PETROLOGY OF INCLUSIONS from some LATE PALAEOZOIC BRITISH VOLCANIC ROCKS

by

NEIL A. CHAPMAN, B.Sc.

Thesis presented for the Degree of Doctor of Philosophy of the University of Edinburgh in the Faculty of Sciences.

1974

DECLARATION.

I hereby declare that all the work presented in this thesis is my own, unless otherwise stated within the text, and that the thesis has been composed by myself.

N.A.Chapman.

ABSTRACT

Ultrabasic inclusions in basanitic rocks are of restricted occurrence in Britain, being found only in rocks of Carboniferous or Permian age. As such they are amongst the oldest known occurrences in the world and yet have never been studied in detail.

The present work has concentrated on a series of late Carboniferous or early Permian tuff-pipes and minor intrusions on the Fife coast near Elie. These contain a wide variety of fragmental materials and megacrysts. Further detailed work was carried out on a vent at Duncansby Ness, Caithness, which is host to spinel-lherzolite, spinel-wehrlite and spinel-pyroxenite nodules. Samples of inclusions were also studied from Fidra, Kidlaw and Weak Law, East Lothian; Hawk's Nib, Bute and Calton Hill, Derbyshire. Geochemical data collected from this material are described, and these, along with results of high-pressure experiments, are used to postulate a petrogenetic model for the Fife volcanics.

Of the six diatremes studied along an 8km stretch of the Fife coast, the Elie Ness vent contains the widest variety of fragments and megacrysts of basic and ultrabasic material. Five types of coarse-grained, alkaline, mafic and ultramafic fragments (Elie-type nodules) were distinguished:-

Type 1. Kaersutite-olivine-pyroxenite.

Type 2. As Type 1 plus oligoclase.

Type 3. Biotite-pyroxenite.

Type 4. Sodic amphibole-biotite-albite.

Type 5. Biotite-albite.

Megacrysts of sodic anorthoclase of high-temperature structure, pyrope, sub-calcic augite and kaersutite are also common in the tuff, and scattered representatives of similar Elie-type nodules and megacrysts occur in other vents. The basaltic rocks associated with this material are alkali-basalts trending via basanites toward monchiquites, with normative nepheline from 1-17%. The most undersaturated rocks, found at Elie Harbour and Chapel Ness, contain no Elie-type nodules or megacrysts. The Ruddons Point basalt (RPB), one of the most basic rocks, contains spinel-lherzolite inclusions, and in common with the other lherzolite-bearing sheet at Coalyard Hill is free of Elie-type nodules.

The composition of the augite and pyrope megacrysts indicates crystallisation from a basic alkaline liquid. Experimental studies show that these phases could have coprecipitated from an alkaline basalt magma at P > 25kb, T = 1300-1450°C. It is proposed that the primary magma for the Fife volcanics was formed by 10-15% partial melting of a vapour-free, mica-bearing garnet-lherzolite at a depth of ca. 100kms, and that the 'eclogitic' pyrope and augite mixture crystallised from this liquid at depths > 70 kms. Geochemical studies of pyroxenes from the Elie-type nodules indicate that they crystallised within the lower crust. It is proposed that the Types 1 and 2 nodules are cumulates from the alkaline liquid, with intercumulus kaersutite representing the composition of liquids intermediate on the Fife basalt trend. Advanced fractionation of pyroxene could

produce the most undersaturated, nodule-free eruptives. The Type 3 nodules may represent basaltic liquids, at the basic end of the Fife trend, crystallised at pressures from 10-15kb. Types 4 and 5 nodules may represent crystallisation products of a trapped body of hydrous liquid, possibly remnant from the formation of Type 3 nodules.

Experimental work on the stability of anorthoclase in RPB shows it to be present in the liquid field at $P < 9$kb (dry), and it is thought that crystallisation of anorthoclase may be the final phase of Types 4 and 5 nodule formation. The build up in volatile pressure led to an eruption so violent as to strip the cumulates from the lower crust, sample fragments of basement rock, and carry unresorbed garnet and augite from depths of over 70kms. This may indicate that a magma column up to 50kms long existed prior to eruption. The spinel-lherzolite inclusions from other localities may represent crystal-cumulates from a late-stage basic liquid, injected into ring-fractures and as sheets within vents.

Experimental studies on black, pleonaste-clinopyroxenites from Duncansby Ness, Caithness, show that up to 5 wt % of the spinel could have been exsolved from the augite at pressures close to 18kb and temperatures of about 1300°C under dry conditions. The large size of these pyroxenites, together with their lack of subsequent low-pressure or hydrous recrystallisation indicates that a deep-seated, violent, eruptive episode similar to that postulated for Elie Ness may have taken place.

CONTENTS

CHAPTER ONE

Introduction and General Geology

Introduction

'Trying to reconstruct the depth of origin and process of formation of xenoliths in any one individual tuff or flow is akin to trying to map the geology of an inaccessible highland area by looking at the boulders in the bed of an emergent stream. Multiple origins and differences in distances of transport of fragments, even those deposited side by side, might as well be assumed in both cases, and generalisations ought to be made with extreme care.'

This quotation from Jackson (1969) adequately sums up the problems encountered in trying to draw meaningful conclusions about the composition of the earth's mantle from a study of ultrabasic inclusions in basalts. The important theory that such inclusions may be mantle fragments has only become fashionable in the last fifteen years and since then, with the increasing need of petrologists seeking the answers to basalt genesis to have a workable model for mantle composition, there has been a strong motivation to study inclusions and nodules in detail. The bulk of recent work has been centered on inclusions containing high-pressure assemblages such as garnet- and spinel-lherzolites, as these would most closely approximate to what may be upper-mantle fragments. Since the early review paper by Ross, Foster and Myers (1954) the argument as to whether peridotite inclusions are in fact mantle xenoliths or cognate accumulates from basalts has expanded to take in modern isotope

techniques and phase-equilibria studies, but is as yet still unresolved. A fuller discussion of this controversy is presented in Chapter 7. The increasing interest in peridotitic inclusions led to international conferences such as the Penrose (Flagstaff) Conference (1970) and a number of far-reaching review papers have summarised a great deal of the worldwide geochemical data on such rocks. The most notable contributions have been made by Harris, Hutchison and Paul (1972), Forbes and Kuno (1964), Kuno and Aoki (1970), Kuno (1967), O'Hara (1967), and Yamaguchi (1964). Wyllie has contributed much by assembling data from many authorities in 'Ultramafic and Related Rocks' and 'The Dynamic Earth' (1967, 1971).

In 1961 Wilshire and Binns published data on the other lesser studied groups of inclusions and megacrysts which are of more probable cognate origin, such as amphibole- and mica-bearing pyroxenites, gabbros and wehrlites, and feldspar and pyroxene megacrysts. Since then more work has been concentrated on these types of inclusion and similar review papers to those on peridotitic inclusions have been published (Binns, Duggan and Wilkinson 1970, Aoki and Kushiro 1968).

That many of the above 'alkali' inclusions are often found in the same rocks as lherzolite and dunite fragments, and are almost totally confined to under-saturated rocks, has prompted more research into the whole spectrum of inclusion types with a view to reaching conclusions on the petrogenesis of alkali-basalts. It was with these points in mind that the present work was undertaken.

Scope of present research.

The most interesting points regarding the Scottish inclusion-bearing localities and which make them a worthwhile research project are:-

a) They possess many of the features displayed by the classical localities studied in the '50s and '60s and have yet not been studied in any detail.

b) Whilst almost all other known localities for lherzolite inclusions in basalts are late Mesozoic to Recent in age the late Palaeozoic Scottish localities are the oldest known in the world. If the lherzolitic inclusions are in fact mantle fragments then the Scottish localities offer an unrivalled chance to compare modern samples with those up to 300my older.

c) The unusual presence of pyrope garnet in the tuff at Elie Ness in Fife makes this locality one of the few known in the world where very high-pressure megacrysts are found associated with lower-pressure phases such as amphibole and anorthoclase.

d) The use of modern high-pressure and temperature equipment facilitates the study of phase-relationships and stability limits of some of the little-studied phases found as megacrysts, the results of which could be directly applicable to similar occurrences elsewhere.

Added to these points a further advantage of studying a reasonably well-exposed British locality is the well-documented nature of the associated basalts, due to previous mapping by the Geological Survey. With these points in mind it was decided to

carry out detailed chemical work on the nodule and megacryst phases in the hope of being able to fit them into a viable petrogenetic scheme. Owing to the highly altered nature of the lherzolitic inclusions the majority of the work has been centred on the 'alkali' inclusions and megacrysts, though comparative geochemical work was performed on the lherzolites. In general then the aim of the present work is both to provide an accurate account of some of the most important Scottish inclusion localities, as yet unstudied, and to provide geochemical and experimental data that may be of use in contributing to the understanding of similar occurrences abroad.

Layout of the thesis

In order to facilitate the reader's study of the thesis it is intended to give a general outline of the layout. The chapters are arranged in such an order as to become progressively more detailed studies of individual topics discussed in previous chapters. The final two chapters (6 and 7) are respectively devoted to experimental studies and the main conclusions which can be drawn from the work as a whole. The current chapter goes on to discuss the overall geology of the Scottish inclusion areas, with a more detailed study of the local geology of individual localities and a survey of previous work on them.

Chapter 2 outlines the petrography and mineralogy of material from all the localities, whilst Chapter 3 studies the detailed whole-rock geochemistry of this material. In Chapter 4 the chemistry of discrete minerals from the samples is discussed, and Chapter 5

presents a more detailed examination of clinopyroxenes only. All analyses of rocks and minerals are presented in Appendix 1. Experimental and computer techniques and estimates of accuracy are outlined in Appendices 2-4.

British Inclusion Localities

Ultrabasic inclusions in basaltic rocks are of restricted occurrence in the British Isles. All the known localities are Carboniferous or early Permian in age, and the great majority of these are found in the Midland Valley of Scotland where Carboniferous volcanic activity was most intense. Inclusions are also found associated with other centres of activity, notably in Derbyshire, Co. Cork, Caithness and in east-west dykes scattered across the western Highlands. All the inclusion suites are found in, or associated with, strongly undersaturated basanitic or monchiquitic rocks. There are over twenty known occurrences of ultrabasic inclusions and associated megacryst assemblages in the Midland Valley, and when one considers that the majority of these localities are only known because of good coastal exposure it seems fair to assume that their occurrence is widespread.

The Midland Valley, whilst being a well-defined structural unit well back in to the early Palaeozoic, did not develop into a true rift-valley until the Devonian. Sedimentation was continuous and rapid throughout the Carboniferous, keeping pace with the gradual sinking of the graben. The widespread volcanic activity during this period is well documented, and it will not be reviewed in

detail in this work. The general trend of the alkaline volcanic sequence throughout the lower and middle Carboniferous is from basic through to acidic eruptives with a marked decline in activity in the Westphalian. The later volcanism is represented by more alkaline lavas and intrusives. The increasingly undersaturated nature of the magma was associated with explosive activity and it is in the resulting tuffs and their contemporaneous flows and intrusions of basanites and monchiquites that inclusions and fragments of ultrabasic material are found. The youngest members of this sequence are found in the Mauchline Basin in Ayrshire, and were considered to be Permian, but are now thought to be Stephanian (Mykura, 1967).

Previous descriptions of the inclusions and their kindred megacrysts have tended to be 'en passant' references in descriptions of local geology, and are mainly found in the Survey Memoirs for East Fife, East Lothian, Central Ayrshire and Caithness, some of which date back to the turn of the century. The only two recent studies in any depth are those of Hamad (1963) on the lherzolites from Calton Hill, Derbyshire, and Colvine (1968) on garnet megacrysts from Elie Ness in Fife. Heddle performed the earliest experimental work on spinel-pyroxenites from Caithness in 1878 and described many of the minerals found as megacrysts from Fife in his 'Mineralogy of Scotland' (1901). In 'Chapters on the Mineralogy of Scotland' (1879) Heddle describes attempts to melt the black augite nodules from Duncansby Ness (Caithness), in which he heated some chips and powder of the pyroxenite in a platinum crucible; "only when the crucible was at the point of bright ignition.... did the powder coalesce and liquefy". This, he states, "accords with a

temperature of 2200 to 2250°F".

A summary of the findings of previous published work is laid out in Table 1-1.

Areas studied in present work. (See Fig.1-1).

Most of the work in the present study has centred on localities in the eastern Midland Valley, in East Lothian, and on the Fife coast. Detailed work has also been carried out on the Duncansby Ness vent near John o' Groats in Caithness. Representative collections have been taken from Calton Hill in Derbyshire and Hawk's Nib in Bute for comparative geochemical work. The following section is intended to give an outline of the local geology of the areas studied and describe the general field relations of specific localities.

Fife. (Fig. 1-2).

Geikie (1902) stated that he had found at least eighty volcanic necks in the stretch of land between St. Andrews and Lundin Links, from the coast to six or eight miles inland. He also noted that many more had probably escaped detection in the poorly exposed inland area. The coastal section between St. Monance and Ruddons Point reveals eleven well-dissected diatremes and associated minor intrusions. Their state of preservation led Geikie to say "perhaps nowhere in the world have such vents been dissected in so instructive a manner..."

The present work concentrates on six of these vents, four of them

Table 1-1

Summary of previous published data on inclusions in basaltic rocks of Britain.

LOCALITY	ESTIMATED AGE	HOST INTRUSION	ROCK TYPE	INCLUSION TYPES	MEGACRYSTS	REFERENCES
a) FIFE						
Elie Ness	Upper Carb.	Vent	Agglomerate	Hb. pyroxenites	Il, Gt, Aug, Hb, Bi, Or.	Balsillie 1927 Heddle 1901 Geikie 1902 Colvine 1968
Kellie Law	Upper Carb.	Dykes	Basanite	-----	Hb, Or, Bi.	Geikie 1902
Carnbee Law	" "	Dykes	Limburgite	-----	Hb, Or, Bi.	"
Coalyard Hill	" "	Dyke	Unspecified	-----	Hb, Or, Bi.	"
Chapel Ness	" "	Sheet	Basalt	-----	Or.	"
Rudions Point	" "	Sheet	Unspecified	-----	Gt, Il.	Heddle 1901
Largo	" "	Vent	Agglomerate	-----	Or.	Geikie 1902
Kinkell Ness	" "	Vent	Agglomerate	-----	Aug.	Heddle 1901
b) EAST LOTHIAN						
Kidlaw	Upper Visean	Sill	Anal. basanite	Spinel lherzolite	-----	Bailey 1910
	" "	Plug in vent	" "	" "	-----	Simpson 1932
Gullane	" "	Sill	Teschenite	Olivine nodules	-----	Bailey 1910
The Lamb	" "	Sill	Anal. basanite	Spinel wehrlite	-----	"
Fidra	" "	Sill	" "	Olivine-pyroxenite	-----	"
Chesters	" "	Sill	" "	" "	-----	"
Weak Law	? L. Carb.	Vent	Agglomerate	Spinel dunite	-----	Duncan 1972
c) AYRSHIRE						
Carnochan, Patna and Kirklafin.	Permian	Vents and dykes	Agglomerates	Spinel peridotites	An, Hb, Bi.	MacGregor 1949
Carskeoch Hill	"	Sills	Monchiquite	-----	Hb, Bi, Alk.Fsp.	"
Patna Tower	"	Dyke	Monchiquitic anal. basanite	Spinel-olivine-pyroxenites.	-----	"
Meikleholm	"	Sill	Monchiquite	Olivine pyroxenite, hb. pyroxenite.	Hb, Bi, Ap, Alk.Fsp.	"
"	"	Dykes	Monchiquite	Olivine nodules	-----	"
Dunaskin	"	Sill	"	-----	Hb, Bi, Alk.Fsp.	"
Heads of Ayr	Upper Carb.	Vent	Agglomerate	Spinel lherzolite	-----	Tyrell 1918 Whyte 1963
Greenan Castle	"	?Vent	Agglomerate	Spinel lherzolite	Alk.Fsp.	MacGregor 1949
Black Rock (Fairlie)	"	Vent	"	Mica pyroxenite	Aug.	Smellie 1915
d) BUTE						
Hawks Nib	Lower Carb.	Dyke	Olivine basalt	Anorthosite, dunite, pyroxenite, gabbro, serpentinite, olivine-pyroxenite.	-----	Smellie 1915
e) CAITHNESS						
Duncansby Ness	-----	Vent and sheet	Agglomerate, basanite.	Spinel wehrlite, spinel pyroxenite.	Bi.	Flett 1914 Heddle 1878
f) INVERNESS						
Glenfinnan	? Permian	Dyke	Monchiquite	Spinel lherzolite, pxte.	-----	Walker and Ross 1954
g) DERBYSHIRE						
Calton Hill	Lower Carb.	? Sheet	Anal. Basalt	Spinel lherzolite	-----	Hamad 1963
h) Co. CORK						
Black Ball Head	" "	Vent	Agglomerate	Hb. pyroxenites	Bi, Hb, Il.	Coe 1966
i) DUMFRIES						
Gateside Pit, Sanquhar	Permian	Dyke	Monchiquite	Peridotites	-----	Simpson and Richey 1936

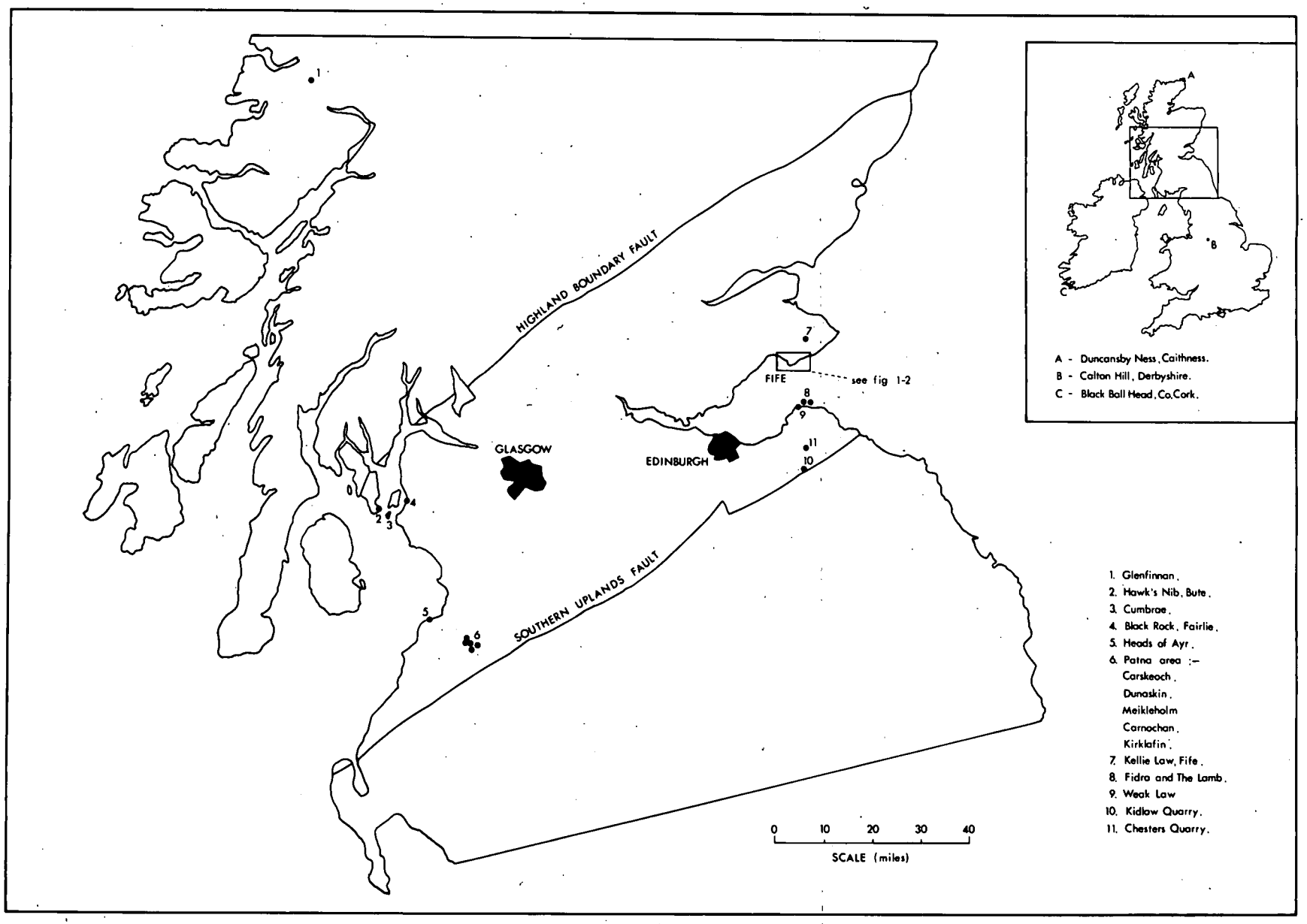
HIGHLAND BOUNDARY FAULT
SOUTHERN UPLANDS FAULT
GLASGOW
EDINBURGH
FIFE
see fig 1-2
SCALE (miles)
0 10 20 30 40
A - Duncansby Ness, Caithness.
B - Calton Hill, Derbyshire.
C - Black Ball Head, Co. Cork.
1. Glenfinnan.
2. Hawk's Nib, Bute.
3. Cumbrae.
4. Black Rock, Fairlie.
5. Heads of Ayr.
6. Patna area :-
Carskeoch.
Dunaskin.
Meikleholm
Carnochan.
Kirklafin.
7. Kellie Law, Fife.
8. Fidra and The Lamb.
9. Weak Law
10. Kidlaw Quarry.
11. Chesters Quarry.

Fig. 1-2

Volcanic vents and allied structures along the Fife coast near Elie and Earlsferry. (after Francis, 1970 and Francis and Hopgood, 1970).

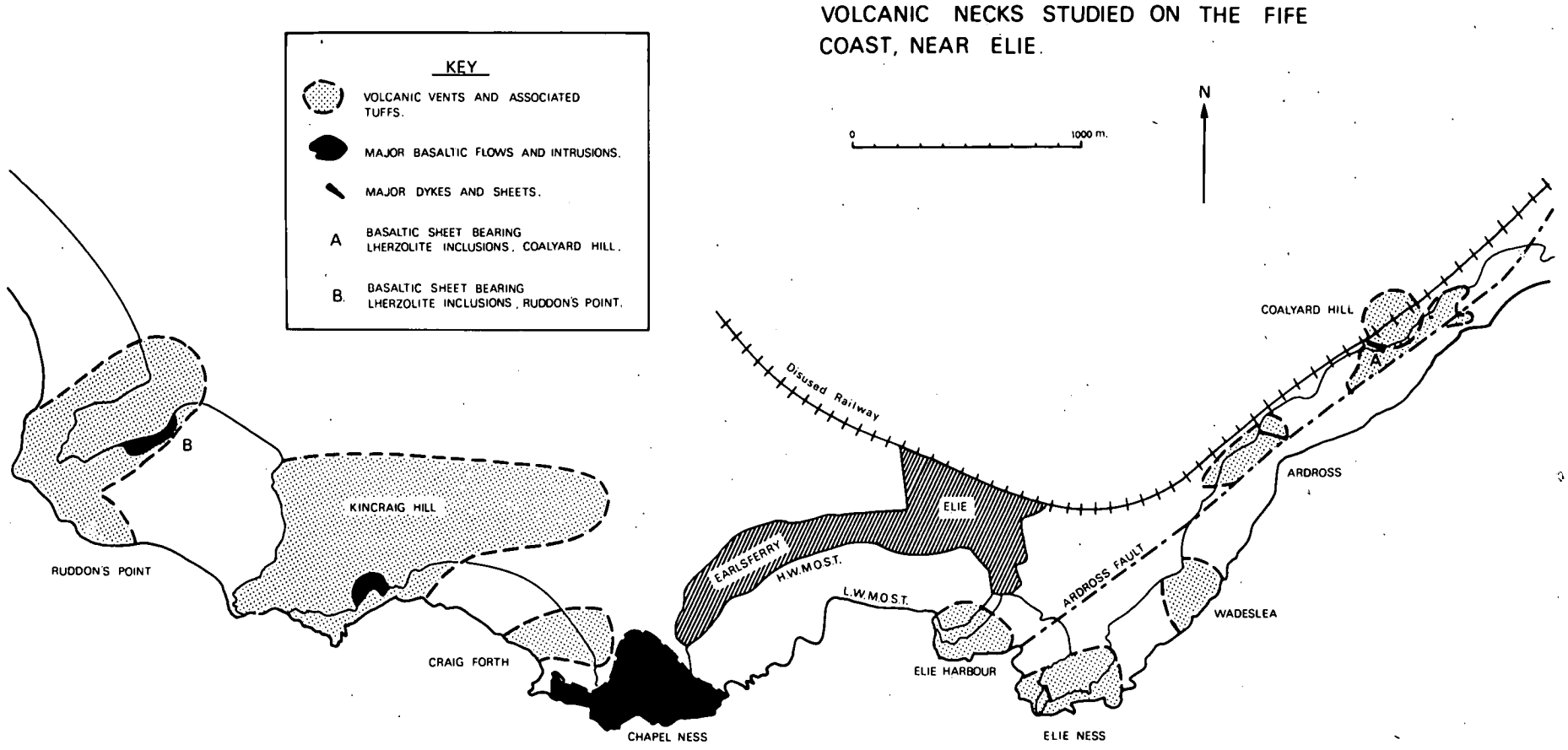
VOLCANIC NECKS STUDIED ON THE FIFE COAST, NEAR ELIE.
KEY
VOLCANIC VENTS AND ASSOCIATED TUFFS.
MAJOR BASALTIC FLOWS AND INTRUSIONS.
MAJOR DYKES AND SHEETS.
A BASALTIC SHEET BEARING LHERZOLITE INCLUSIONS. COALYARD HILL.
B. BASALTIC SHEET BEARING LHERZOLITE INCLUSIONS, RUDDON'S POINT.
N
0
1000 m.
COALYARD HILL
A
Disused Railway
B
KINCRAIG HILL
RUDDON'S POINT
ELIE
EARLSFERRY
H.W.M.O.S.T.
L.W.M.O.S.T.
ARDROSS FAULT
ARDROSS
WADESLEA
CRAIG FORTH
ELIE HARBOUR
CHAPEL NESS
ELIE NESS
FIRTH OF FORTH

which lie adjacent along a 4 km stretch of coast between Coalyard Hill and Elie, where the Ardross fault is the dominant structural feature. The internal structure of the whole series of vents, together with the structure and contact relationships of the penetrated country-rock has recently been studied in detail by Francis (1960, 1969, 1970) and Francis and Hopgood (1970). The vents are filled with basaltic tuff and agglomerate, and fragments of country-rock including the surrounding lower Carboniferous sandstones, shales and limestones. The Elie Harbour vent contains a large raft of foundered sediments including a garnetiferous sandstone. Many of the vents exhibit downturning of the surrounding sedimentary rocks at their margins. This, along with the internal bedding structures in the tuff-pipes, led Francis (1970) to propose that cauldron subsidence of up to 500m had taken place after the cessation of explosive activity. Emplacement of minor intrusions had accompanied the subsidence, particularly along the ring-fractures around the pipe margins. This phenomenon is exhibited at Coalyard Hill, where an inclined sheet containing lherzolite inclusions has been intruded along the western margin of the vent. Elsewhere the associated intrusions take many forms, from impersistent dykes and sheets, often merging into the tuff, to large plugs and bosses such as that of Kincraig Hill. This mass of columnar basalt which occupies the central area of the vent is thought to have an inverted cone-shaped structure floored by tuff, rather than being a true plug (Francis, 1970). A general feature of the intrusions is their lack of sharp margins and their previously noted tendency to merge into the surrounding tuff, all of which suggests the tuff to have been in

a relatively unconsolidated state at the time of intrusion.

The vents range in size from 0.7 to 1.3kms across (Francis, 1970), the largest being at Kincraig Hill, where the tuff forms high cliffs and a broad wave-cut platform dissected by dykes. None of the vents is completely exposed even at low-tide, as they tend to be drift or sand covered on the landward sides. Owing to the presence of carbonised plant remains and fossil wood in the tuff Geikie suggested that the vents were formed subaerially. This is further substantiated by the impact marks found in the tuff under some of the larger blocks and the general lack of graded bedding. Two vents do show thin layers of tuffites (mudstones, clays etc. containing volcanic detritus) indicating evidence of at least minor underwater sedimentation, though Francis (1970) takes this to represent sedimentation in temporary crater-lakes.

At Kellie Law, 5kms inland from St. Monance, a conspicuous hill is composed of agglomeratic tuff dissected by numerous dykes (Geikie, 1902). The exposure is poor, though a large mass of basaltic material on the western flank of the hill by the roadside yielded rare anorthoclase megacrysts.

East Lothian.

Apart from the isolated occurrence of probable lherzolite inclusions in a (?) lower Carboniferous vent at Weak Law the remainder of the inclusion-bearing rocks are sills and plugs, most probably of upper Visean age. These sills are of fine-grained analcime-basanite or monchiquitic rock and Clough (1910) grouped them together as

probably post-dating the Calciferous Sandstone Series lavas. Chesters quarry is no longer accessible, though Clough reported the occurrence of 'olivine-nodules' from a monchiquite sill at this locality. The analcime-basanite of Kidlaw Quarry was originally described by the Survey as a sill, but later work (Simpson, 1932) revealed the presence of tuff to the south side of the quarry which had a steep junction with the basanite indicating a plug-like structure. Whether this is a true plug or merely a large floored boss as at Kincraig Hill in Fife is uncertain. The quarry itself is transected by an east-west fault and lies only about 300m north of the S. Uplands fault itself. Upton and Macdonald (in press) have reported the presence of granitic fragments in the tuff, possibly of Caledonian origin, and Bennett (1939) also noted granitic fragments and Palaeozoic sediment xenoliths in the fault-breccia. Cavities in the compact basanite represent the weathered-out remnants of lherzolite inclusions.

The islands of Fidra and the Lamb lie 2kms apart and to the west of North Berwick, about 0.7kms offshore. The two islands may well represent outcrops of the same analcime-basanite sill. Spinel-bearing wehrlites were collected by the Survey (1910 Memoir) from the Lamb. Fidra only was visited in the course of the present work. The sill exhibits columnar jointing, and on the northern side of the island is 20m thick. Rare spinel-lherzolite and spinel-wehrlite inclusions, together with anorthoclase megacrysts are found in the lower part of the sill, large xenoliths of limestone and sandstone also being common.

The vent at Weak Law on the coast opposite Fidra is associated with flows of alkali-olivine basalt, mugearite and trachyte (Duncan, 1972). The vent itself is poorly exposed and the agglomerate rich in fragments of country-rock, particularly sandstones and feldspar-phyric basalt. Fragments of probable spinel-lherzolite are found in the agglomerate on a small wave-cut platform.

Caithness.

Two volcanic vents occur on the north coast of Caithness, at Duncansby Ness and Dunnet Head. The former penetrates Middle Old Red Sandstone (ORS), the latter, Upper ORS. Five thin monchiquitic dykes cut the M.ORS on the coast north of Castletown and similar dykes are found on the eastern side of Dunnet Bay, possibly being continuations of the same dykes. Apart from rare monchiquitis dykes further south these rocks furnish the only evidence of volcanic activity in Caithness (Flett, 1914). The Dunnet Head vent is poorly exposed in a dry stream bed on the eastern side of the promontory, and consists of a fine-grained agglomerate composed largely of sand-grains from the surrounding ORS in a basaltic glass. No ultrabasic blocks have been found in this vent.

Partly concealed by low sand-dunes, the Duncansby Ness vent is exposed in reefs between water-marks, where its maximum width is 200m. A further small exposure of tuff occurs on the western side of the Ness, but as this also disappears under the sand, it is not possible to say if this is part of the same vent. The tuff in the main exposure is transected by nepheline-basalt dykes (Flett, 1914)

and larger intrusive bodies to the west. Both the tuff and the intrusions contain ultrabasic fragments and inclusions. Flett (1910) left the age of these rocks open to conjecture, ruling out neither the possibility that they were associated with the Devonian volcanics of Orkney nor the possibility that they may be Tertiary. Potassium-Argon dating of basaltic material from the intrusions in the Duncansby Ness vent (present work) shows this locality to be early Permian in age (255my) and there is a strong possibility that the monchiquitic dykes may be contemporaneous. This correlates with the radiometric ages of the Fife diatremes.

Bute.

The island of Bute is transected by the Highland Boundary Fault in the north, placing the southern 12kms within the structural confines of the Midland Valley. The southern tip of the island is largely composed of flows and minor intrusions of lower Carboniferous volcanics which, in places, overlie Calciferous Sandstone Series sediments. The volcanics comprise basaltic and trachytic lavas, rare agglomerate-filled vents, tuff beds and minor intrusions (Smellie, 1915). A small outcrop, 20m by 30m, lying between water-marks at Hawks's Nib south of Kilchattan on the east coast comprises a basanitic intrusion containing a wide variety of basic and ultra-basic inclusions. The intrusion has a steep southerly dip and penetrates Calciferous Sandstone Series cornstones, sandstones and clays (Smellie, 1915), lying along the northern margin of the main volcanic sequence. The volcanic flows and dykes of Little Cumbrae,

an island to the east of Bute, probably represent a continuation of this sequence, and ultrabasic inclusions have recently been reported from this locality (C. Chaplin, pers. comm.).

Derbyshire — Calton Hill.

The massive limestone deposits of the lower Carboniferous sequence in Derbyshire are intercalated with lavas and tuffs and rarer agglomerate-filled vents. The lavas, locally known as 'toadstones', are mainly of porphyritic olivine-basalt grading to olivine dolerite. Pillow-lavas are found in the Hope district. An analcime-basanite body forms a low hill formerly quarried for roadstone at Calton Hill, 7kms east of Buxton, and contains spinel-lherzolite inclusions (Hamad, 1963). No other ultrabasic material has been reported from the local tuffs or lavas.

Sampling techniques and problems of alteration.

Owing to the age of the rocks studied and their predominant coastal exposure severe problems have been encountered in gaining fresh material, particularly for whole-rock analysis. In the majority of the rocks sampled, both from inclusions and basaltic blocks and intrusions, olivine has very rarely been fresh and is generally pseudomorphed. Calcitisation of basaltic material is often extreme and the resulting 'white-trap' noted by the Survey is common. The ultrabasic inclusions from Coalyard Hill are severely calcitised. The amphibole- and mica-bearing pyroxenites and related material such as that from Elie Ness is, however, generally quite fresh, with

the exception of olivine. The depth to which weathering has proceeded in basaltic material is such that only the largest blocks in tuff are reasonably fresh in the centre.

To combat this problem of deep-weathering a small petrol-engined rock drill with a one-inch diamond bit was utilised at several localities. The machine is a converted chain-saw, hand-held, with a maximum depth of penetration of about 25cms. At many localities this was still insufficient to gain really fresh material, notably at the lherzolite-bearing outcrop of Coalyard Hill, where calcitisation seems to be almost complete. At Kidlaw, however, where the compact basanite outcrops in smooth faces, it was found particularly useful in gaining the only reasonably fresh inclusion samples.

At Elie Ness a series of five-metre squares were laid out on a traverse across the level tuff platform, from the centre to the eastern margin of the vent. Detailed sampling was then carried out in the quadrats, though the only measurable result of this type of sampling over a random method was merely to reinforce the observation that sedimentary material increased in proportion towards the vent margin. Wilshire et al. (undated) compiled a report on ultrabasic nodule sampling techniques for the National Aeronautics and Space Administration as a guide to any future search for such material on the moon. Their conclusions were based on observations of several localities in North America. The tendency for inclusions within flows and intrusions to congregate at the base of the mass is noted, but when dealing with tuff-pipes they found that whilst

ultrabasic blocks are commonest within agglomerates, they are equally abundant anywhere within the agglomerate at up to twice the crater diameter away from the vent. It was also pointed out that there is no morphological difference between cones or basalt bodies which are nodule-bearing or nodule-free. They concluded that many occurrences of nodules in tuffs and agglomerates showed little variation in nodule types from point to point. In theory all sampling could be done at one point, although exceptions do rule out this method as imprecise. It would seem that a random sampling technique within any locality is the best compromise. Observations of nodule location and frequency of occurrence within the Fife diatremes tends to support this supposition.

Radiometric ages of Fife and Caithness volcanism.

Owing to the uncertainty of the exact ages of the Fife tuff-pipes and the lack of any stratigraphic evidence to date the Duncansby Ness vent as anything other than post-Devonian, it was decided to carry out a small-scale survey using potassium-argon dating techniques. This is being carried out in co-ordination with Dr. R. M. Macintyre of the Scottish Reactor Research Centre, East Kilbride, and at the time of writing the programme is still in progress. As it is intended to publish the complete results, only a general outline of the work so far will be discussed here.

Table 1-2 lists the uncorrected results obtained so far from Fife and Caithness materials and as such serves only as a rough guide to the radiometric ages. Amphiboles and micas from two Elie Ness

Table 1-2

Potassium-argon data from Fife and Caithness (uncorrected).

LOCALITY	SAMPLE	SAMPLE DESCRIPTION	ANALYSED MINERAL	K %	Ar^{40} $x10^{-2}$ ppm	ATMOS %	AGE my
Elie Ness	Q2-13	Kaersutite-olivine pyroxenite nodule.	Kaersutite	1.029 1.054 1.152	2.376 2.348 2.501	8.8	309 291 288
Elie Ness	Q4-13	Elie-type 4 nodule	Mica	5.70 6.19 3.83	13.48 13.35 8.69	2.4 1.4 2.1	306 288 297
Elie Ness	P-21b	Basanite block	Whole-rock	-	-	-	260
Elie Harbour	P-25	Basanite block	Whole-rock	-	-	-	254
Duncansby Ness vent.	DH-24 DH-25	Monchiquite "	Whole-rock Whole-rock	- -	- -	- -	256 259

All analyses were performed by Dr. R. M. Macintyre at S.R.R.C.

nodules yielded acceptable results, as did whole-rock determinations on basalts from the Elie Ness, Elie Harbour and Duncansby Ness vents. Further work is in progress on anorthoclase megacrysts from Fife.

As can be seen from the results the nodules from the Elie Ness vent give an age roughly 40 my older than the basalts. Whether this is in fact an effect of excess argon in the nodules is not known at this stage. The 297my age would place the Fife volcanism in the Stephanian (Fitch, Miller and Williams, 1970) whereas the basalt ages of 250-260my are lower Permian. In either case it would appear that the two vents are younger than the Namurian age estimated by Francis and Hopgood (1970) from statigraphic data. Recent work carried out by IGS for the new East Fife Memoir (in press) has dated material from some of the Fife vents and arrived at similar ages ($\sim$ 280my) for the coastal group (Mr. I. Forsyth, pers. comm.). It is possible that the slow cooling of a basalt flow may result in argon escape and hence a young date, whereas the rapid chill experienced by the Elie nodules and megacrysts may give a more reliable answer. It remains to be seen if the anorthoclase dates support those from the nodules.

The Duncansby Ness vent is apparently contemporaneous with the Fife volcanism, also falling in the lower Permian, though being in a tectonically stable region during this period compared to the active graben of the Fife area.

CHAPTER TWO

Petrography and Mineralogy.

Notes on nomenclature.

The classification of undersaturated basaltic rocks, and in particular the dividing line between basanites and alkali-basalts has long been a point of controversy. A wide variety of both terminology and methods of classification have been used by various authors. Many rock names are now little used or obsolete. In an effort to clarify this problem Coombs and Wilkinson (1969) proposed a normative classification scheme to locate the transition between basanites and alkali-basalts. They point out that although a rock may have up to 5% ne in its CIPW norm it is often impossible to optically determine nepheline in the mode. Above 5% ne it is usually possible to identify nepheline either optically or by XRD methods. They also note that rocks with less than 5% ne are usually part of a trend resulting in trachytic differentiates, whereas those with more than 5% ne usually lead to phonolitic differentiates.

In the present study the rocks encountered have ne ranging from 1-17% (Fig. 3-1) although modal nepheline is not generally found, the sodic phase being analcime. Even in the most basic samples 5-8% modal analcime is present. Coombs and Wilkinson note that it often requires 10% modal analcime to be present before ne is 5.5%, or in other words the presence of 10% modal analcime would

only just qualify the rock for their basanite field. Since it is only the more basic rocks from Fife which fall below the 5% ne divide, and since these rocks are part of a sequence leading well into the basanite field, it is proposed to term those with less than 5% ne 'analcimic-basalts', and those with more than 5% ne 'basanites' for the sake of clarity.

The use of the term 'monchiquite' to describe some of the more under-saturated rocks gives rise to further problems of classification. The lamprophyres are probably one of the most ill-defined rock-groups and little has been done to clarify the issue since Rosenbusch first laid out a classification in 1910. To quote from Métais and Chayes (1963) 'The resulting chaos has been admirably described by Knopf (1936) who points out that a particularly well-known sample he himself describes as vogesite had been described previously by Pirrson as minette, by Rosenbusch as camptonite, and by Beger as monchiquite'. Métais and Chayes summarised the available data on rocks which had been termed lamprophyres, which included 633 analyses falling into some 33 different groups. Only the six major groups had any number of analyses. Minettes, vogesites, kersanites and spessartites were found to be indistinguishable on a chemical basis, though monchiquites and camptonites were markedly less siliceous and richer in iron.

In generally accepted terminology lamprophyres containing olivine and augite phenocrysts, amphibole microphenocrysts and analcime instead of feldspar are termed monchiquites. In this respect only one of the Fife rocks, a block from the Elie Ness tuff,

could be described as a monchiquite in that it fits the above description and contains very little feldspar. It should, however, be noted that whilst in the sense of Rosenbusch the camptonite-monchiquite group is olivine-titanaugite rich, the type monchiquite from Rio de Janeiro is in fact olivine-free. (Knopf, 1936). The camptonites are generally more amphibole-rich than the monchiquites, having amphibole phenocrysts.

The term monchiquite has been used frequently by most authors discussing the volcanics of the Midland Valley, but it is proposed that in the present work the term is not to be used in the form of a strict classification. The trend in the Fife rocks to increasingly basanitic compositions with ne steadily increasing is reflected by a predominance of modal analcime over feldspar. That some of the rocks are lamprophyric in character is not disputed, but bearing in mind the restrictions in nomenclature brought out in the previous discussion it is proposed that only those with primary modal amphibole be termed 'monchiquitic'. The chemistry of these rocks correlates closely with the camptonite-monchiquite group of Metais and Chayes.

Use of the term 'inclusion'.

In the present work 'inclusion' will be used only to denote those fragments of cognate or accidental material included within a magma body (e.g. dykes, sills, flows). Whilst similar material occurs in tuffs and agglomerates the fragments are clastic and not inclusions sensu-stricto. Here they will be termed blocks, fragments

or nodules.

Xenocrysts and megacrysts.

Strictly speaking the term 'megacryst' means no more than 'big crystal' and can equally apply to both cognate and accidental material. In this work it is proposed to use the term in that sense, for discrete crystals found in both tuffs and basaltic bodies. Where a crystal can be clearly shown to have originated from the mechanical breakdown of an ultrabasic inclusion or nodule it will be termed (cognate) xenocryst.

Modal data.

Table 2-1 presents data on the major modal constituents of some of the more important rock-types discussed below, including the five Elie nodule-types. Modal data on lherzolitic inclusions from Fife and Calton Hill are discussed in Chapman (1974, in press).

2.1 The Fife localities.

Introduction.

Before describing in detail the material sampled from the volcanic vents in Fife it is proposed to outline some of the features which the vents have in common. The clastic material in all the vents is composed largely of angular to sub-angular blocks of basaltic rock and fragments of sedimentary material in a tuffaceous matrix. The sediment fragments are predominantly sandstones and limestones with subordinate shales and coals, thought to be mainly Carboniferous in age (Francis, 1970). The Elie Ness vent contains the widest

Sample	Locality and type	Major modal constituents								
		Ol	Cpx	Anal	Plag	Alk.Fsp	Amph	Mica	Glass	Ore
EHB	Elie Harbour basanite block	17	26	35	12	-	-	-	-	10
Q2-32	Elie Ness basalt block	16	29	11	14	-	-	-	21	9
XR-8	Kincraig plug basalt	17	27	6	23	-	-	-	17	10
RPB	Ruddons Point basalt	11	27	8	18	-	-	-	25	11
XR-44	Kellie Law basalt	12	30	10	10	-	-	-	26	12
DH-24	Duncansby monchiquitic boss	18	15	-	-	5	-	-	-	6
		(indefinable groundmass- 56)								
Q2-23	Elie Ness Type 1 nodule	22	48	-	-	-	30	-	-	-
Q2-5	Elie Ness Type 1 nodule	5	40	-	-	-	55	-	-	-
Q3-16	Elie Ness Type 2 nodule	6	28	-	9	-	57	-	-	-
Q2-6	Elie Ness Type 3 nodule	-	55	-	-	-	-	45	-	-
Q4-13	Elie Ness Type 4 nodule	-	-	-	21	-	60	19	-	-
Q2-27	Elie Ness Type 5 nodule	-	-	-	40	-	-	60	-	-

variety of fragmental material other than that described above, and for this reason will be described in detail first to serve as a reference to the other Fife localities.

a) Elie Ness vent.

The clastic material within the tuff falls into five major groups; basaltic and sedimentary blocks, fragments of deeper crustal origin, and fragments of ultrabasic material together with associated megacrysts. The first two groups predominate. Angular to sub-angular blocks of basaltic material range in size from a few centimetres to over a metre across, though rarely attaining this size. There is a marked decline in their frequency towards the exposed eastern margin of the vent where sedimentary material predominates. Xenoliths of sandstone, shale and limestone of supposed Carboniferous age make up the bulk of the remaining clastic debris. Occasional fragments of carbonised wood and fossil plant remains in the tuff indicate subaerial eruption, as previously noted.

The basaltic blocks are analcimic-basalts and basanites, having ne ranging from 2.5 to 8%. They are porphyritic with euhedral to subhedral pseudomorphed olivine phenocrysts and subsiduary augite phenocrysts in a groundmass of titanaugite, titanomagnetite, and varying amounts of chlorite, brown-glass, plagioclase and analcime. The overall fine-grained nature of the groundmass and the predominance of glassy material present in the majority of the basalts is thought to indicate a rapidly chilled origin. A general trend towards the more basanitic types is indicated by the increase of

analcime at the expense of plagioclase, a trend common throughout the Fife localities. The augite phenocrysts are strongly zoned, showing pale-purple titanaugite rims, and occasionally small glomeroporphyritic aggregates of augite occur. A less common vesicular basanite is present, the vesicles being filled with calcite, analcime and other zeolites. Rare monchiquitic blocks with ne 13% have pseudomorphed elongate olivine phenocrysts and amphibole microphenocrysts in a matrix of titanaugite, titanomagnetite and analcime. Plagioclase (andesine) is present in minor amounts in the groundmass (Plate 1). Occasional megacrysts of oligoclase up to 5 mms across and exhibiting corroded rims, together with aggregates of amphibole and clinopyroxene reminiscent of the Type 1 nodules described below are found in these monchiquitic blocks.

A highly altered fragment of feldsparphyric basalt, possibly of Devonian age, and a small block of mica-schist, also very altered, were collected from the tuff. These two fragments represent materials which must have been brought up from considerable depths. The nearest occurrence of mica-schist is in the Dalradian north of the Highland Boundary Fault in Perthshire, but the presence of schistose material within the tuff at Elie may indicate that similar material forms basement rocks below this area of the Midland Valley graben. Whilst it is not intended to enter into any discussion of the Palaeozoic plate-tectonic theories of origin of the Midland Valley, this particular discovery suggests the presence of continental-crustal material beneath this part of the Midland Valley during the Carboniferous, rather than the remnant oceanic crust of a closed

proto-Atlantic Ocean. (cf. Dewey, 1969, Fitton & Hughes, 1970).

The fourth group of clastic material comprises nodules of coarse-grained ultrabasic rock (Plate 10) which display a wide variety of textural and mineralogical types. These have been split into five Types, described below in order of decreasing abundance.

Type 1. Those containing essential olivine, augite and kaersutite.

These can be further subdivided into three subgroups on textural grounds.

a) The first subgroup consists of euhedral to subhedral olivines and augites, the latter showing some evidence of rim-corrosion, which are poikilitically enclosed by large, interlocking kaersutite grains. The amount of olivine present is variable, from rare crystals to large aggregates. Alteration of the olivine is almost invariably total. (Plate 2).

b) The second type has euhedral olivines (up to 3mms), usually completely pseudomorphed, surrounded by an equigranular mosaic of small augite and kaersutite crystals, commonly exhibiting three-point junctions. (Plate 3).

c) The third subgroup contains kaersutite as a secondary alteration from augite. The texture is one of fresh interlocking augite and rarer pseudomorphed olivine crystals, with kaersutite occurring mainly along grain boundaries and cleavage traces in the pyroxene, though sometimes forming well-developed crystals. (Plate 4).

Type 2. Nodules of Type 1 containing feldspar. (Plate 5)

Whilst this group has the same essential mineralogy as the previous group the texture varies and potassic oligoclase occurs interstitially. Large, deep-brown kaersutite crystals compose up to 60% of the rock, whilst the augite and rare pseudomorphed olivines exhibit poorly developed crystal-forms and show signs of incipient alteration. In many of the kaersutite-bearing fragments, though particularly in this group, the amphibole displays exsolution of ilmenite and associated opaque minerals.

Type 3. Nodules containing augite and titanbiotite only. (Plate 6)

This type is much less common than the previous groups and consists of a well-developed pyroxenite containing large patches of pale-brown, pleochoic titanbiotite, much of which appears primary, though a certain amount appears to be formed at the expense of the augite.

Type 4. Those containing essential green-amphibole, biotite and albite. (Plate 7)

A deep-green, sodic edenite-hornblende with interstitial albite forms the bulk of this rock. The biotite occurs in evenly-spaced, well-formed, radiating clumps throughout the rock. The albite lies in the range An_{5-7}.

Type 5. Nodules containing biotite and albite only. (Plate 8)

This uncommon group comprises deep-brown titanbiotite in approximately equal proportion to interstitial potassic albite.

Chlorite occurs as an accessory mineral. Many of the rocks described above contain minor amounts of iron pyrites (FeS_2) and titanomagnetite. Apatite occurs as an accessory in some inclusions.

The first two Types could be broadly classed as 'alkali-pyroxenites', and are comparable with many similar occurrences in alkali-basaltic rocks described by various authors (c.f. Dawson, 1973). Due to their friable nature the nodules are subrounded in outline with a maximum size of about 6cms. Some of the megacrysts within the tuff may in fact be xenocrysts from the breakdown of the nodules though this cannot be verified by field observation.

The megacrysts are of three types (Plates 9 and 10). The first is a deep green augite occurring in conchoidally fractured, glassy fragments, often rounded and up to 1.5cms in size. This pyroxene exhibits no crystal structure, and cleavage is not seen in thin section. It is substantially less calcic and more magnesian than pyroxenes from the nodules. A darker green augite of similar chemistry, though generally more calcic than the glassy megacrysts, is found. This variety displays normal pyroxene structure and cleavage. The second megacryst type is garnet, of two varieties. One is a deep-red, clear, glassy pyrope-rich garnet, the other is a pale-pink variety. The former can be found up to 1.5cms in size and has never been found in any nodule. The latter garnet is thought to be a detrital mineral from the breakdown of garnetiferous sandstones of Carboniferous age such as those found in the sediment raft in the Elie Harbour vent.

Cloudy, reddish-brown anorthoclase megacrysts up to 1cm in size

are found both in the tuff and in a dyke east of the lighthouse. This basanitic dyke cuts the tuff, wedging out to the seaward side of the vent. It is marginally composed of tuffaceous material, and is highly weathered. The pseudomorphed remains of olivine phenocrysts together with fresh augites lie in a cloudy, isotropic base, possibly of analcime, containing scattered titanomagnetite. As noted, the dyke contains rare anorthoclase megacrysts and small amphibole-bearing inclusions.

Amphibole also occurs as discrete, often euhedral crystals in the tuff. It is of similar chemistry to the kaersutite from the nodules and may be xenocrystal in origin.

b) Kincraig Hill vent.

Clastic deposits in the Kincraig Hill vent closely resemble those at Elie Ness, being largely composed of basaltic and sedimentary blocks, with occasional fragments of coal and plant remains. As previously noted the central part of this well dissected vent contains a large columnar boss of basaltic material thought to represent a shallow inverted cone.

As at Elie Ness the majority of the basaltic blocks are analcimic-basalts or basanites (ne = 3-11%) and are of similar mineralogy. The central plug basalt has fresh olivine phenocrysts zoning outwards from Fo_{85-76}. Glomeroporphyritic aggregates of augite are present in this analcimic-basalt.

Pyroxenite nodules are comparatively rare in the tuff at Kincraig, the specimens sampled all being of Elie Types 1 or 2.

c) Coalyard Hill vent.

Tuff of a predominantly sedimentary nature is found to the west of the main basaltic tuff which infills the vent proper. A 1.5m thick inclined basaltic sheet containing a suite of spinel-lherzolite, wehrlite and pyroxenite inclusions is intruded into the ring-fracture around the western margin of the vent. A smaller horizontal sheet merging into the tuff and containing alkali-pyroxenite inclusions and large, well-formed anorthoclase megacrysts, outcrops to the south-east of this below High-Water Mark.

Samples of basanitic and monchiquitic blocks from the tuff show a more undersaturated mineralogy than the material from Elie Ness or Kincraig (ne = 5-11%). Plagioclase is less common and analcime predominates in the groundmass. No pyroxenite nodules have been discovered in the tuff.

The material composing the horizontal sheet is of similar mineralogy to the sampled blocks, being analcime-rich and very poor in plagioclase. Abundant rounded kaersutite megacrysts are present in the sheet and are invariably rimmed by broad reaction bands of magnetite. Anorthoclase megacrysts are also present, the larger ones being rounded and shattered with titanbiotite developed along the fractures. The largest specimen found is a perfect euhedral twin, 8cms long (Plate 10). An alkali pyroxenite inclusion of Type 1c was found, in which the contacts between the kaersutite and the host-rock show magnetite reaction rims.

The inclined marginal sheet is the main feature of interest at Coalyard Hill. Titanaugite is the main phenocryst phase, and together with plagioclase and titanomagnetite it forms the bulk of the groundmass. Analcime is a subsidiary phase and is present in small enough amounts to place this rock in the analcimic-basalt group. Estimation of the proportion of phenocrystal olivine is confused by the large amounts of xenocrystal material derived from the included lherzolites. Xenocrysts of enstatite from the lherzolites are rimmed by narrow reaction bands thought to be olivine, which in turn display overgrowths of titanaugite. (Plate 11). Diopside xenocrysts from the same source also act as nuclei for titanaugite overgrowths. Spinel xenocrysts generally show marginal alteration to magnetite. Fractures in some of the inclusions have been invaded by the host-liquid and contain titanaugite and a slightly more sodic labradorite than that found in the bulk rock. Small euhedral chrome-spinel crystals also occur in these veins, showing marginal alteration to magnetite (Plate 12).

The majority of the inclusions are accumulated in the lower part of the sheet where they comprise up to 70% of the rock volume, and are surrounded by radiating contraction fractures, generally calcitised, in the host basalt. Chrome-spinel lherzolites are the predominant variety of inclusion and are highly altered, many having little or no fresh olivine present. Their textures are granoblastic, showing signs of partial recrystallisation amongst the olivines which are generally equigranular with triple-point junctions. (Plate 13).

The orthopyroxenes are the largest crystals present showing no signs of recrystallisation. The diopsides show rare spinel exsolution (Plate 14). Little evidence of shearing is seen other than one sample which comprises a 4cm diopside, twisted along its length and surrounded by a mosaic of altered olivine. The spinel is pale-brown and globular in appearance. The inclusions are subrounded to subangular and reach up to 30cms in size.

Rarer inclusions are black clinopyroxenites, composed of salitic augite with uncommon interstitial labradorite, and wehrlites. The latter exhibit cumulate textures with euhedral to subhedral olivine, partially pseudomorphed, enclosed by large crystals of intercumulus augite. No alkali pyroxenites have been found in this sheet.

d) Ruddons Point vent.

A small vent partially covered by sand-dunes contains an analcimic-basalt sheet with sparse inclusions and anorthoclase megacrysts. The sheet (ne = 3%) has phenocrysts of olivine and augite in the usual glassy, analcimic groundmass. Xenocrysts from the spinel-lherzolite inclusions are common. As at Kincraig and Elie Ness glomeroporphyritic 'pyroxenites' are present.

The inclusions found in this sheet are mainly chrome-spinel lherzolites of two textural varieties, the first being similar to the Coalyard Hill inclusions. Large ortho- and clinopyroxenes are enclosed in a matrix of partially recrystallised olivine. In the second variety all the phases are intensely sheared and elongated

with long trails of pale-brown spinel running through the rock. Only rare orthopyroxenes remain unsheared (Plate 15) though they are generally rounded with shattered margins. A certain amount of recrystallisation seems to have taken place, especially amongst the olivines. The inclusions are rarely more than 10cms in size and are sub-angular to rounded.

Gabbroic inclusions also occur in this sheet though less commonly than the lherzolites. They are generally quite fresh and coarse to medium grained, showing a cumulus texture. Large plagioclase laths form the main phase together with euhedral olivines and elongate clinopyroxene. The intercumulus phases are magnetite and (?) analcime (Plate 16) together with a little chlorite. Rare black pyroxenite inclusions are present in this sheet.

Pale-brown, cloudy anorthoclase megacrysts up to 3cms in size are common. They are rounded though often shattered. No other megacryst phases were noted.

e) Elie Harbour Vent and Chapel Ness.

A large raft of tuff-penetrated sediment including the garnetiferous sandstone from which the pale-pink garnets of Elie Ness are thought to be derived occupies the western margin of this small vent. Basanitic blocks up to half a metre in size form the bulk of the clastic material, with the remainder being sedimentary rocks, mainly of Carboniferous age. No nodules or megacrysts have been found in either the tuff or the basanitic blocks at Elie Harbour. The blocks are almost constant in mineralogy and chemistry throughout

the vent, and they represent the most undersaturated rocks in the area studied (ne = 11-18%). Whilst they display the same essential mineralogy as other vent blocks described above, analcime forms up to 35% of the mode. (Plate 17)

At Chapel Ness, 1.5kms to the west of Elie Harbour, a flow of basanite (ne = 16.8%) occurs just above high-water mark. This is chemically and mineralogically almost identical to the blocks from the Elie Harbour vent, and similarly is barren of inclusions or megacrysts.

f) Ardross vent.

The tuff is cut by a metre-wide basanitic dyke containing micaceous inclusions and anorthoclase megacrysts. The dyke material is olivine-phyric with euhedral pseudomorphed olivine phenocrysts. Augite occurs as phenocryst and groundmass components. The glassy analcimic groundmass is severly altered. The micaceous inclusions are unlike any of those previously mentioned and are also highly altered. Dark-brown mica crystals up to 6mms in length lie in a highly altered matrix exhibiting possible olivine and pyroxene pseudomorphs and a glassy or analcime rich indeterminate groundmass. Apatite needles up to 2mms in length occur throughout the inclusion. Plagioclase laths are aligned parallel to the inclusion rim in the host rock.

The anorthoclase megacrysts are rounded, pale-brown to colourless, and clear. They range in size up to about 4cms across and are generally smooth and rounded. The tuff contains basaltic and

sedimentary blocks, though no nodules have been found in it.

g) Kellie Law.

The grass-covered rounded hill of Kellie Law has several small outcrops of basaltic material around its western margin and summit. In a small outcrop near the roadside to the west of the hill a dark-grey, compact analcimic-basalt (ne = 3.6%) contains rare, colourless to greenish sanidine megacrysts up to 2cms in size. The host rock displays similar mineralogy to the coastal basalts, with patchy analcime occurring throughout the matrix. It is not known how this basalt is associated with the Kellie Law vent due to the poor inland exposure.

2.2 Other areas studied.

a) East Lothian--Kidlaw Quarry.

A compact, jointed body of analcime-basanite is associated with poorly exposed tuffs in the small roadside quarry near Kidlaw. The basanite contains sparse inclusions of spinel-lherzolite, generally highly altered and often noticeable only by eroded cavities on the rock surface. The inclusions are subangular and up to 8cms in size. Texturally they closely resemble the unsheared granoblastic types from Fife and contain a dark-green to pale-brown chrome-spinel. The host rock shows a characteristic platy fracture due to the large (up to 3mms) crystals of analcime in the groundmass. It is a scantily porphyritic rock with only occasional olivine and augite phenocrysts. Magnetite is present in great quantity in the

groundmass with augite, plagioclase, analcime, biotite and a little orthoclase. This rock type has unusual features, such as the large poikilitic analcimes in the groundmass, the presence of biotite in some quantity and patches free of augite and magnetite, usually containing radiating feldspar crystals. These features led Bailey (1910) to classify it in a group apart from the other East Lothian intrusions.

b) East Lothian--Fidra and Weak Law.

The island of Fidra is composed of a compact basanite sill (ne = 14.6) showing columnar jointing, particularly on the southern margin. The sill contains scarce inclusions of spinel-lherzolite and spinel-wehrlite, together with rare megacrysts of anorthoclase. The basanite is superficially similar to that of Kidlaw in both hand-specimen and section. It exhibits the same platy fracture, with analcime composing much of the groundmass. Microphenocrysts of olivine and larger, zoned titanaugite phenocrysts lie in a fine-grained groundmass of augite, plagioclase and titano-magnetite, with large poikilitic analcimes making up the matrix. No mica is present in this rock.

The inclusions are subangular and up to 5cms in size, being generally quite fresh. The wehrlite inclusions are similar to those noted from Coalyard Hill, with euhedral pseudomorphed olivines lying poikilitically enclosed by clinopyroxene. The Fidra wehrlites contain scattered grains of chrome-spinel in the augite (Plate 18). The majority of the inclusions are chrome-spinel lherzolites, some

verging on more harzburgitic compositions. Sheared and partially recrystallised textures are common, the olivine often showing strain-banding. Unlike lherzolite inclusions from previously mentioned localities the Fidra specimens are more or less equigramular with no size preference for the orthopyroxenes. Narrow magnetite reaction rims are sometimes found around the inclusions in the host basanite.

Inclusions of spinel-wehrlite have been reported from the Lamb in the East Lothian Memoir. At Weak Law, on the mainland west of Fidra, a poorly exposed tuff-filled vent associated with trachytic and olivine-basalt flows contains scattered spinel-bearing blocks first noted by Duncan (1973). These occur in predominantly sediment-bearing tuff and are in an extreme state of calcitisation, pale-brown spinel being the only fresh primary mineral. The texture of the calcitised matrix suggests olivine to have been the major component, the presence of pyroxene being indefinite. These fragments are rounded, pale-green and friable, being up to 15cms in size.

c) Caithness—Duncansby Ness.

This isolated vent is well exposed at low tide and exhibits a clear-cut margin with the Old Red Sandstone country-rock to the western edge. The tuff penetrates deep fractures in the sandstone, and blocks of country-rock are common in both the tuff and the associated monchiquitic body. A wide variety of igneous and sedimentary fragments are included in the vent. (Plate 19)

Two phases of tuff are distinguishable, the first being a dark

grey basaltic variety coating the ultrabasic fragments and some of the larger sandstone blocks, the second being a pale-brown, sandy type forming the mass of the tuff body and containing much sedimentary material, including shales mudstones, sandstones and quartz grains. To the west of the vent a monchiquitic (ne = 8%) basalt rich in sandstone fragments, merges downwards into the tuff. The rock is porphyritic with euhedral pseudomorphed olivines and zoned titanaugite phenocrysts in a very fine-grained indeterminate groundmass containing small augite laths and scanty magnetite microphenocrysts, plagioclase being absent. Patchy areas of anorthoclase and zeolite are found in the matrix with occasional small brown biotites. Rounded quartz and twinned feldspar grains, presumed to be xenocrysts from the arkosic ORS xenoliths occur in the groundmass. The quartz is invariably severely corroded and surrounded by a fine-grained reaction corona. The feldspars (oligoclase and anorthoclase/sanidine) display no such reaction margins and appear to have been stable in the liquid. (Plate 20)

Highly altered fragments of chrome-spinel bearing rock, up to 10cms in size and generally well-rounded, occur in both the tuff and the monchiquitic body. Many of these fragments are wehrlitic, though spinel-lherzolites are also present. Their textures show no evidence of shearing and are generally equigranular with well-developed triple-point junctions indicating recrystallisation. Clinopyroxenes around the margins of the inclusions in the monchiquite often display overgrowths of titanaugite into the host rock. One of the inclusions was found to contain phlogopite.

A uniform group of compact, black, coarse-grained spinel-clinopyroxenites (Plate 19) form the bulk of the ultrabasic material in the tuff. They vary in size from a few millimetres to 15cms across and are subrounded. One euhedral crystal of this salitic augite was found, measuring 7cms by 4cms in basal section, and containing deep green chrome-free spinel (Plate 21). These fragments are characteristically very coarse-grained, many of the largest specimens being composed of only five or six large augite crystals with small granular crystals along grain-boundaries. The spinel forms anhedral, often angular blebs and tends to clump together or trail out on, or close to, grain boundaries, cleavage traces or other lines of weakness in the pyroxene. Some of these spinels are up to 2cms across. Chloritic areas in some nodules may indicate that olivine has been present. The texture of these pyroxenites indicates that spinel may have been exsolved from the pyroxene and have been mobile enough to accumulate along lines of weakness. Some specimens contain a pale-brown amphibole as an alteration of the augite.

Small accumulations of a green amphibole, and some of kaersutite, also occur rarely in the tuff, and fragments of tonalite or diorite are also noted. The latter contain a variety of plagioclase compositions from oligoclase to basic labradorite with some interstitial feldspathoidal material and primary quartz and biotite.

d) Bute—Kilchattan (Hawks Nib).

Smellie (1915) first described this minor intrusion as an alkali-olivine basalt containing a host of inclusion types from anorthosites through gabbros to dunites and olivine-pyroxenites. The sheet has a

steep southerly dip, the bulk of the inclusions having sunk to the base.

The host-rock is an analcimic-basalt containing a substantial amount of analcime in the groundmass. Small cavities in the rock are zeolite-filled. Euhedral olivine and zoned augite phenocrysts in a groundmass of titanaugite, tianomagnetite and plagioclase give the rock a similar appearance to many of the Fife basalts. Xenocrystal olivine, usually much fresher and more transparent than the phenocrysts, and xenocrysts of pyroxene are abundant. Some orthopyroxenes show titanaugite overgrowths. Occasional glomero-porphyritic clinopyroxene aggregates are found.

The inclusions sampled were mainly wehrlites, with euhedral to subhedral olivine poikilitically enclosed by a pale-brown augite. Texturally these are similar to those from Fidra and Coalyard Hill. The majority of the inclusions are subangular and range in size from 2 to 10cms.

Harzburgites showing a marked degree of recrystallisation are also common. These are spinel-free with scattered magnetite and sulphide developed. A massive black clinopyroxene inclusion, consisting of one 5cm crystal with a margin of smaller augites, one of which showed orthopyroxene exsolution lamellae (Plate 22) was sampled. Some highly altered inclusions proved to contain only minor amounts of a fresh pale-brown spinel, though the calcitised matrix texturally resembled lherzolite. There is little evidence of material of sedimentary origin in this sheet, though one small pebble of white quartzite was found.

e) Derbyshire--Calton Hill.

The analcimic-basalt of Calton Hill and the spinel-lherzolite inclusions found in it have been described in detail by Hamad (1963). A small collection of material has been made for comparative geochemical purposes.

The host-rock is a typical fine-grained analcimic-basalt (ne = 1.9%) displaying a similar texture and mineralogy to the examples from Fife. The only inclusions sampled from this locality were spinel-lherzolites which are generally quite fresh and unsheared. Hamad considered these inclusions to be genetically unrelated to their host basalt and to be fragments of a deep-seated peridotite body.

Plate 1.

Monchiquite block, Elie Ness vent, showing phenocrysts of augite and microphenocrysts of kaersutite, titanaugite and titanomagnetite. P.P. light, x 20 (Q3-20)

Plate 2.

Elie Type 1(a) nodule (Q2-5) showing three large poikilitic kaersutite crystals enclosing subhedral olivine and pyroxene. Unpolarised light. Approx. x 2.5

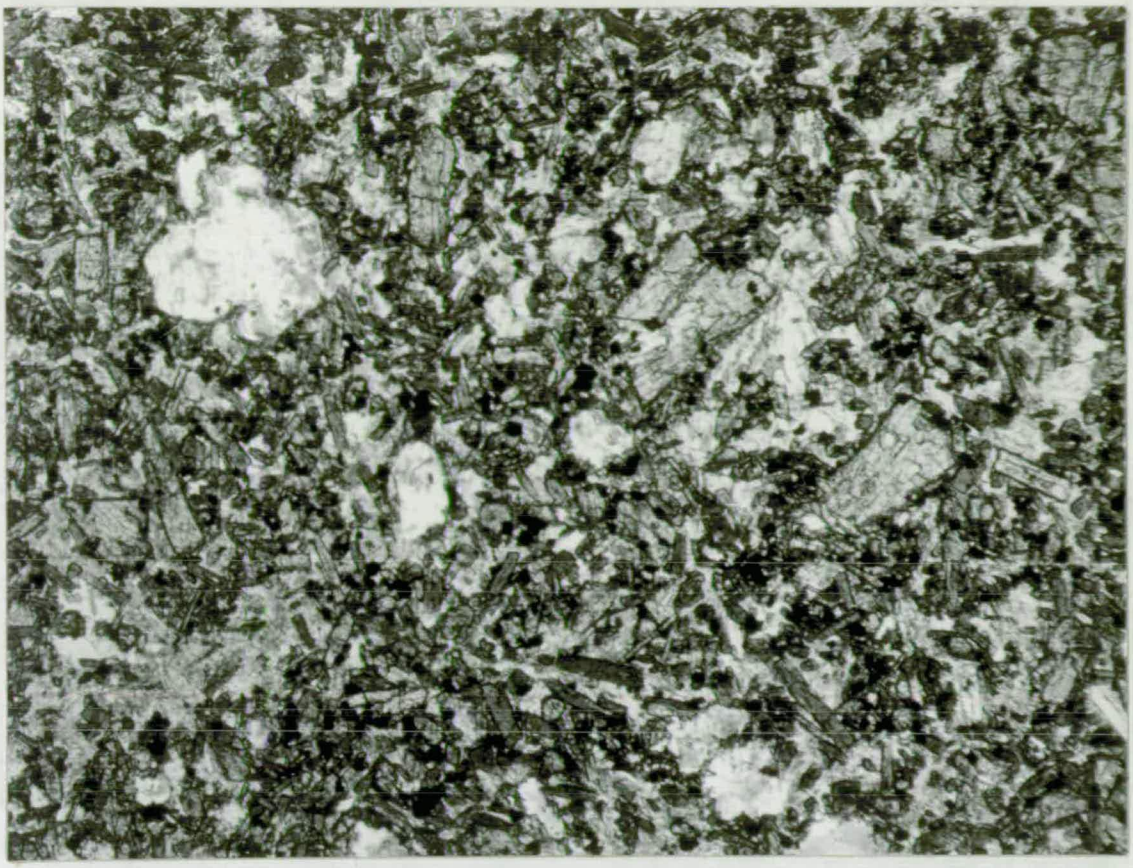

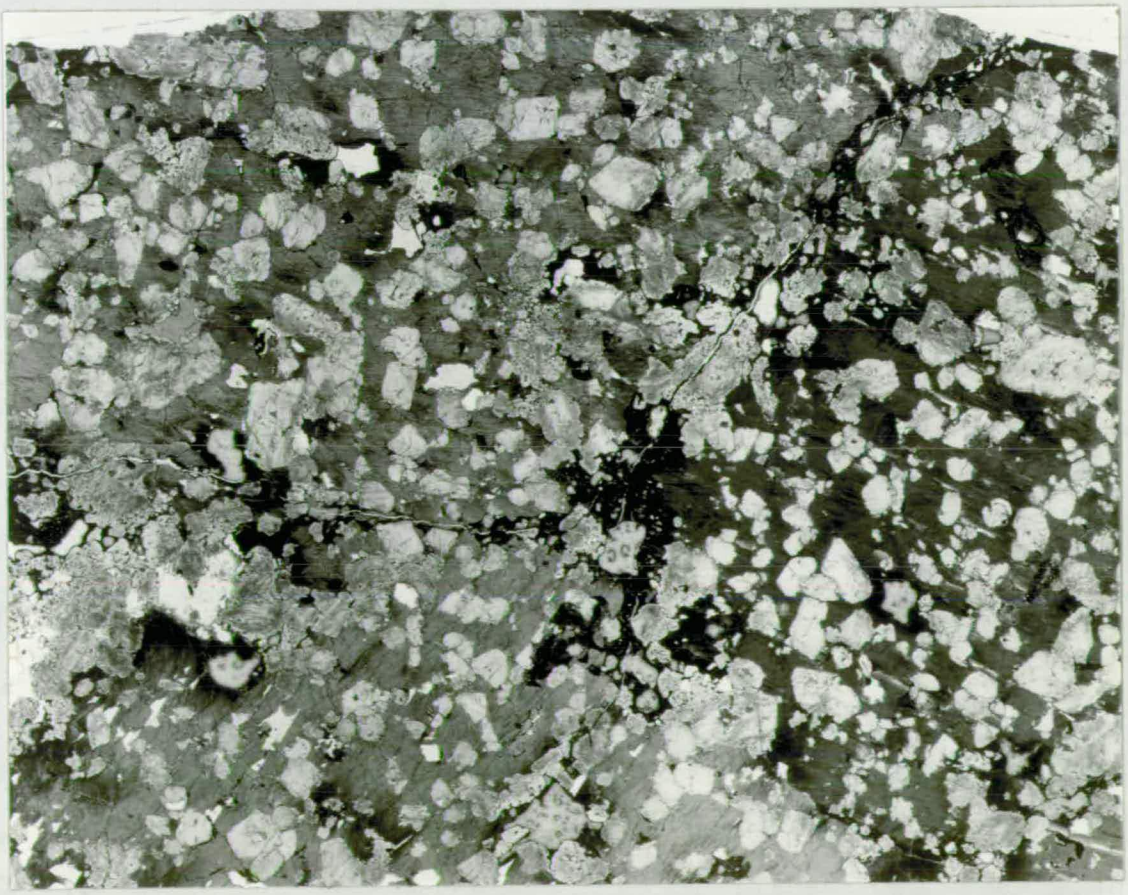

Plate 3.

Elie Type 1(b) nodule (N2) showing large subhedral olivine crystals enclosed by an almost equigranular mosaic of kaersutite and augite.
Unpolarised light. Approx. x 5

Plate 4.

Elie Type 1(c) nodule (N7) composed mainly of augite with rare olivine. Kaersutite is seen as alteration of the augite and as large primary crystals, sparsely poikilitic (centre).
Unpolarised light. Approx. x 2.5

Plate 5.

Elie Type 2 nodule (Q3-16). Dark kaersutite encloses areas of altered and poorly developed augite containing plagioclase and rare olivine.
Unpolarised light. Approx. x 2.5

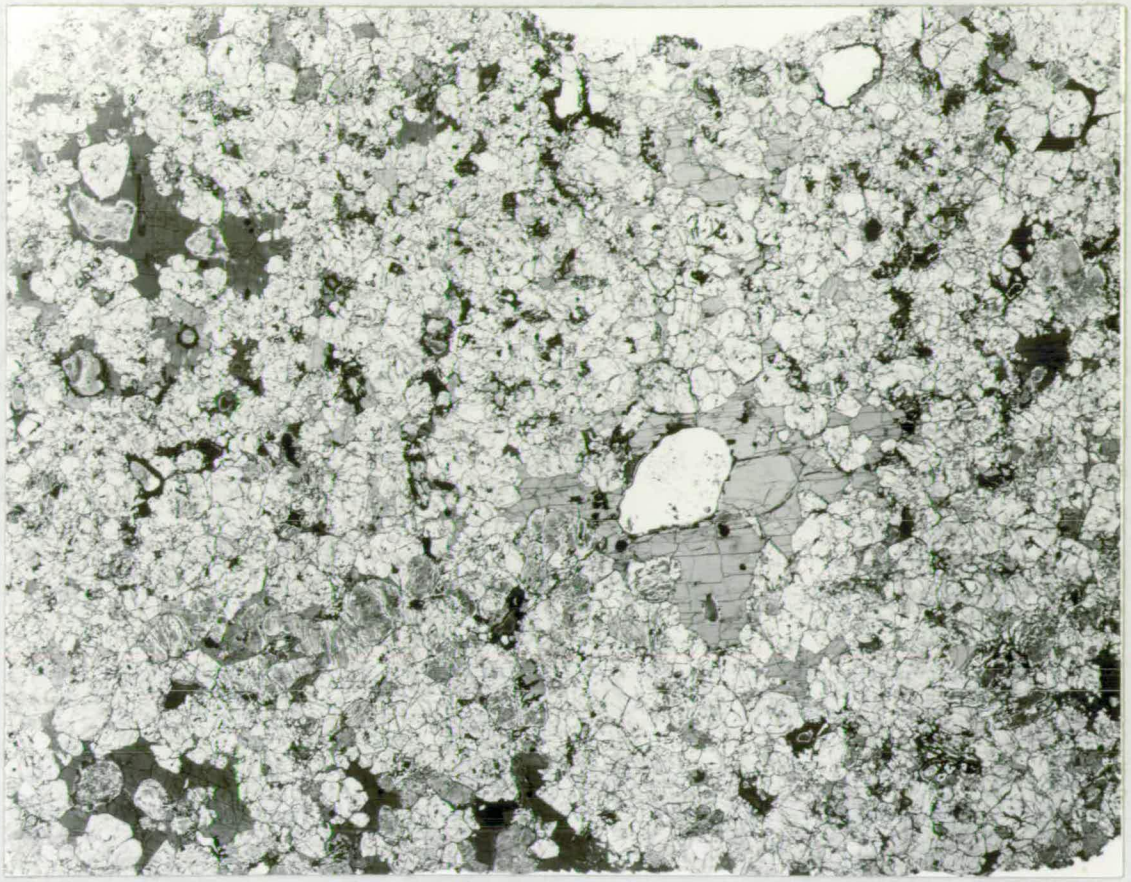

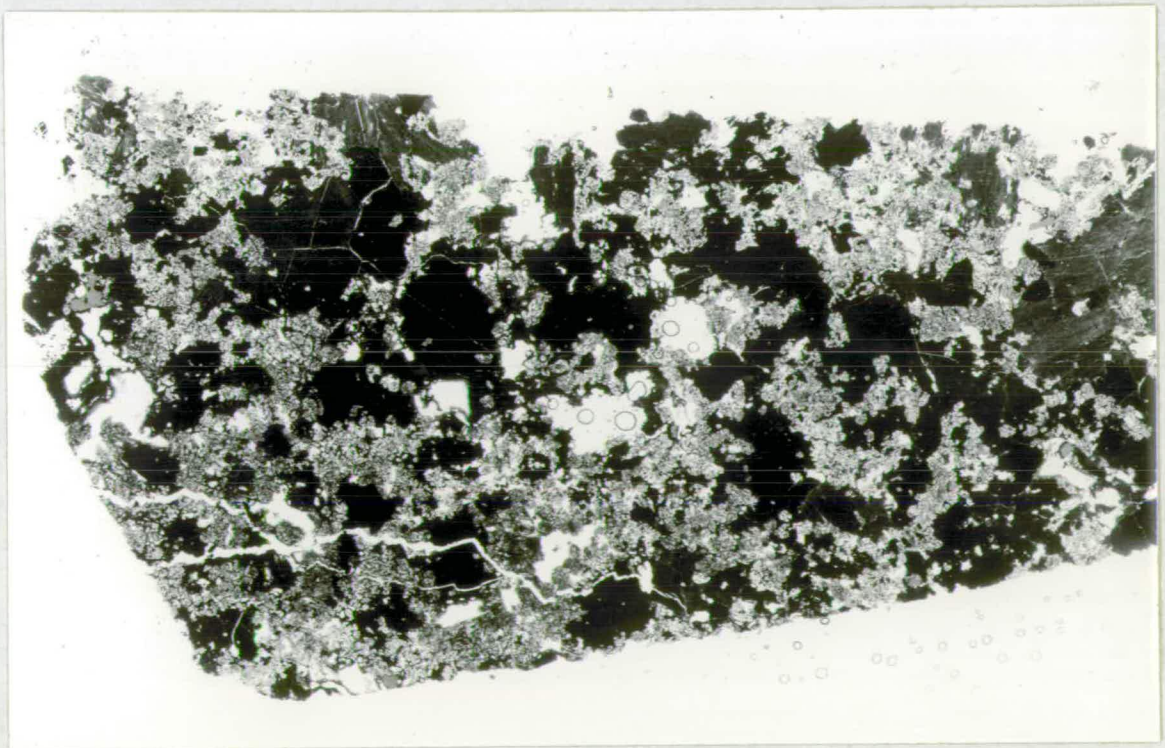

Plate 6.

Elie Type 3 nodule (Q2-6). Biotite-pyroxenite with augite showing signs of marginal corrosion. Unpolarised light. Approx. x 2.5

Plate 8.

Elie Type 5 nodule (Q2-27). Well developed titan-biotite crystals with interstitial albite. Unpolarised light. Approx. x 2.5

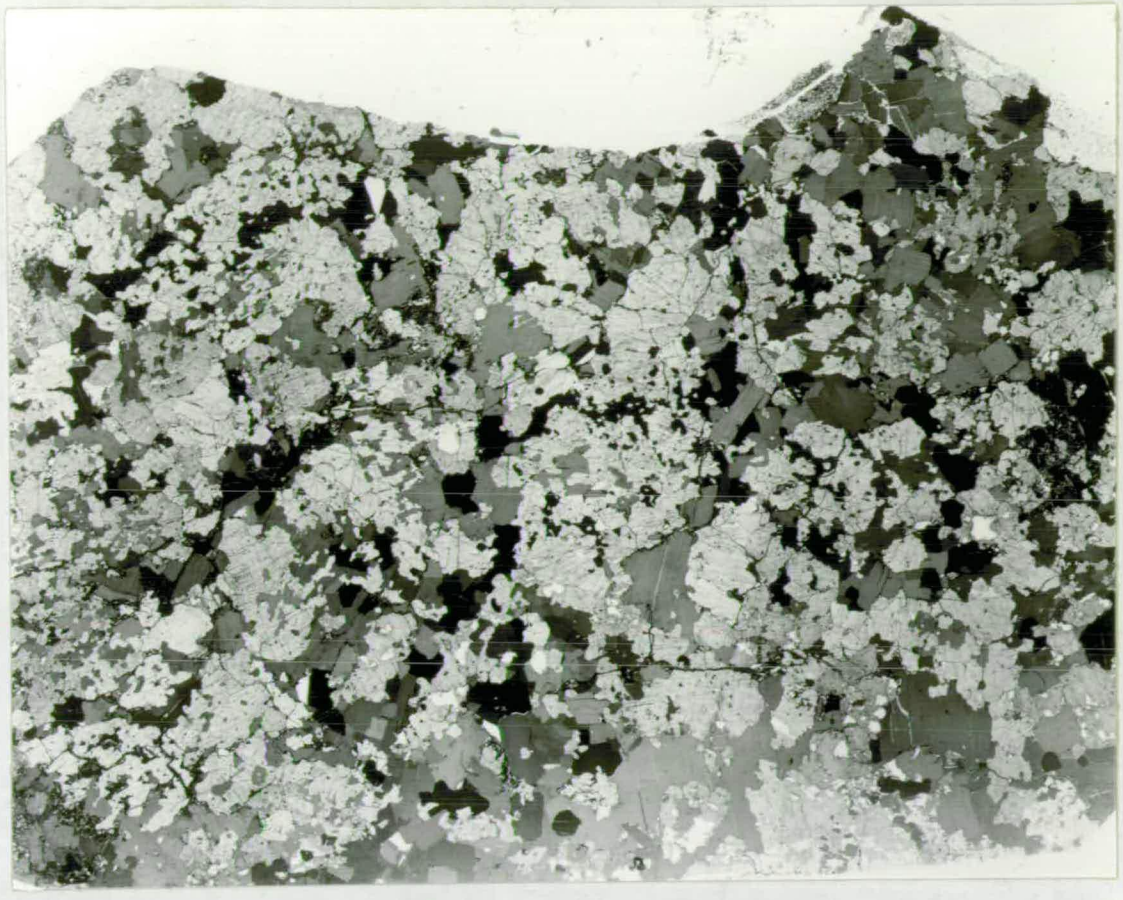

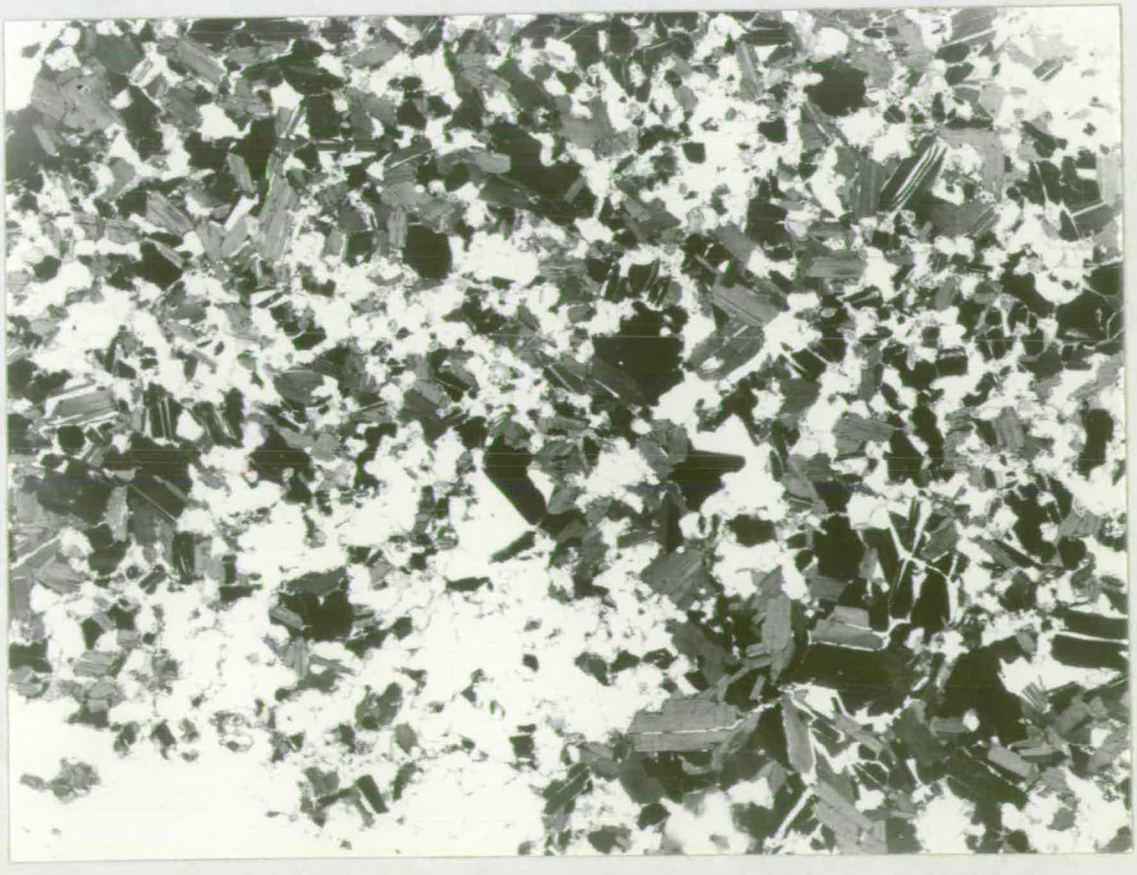

Plate 7.

Elie Type 4 nodule (Q4-13). Clumps and aggregates of biotite enclosed in microcrystalline sodic-amphibole and albite (transparent).
Unpolarised light. Approx. x 5

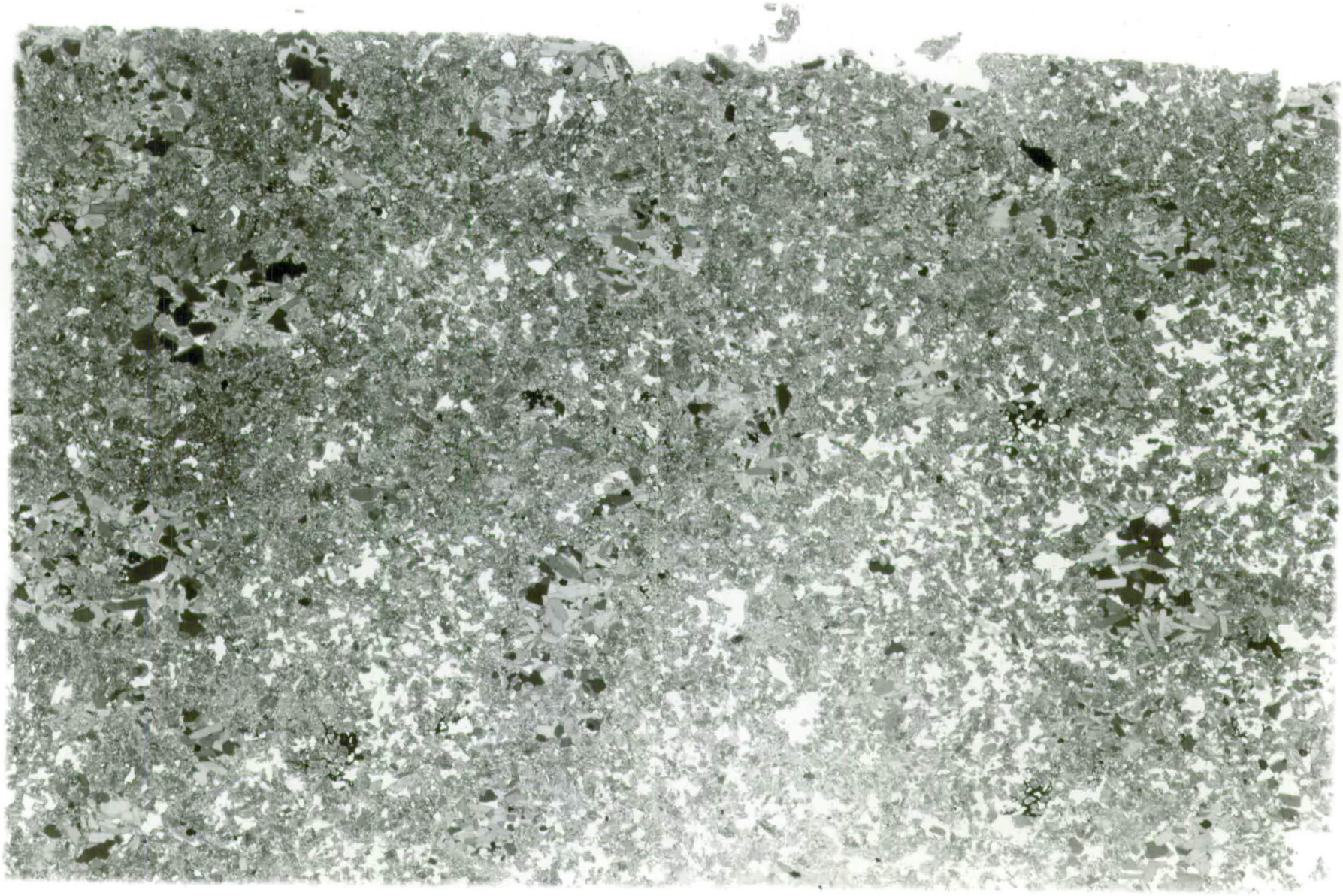

Plate 9.

High-pressure megacrysts from the Elie Ness tuff. Left- pyrope garnet. Right- glassy sub-calcic augites. x 2.5

Plate 11.

Orthopyroxene xenocryst from lherzolite inclusion, Coalyard Hill sheet. The enstatite displays a granular reaction corona with the host basalt, most probably of olivine, which is in turn rimmed by an overgrowth of titanaugite.
X polars. x80

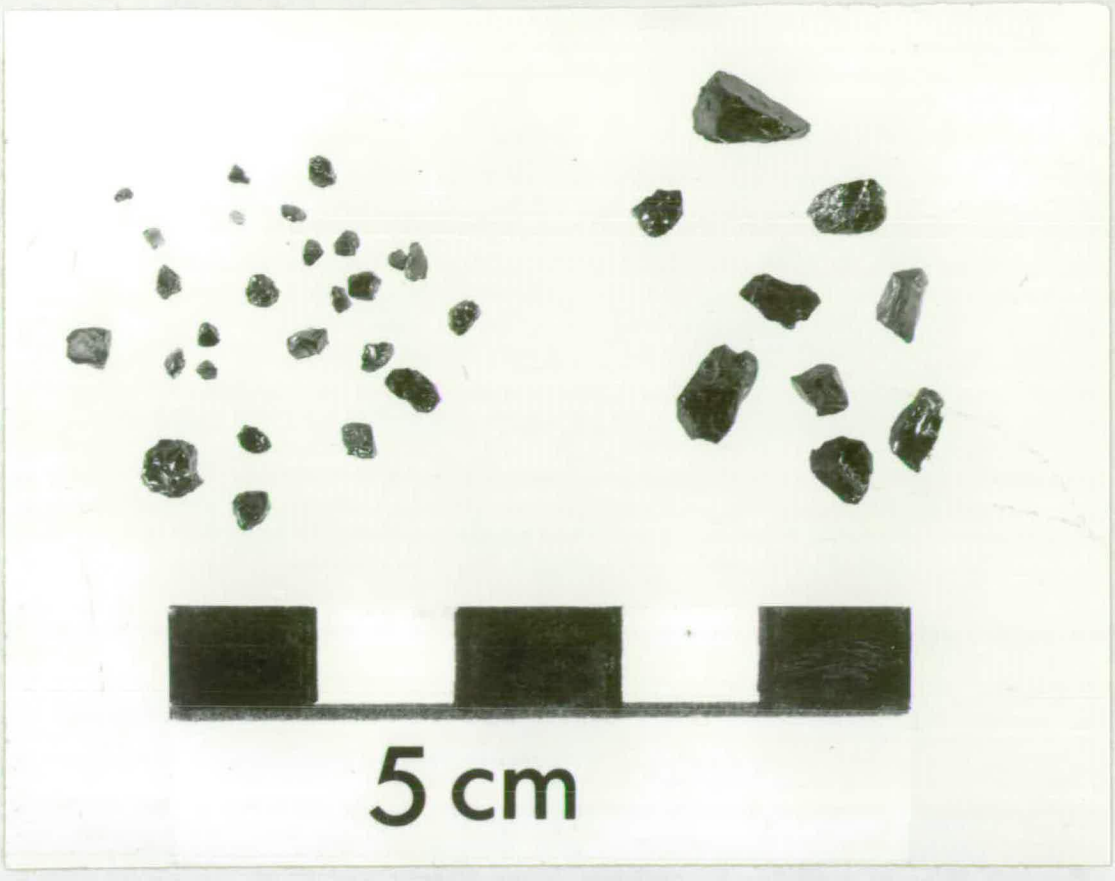
5 cm

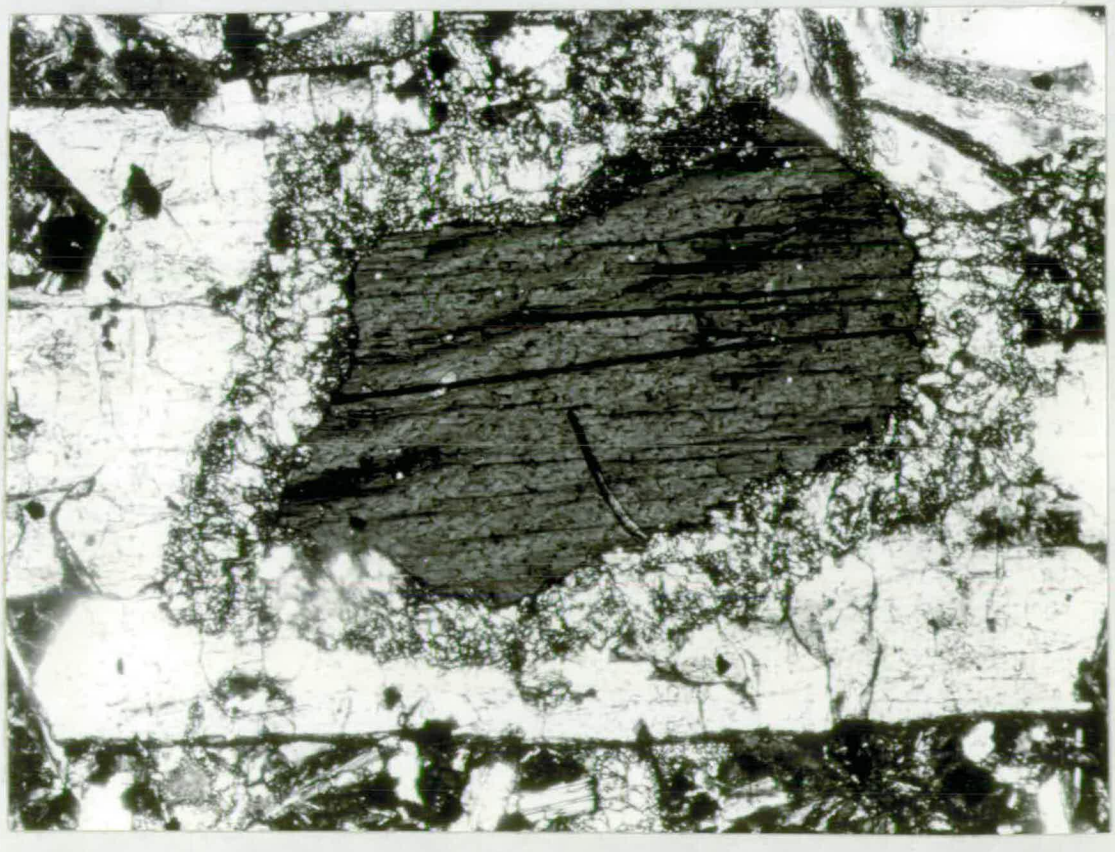

Plate 10.

Elie-type nodules (top) and euhedral, twinned anorthoclase megacryst from Coalyard Hill monchiquitic sheet (bottom).


5 cm

Plate 12.

Euhedral spinel crystal in quench vein within lherzolite inclusion from Coalyard Hill. Note marginal alteration to magnetite. The black spots in the centre of the crystal are burn-marks from microprobe analysis. (P14-A).
P.P light, x200

Plate 13.

Calcitised and serpentinised lherzolite inclusions (CH-7) from Coalyard Hill. Spinel is dark, the larger crystals being enstatite. Note granoblastic texture in the recrystallised olivines.
Approx x 2.5, unpolarised light.

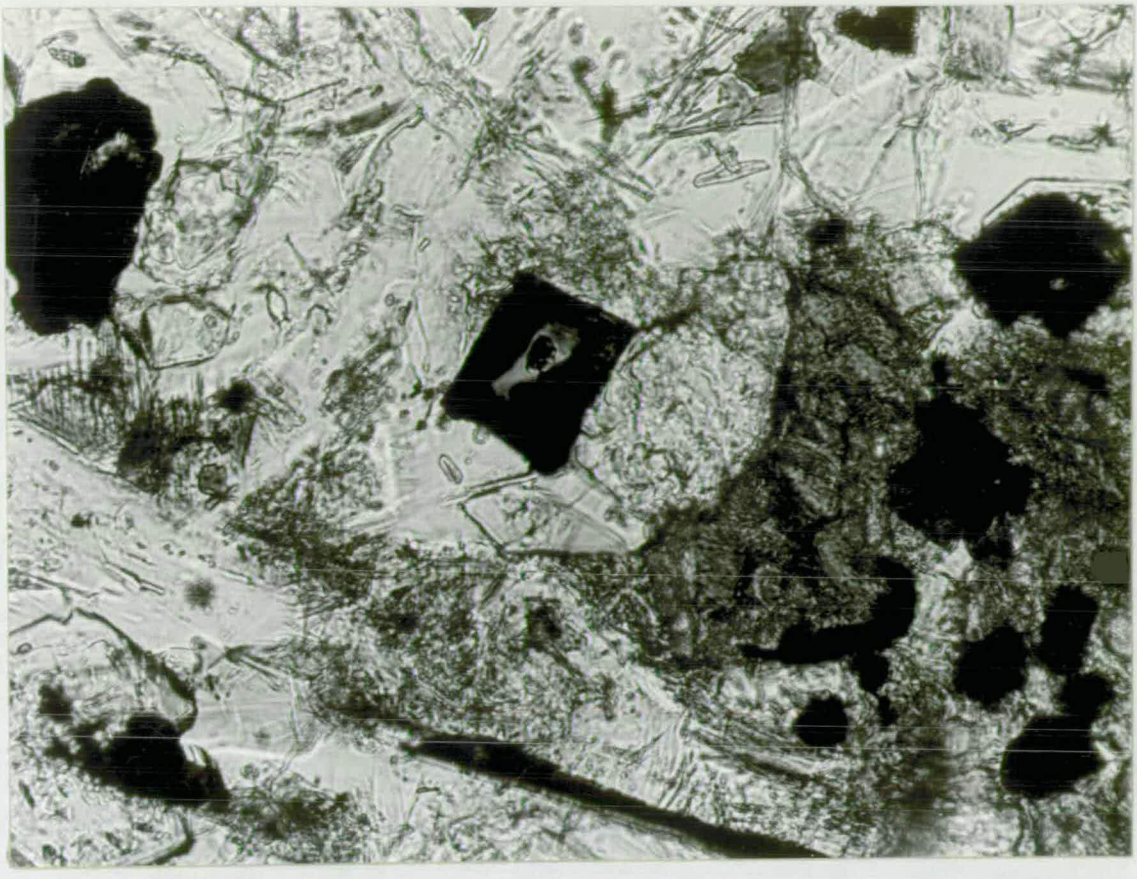

Plate 14.

Spinel exsolution lamellae in diopside from Coalyard Hill lherzolite inclusion (P14-A). Diagonal bands across the picture are strain bands in the pyroxene.
X polars, x 80

Plate 16.

Gabbro inclusion, Ruddons Point.
Approx. x 2.5, unpolarised light.

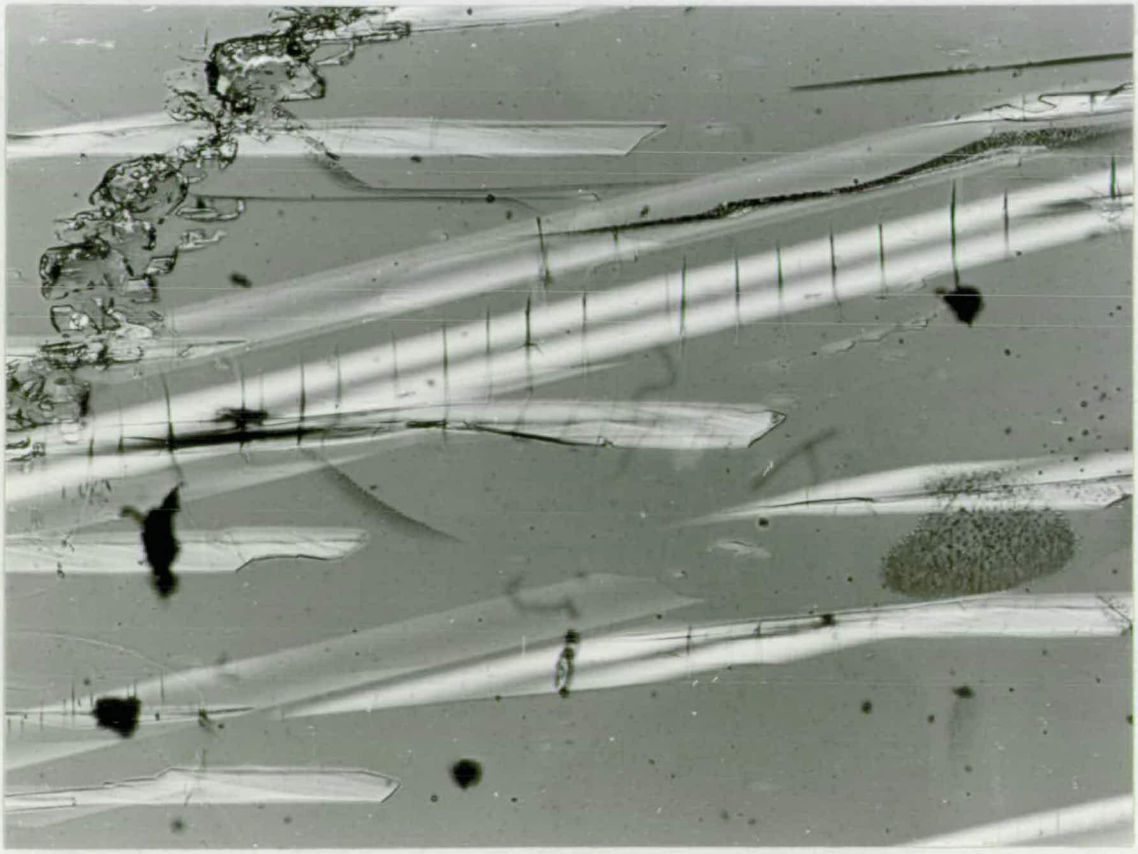

Plate 15.

Sheared and partially recrystallised lherzolite inclusion (E-1) from Ruddons Point. Note extended trails of spinel (black) and rare, large orthopyroxene crystals.
Unpolarised light, approx. x 5

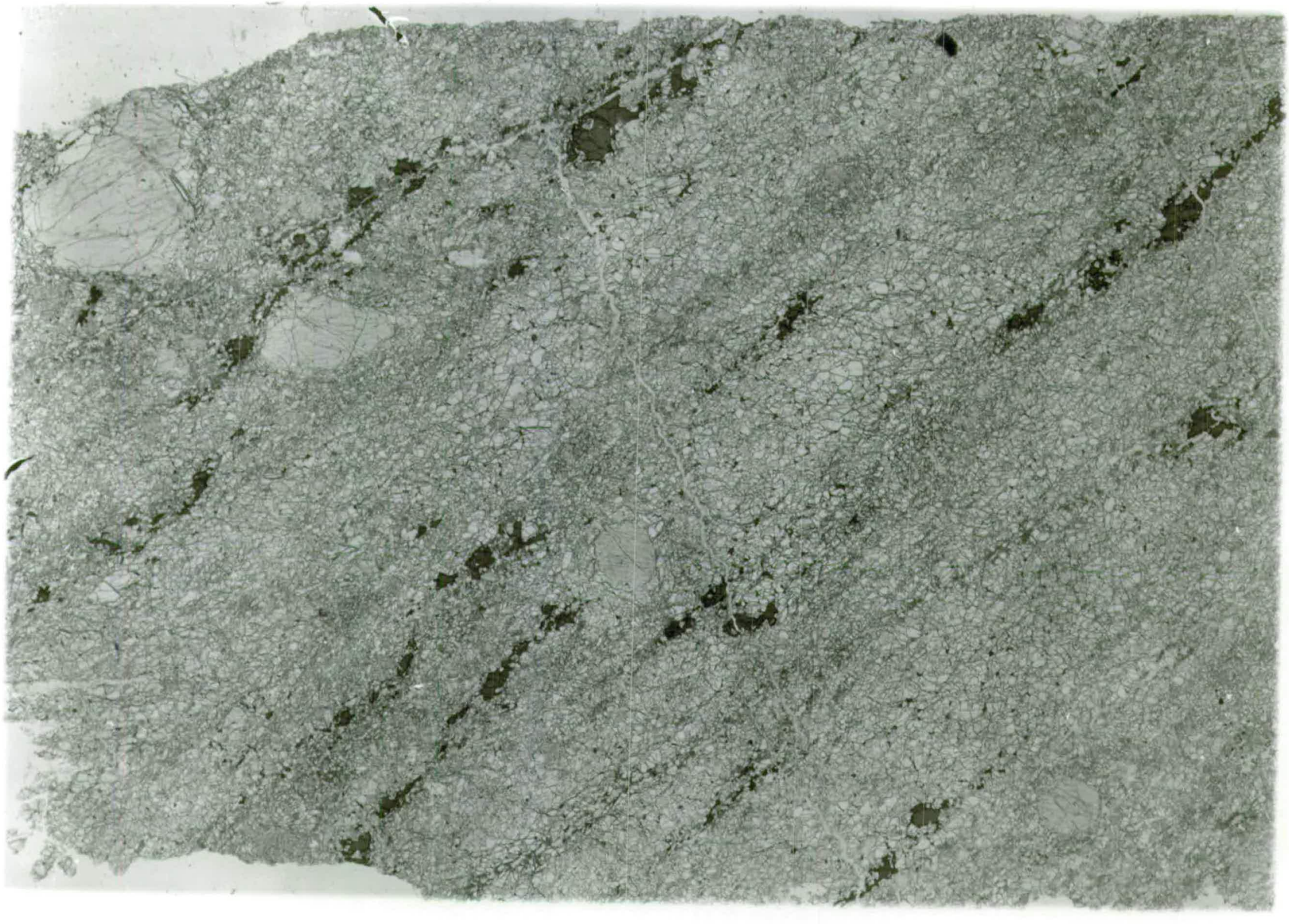

Plate 17.

Basanite block, Elie Harbour vent, showing pseudomorphed olivine phenocrysts (top and bottom left) and zoned titanaugite phenocrysts (right) in analcime-rich base.
P.P light, x 20

Plate 18.

Wehrlite inclusion, Fidra island. Pseudomorphed subhedral olivines (dark) enclosed by interlocking augite grains. Smaller opaque grains are chrome-spinel.
Unpolarised light, approx. x 2.5

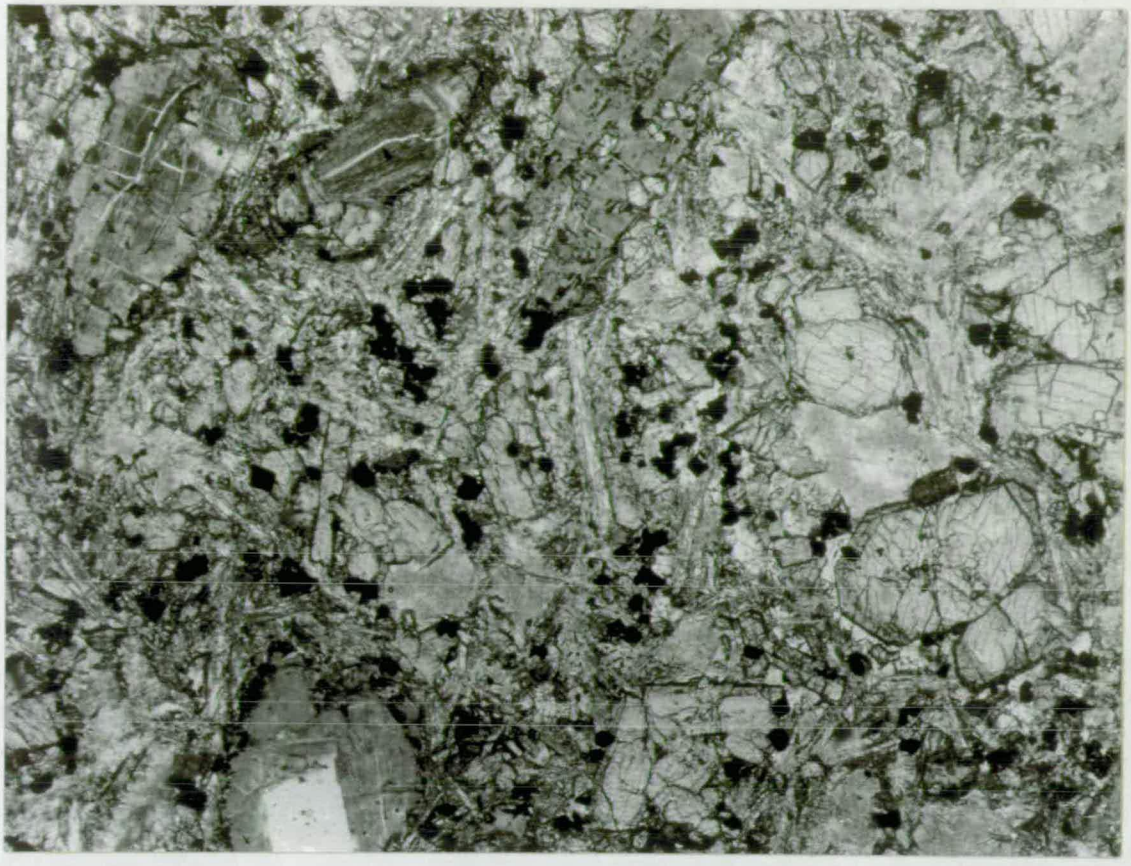

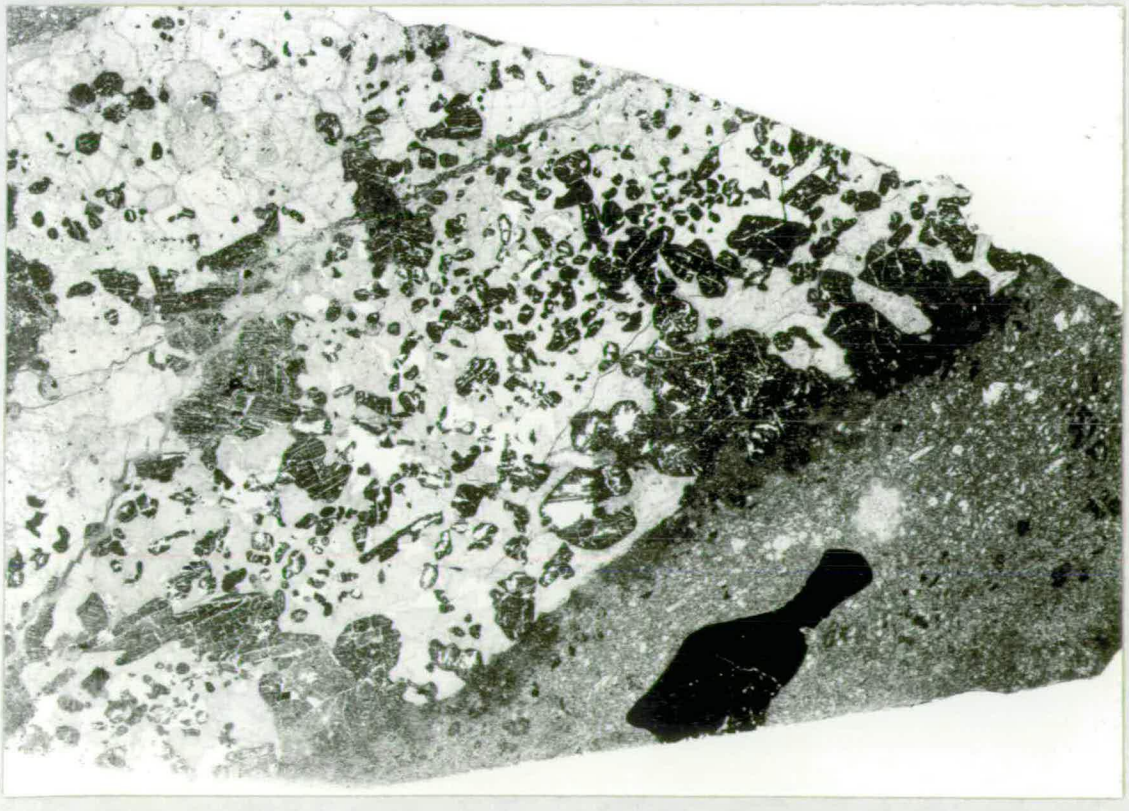

Plate 19.

Nodules from the Duncansby Ness vent. Top left -- highly carbonated ?lherzolite inclusion, showing only fresh spinel. Top right - spinel clinopyroxenite nodule (dark spinel) and similar nodule (bottom) showing contact with tuff, and darker, more basic, tuff rim (upper centre of section).


5 cm

Plate 20.

Alkali feldspar xenocryst in Duncansby Ness monchiquite, thought to be derived from the Old Red Sandstone. (DH-24)
X polars, x 200

Plate 22.

Orthopyroxene exsolution lamellae in augite from Bute clinopyroxenite inclusion (P-29).
X polars, x 80

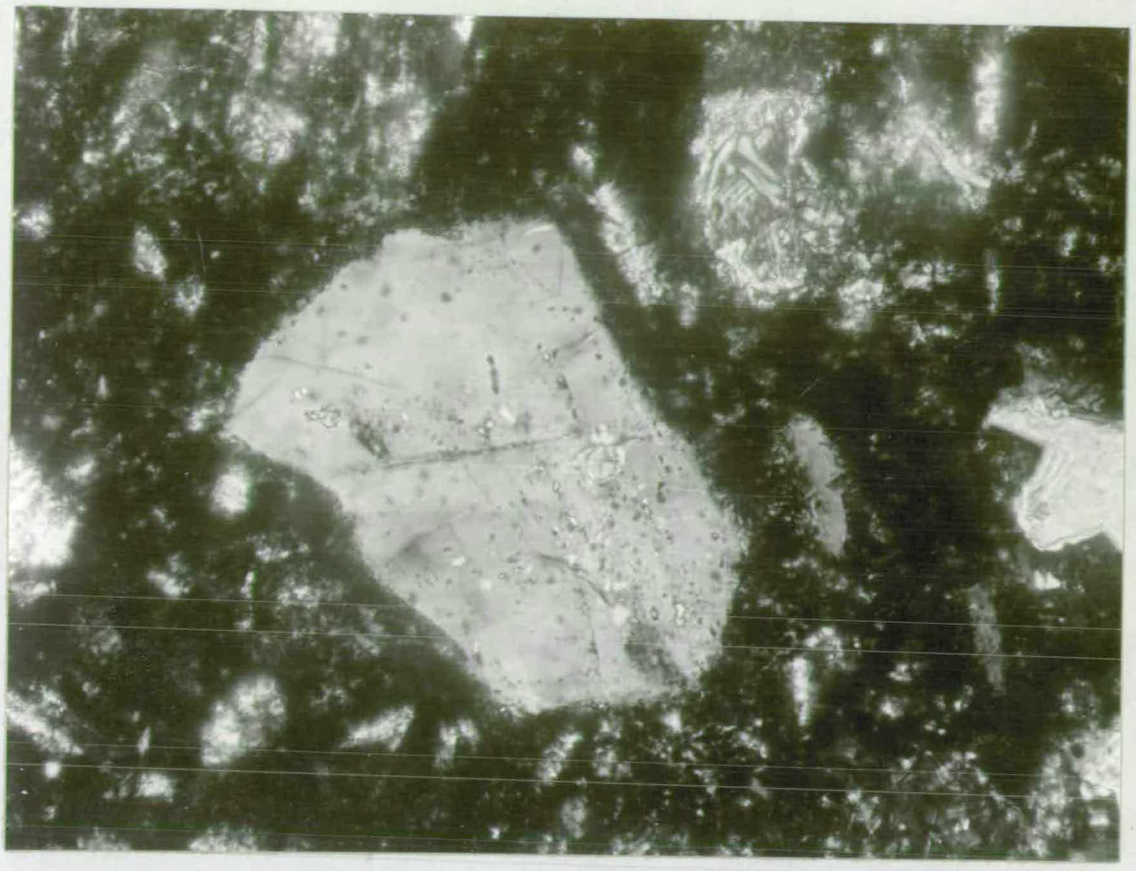

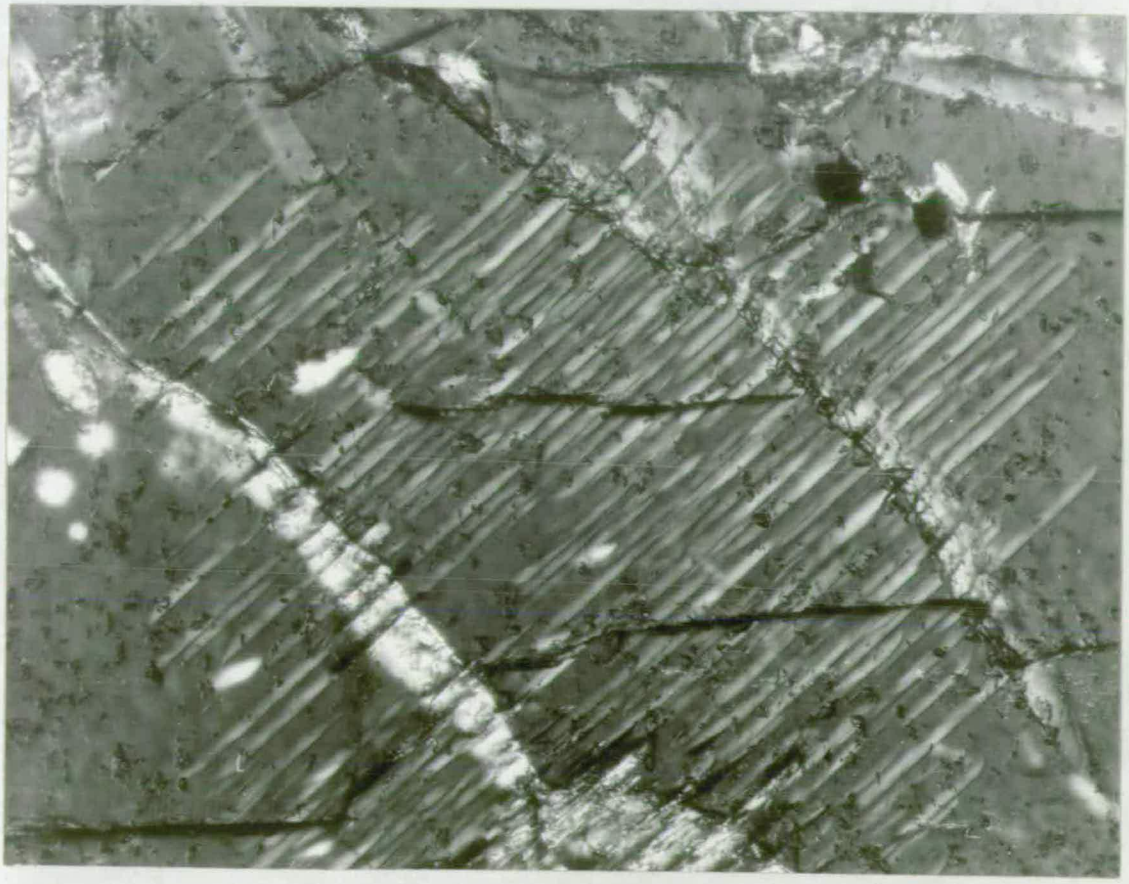

Plate 21.

Complete basal section of augite crystal occuring as discrete spinel-clinopyroxenite nodule in Duncansby Ness tuff, showing pleonaste spinel, thought to be exsolved from the augite.
Unpolarised light. Actual size 8x4 cms.

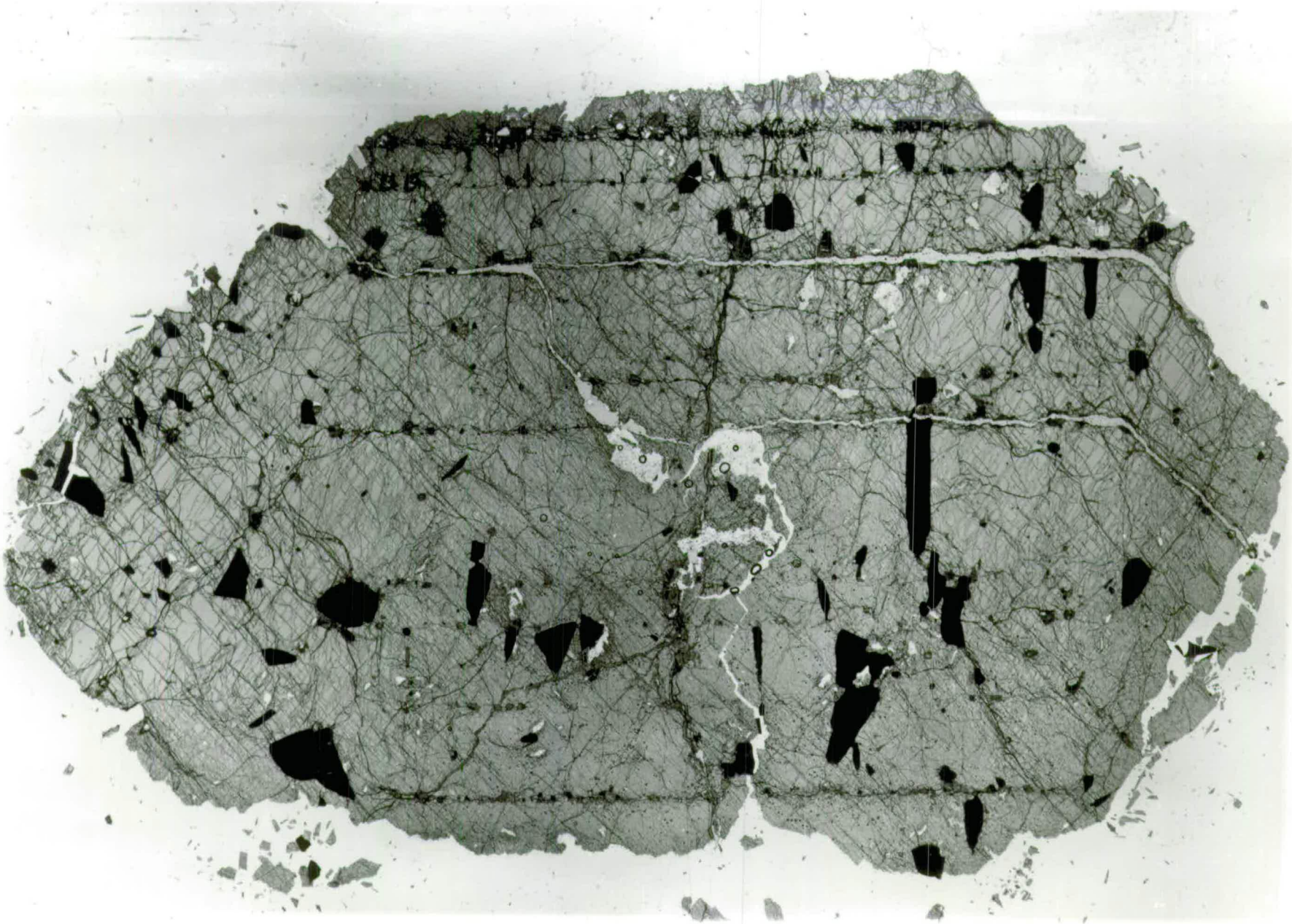

CHAPTER THREE

Whole-rock geochemistry.

Preliminary note on analyses

The problem of deeply weathered material has been discussed previously. When choosing material for analysis the problem is more acute than in straightforward petrographic examination, as extreme oxidation of a sample radically affects its normative components and leaching of some elements can lead to analyses which by no means reflect the original chemistry of the unaltered rock. The freshest obtainable material has been used wherever possible, but in many cases quite severely altered specimens are the only material available, especially when dealing with rock-types which are comparatively rare and only occur as isolated small blocks within tuff. These are usually weathered through, and similarly small ultrabasic fragments are often calcitised as well as having undergone various degrees of alteration.

A further problem exists when analysing samples rich in inclusions and disseminated xenocrysts. Attempts to remove this material prior to analysis can only meet with a certain amount of success as the finest grains cannot be extracted which inevitably leads to erroneous results. It was decided, however, that in many cases an analysis was essential, but the above qualifications on their accuracy should be borne in mind.

Methods of analysis.

Details of analytical technique, together with error estimates, are given in Appendix 2. Whole-rock analysis for major and trace-elements was performed by X-ray fluorescence on compressed rock-powder discs. Ferrous iron was determined wet-chemically, as were several sodium analyses as a check on the XRF method. Since it was not intended to perform complete analysis, water and carbon-dioxide were not determined, and their absence is reflected in the analysis totals in Appendix 1. All the analyses, together with their CIPW norms are listed in this appendix.

Note on the calculation of CIPW norms.

Coombs (1963) points out the effect of secondary alteration on the calculated norms of basaltic rocks, particularly the effect of change in the Fe_2O_3/FeO ratio. Increased oxidation tends to increase normative hy at the expense of ol as well as increasing ne. Serpentinisation of olivine also increases hy at the expense of ol and chloritisation of glass decreases di with respect to hy and ol. In order to attain some degree of internal consistency Coombs suggests reducing Fe_2O_3 to some arbitrary value throughout the given series. Since the value of normative nepheline is used to classify the basalts in the present work it was considered advisable to perform such a normalising procedure. An examination of the oxidation ratios of the analysed rocks from Fife shows two clear groupings. The more altered material such as that occurring as blocks within vents has an $Fe_2O_3/FeO+Fe_2O_3$ average of 0.53 with a distribution of $\pm$0.06 (excluding the most extreme members). The

freshest material occurring in some of the intrusions and flows, usually with some fresh olivine, has a mean oxidation ratio of 0.33 with a maximum distribution of $\pm$0.03. These groupings are considered merely to represent degrees of secondary alteration, and no genetic significance is attached to them. For this reason the value of 0.33 has been used as an overall normalised oxidation ratio in calculating the CIPW norms for the Fife rocks. For the other localities where no definite rock series exists, the norms have been calculated on an unstandardised basis. Fig 3-1 illustrates the values for the Fife series. The diagram is a projection from plagioclase on to the plane ne-di-ol in the normative basalt tetrahedron di-ol-ne-qz of Yoder and Tilley (1962). The substantially ne normative nature of the rocks can be seen, and the postulated evolutionary trend has been inserted.

The Fife series.

Note on variation diagrams.

The Fife volcanics are the only rocks studied in this work which form a distinct group and hence lend themselves to any form of variation analysis. How far this grouping can be explained in terms of chemical trends can best be seen in the form of oxide:oxide variation diagrams and ternary oxide plots. Criticism has been levelled at conventional Harker diagrams (e.g. Pearce, 1968) in that they tend to distort chemical trends, but they still provide the simplest method of bulk data presentation. Other methods such as Principle Latent Vector analysis which take all possible oxide:oxide

Fig. 3-1

Normative composition of Fife basalts projected onto the plane Ne-Di-Ol from plagioclase in the system Di-Ol-Ne-Qtz, showing the postulated evolutionary trend.

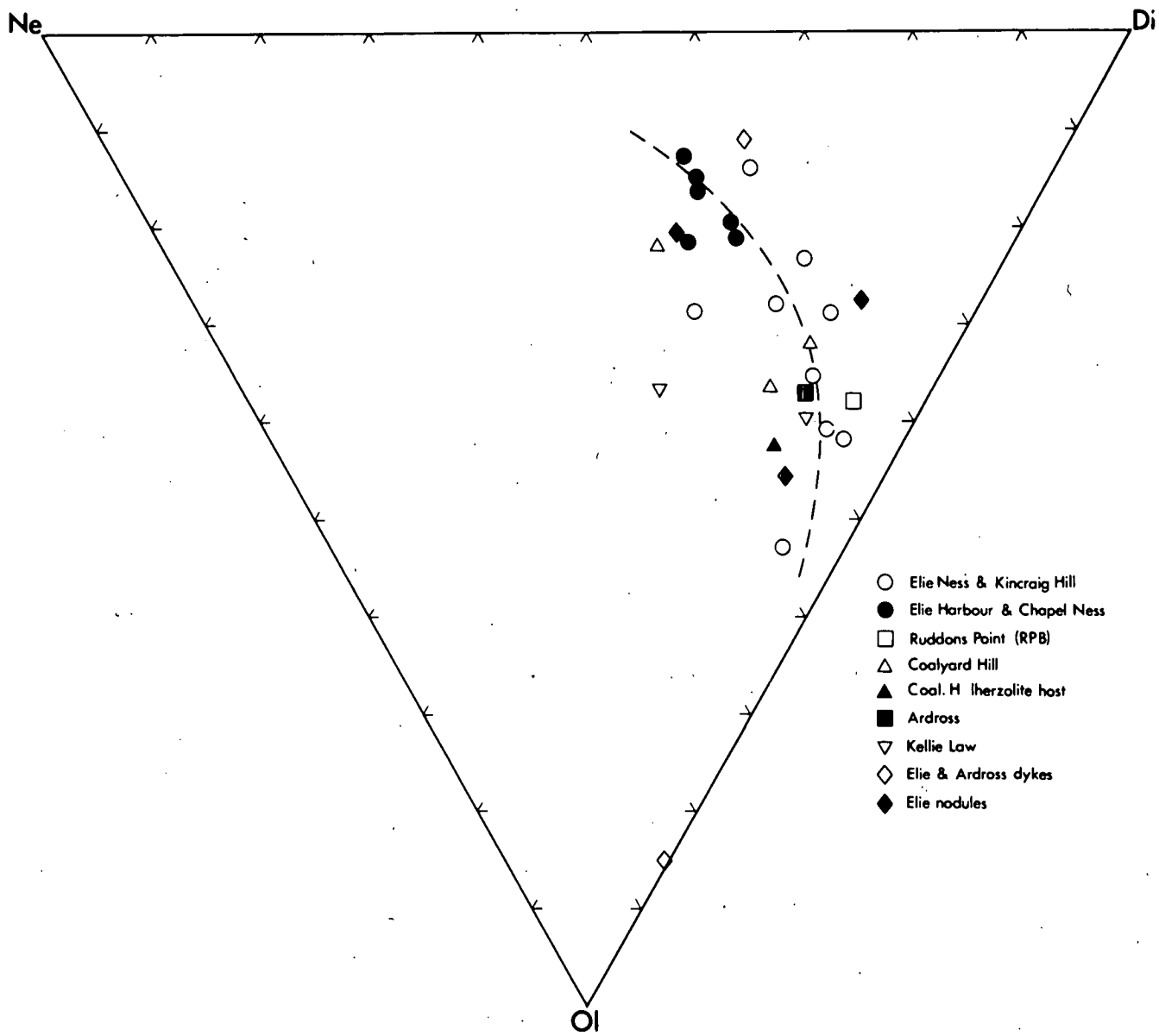
Ne
Di
Ol
Elie Ness & Kincraig Hill
Elie Harbour & Chapel Ness
Ruddons Point (RPB)
Coalyard Hill
Coal. H lherzolite host
Ardross
Kellie Law
Elie & Ardross dykes
Elie nodules

variations and extract three abstract vectors of variation (usually accounting for upwards of 97% of the total variation) also give a simple condensed graphical presentation (Le Maitre, 1968). These methods, however, are complex and due to the abstract nature of results not as easily applicable as simpler methods.

Two graphical methods are presented here; oxide:oxide variation diagrams and their equivalents for trace-elements, and ternary plots such as the CIPW norm described above and total alkalis-magnesia-iron (fig 3-5). Projections within the quaternary system C-M-A-S are illustrated in Chapter 7.

Before proceeding to discuss these diagrams two points relevant to their construction must be raised:-

a) In order to gain any useful data on the evolution of a group of basalts they must be shown to be a series of genetically related rocks, as in the case of a simple lava-pile. The Fife rocks are not as simply dealt with, as the samples come from a wide variety of environments and several localities. Blocks within tuff and samples from dykes, flows, sheets and plugs have all been analysed. That they form a group is indisputable, but whether they form a definite series related by the same fractionation trends can only be discerned from a study of their chemistry.

b) When plotting Harker diagrams the oxide which displays the greatest variance is normally chosen as the abscissa. This is usually silica or magnesia. Table 3-1 lists the variance

Table 3-1

Major-oxide mean, standard deviation, and variance of 27 analysed basalts from Fife.

Oxide	Mean	σ	σ^2	Variance %
SiO_2	43.52	2.143	4.593	21.93
Al_2O_3	14.54	1.182	1.397	6.67
FeO (Tot)	11.98	1.918	3.697	17.57
MgO	9.04	2.325	5.406	25.81
CaO	9.57	1.802	3.247	15.51
Na_2O	3.26	1.239	1.536	7.34
K_2O	1.60	0.735	0.540	2.58
P_2O_5	0.92	0.582	0.338	1.61
MnO	0.50	0.333	0.111	0.53
TiO_2	2.97	0.308	0.095	0.45
Total	97.90		20.942	100.00

of the major-oxides for 27 analysed basalts from Fife. As can be seen, no one oxide accounts for a substantial amount of the variation, although MgO has the highest single variance. The fact that silica also accounts for a comparatively high percentage reflects the trend to increasingly nepheline normative compositions. This general lack of conclusiveness is also indicated by the scattering of data-points seen in some of the variation diagrams and is relevant to the previous discussion on how far the rocks can be related to the same fractionation trends.

Major-oxide variation diagrams.

Major-oxide variation diagrams are presented in Figs 3-2a and 3-2b. Despite the scatter of points some features show through clearly. With decreasing magnesia:-

i) Silica shows a slight increase and alumina and soda increase substantially.

ii) Both Fe_2O_3 (total iron) and CaO decrease sympathetically.

iii) Potash shows an initial decrease to 10% MgO then rises.

iv) TiO_2 remains almost constant.

Some of the minerals closely related to the Fife rocks as phenocrysts and megacrysts have been plotted on the diagrams, and also a lherzolite inclusion from Ruddons Point. The following features can be noted:-

a) Olivine and titanaugite form the phenocryst phases in all the analysed rocks, but there is no consistent geometrical indication

Fig. 3-2 (a and b)
(overleaf)

Major-oxide variation (wt %) of Fife basalts plotted with MgO as the abscissa.

Dashed lines represent estimated paths, or limits of possible paths, of differentiation.

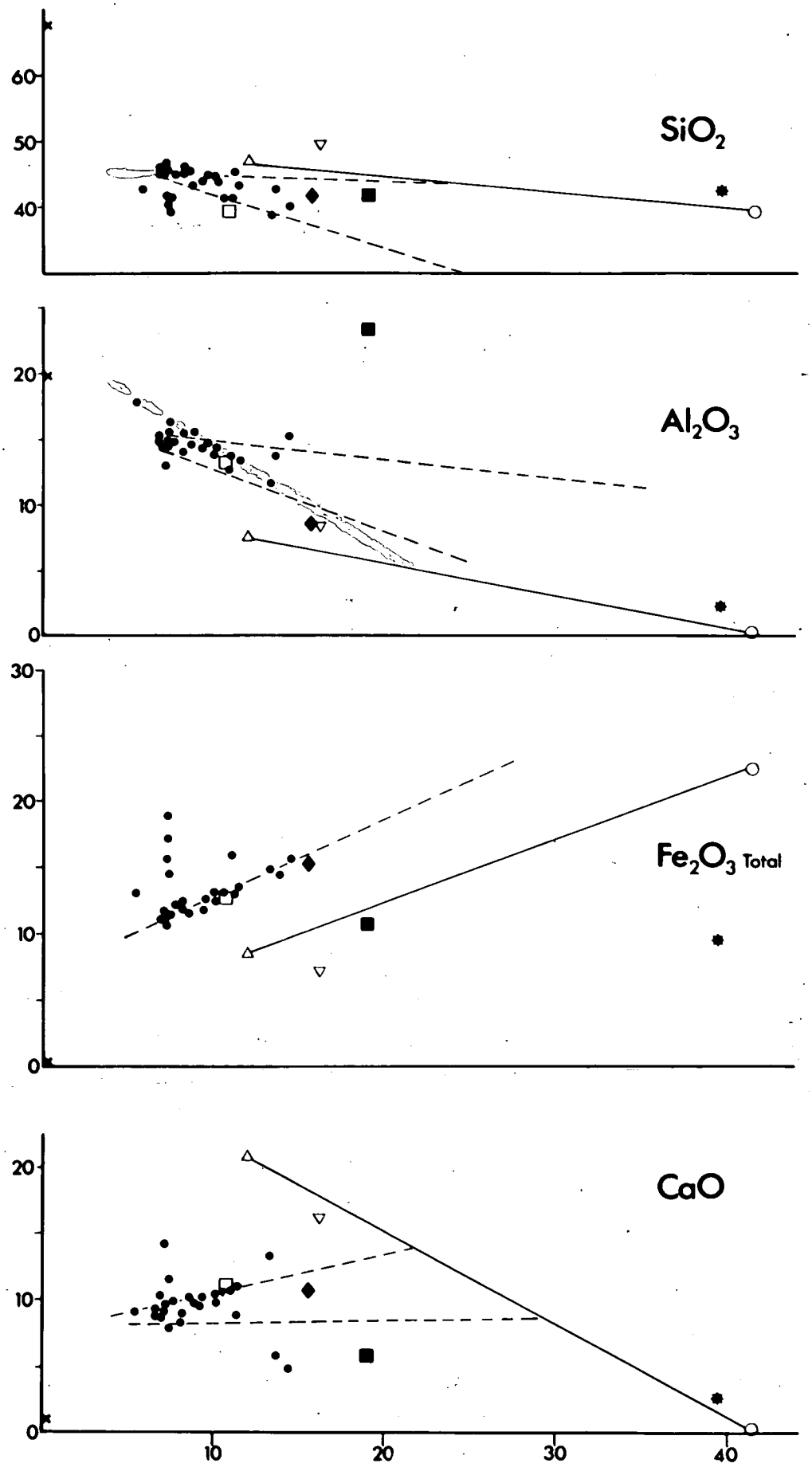
60
50
40
SiO_2
20
10
0
Al_2O_3
30
20
10
0
Fe_2O_3 Total
20
10
0
CaO
10
20
30
40

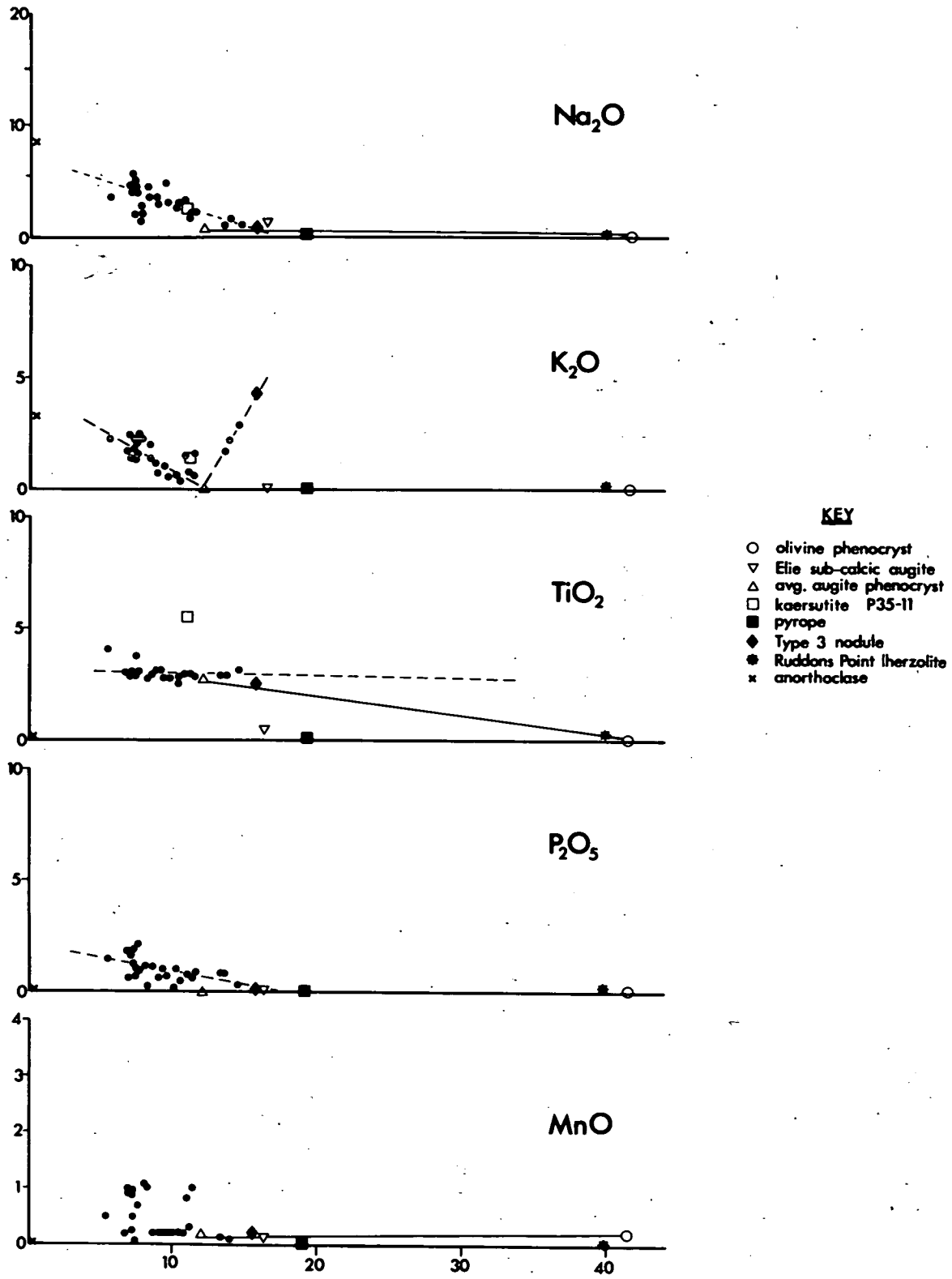
Na_2O
K_2O
TiO_2
P_2O_5
MnO
20
10
0
5
4
3
2
1
10
20
30
40
KEY
olivine phenocryst
Elie sub-calcic augite
avg. augite phenocryst
kaersutite P35-11
pyrope
Type 3 nodule
Ruddans Point lherzolite
anorthoclase

of a trend in all the oxides controlled solely by extraction of these phases. The trends exhibited in the estimated lines of evolution for silica, alumina and lime may indicate some control by olivine-augite fractionation. The latter are major components of Types 1 and 2 nodules, and are also the phenocryst phases in the Fife basalts. There is no consistent geometrical indication of the relative proportions of these minerals which might possibly account for the variations shown.

b) The composition of kaersutite from the Elie Ness nodules lies consistently amongst the more basic members of the group.

c) Fractionation of none of the megacryst phases <u>alone</u> could account for all the variation noted.

d) The decrease in total-iron may reflect extraction of titano-magnetite which would swing the 'control-line' away from the pyroxene-olivine tie-line.

e) Na_2O, K_2O and P_2O_5 increases are unrelated to olivine fractionation, but may be controlled by pyroxene crystallisation, leading to higher concentrations in the later formed rocks. The unusual trend exhibited by K_2O will be discussed in Chapter 7.

It might be concluded from the above observations that the Fife rocks comprise a comagmatic series of limited variation, much of which can be accounted for by simple crystallisation models involving extraction of olivine and pyroxene together, or pyroxene alone. The scatter of data may represent degrees of alteration of analysed

material or fractionation of phases other than those present in the mode. It is clear, however, that the chemistry of these rocks shows no signs of having been significantly controlled by the crystallisation of the megacryst phases, and hence that these phases and some of the nodule phases considered to be cognate may have crystallised from liquids of which there are no surface manifestations. The close correlation of kaersutite compositions with those of the more basic Fife rocks indicates that this may have been a late-stage mineral, which is supported by its poikilitic texture in some nodules, and which reflects the composition of the liquid from which it crystallised. These conclusions will be further discussed in Chapter 7.

Trace-element variation diagrams.

Analysed trace-elements fall into the two groups described by Ringwood (1966) of 'incompatibles' (Ba, Sr, Zr, Rb, Ce, La) and the 'compatible' elements (Ni, Cr, V). The former group derives its name from the inability of certain elements to enter the stable crystal lattices of many igneous minerals, and hence remain in the liquid, being gradually enriched in the later fractions. Whether an element is incompatible or not depends on what crystalline phases precipitate. Barium, for example, is normally considered incompatible, but as it can proxy for potassium it can become compatible if mica or alkali-feldspar are present. Similarly, strontium can proxy for calcium in feldspars and apatites. Generally speaking then, one would expect a truly incompatible element to

display a regular, linear increase in concentration with the evolution of magmas during fractional crystallisation, whereas the compatible elements would reflect the composition of the phases extracted.

The trace-element variation diagrams (again with MgO as the abscissa) are presented in Figs 3-3a and 3-3b. Several points are worthy of note:-

a) A scatter of data-points similar to that of the major-oxides is prevalent in most of the diagrams.

b) The incompatible elements Ba, Sr, Zr, Ce, and La all increase with decreasing MgO. However, both Ba and Sr have a very wide field and are not confined to a linear trend as would be expected if they were truly incompatible. This may be merely a function of secondary alteration, though anorthoclase is associated with or present in some of the rocks. If anorthoclase was crystallising in sufficient amounts in the liquid both Ba and Sr may become compatible before crystallisation of plagioclase.

c) The trend exhibited by Rb in decreasing until MgO=12% and then gradually increasing closely parallels that shows by K_2O.

d) Both Cr and Ni decrease with decreasing MgO but V remains relatively constant, a trend also displayed by TiO_2. V is most probably present in the titanomagnetites found in the groundmass of the basalts.

Fig. 3-3 (a and b)
(overleaf)

Trace element variation of Fife basalts (ppm) plotted with MgO as the abscissa.

□ Elie-type nodules

◆ Type 3 Elie nodule (Q2-6)

■ Ruddons Point lherzolite inclusion. (E-1)

Dashed lines as in Fig. 3-2. (estimated paths of evolution).

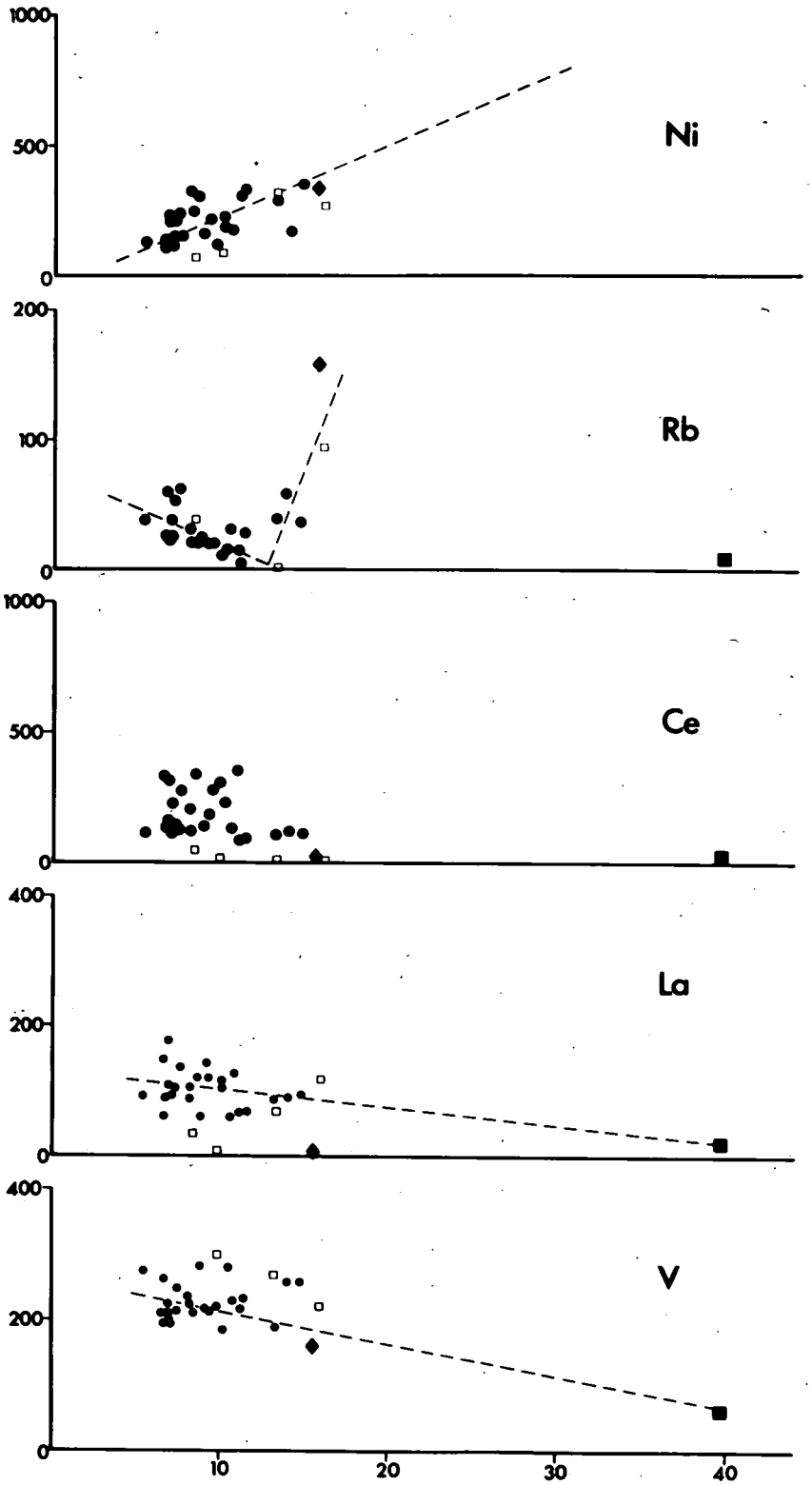
1000
500
0
Ni
200
100
0
Rb
1000
500
0
Ce
400
200
0
La
400
200
0
V
10
20
30
40

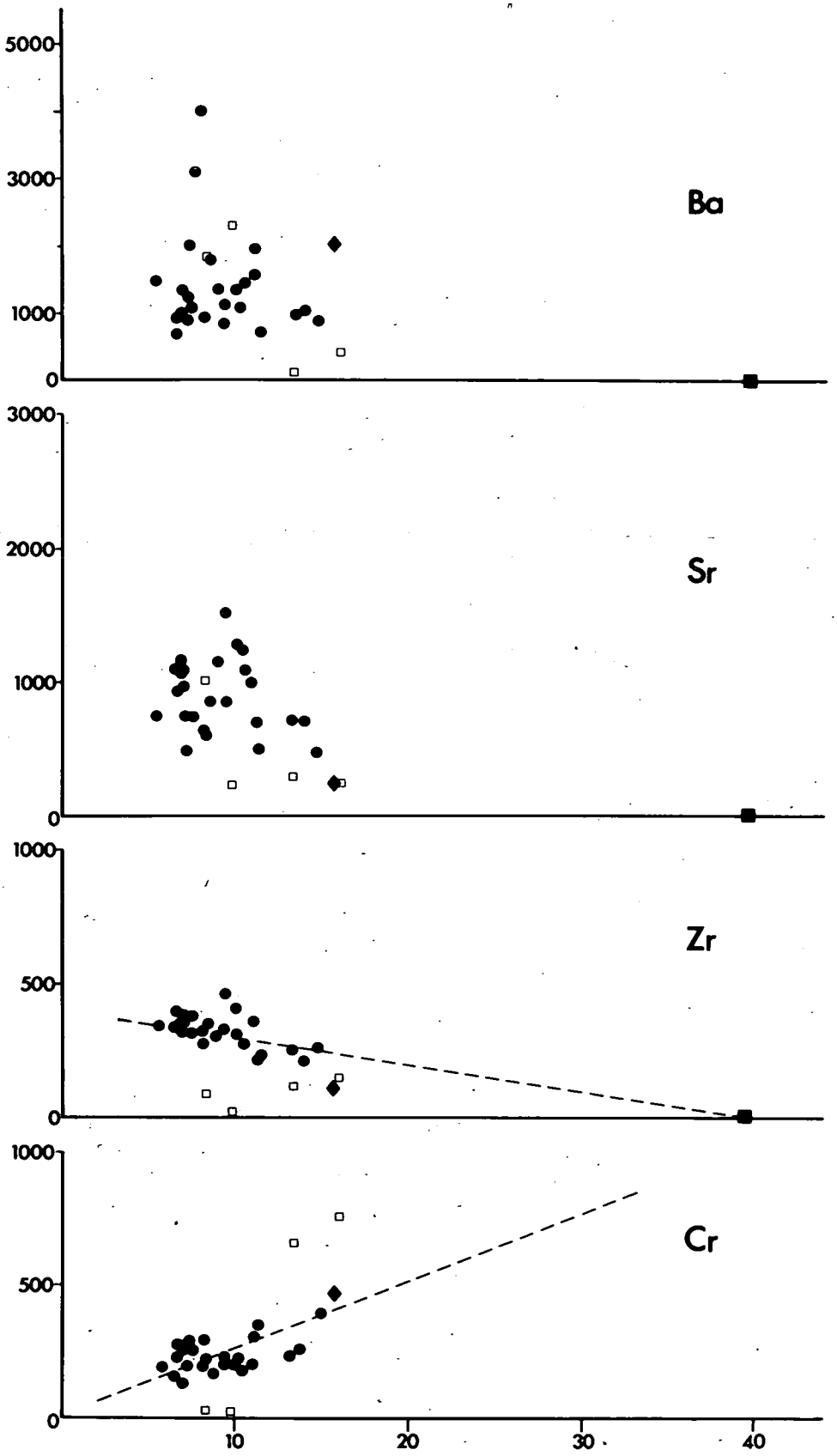
5000
3000
1000
0
Ba
3000
2000
1000
0
Sr
1000
500
0
Zr
1000
500
0
Cr
10
20
30
40

Potassium and Rubidium.

A strong positive correlation (r=0.79) exists between K and Rb in the Fife basalts. Fig 3-4 illustrates the relationship between the two elements and shows the basalts to have a K/Rb ratio from 250-600, which is within the general field for alkali-basalts (Gast, 1968).

'F.M.A.' diagram.

Fig 3-5 shows the Fife basalts plotted in the system Total-Alkalis (Na_2O+K_2O)-Total iron-MgO. Here again an inconclusive scatter of data-points is seen. The trends of Hawaiian alkali-basalts (MacDonald and Katsura, 1964) and the analcime-rich igneous rock trend of Wilkinson (1962) are also shown for reference. The latter shows the trends from analcime-basalts on the right to blairmorite and analcime-tinguaite on the extreme alkaline side. A postulated trend for the Fife basalts which ignores the more aberrant points is also indicated, and shows little in the way of iron-enrichment. The transitional nature of the rocks from analcimic-basalts to basanites can be clearly seen.

Other localities.

Major and trace-element data for rocks from the other areas visited are also presented in Appendix 1. In order to avoid confusion these isolated analyses have not been plotted on the previous diagrams. Where relevant they will be discussed in Chapter 7.

Fig. 3-4

Potassium / rubidium correlation of Fife basalts plotted on a logarithmic scale. Parallel lines refer to K/Rb ratios.

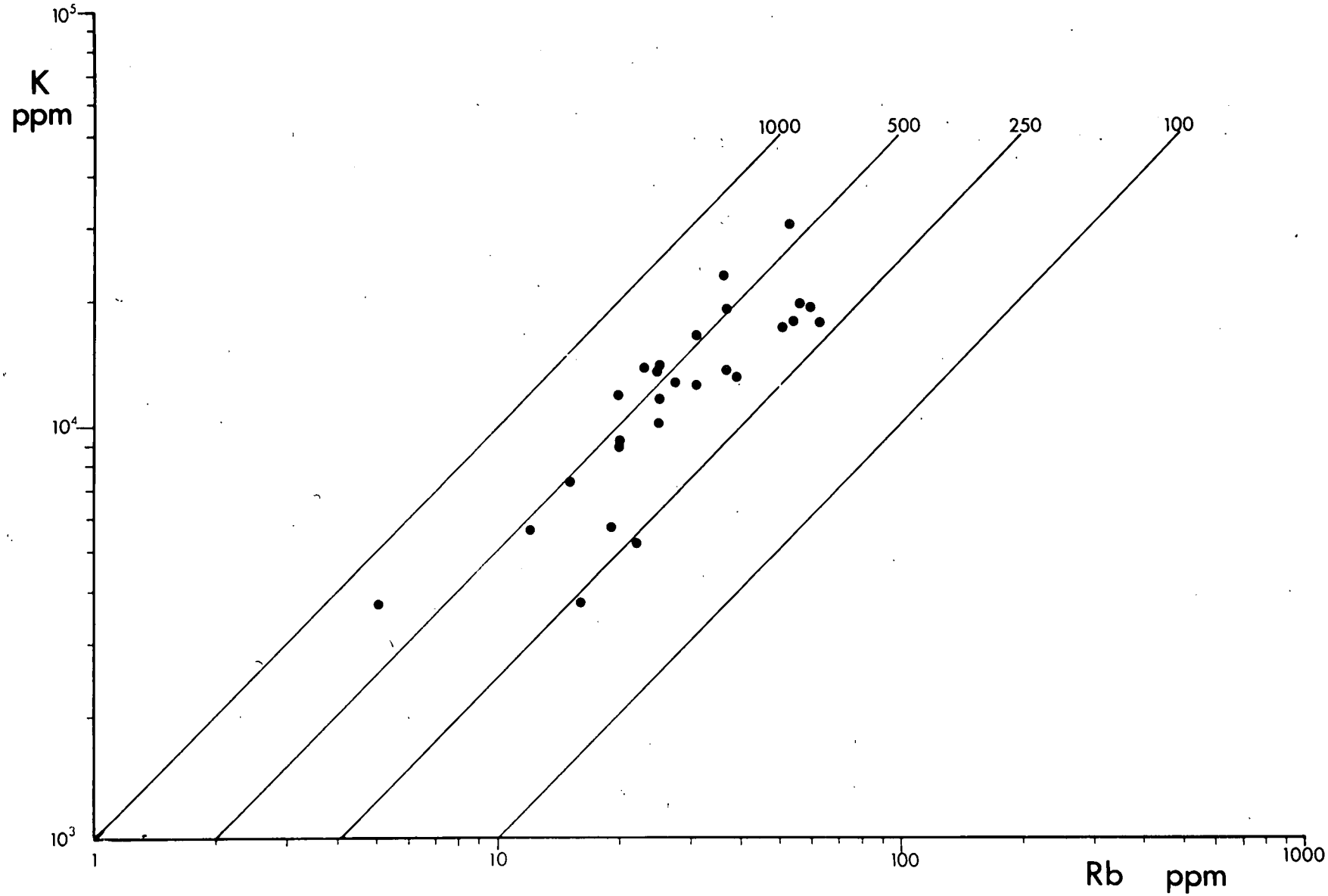
10^5
K
ppm
10^4
10^3
1000
500
250
100
1
10
100
1000
Rb ppm

Fig. 3-5

' F - M - A ' diagram for Fife basalts.

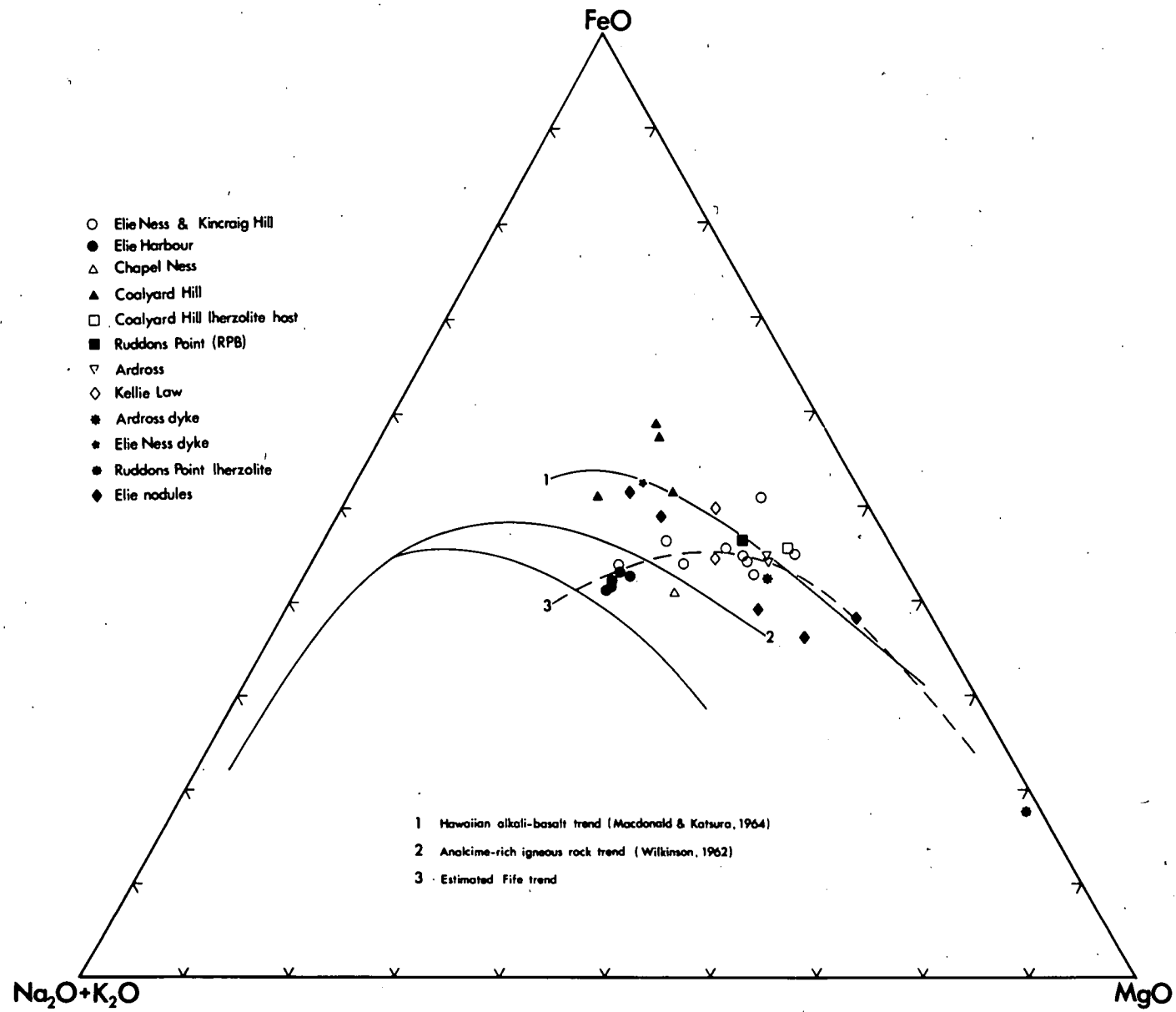
FeO
Na2O+K2O
MgO
Elie Ness & Kincraig Hill
Elie Harbour
Chapel Ness
Coalyard Hill
Coalyard Hill lherzolite host
Ruddons Point (RPB)
Ardross
Kellie Law
Ardross dyke
Elie Ness dyke
Ruddons Point lherzolite
Elie nodules
1
2
3
1 Hawaiian alkali-basalt trend (Macdonald & Katsura, 1964)
2 Analcime-rich igneous rock trend (Wilkinson, 1962)
3 Estimated Fife trend

CHAPTER FOUR

Mineral Chemistry.

Introduction.

This discussion of mineral chemistry is divided into two sections. The modal constituents of the basaltic material will be dealt with first. In order to prevent repetition the basalts from all the areas studied will be considered together and wherever practical data from all these sources will be presented on the same diagrams. The second section deals with nodules, inclusions and megacrysts, and for clarity will be subdivided into areas. As with the first section it is often possible to present data from different areas on the same diagrams without causing undue complication. Unless otherwise stated all analyses were performed by electron-microprobe, and are presented in Appendix 1.

4.1 Minerals from the basalts.

a) Olivines

Whilst olivine forms the main phenocryst phase along with augite it has already been noted in Chapter 2 that it is generally pseudomorphed in all but the freshest rocks. Fresh olivine phenocrysts from the central plug analcimic-basalt of Kincraig Hill have an average composition of Fo_{79}, zoning outwards from Fo_{86} to Fo_{75}, a relatively high Fo content for the cores which indicates an initially quite magnesian liquid.

b) Clinopyroxenes.

Augite occurs both as phenocrysts and in the groundmass of the majority of the rocks studied. Analyses of 56 groundmass and phenocryst core and rim pyroxenes are presented on the pyroxene quadrilateral in Fig. 4-1.

The majority of the phenocrysts and all the rim and groundmass pyroxenes fall into the salitic-augite field. A general trend towards more calcic compositions with little change in the FeO/MgO ratio is indicated. This lack of any substantial iron enrichment in the later crystallised pyroxenes is also reflected in the whole-rock chemistry previously discussed, a number of the groundmass-rim analyses plot outside the upper limit of the quadrilateral, being very calcic. It has already been noted that the phenocrysts zone outwards into increasingly titanium-rich compositions, TiO_2 substituting for SiO_2. Titanium is present in the clinopyroxenes in the Ti-Tschermak molecule ($CaTiAl_2O_6$) (see Chapter 5) and hence any enrichment in Ti would be reflected by a parallel enrichment in both Ca and Al, explaining the highly calcic nature of the late pyroxenes. It will be noted from the analyses that these pyroxenes are very aluminous (up to 8% Al_2O_3) and within this particular group of phenocryst-groundmass pyroxenes such a trend towards increasing alumina with degree of crystallisation can be noticed. The petrogenetic significance of Ca-Ti-Al-Na variations will be dealt with in Chapter 5.

Two further points will be mentioned at this stage. Firstly the pyroxenes from small glomeroporphrytic aggregates present in

Fig. 4-1

Groundmass and phenocryst clinopyroxenes plotted in the mole % C-M-F system. Pyroxene fields after Deer, Howie and Zussman.

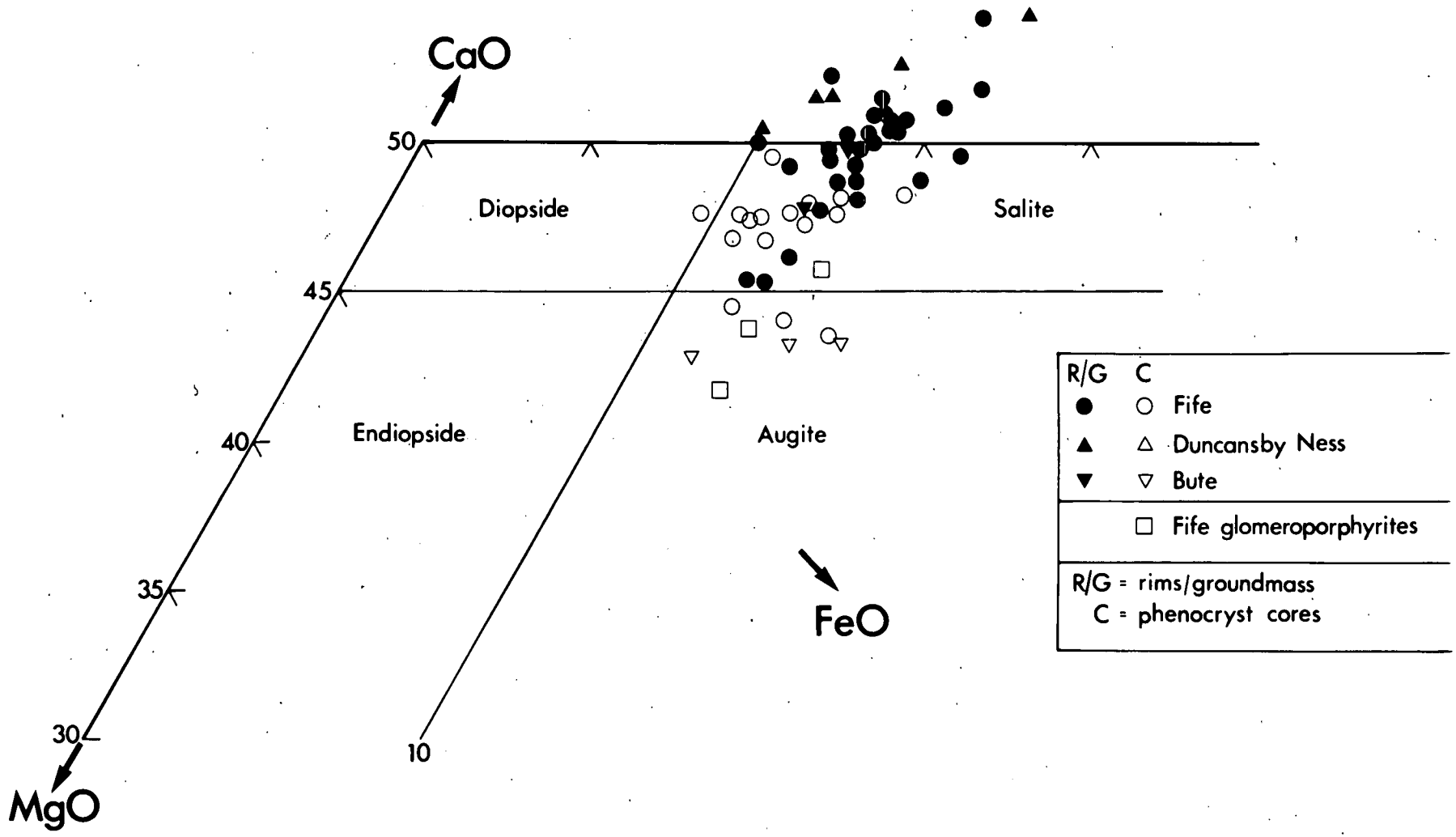
CaO
50
45
40
35
30
MgO
10
Diopside
Salite
Endiopside
Augite
FeO
R/G C
Fife
Duncansby Ness
Bute
Fife glomeroporphyrites
R/G = rims/groundmass
C = phenocryst cores

some of the Fife rocks are noticeably less calcic than corresponding phenocryst cores from the same rocks, and secondly the core analyses from the Bute host-rock are less calcic and poorer in TiO_2 than those from other localities.

c) Plagioclase.

Plagioclase is an important groundmass phase in the majority of the basalts, though in the most undersaturated rocks it is subordinate to analcime. Fig. 4-2 illustrates the normative composition of groundmass plagioclases from the Fife rocks. The majority of these are labradorites, being mildly zoned towards more sodic rims. Those of the monchiquitic block from the Elie Ness tuff are substantially more sodic, falling in the andesine field, which may indicate a lower P_{H2O} of crystallisation than that of the basanitic rocks (cf. Yoder, 1969). Two analyses of core and rim from the Bute host-rock are presented in Fig. 4-3, showing normal zoning towards a more sodic labradorite rim, and falling within the same general field as those from Fife.

d) Analcime.

The cloudy analcime present as the matrix in the basalts is not easily analysed by electron-'probe as the mineral is unstable under the beam and Na evaporates rapidly. Appendix 1 lists analyses of analcime from blocks in the Elie Ness vent. Little replacement of Na by K had taken place, the only noticeable variation being the partial substitution of Na and Al for Si. Deer et al. (1966) ascribe this substitution to the lowering of temperature during igneous

Fig. 4-2

Normative compositions of feldspars from Fife.
wt %

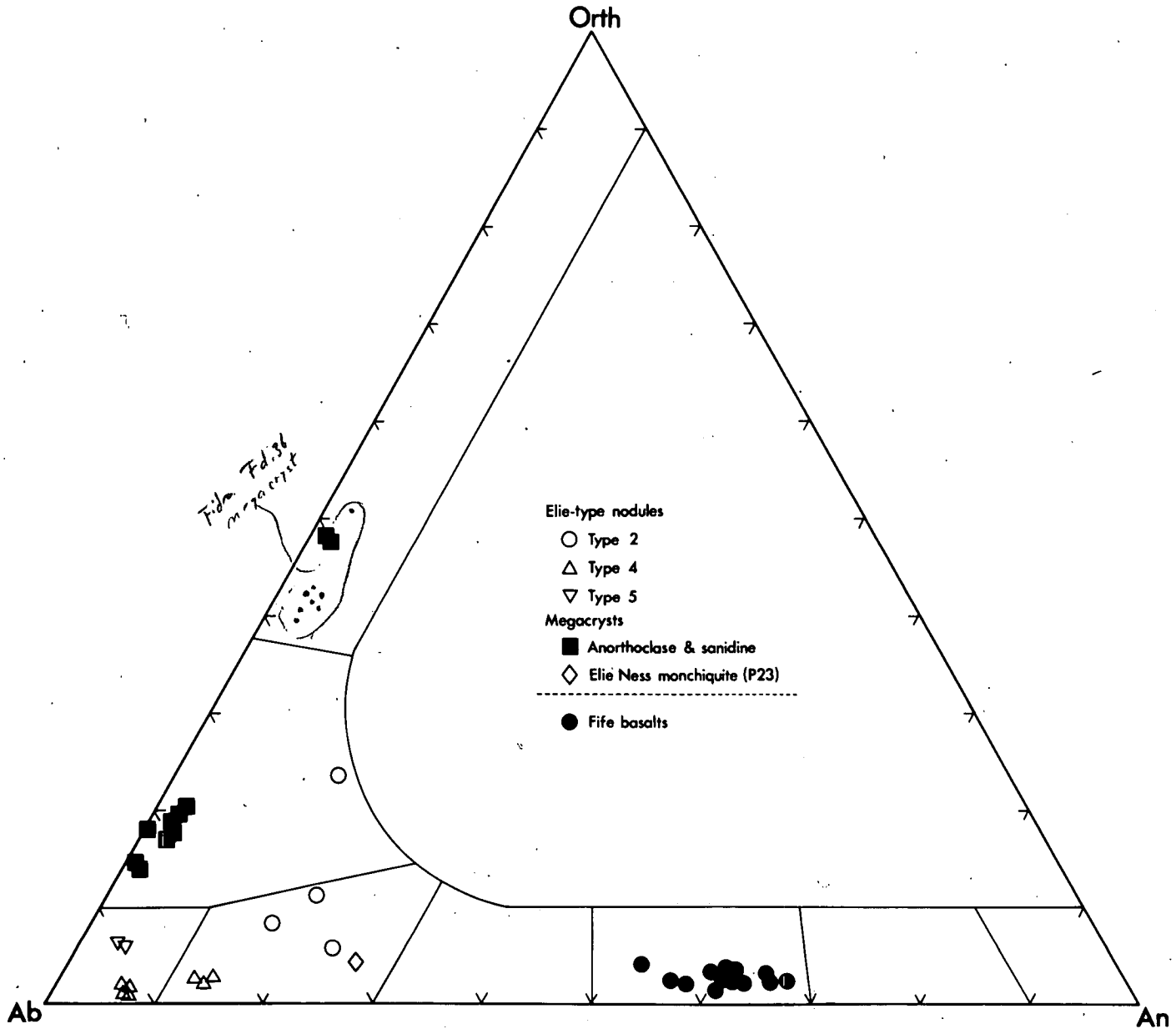
Orth
Ab
An
Fife Fd, Sb megacryst
Elie-type nodules
Type 2
Type 4
Type 5
Megacrysts
Anorthoclase & sanidine
Elie Ness monchiquite (P23)
Fife basalts

Fig. 4-3

Normative composition of feldspars from localities other than Fife. (wt %)

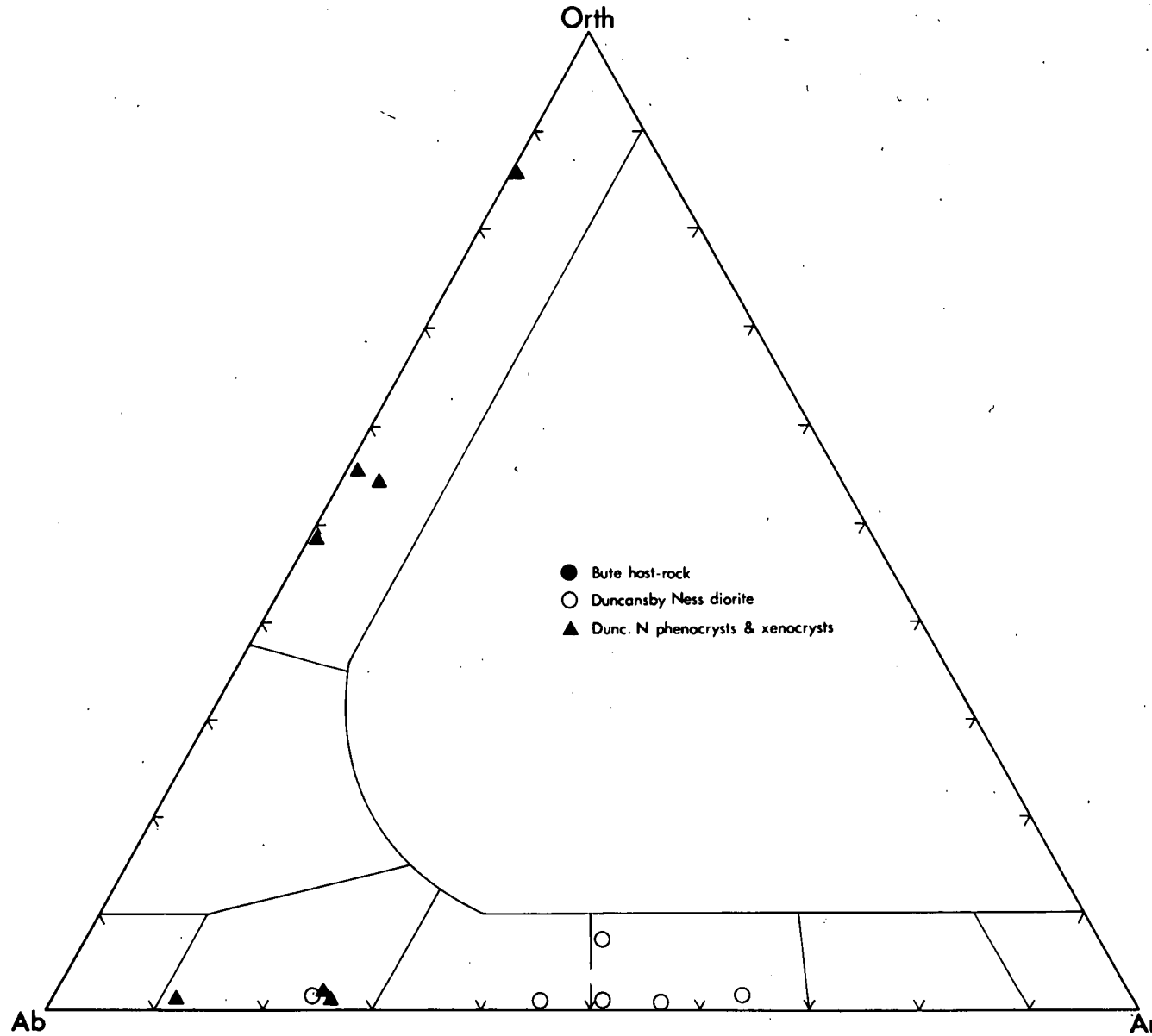
Orth
Ab
An
Bute host-rock
Duncansby Ness diorite
Dunc. N phenocrysts & xenocrysts

crystallisation, although the degree of substitution within the analysed specimens is not sufficiently significant to allow any conclusions to be drawn on the temperatures of formation of rocks which are chemically very similar.

e) Opaque phases.

Small, often euhedral, titanomagnetite microphenocrysts form up to 12 modal percent of the basaltic material, rarely falling below 6%. Analyses of 5 titanomagnetites from the basalts are presented. Whilst they cover a range of compositions they show no sign of exsolution. Vincent et al (1957) describe a great degree of magnetite-ilmenite-ülvospinel solid-solution at temperatures above 600°C, with exsolution taking place on slow cooling below that temperature. The lack of un-mixed textures in the titano-magnetites studied suggests a fairly rapid quench, which is supported by the generally glassy and chilled nature of the groundmass in the bulk of the rocks.

A little pyrite is found in the groundmass of some of the basaltic blocks and most probably represents late-stage formation.

f) Amphibole.

Amphibole occurs in the monchiquitic block from Elie Ness as micro-phenocrysts of kaersutite. Classification of the amphiboles has been based on Leake's (1968) system and all the analysed amphiboles are plotted on this grid in Fig. 4-4. The kaersutite from the monchiquitic block is very similar in composition to those from the Elie Ness nodules, and to amphibole formed as an alteration of

Fig. 4-4

Amphiboles from Fife classified according to the system of Leake (1968).

mg...'Niggli number' (Mg/ Fe(3) + Fe(2) + Mn + Mg)

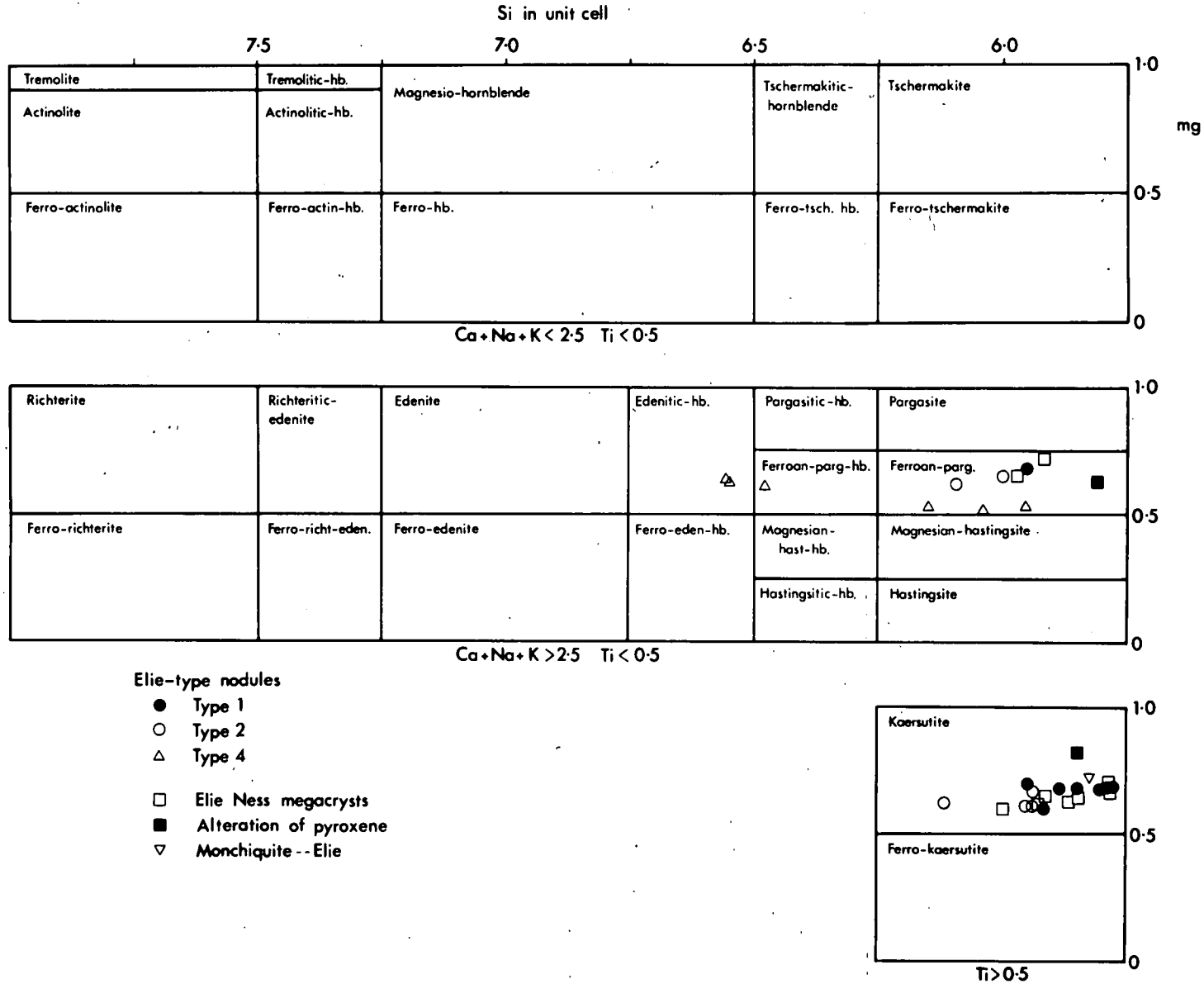
Si in unit cell
7·5
7·0
6·5
6·0
Tremolite
Actinolite
Tremolitic-hb.
Actinolitic-hb.
Magnesio-hornblende
Tschermakitic-hornblende
Tschermakite
Ferro-actinolite
Ferro-actin-hb.
Ferro-hb.
Ferro-tsch. hb.
Ferro-tschermakite
1·0
0·5
0
mg
Ca+Na+K < 2·5 Ti < 0·5
Richterite
Richteritic-edenite
Edenite
Edenitic-hb.
Pargasitic-hb.
Pargasite
Ferroan-parg-hb.
Ferroan-parg.
Ferro-richterite
Ferro-richt-eden.
Ferro-edenite
Ferro-eden-hb.
Magnesian-hast-hb.
Magnesian-hastingsite
Hastingsitic-hb.
Hastingsite
Ca+Na+K > 2·5 Ti < 0·5
Elie-type nodules
Type 1
Type 2
Type 4
Elie Ness megacrysts
Alteration of pyroxene
Monchiquite--Elie
Kaersutite
Ferro-kaersutite
Ti > 0·5

clinopyroxene.

4.2 Nodules, inclusions and megacrysts.

Elie Type nodules and megacrysts.

a) Clinopyroxenes.

Clinopyroxene forms a major part of the Types 1, 2 and 3 nodules from the Elie Ness tuff. Fig. 4-5 shows the pyroxenes from these nodules in the C-M-F system, where they fall within a restricted area in the field of salitic-augite. Comparison with Fig. 4-1 shows them to plot in the same compositional zone as the phenocryst cores from the associated basalts. There is, however, no discernible variation within the C-M-F system between the nodule groups, though those from the biotite-pyroxenites (Type 3) are much poorer in TiO_2 than those from the other two types. They are correspondingly richer in silica and also less aluminous. On more detailed examination the augites from Types 1 and 2 nodules are also found to be slightly different in chemistry, the former being poorer in silica and soda and richer in alumina and titania than the latter. In overall composition the augites from Type 1 nodules are very similar to the phenocryst cores discussed above.

Clinopyroxene megacrysts of two forms are found in the Elie tuff, the 'glassy' structureless variety and the darker, well-cleaved type. Both varieties are relatively sub-calcic augites and notably less calcic and more magnesian than the nodule pyroxenes, particularly the glassy megacrysts. This indicates a substantial

Fig. 4-5

Clinopyroxenes from Elie-type nodules and megacrysts in the mole % C-M-F system. (see Fig. 4-1)

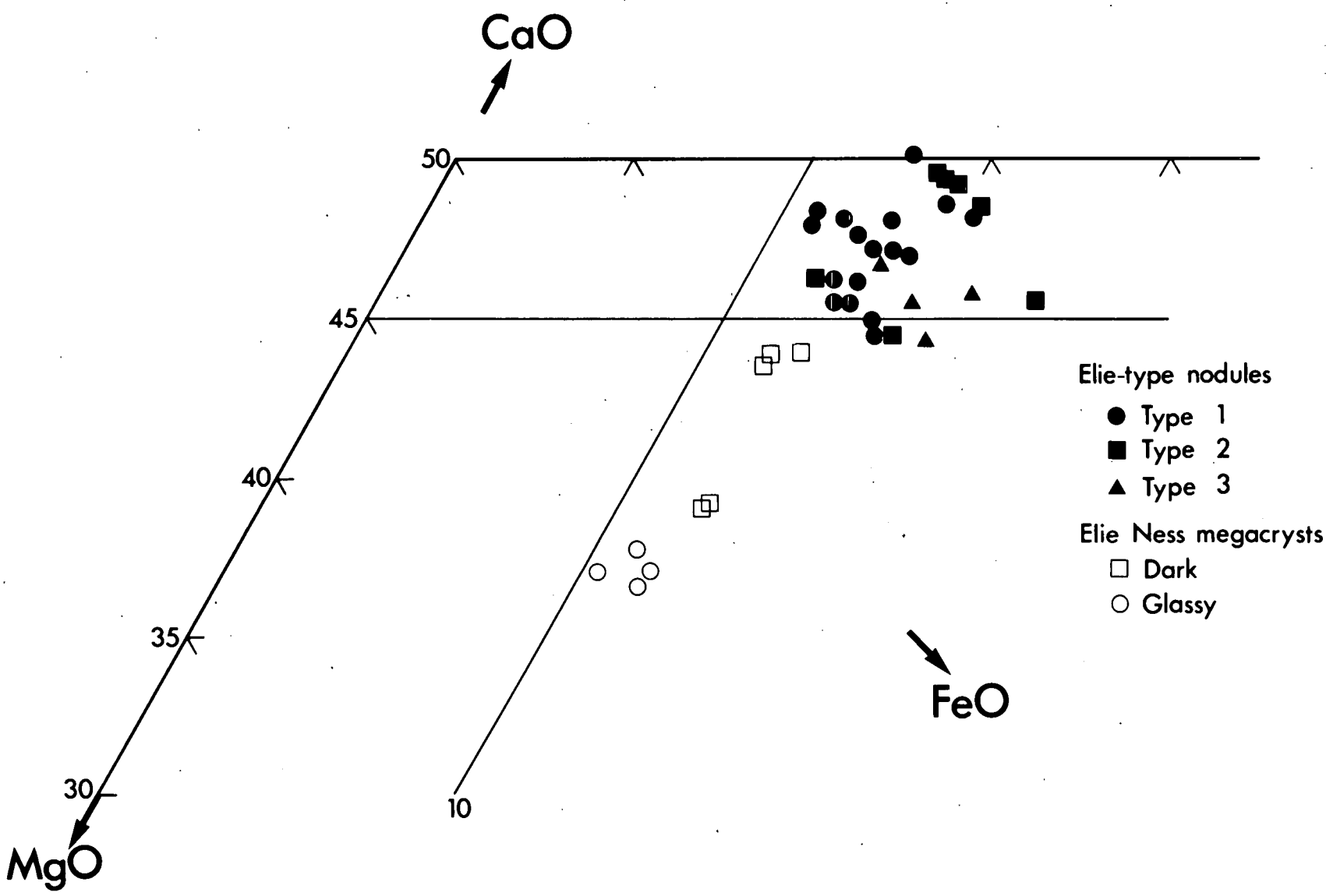
CaO
50
45
40
35
30
MgO
10
FeO
Elie-type nodules
Type 1
Type 2
Type 3
Elie Ness megacrysts
Dark
Glassy

amount of the enstatite component (up to 45 mole %) to be in solid-solution, and as no orthopyroxene is exsolved it can be assumed that these megacrysts must have moved rapidly to the surface. The megacrysts also differ from the nodule pyroxenes in their higher sodium and aluminium contents. TiO_2 is lower than in the group 2 augites. The overall chemical variations in the clinopyroxenes from nodules, megacrysts and phenocrysts (cores and rims) are summarised in Fig. 4-6. This diagram assumes that all the phases represented are cognate in origin, with fractionation taking place from right to left. Several points are worthy of note:-

i) The augites from Types 1, 2 and 3 nodules have perfect linear correlation for every oxide except MgO and CaO, though these too are almost linear.

ii) Phenocryst cores and Type 1 nodule augites are, as already noted, very similar.

iii) The antipathetic variations between MgO and CaO, and silica and alumina are clearly displayed.

iv) Alumina decreases sharply from the high values of the megacrysts, proceeding then to rise steadily, a trend which is reversed in both SiO_2 and FeO.

Whilst it is not intended to discuss petrogenesis at this stage, several deductions might be made from this diagram which will be useful in further discussion. These are based on the assumption that all the phases are cognate.

a) The linear correlation within the three nodule groups suggests

Fig. 4-6

Average compositions of Fife clinopyroxenes.

PR...phenocryst rims
PC...phenocryst cores
1...Elie-type 1 nodules
2...Elie-type 2 nodules
3...Elie-type 3 nodules
D...Elie Ness dark megacrysts
Gl...Elie Ness glassy megacrysts

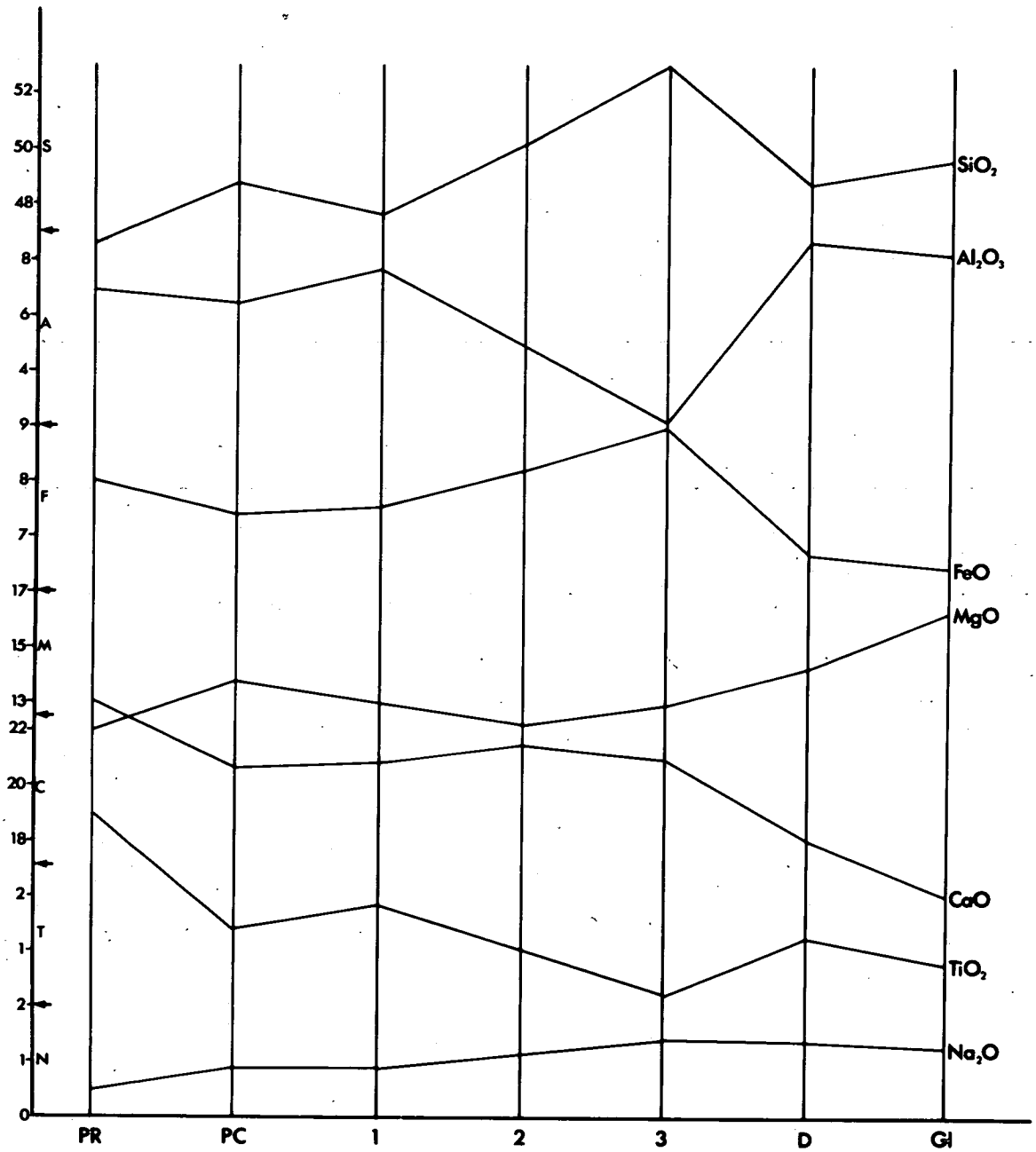
52
50
48
8
6
4
9
8
7
17
15
13
22
20
18
2
1
2
1
0
S
A
F
M
C
T
N
PR
PC
1
2
3
D
GI
SiO2
Al2O3
FeO
MgO
CaO
TiO2
Na2O

them to be closely related in origin and to have crystallised in the order shown.

b) The Type 1 augites formed under very similar conditions to those under which the phenocryst cores began to crystallise.

c) The initial decrease in alumina and its subsequent gradual increase could be explained in terms of pyroxene end-members (Chapter 5). The alumina 'low' may mark the point at which P-T conditions are no longer sufficient for extensive formation of jadeite or Ca-Tschermak molecules, but are also too extreme to allow the Ti-Tschermak component to form in substantial amounts. The progressive decrease in Na_2O and TiO_2 support this.

b) Amphiboles.

Amphibole is an important phase in both nodules and megacrysts from Fife, and to a lesser extent in nodules from Duncansby Ness. As noted in 4.1f all analysed amphiboles are presented in Fig. 4-4 on the basis of Leake's classification. There is little overall variation in chemistry and all amphiboles from nodules and megacrysts apart from Type 4 nodules fall into the fields of kaersutite or ferroan-pargasite. The dividing line between these fields is dependent solely on the amount of Ti in the half unit-cell. ($Ti > 0.5$, kaersutite : $Ti < 0.5$, ferroan-pargasite). In fact actual variation around the figure of 0.5 is relatively small, and the majority of the amphiboles are markedly titaniferous. The green amphibole occurring in Type 4 nodules straddles the compositional

fields of ferroan-pargasite, ferroan-pargasitic hornblende, and edenitic hornblende and is substantially more sodic and poorer in TiO_2 than the brown amphiboles. Amphibole occurring in nodules as an alteration of augite is also very similar in chemistry to the nodule and megacryst amphiboles. Owing to the similarity in composition of megacrysts and nodule amphiboles it is not possible to say whether the megacrysts in fact formed discretely or whether they are merely xenocryst from the nodules.

c) Feldspars.

Feldspar occurs in the Types 2, 4 and 5 nodules, as megacrysts in tuffs and basalts from Fife and East Lothian, and as presumed xenocrysts from the ORS in monchiquite from Duncansby Ness. Those occurring as megacrysts and in nodules from Fife are presented in Fig. 4-2. Type 2 nodules contain potassic oligoclase (one analysis falls within the lime-anorthoclase field) similar in composition to a megacryst from the Elie Ness monchiquitic block. The Type 4 nodules containing green-amphibole have low-potash plagioclase in the region of calcic albite to sodic oligoclase. The bimineralic Type 5 biotite-plagioclase nodules contain potassic albite.

Megacrysts of alkali-feldspar are widespread in Fife and samples have been analysed from the Elie Ness Tuff, the Elie Ness dyke, Ardross dyke, Coalyard Hill monchiquitic sheet, Ruddons Point lherzolite-bearing sheet and the Kellie Law basalt. Apart from the Kellie Law sample which is a potassic sanidine, all the remainder are of very limited composition, lying in the anorthoclase field. Structural

state analyses have been performed on all these samples including a megacryst from Fidra after the method of Wright (1968). The results are shown on Fig. 4-7. An oscillating scan X-ray diffraction technique using Cu-Kα radiation was found to give a high degree of reproducibility when measuring the positions of 060, $\bar{2}04$, and $\bar{2}01$ peaks, with an estimated precision of $\pm 0.02^{\circ}$ 2θ. Apart from the Fidra specimen all results are slightly offset from the High Albite-High Sanidine series indicating a very high temperature of formation. The Fidra sanidine also plots close to the above series and within the bounds of the quadrilateral, again indicating a high temperature origin. Results of Hoffer and Hoffer (1973) who studied a similar occurrence of alkali-feldspar megacrysts from New Mexico are also shown, and are again seen to be offset from the high albite-high sanidine series and within the same region as the Fife megacrysts.

Fig. 4-3 shows analyses of oligoclase and orthoclase feldspar from the Duncansby Ness monchiquite. As these are closely associated with partially resorbed quartz crystals and xenoliths of arkosic ORS it is thought that they represent xenocrysts from the sandstone fragments. Also presented on this diagram are six analyses of plagioclase from the large tonalite nodule found in the tuff at Duncansby Ness. Small nodules of this type are sparsely scattered throughout the tuff. The plagioclase ranges in composition from basic labradorite to oligoclase.

Fig. 4-7

Structural state of anorthoclase megacrysts and sanidine from Fife and East Lothian based on the method of Wright (1968). Puye, high albite and sanidine, low albite and maximum microcline are standards used by Wright.

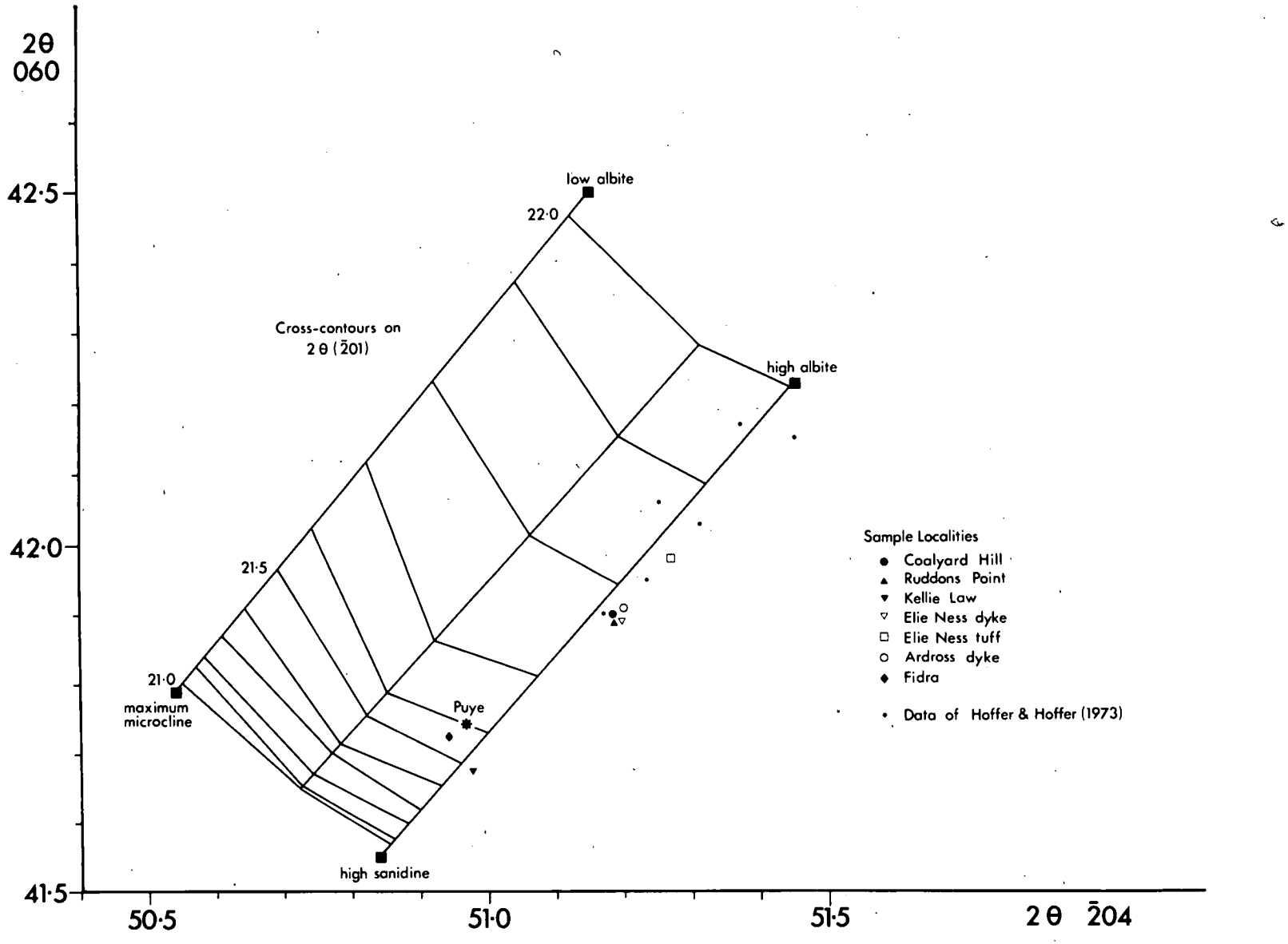
2θ
060
42·5
42·0
41·5
50·5
51·0
51·5
2θ 204
low albite
22·0
high albite
Cross-contours on
2θ (2̄01)
21·5
21·0
maximum
microcline
Puye
high sanidine
Sample Localities
Coalyard Hill
Ruddons Point
Kellie Law
Elie Ness dyke
Elie Ness tuff
Ardross dyke
Fidra
Data of Hoffer & Hoffer (1973)

d) Mica.

Mica occurs in the Types 3, 4 and 5 nodules, in the Duncansby Ness tonalite nodule and as a secondary mineral in fractures in anorthoclase megacrysts from Fife. These dark, iron-rich micas lie in the general biotite-phlogopite compositional field. Following the convention of Deer et al., whereby only those members of this group with Mg/ Fe > 2 are termed phlogopites, all the analysed micas in this group are biotites, with Mg / Fe = 0.4-1.2. They are also substantially titaniferous and will be referred to as titanbiotites.

Those from Types 3 and 4 nodules are chemically quite similar, with Mg / Fe ratios close to 1.1. The Type 5 titanbiotites, however, are much richer in FeO (Mg / Fe = 0.39) and titanium and poorer in alumina. The mica from the tonalite-diorite nodule is aluminous and iron rich (Mg / Fe = 0.5) with lower titanium than the other analysed micas. Nockolds (1941) discussed the change in composition of biotites relative to a fractionating liquid in his work on the Garabal Hill-Glen Fyne complex. He noted an increase in Al and Fe and a decrease in Si, Ti and Mg with differentiation. In a later paper (1947) Nockolds came to the conclusion that biotite compositions are not related to the silica content of the liquid, but that the ratio of Al_2O_3 to FeO + MgO is determined by their paragenesis. The FeO:MgO ratio depends merely on degree of fractionation. These conclusions are summarised in Fig. 4-8. The three fields denoted are related solely to alumina content. It can be seen that the biotites from the Elie nodules and the tonalite nodule fall within Nockolds field 3, which is biotite associated

Fig. 4-8

Biotites in the wt % MgO-FeO-Al_2O_3 system of Nockolds (1947).

Field 1....Biotites associated with muscovite
Field 2....Biotites associated with other mafic minerals
Field 3....Biotites associated with hornblende, pyroxene or olivine.

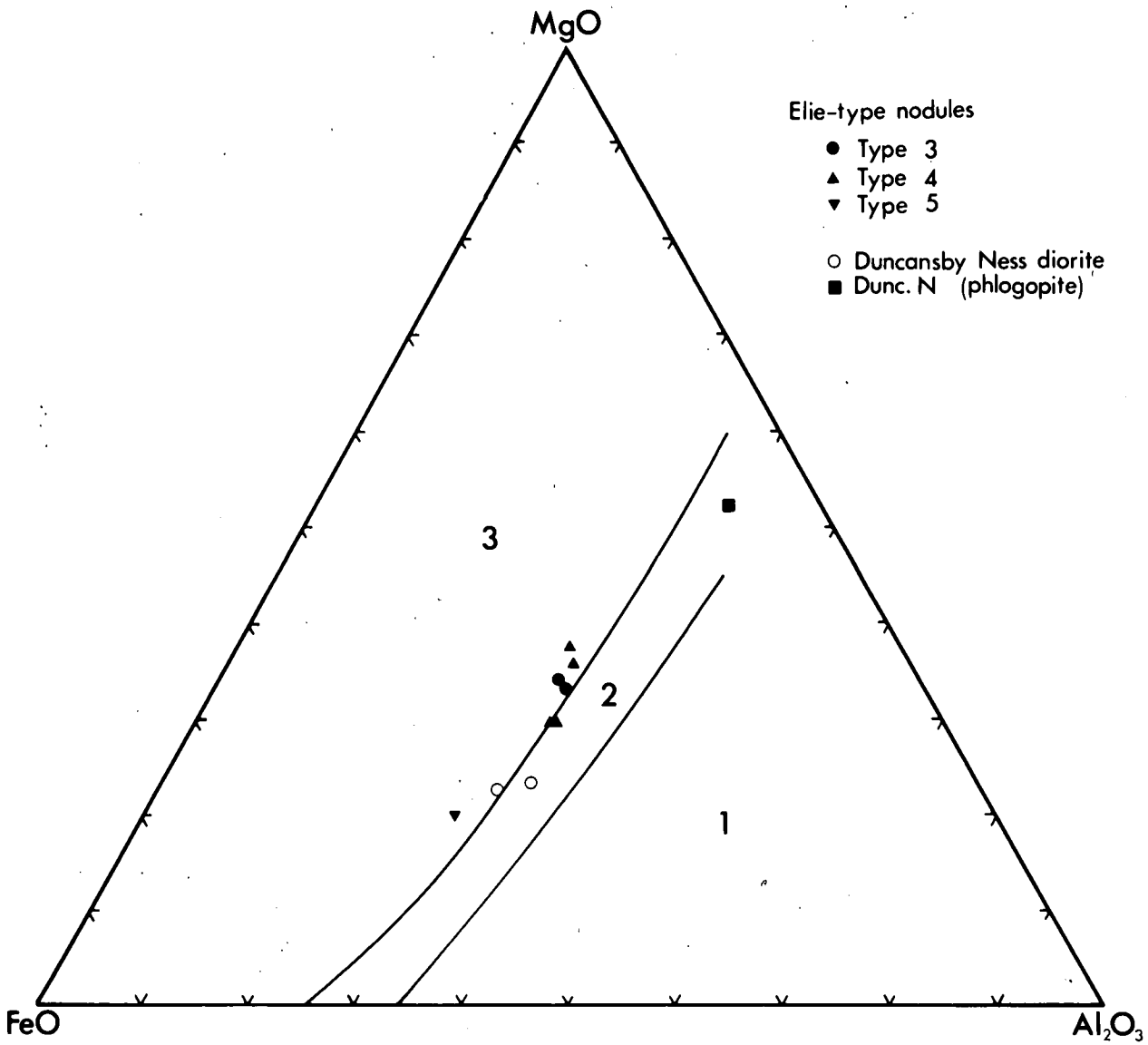
MgO
FeO
Al_2O_3
3
2
1
Elie-type nodules
Type 3
Type 4
Type 5
Duncansby Ness diorite
Dunc. N (phlogopite)

with hornblende, pyroxene or olivine. The FeO:MgO variation shows that biotites from groups 3 and 4 nodules formed before those from group 5 nodules, assuming a cognate origin. This is supported by the more titaniferous nature of the group 5 biotites.

e) Garnet.

Garnet is only found as megacrysts in the tuff at Elie Ness. Of the two varieties previously described, the supposed xenocrystal pink almandine has not been studied in detail. The deep-red, glassy garnets are chemically consistent and no great variations have been noted from one specimen to another, or within any particular crystal. Their average composition is pyrope-rich, $Alm_{20}Py_{66}Gr_{14}$. The low Cr_2O_3 content is variable from 0.01 to 0.19% being most consistent at 0.08%. Similarly the TiO_2 content is relatively high at 0.4%. Colvine (1968) compared the chemistry of the Elie pyropes to those garnets of similar bulk compositions found in crustal and nodular garnet-peridotites and eclogites and as xenocrysts in kimberlites and diatremes. Chrome and titanium content of the Elie pyropes set them apart from the majority of the other occurrences, chrome generally being much lower and titanium much higher in the Elie specimens. The only closely corresponding garnet was pyrope from an alnöitic breccia pipe. Colvine concluded that owing to the Elie pyrope's dissimilarity with the garnets from other environments it was unlikely to be a xenocryst from the breakdown of an ultrabasic body, and that it may have crystallised from basic alkaline magma at depth. The high MgO and low Fe_2O_3 (0.4%) content of the pyrope

suggested either a highly magnesian magma or a highly oxidised magma, the latter case allowing little FeO to enter the garnet structure. The relative contents of TiO_2 and Cr_2O_3 in the pyrope tend to support Colvine's theory that they crystallised from an alkalic melt, the generally titaniferous and chrome-poor nature of other phases crystallised from the Fife rocks having already been noted.

f) Opaque phases.

Titanomagnetite and ilmenite are the main opaque minerals occurring in the nodules together with scattered pyrite. Types 3 and 5 nodules are apparently free of opaque phases, and within the limits of available data there seems to be little significance in the variation in chemistry of those occurring in the other nodule groups. One specimen (P32) of a Type 2 nodule shows minor ilmenite-titanomagnetite exsolution which indicates a slow rate of cooling compared to the titanomagnetites of the basalts. Where sulphide occurs in nodules it is generally surrounded by calcite which tends to indicate a late-stage origin.

Lherzolitic, wehrlitic and clinopyroxenite nodules and inclusions.

This section deals with the nodules and inclusions of lherzolite, wehrlite, and clinopyroxenite from all the localities studied.

a) Clinopyroxenes.

Data from all samples and localities is presented in the C-M-F system in Fig. 4-9 together with the associated orthopyroxenes and olivines, where present.

Fig. 4-9

Clinopyroxenes, orthopyroxenes and olivines from lherzolites, wehrlites and pyroxenites in the mole % C-M-F system.
X denotes the area within which all the analysed orthopyroxenes and olivines from spinel-lherzolite inclusions fall.

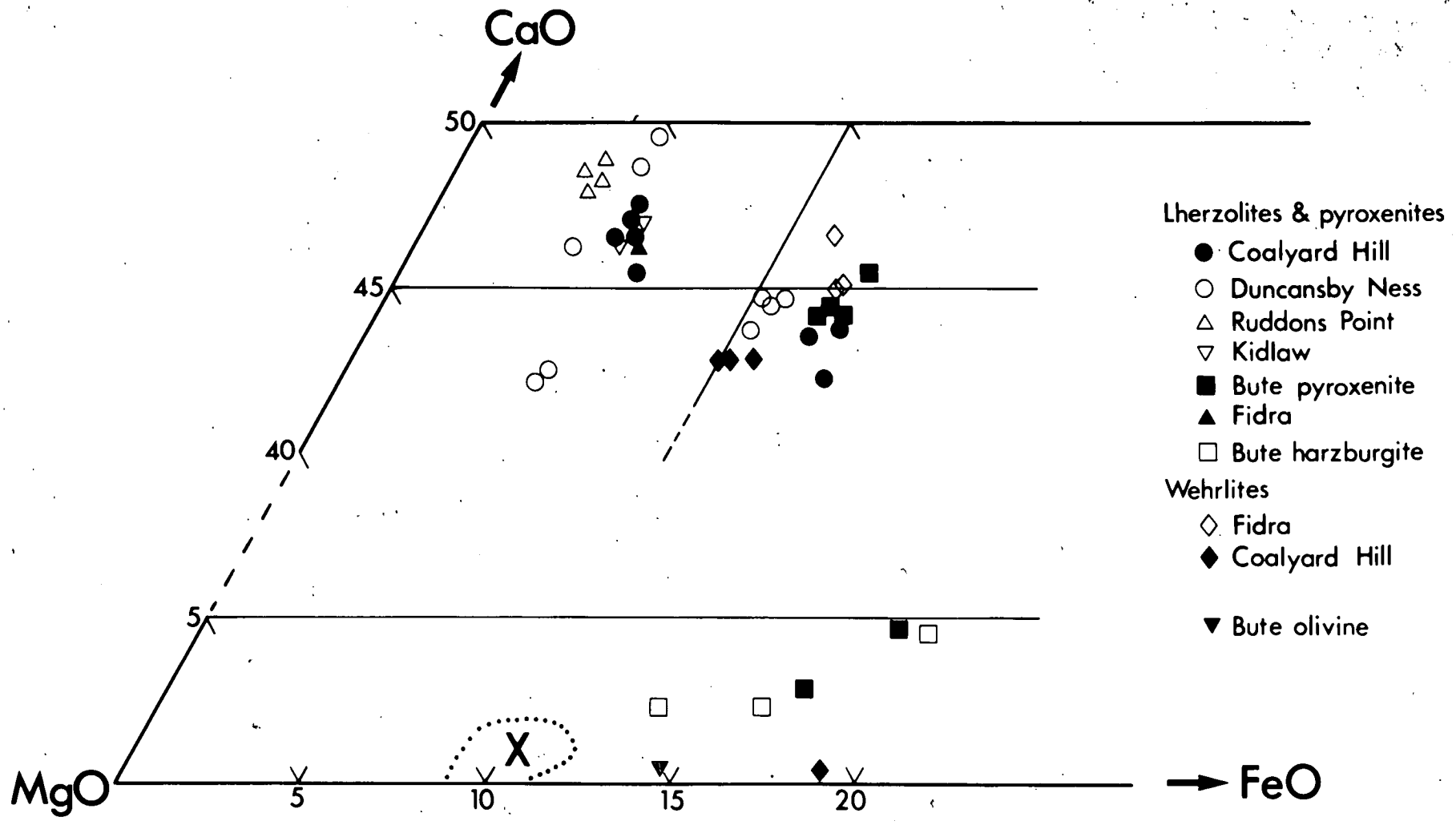
CaO
50
45
40
5
MgO
5
10
15
20
X
FeO
Lherzolites & pyroxenites
Coalyard Hill
Duncansby Ness
Ruddons Point
Kidlaw
Bute pyroxenite
Fidra
Bute harzburgite
Wehrlites
Fidra
Coalyard Hill
Bute olivine

Dealing first with the clinopyroxenes from lherzolites and the Duncansby Ness spinel-wehrlites; all the analyses plotted to the left of the 10% FeO line in fig. 4-9 fall into this group. All the clinopyroxenes from lherzolites plot in the diopside field and contain from 0.5 to 0.7% Cr_2O_3 which is within the range of chrome-diopsides from peridotite nodules in basalts and kimberlites, though generally lower than average. Alumina varies from 4.5 to 7.5% with TiO_2 generally less than 0.6%. Alumina in the Duncansby Ness diopsides is lower (4.5 - 5%) than in the Fife and East Lothian diopsides (6.5-7.5%). Variation in the FeO/MgO ratio is minimal. As with alumina Na_2O is lower (0.8%) in the Duncansby diopsides than in those from other localities ($\simeq$ 1.8%).

Clinopyroxenes from a spinel-wehrlite nodule from Duncansby Ness are less calcic than the diopsides from the lherzolites, falling in the endiopside field. Alumina is the lowest (4.3 to 4.6%) of any of the clinopyroxenes analysed from peridotite nodules and inclusions, though soda (1.74%) and TiO_2 (0.57%) are comparable with the Fife and East Lothian material. Cr_2O_3 is substantially higher at 1.71% than in the lherzolite diopsides.

The clinopyroxenes from pyroxenites and the Fidra and Coalyard Hill wehrlites all plot to the right of the FeO = 10% line in Fig. 4-9. The clinopyroxenites from Bute and Coalyard Hill are monominerallic, whilst those from the Duncansby Ness tuff contain approximately 5% spinel thought to be exsolved from the pyroxene. All plot in the high-magnesium augite or salitic-augite field. Alumina content varies between localities, the Bute augites having

7.1 to 7.8%; Coalyard Hill 8.0 to 8.3% and Duncansby Ness 9.0 to 9.2%. Na_2O content in the Duncansby Ness and Coalyard Hill augites is higher (1.1 to 1.4%) than in those from the Bute clinopyroxenite (0.9%). The Duncansby Ness augites are more magnesian than those from the other two localities.

Augites from the two wehrlite inclusions plot within the same area on Fig. 4-9 as those from clinopyroxenites. The Coalyard Hill specimen is less calcic than the spinel-bearing augite from Fidra. It is also less aluminous and titaniferous, but richer in silica, soda and magnesia. The Fidra augite is slightly richer in chrome.

b) Orthopyroxene.

Orthopyroxene is present as a primary phase only in the lherzolite and harzburgite inclusions, and also as rare exsolution lamellae in the Bute clinopyroxenite. All the orthopyroxenes from lherzolites plot in a restricted field close to the enstatite-bronzite boundary in Fig. 4-9. Those from the Bute harzburgitic inclusion and those exsolved from the Bute clinopyroxenite are more calcic (up to 2.3% CaO) and richer in iron, falling in the bronzite field.

There is little significant chemical variation within the enstatites, all are aluminous with Al_2O_3 from 3.3 to 4.8%, corresponding to similar orthopyroxenes from peridotite inclusions in basalts.

c) Olivine.

Owing to the high degree of alteration of olivine it has only

been possible to analyse samples from two of the lherzolites, from Fidra and Ruddons Point, and the harzburgite from Bute. As was noted with the orthopyroxenes the Bute olivine is also more iron-rich than its counterparts from the other two localities. The latter are very similar in composition (Fo_{90}) and plot within the enstatite field of lherzolites on Fig. 4-9, on the forsterite-chrysolite boundary. The Bute olivine has Fo_{85} and hence falls into the chrysolite group.

Only one analysis was obtained from the wehrlite inclusions, and is also a chrysolite (Fo_{81}) from the Coalyard Hill specimen. This compares in composition with the more magnesian phenocrysts discussed in 4.1a.

d) Spinel.

Chrome-spinel is a common phase in the lherzolite inclusions and is also found in the Fidra wehrlite. Microscopic exsolution lamellae of chrome-spinel have been found in diopside from a Coalyard Hill lherzolite inclusion (Plate 14). Both Cr_2O_3 content and FeO/MgO ratio are often slightly variable within spinels from any one inclusion, though Cr_2O_3 is always between 8 and 12% in those from lherzolite inclusions. The spinel found as exsolution in diopside is very similar in composition to the other spinels from the same inclusion although it is slightly less chromian.

The FeO/MgO ratio of the spinels from lherzolites in Fife and East Lothian are all closely clustered around 0.5 whereas the Dunsansby Ness lherzolite has a more chromian spinel with FeO/MgO =

0.83. Similarly, the spinel from the Fidra wehrlite is very iron-rich (FeO/MgO = 1.5) and much less chromian (3 to 5%) than those of the lherzolite inclusions.

Chrome-free ($< 0.05\%\ Cr_2O_3$) spinel-hercynites are found in the massive clinopyroxenites from Duncansby Ness and as has been previously noted, are thought to have exsolved from the augite. These are highly aluminous spinels with FeO/MgO ratios of 0.9, lying between the spinel and hercynite solid-solution end-members.

e) Mica.

Mica, considered to be a primary phase, has only been noted in one nodule, a wehrlite from Duncansby Ness. It is highly magnesian and using Deer et al's convention noted in 4-2d it falls well into the phlogopite field with MgO/FeO = 5.8 and is also mildly titaniferous (TiO_2 = 3.8%). The analysis is plotted on Fig. 4-8. Both Na_2O and Cr_2O_3 are enriched compared with most phlogopites (cf. Dawson and Smith, 1973).

CHAPTER FIVE

Clinopyroxene solid-solutions and alumina variations as indicators of P-T-X conditions of origin.

Analyses of clinopyroxenes show that they contain several pyroxene components in varying proportions. The relative amounts of these components seem to be closely related to the physico-chemical conditions under which the pyroxene crystallised or equilibrated. Kushiro (1962) proposed that the Ca-Tschermak ($CaAl_2SiO_6$) component in particular is a strong indicator of P-T-X conditions and White (1964) proposed that the ratio of Ca-Tschermaks molecule to jadeite ($NaAlSi_2O_6$) could be used to distinguish eclogitic pyroxenes from granulitic pyroxenes. Aoki (1970) notes that recent work indicates that the jadeite and Ca-Ts components are largely P dependent, whereas the Ti-Tschermak ($CaTiAl_2O_6$), Ferri-Tschermak ($CaFe(3)AlSiO_6$) and Ferridiopside ($CaFe(3)_2SiO_6$) components are largely dependent on composition (X) of the liquid from which the pyroxene crystallised. The jadeite and Ca-Ts variations are not in fact simply dependent on pressure (c.f. O'Hara, 1969) and this will be discussed in more detail later in the chapter. Distribution of aluminium between the tetrahedral and octahedral (Al(4) and Al(6)) lattice sites of clinoproxenes can also be used as a physico-chemical indicator. Thompson (1947) suggested that on increasing temperature aluminium preferentially enters four-fold co-ordination whilst with increasing P it enters six-fold co-ordination.

The effects of some of these P-T-X dependent factors has been briefly mentioned in Chapter 4 in respect to some of the chemical trends displayed by the pyroxenes, and it is now intended to examine these more closely. Nine end-member molecules have been recalculated from the microprobe analyses using a computer programme described in Appendix 4. Kushiro's (1962) method has been observed when recalculating the analyses, but this necessitates a knowledge of the ferric and ferrous proportions. The amount of ferric in the pyroxenes has been estimated, assuming stoichiometry, by a charge-balancing method (Appendix 4). The end-members and Al(4) -Al(6) ratios were then calculated using the ferric-corrected analyses.

Al^4 and Al^6 ratios.

Diagrammatic presentation of data for clinopyroxenes from all localities is subdivided in the same manner as Chapter 4 and Al^4-Al^6 ratios for:-

a) Phenocrysts (cores and rims) and groundmass pyroxenes

b) Elie-type nodules and megacrysts

c) Lherzolite, wehrlite, and clinopyroxenite inclusions and nodules are presented in Figs 5-1, 5-2, and 5-3 respectively. The three fields of eclogites, granulites and inclusions in basalts, and igneous rocks are after Aoki and Kushiro (1968).

Fig 5-1 shows a sharp division to exist between phenocryst cores and corresponding phenocryst rims and groundmass pyroxenes, located along the igneous/granulite divide. This suggests that the phenocrysts started to crystallise within the lower granulite

Fig. 5-1

Al(4) and Al(6) values of phenocryst and groundmass clinopyroxenes. The three named fields are after Aoki and Kushiro (1968).

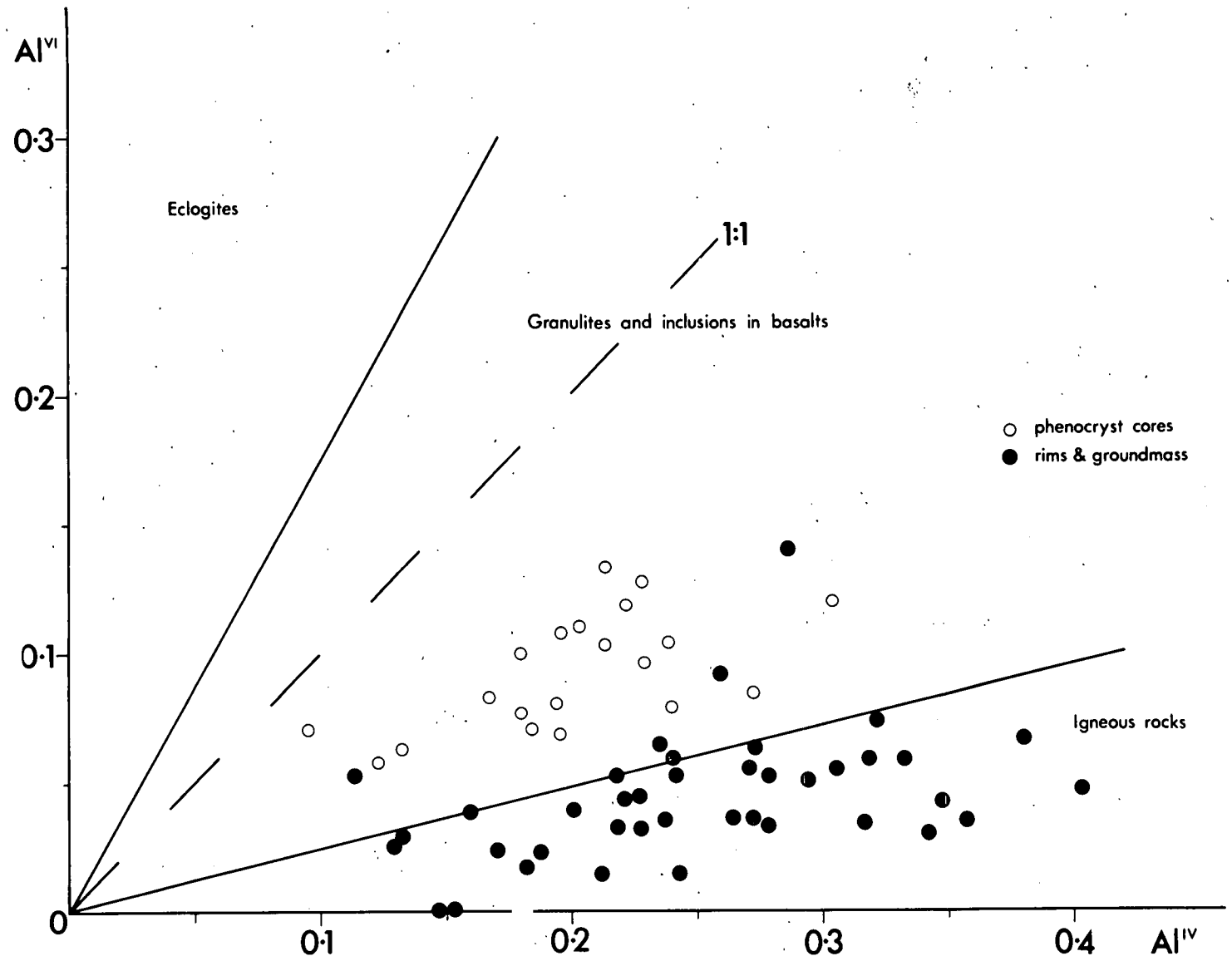
Al^VI
0·3
0·2
0·1
0
Eclogites
1:1
Granulites and inclusions in basalts
phenocryst cores
rims & groundmass
Igneous rocks
0·1
0·2
0·3
0·4
Al^IV

facies, a rather ill-defined PT zone, but probably in excess of 4kb (Turner, 1968). Comparison with Fig 5-2 shows a considerable overlap of the phenocryst core pyroxenes with those from Type 1 nodules (as already noted in Fig 4-6). It is suggested that the pyroxenes from Type 1 nodules and the phenocryst cores crystallised under very similar P-T-X conditions, and hence that the Type 1 nodules are cognate. Pyroxenes from Type 2 nodules have considerably less Al(4) than those of Type 1, though all have similar Al(6) values. The relative values of Al(4) and Al(6) indicate that pyroxenes from Type 2 nodules formed at lower temperature and somewhat higher pressure than those from Type 1, but within the granulite field. The textures and mineralogy of the Types 1 and 2 nodules indicate crystallisation from a similar environment, whereas the more alkaline chemistry of the Types 3, 4 and 5 nodules indicates that these may have formed in a different chemical system, possibly all three in the same one. Pyroxenes from Type 3, mica-pyroxenite nodules lie on both sides of the granulite/eclogite divide and are depleted in Al(4), suggesting a low T and relatively high P origin.

The calcium-poor 'glassy' and 'dark' megacrysts from the Elie Ness tuff show the largest Al(6) content in this group and are comparable in this respect with diopsides from the lherzolite inclusions (Fig 5-3) though also being rich in Al(4), indicating that they must have crystallised at high temperatures and pressures within the upper granulite field, or the lower eclogite field. The 'dark' megacrysts show a generally higher Al(4) than the 'glassy' ones.

Fig. 5-2

Al(4) and Al(6) values of clinopyroxenes from Elie-type nodules and megacrysts.

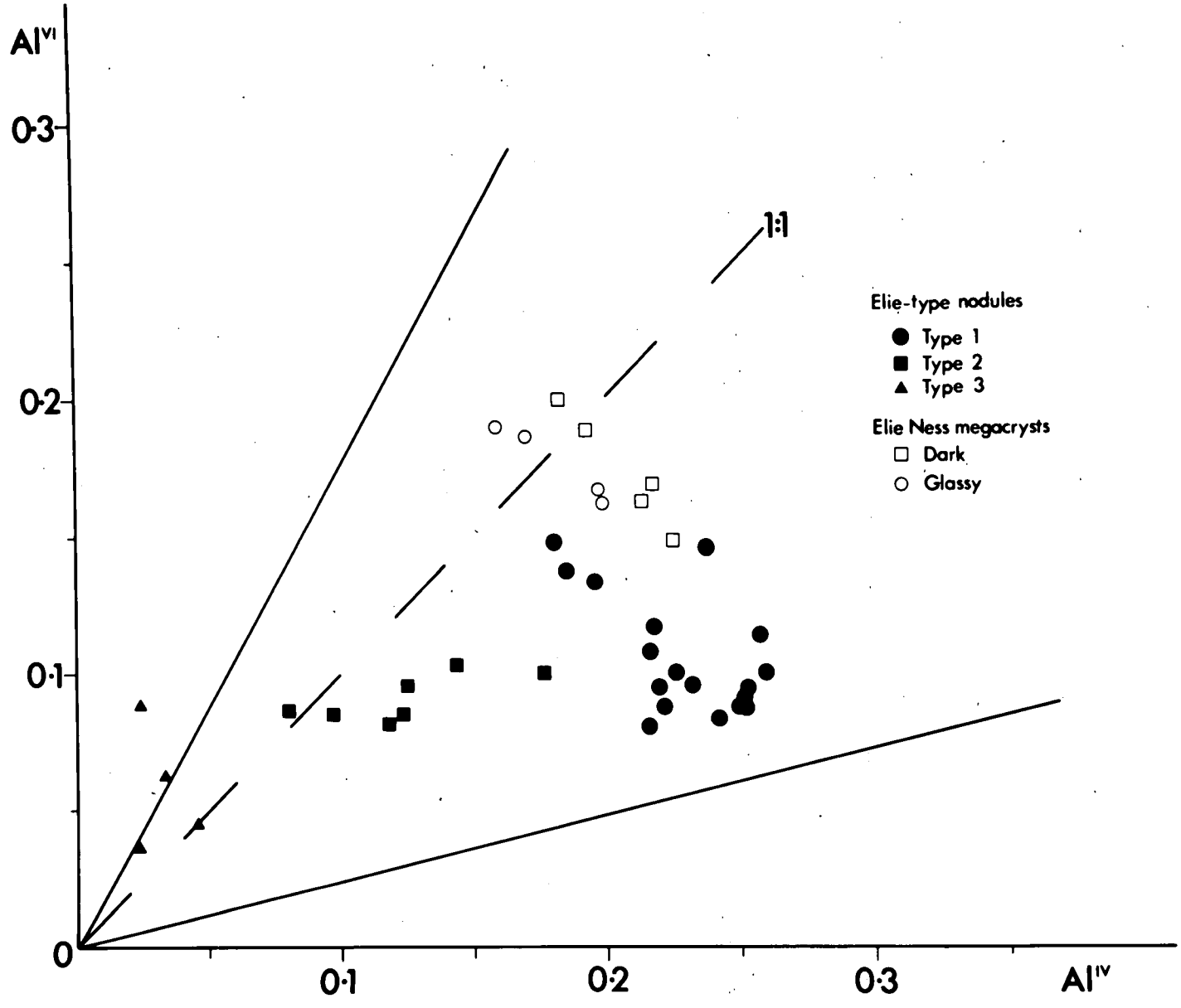
Al^{VI}
0·3
0·2
0·1
0
1:1
Elie-type nodules
Type 1
Type 2
Type 3
Elie Ness megacrysts
Dark
Glassy
0·1
0·2
0·3
Al^{IV}

Fig. 5-3

Al(4) and Al(6) values of clinopyroxenes from lherzolites, wehrlites and pyroxenites.

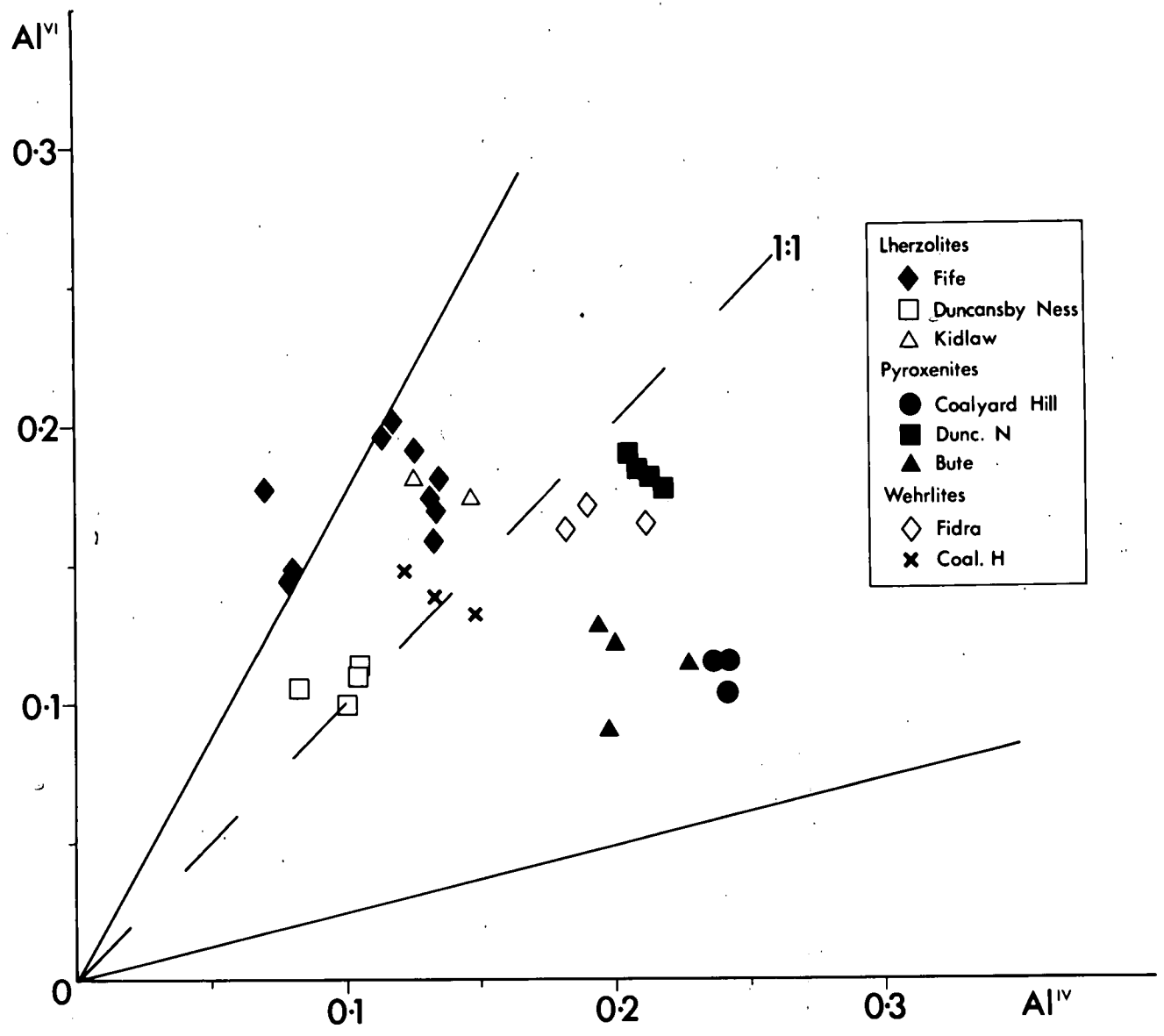
Al^VI
0·3
0·2
0·1
0
0·1
0·2
0·3
Al^IV
1:1
Lherzolites
Fife
Duncansby Ness
Kidlaw
Pyroxenites
Coalyard Hill
Dunc. N
Bute
Wehrlites
Fidra
Coal. H

Diopsides from lherzolite inclusions presented in Fig 5-3 display the highest Al(6) values of pyroxenes studied and are comparable in pressure regime with the Elie megacrysts though of lower T origin. Little variation exists in the diopsides from Fife and East Lothian lherzolites and all lie along the eclogite boundary or in the upper granulite field. Those from the Duncansby Ness lherzolite and wehrlite inclusions are, however, poorer in Al(6), and possibly of a lower P origin. The difference in mineral chemistry of these pyroxenes from that of the lherzolites has already been discussed in Chapter 4.

Turning to the wehrlites, the augites from the Fidra specimen (spinel-bearing) apparently formed at both high P and T, and in fact plot close to the spinel-clinopyroxenites from Duncansby Ness. Augite from the Coalyard Hill wehrlite is poorer in both Al(4) and Al(6) though falling within the upper granulite field.

The monominerallic clinopyroxenites of Coalyard Hill and Bute are probably of lower P origin than the other pyroxenes in this group, and in fact overlap the Type 1 nodule augites in terms of their Al(4) and Al(6) values, though being compositionally different.

End-member variations.

Figs 5-4 to 5-6 show the same pyroxene groupings used previously plotted on what Aoki (1970) suggests to be a largely P-X dependent diagram. Jadeite and Ca-Ts being the P dependent phases are plotted against the X dependent Ti-Ts, Ferridiopside and Fe-Ts molecules. This is an oversimplified view of the actual P-T-X

variations of the pyroxene end-members which will be discussed in more detail later, but serves as an adequate corollary to the Al(4)-Al(6) diagrams.

Recent work suggests that at high pressures Al enters the clinopyroxene structure in the form of Ca-Ts, and as jadeite, thus increasing the Na content above that present as acmite. At lower pressures and in an alkaline environment the Ti-Ts molecule becomes stable. Yagi and Onuma (1968) report Ti-Ts to be unstable above 10kb. The highly aluminous and titaniferous nature of the late-formed pyroxenes show this late enrichment in Ti well. The gradual depletion in Na in the pyroxenes when the liquid is becoming progressively more sodic emphasises the instability of jadeite with decreasing pressure. When discussing Figs 5-4 to 5-6 several points regarding the calculation of the components should be noted:-

a) Acmite ($NaFe(3)Si_2O_6$) is calculated first so that if Fe(3) is greater than Na no jadeite will be formed, but Fe-Ts will.

b) Similarly, if Na is greater than Fe(3) jadeite will be formed but no Fe-Ts.

c) Acmite is present in almost all pyroxenes, but the ferri-diopside component is only rarely present.

This effectively means that pyroxenes with a jadeite component are plotted against Ti-Ts only, whilst those with no jadeite are Ca-Ts Ti-Ts + Fe-Ts plots only. The 1:1 line denotes Aoki's (1970) 'high' and 'low' pressure fields.

Fig 5-4 shows the phenocryst cores and rims and groundmass pyroxene relationships and leads to a similar conclusion to that drawn from Fig 5-1; i.e. that the phenocryst cores formed at high pressures, though no quantitative value can be determined in this manner. Huckenholz (1973) notes a similar trend through increasing Fe-Ts and acmite with fractionation in clinopyroxenite fragments from basanites in the Hocheifel and Dreiser Weiher. The Iki Island phenocrysts studied by Aoki all plotted below the 1:1 line along with their groundmass equivalents.

Comparison with Fig 5-5 reinforces the hypothesis that Type 1 nodule augites come from a similar environment to the phenocryst cores, due to the degree of overlap. Those from Types 2 and 3 nodules again plot well into the high pressure field and the extremely low Ti-Ts (Fe-Ts = 0) content of the Type 3 augites is apparent. This diagram also emphasises the high pressure nature of the Elie megacryst pyroxenes, which are again comparable with the diopsides from the lherzolites.

Fig 5-6 supports some of the correlations brought out by a study of Fig 5-3. The diopsides and endiopsides of Duncansby Ness lherzolites and wehrlites appear much lower down on the 'P' axis than those from Fife and East Lothian localities, and the Fidra spinel-bearing wehrlite again lies close to the spinel-clinopyroxenite of Duncansby Ness, showing a higher pressure origin than the equivalent wehrlite specimen from Coalyard Hill, which is spinel-free.

The clinopyroxenites from Bute and Coalyard Hill, apart from

Fig. 5-4

End-member variations of phenocryst and groundmass clinopyroxenes.

(mole %)

Ca-Ts...Calcium Tschermaks Ti-Ts...Titanium Tschermaks
Fe-Ts...Ferritschermaks FeDi...Ferridiopside

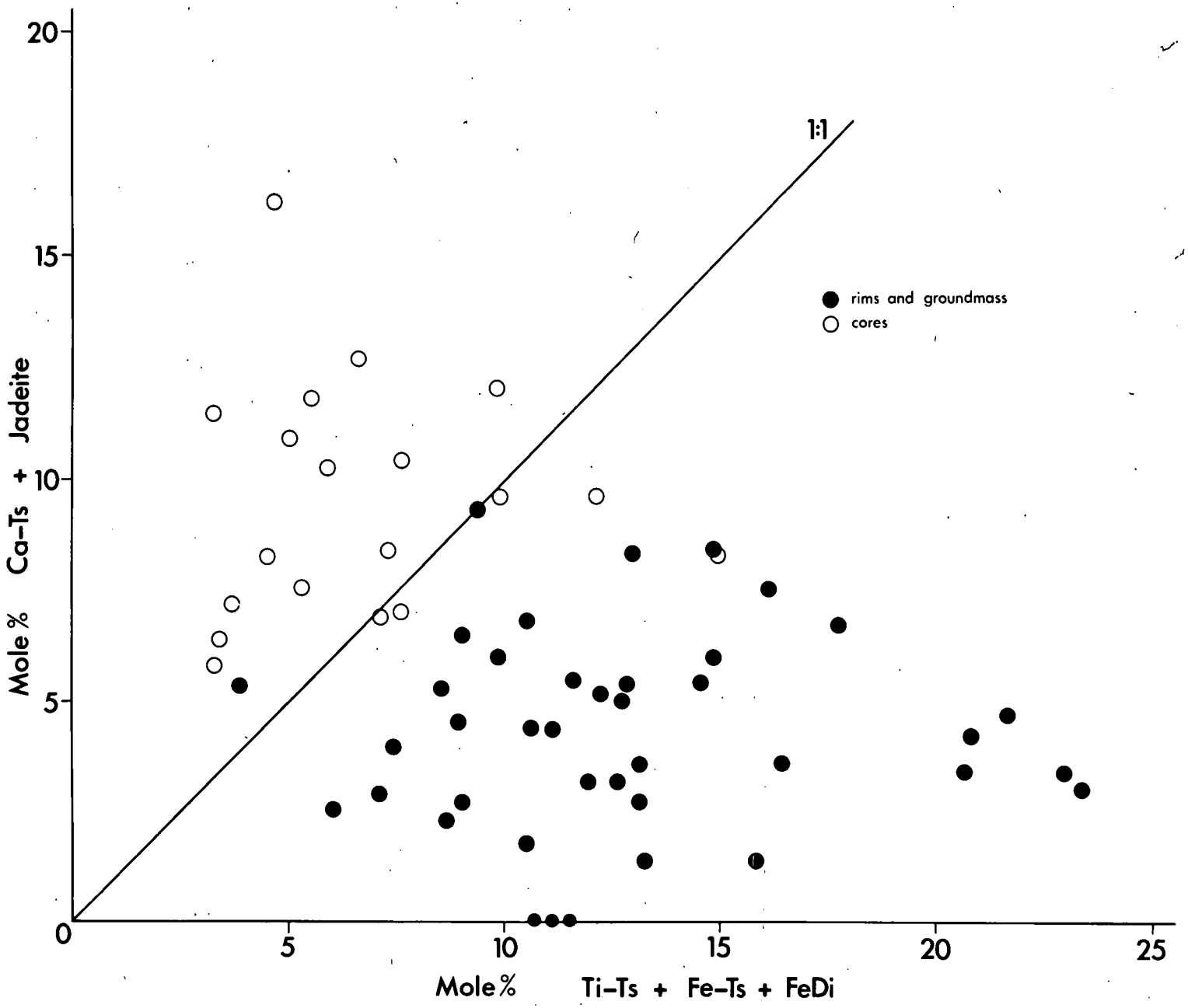
20
15
10
5
0
5
10
15
20
25
1:1
rims and groundmass
cores
Mole % Ca-Ts + Jadeite
Mole % Ti-Ts + Fe-Ts + FeDi

Fig. 5-5

End-member variation of clinopyroxenes from Elie-type nodules and megacrysts. (see Fig. 5-4)

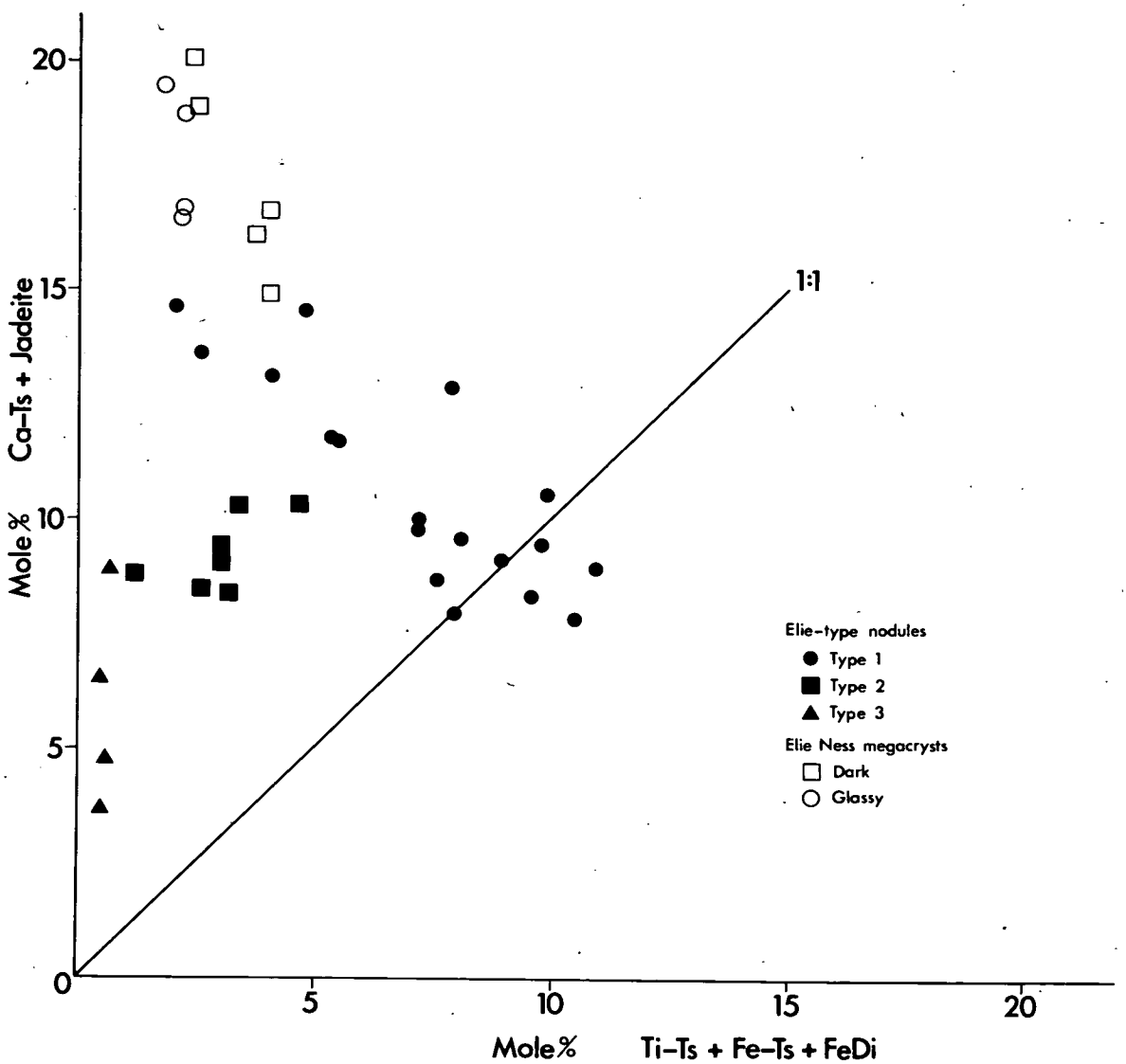
20
15
10
5
0
Mole% Ca-Ts + Jadeite
1:1
5
10
15
20
Mole% Ti-Ts + Fe-Ts + FeDi
Elie-type nodules
Type 1
Type 2
Type 3
Elie Ness megacrysts
Dark
Glassy

Fig. 5-6

End-member variation of clinopyroxenes from lherzolites, wehrlites and pyroxenites. (see Fig. 5-4)

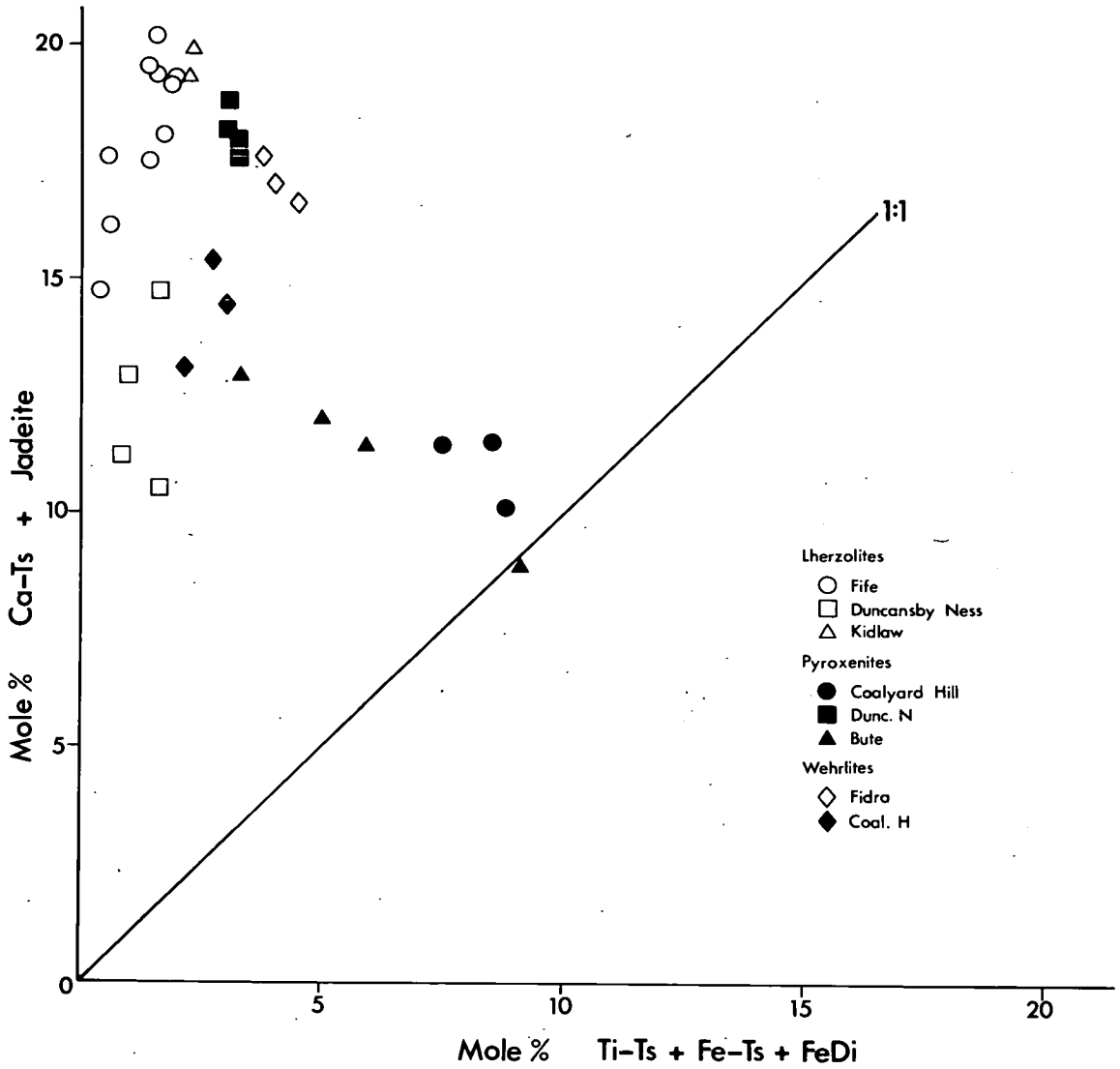
20
15
10
5
0
5
10
15
20
1:1
Mole % Ca-Ts + Jadeite
Mole % Ti-Ts + Fe-Ts + FeDi
Lherzolites
Fife
Duncansby Ness
Kidlaw
Pyroxenites
Coalyard Hill
Dunc. N
Bute
Wehrlites
Fidra
Coal. H

plotting low on the 'P' axis, also have higher proportions of Ti-Ts molecules and overlap the field of Type 1 nodule augites. This would suggest crystallisation under conditions where the Ti-Ts component had attained a large degree of solubility in the pyroxene structure, and following the data of Yagi and Onuma indicates formation at pressures less than 10kb.

Ca-Tschermak : jadeite relationship.

In the foregoing discussion it has been assumed that both Ca-Ts and jadeite are largely P dependent components, though this is a rather simplified explanation.

Cohen, Ito and Kennedy (1967) performed experimental melting work on a tholeiitic basalt (NM5) and found that feldspars on the solidus become progressively more sodic with increasing pressure. Within the granulite facies assemblage the An component dissolves in the clinopyroxene as Ca-Ts, with the Ab component remaining as increasingly sodic plagioclase. Within the eclogite facies the Ab component also dissolves in the clinopyroxene as jadeite, with the final feldspar composition being An_{25-40}. They concluded that the upper pressure limit of feldspar is dominantly the upper limit of albite. If sufficient clinopyroxene is present all the Ab component will enter it and the higher pressure reaction of Ab = jadeite + quartz will be insignificant. Within the eclogite assemblage the aluminous pyroxene breaks down to form garnet. When Ca-Ts and Mg-Ts move out of the pyroxene to form garnet a more sodic pyroxene will remain. The data on NM5 tends to support the theory that Ca-Ts is more stable

within the granulite facies and jadeite more stable in the eclogite region.

Experimental studies on Na-bearing synthetic lherzolite compositions (Herzberg, 1974) show that jadeite does not appear in solidus clinopyroxenes until pressures greater than 17kb, and that in the sub-solidus region the amount of jadeite present in the structure is affected more by pressure than by temperature. Herzberg's data on sodium-free lherzolite compositions also show that in the granulite region the amount of Ca-Ts present in sub-solidus clinopyroxenes is more dependent on temperature than on pressure. Hays (1967) provided direct evidence of the temperature dependance of Ca-Ts stability in his work on the system $CaO-Al_2O_3-SiO_2$. Pure Ca-Ts is not stable below 1160°C and the pressure field of stability is relatively narrow, even at high temperatures. On increasing pressure Ca-Ts breaks down to form grossular and corundum. The presence of the Ca-Ts component in a pyroxene is an indicator of high temperature combined with moderate pressure.

Fig 5-7 shows the clinopyroxenes from nodules, inclusions and megacrysts plotted to show the relationship between Ca-Ts and jadeite on a figure similar to those of White (1964) and Ito and Kennedy (1968). The actual amount of jadeite estimated to be present in a clinopyroxene structure depends on method of calculation. Kushiro's method, used in this work, calculates acmite first and then assigns any remaining Na to jadeite. The amount of acmite present depends on the Fe(3) value and Ito and Kennedy's method of calculation first adds all Cr to the Fe(3) hence increasing acmite at the expense of

Fig. 5-7

Calcium Tschermaks - Jadeite relationships in clinopyroxenes from all inclusion, nodule, and megacryst types.
The 2 · 3 line separates the fields of 'granulites' and 'eclogites' according to Ito and Kennedy (1968).

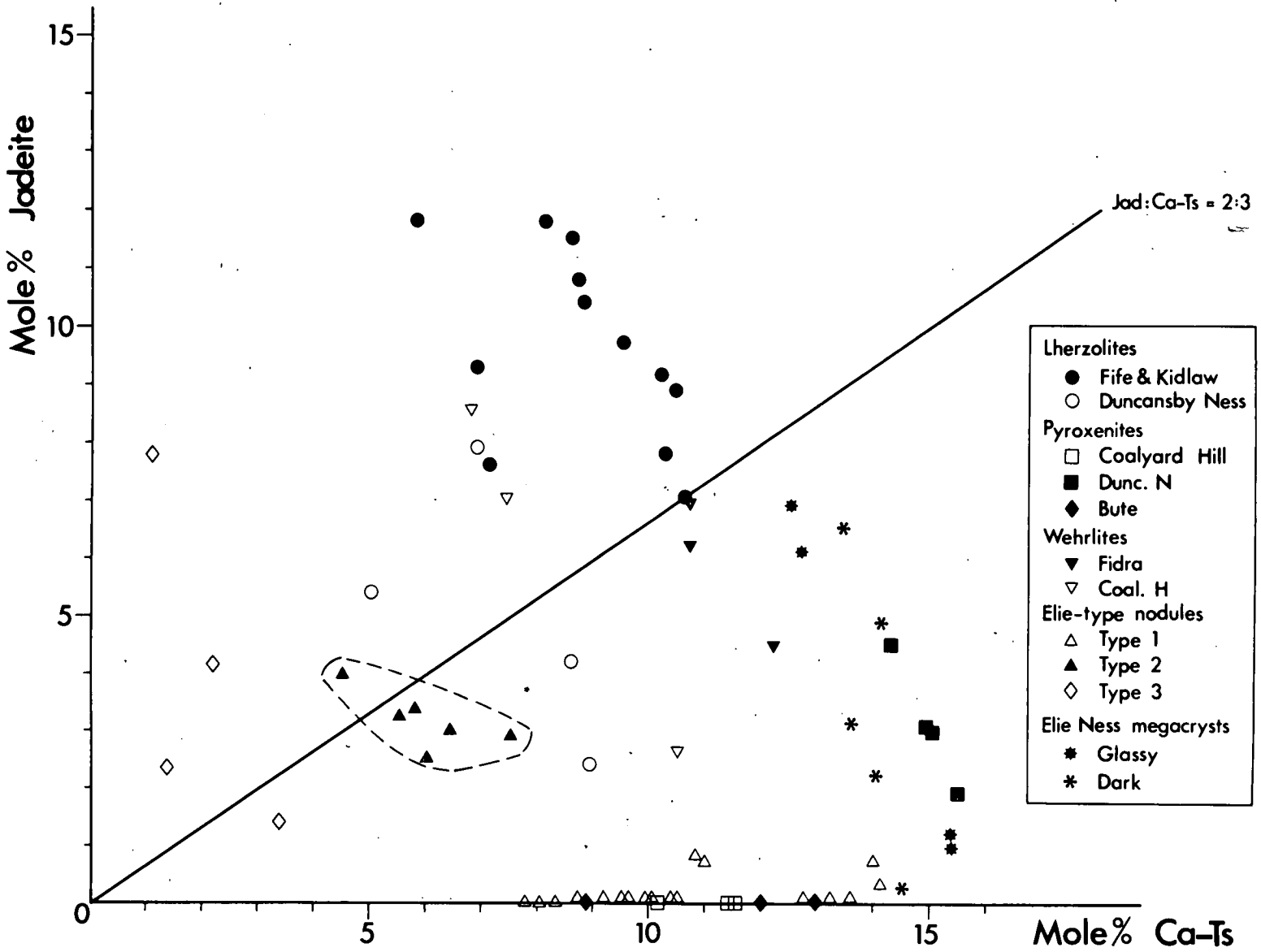
Mole% Jadeite
Mole% Ca-Ts
0
5
10
15
Jad:Ca-Ts = 2:3
Lherzolites
Fife & Kidlaw
Duncansby Ness
Pyroxenites
Coalyard Hill
Dunc. N
Bute
Wehrlites
Fidra
Coal. H
Elie-type nodules
Type 1
Type 2
Type 3
Elie Ness megacrysts
Glassy
Dark

jadeite, whereas Kushiro and White both assign Cr to Al, thereby increasing the Ca-Ts and jadeite values. The behaviour of Cr in the pyroxene structure may follow that of either Al or Fe(3), the latter case allowing for the least possible amount of jadeite, assuming either Cr is present in acmite and Fe-Ts or that a soda-chrome molecule ($NaCrSi_2O_6$) is formed before jadeite. Recalculation to form a soda-chrome component reduces acmite, though jadeite naturally is the same as in Ito and Kennedy's method. Since some weight is put on the amount of jadeite present in the following discussion, the effect of calculating the soda-chrome component has been tested. As might be expected, only those pyroxenes with a significant amount of Cr_2O_3 are affected (i.e. those from lherzolites and wehrlites) and these plot lower on the jadeite axis, straddling the 2:3 line. The other points are only slightly affected. The jadeite : Ca-Ts = 2/3 line separates the 'eclogite' and 'granulite' fields according to Ito and Kennedy. Division into these fields is in fact only valid for low temperature parageneses as O'Hara (1969) noted when discussing the jadeite / Ca-Ts ratio of sub-calcic clinopyroxenes formed in equilibrium with garnet at 30kbs. Whilst plotting well within the 'eclogite' region at 1100°C, isobaric increase in temperature moved the clinopyroxenes well into the 'granulite' field at 1400°C. This correlates closely with Herzberg's findings that the proportion of Ca-Ts solid-solution is more dependent on T than on P. O'Hara's data shows a substantial rise in the Ca-Ts component at the expense of jadeite, which in one instance (A3/10596) moved from 5% jadeite to zero jadeite with a rise of almost 15% in

the Ca-Ts content over a 340°C temperature increase.

Examination of the jadeite content of the analysed pyroxenes shows that none of the phenocryst rims or groundmass pyroxenes contains jadeite and that the phenocryst cores are almost all jadeite-free. Fig 5-7 also shows the augites from Type 1 nodules and the clinopyroxenites from Bute and Coalyard Hill to be jadeite-free, apart from four analyses which all have less than one percent jadeite. As noted previously from Fig 5-6 the similarity between the two clinopyroxenites and the Type 1 nodules suggests them to have crystallised in a similar X environment with the clinopyroxenites crystallised at possibly slightly higher pressure, though less than 10kb. This conclusion was drawn from their overall higher Ca-Ts content, though on Fig 5-7 this can be seen to be less apparent, and as discussed above, may well be more a function of higher temperature of crystallisation.

Augites from Type 2 nodules contain from 2-4% jadeite. They also co-exist with albite. Comparison with Cohen et al's data on the increase in albite content of plagioclase with pressure suggests the Type 2 nodules to have formed at considerably higher pressure or lower temperature than the Type 1 nodule pyroxenes, at some pressure where Na would enter the pyroxene, possible in the upper granulite field. The Type 3 mica-pyroxenite nodules display a wide variety of jadeite contents with a very low Ca-Ts percentage, which may indicate a low temperature origin at high pressure.

A range from 0.5 to 7% jadeite is displayed by the Elie Ness megacrysts, and a range from 12.5 to 15.5% Ca-Ts. Both types of

Table 5-1

Comparison of Elie Ness sub-calcic augite megacryst composition with pyroxenes from garnet-lherzolites and eclogites.

Oxide	Elie Cpx	A	B	C	D
SiO_2	51.00	54.76	55.91	50.20	51.19
Al_2O_3	8.16	8.33	2.54	8.37	8.85
TiO_2	0.62	0.44	0.30	0.51	0.29
Fe_2O_3	0.47	1.30	-	1.58	0.51
FeO	5.84	2.70	5.66	5.72	4.82
MgO	16.73	11.59	21.37	19.00	19.12
CaO	15.86	16.35	13.65	13.28	13.84
Na_2O	1.17	4.63	1.50	0.87	0.85
K_2O	0.00	0.05	-	0.02	0.00
Cr_2O_3	0.18	-	0.32	0.24	0.20
MnO	0.14	0.04	0.15	0.16	0.17
Total	100.17	100.19	101.40	99.95	99.84

A. Eclogite nodule E4, Kao kimberlite pipe, Lesotho. From p.108 of 'Lesotho kimberlites' ed. P.H.Nixon, 1973.

B. Garnet-pyroxenite nodule, 1600 C7B, Thaba Putsoa. From p. 68 of 'Lesotho kimberlites' (ex. Boyd and Nixon).

C. Garnet-pyroxenite xenolith, 68SAL-6, Salt Lake Crater, Oahu. From Yoder and Tilley, 1962, J.Petrol 3, Table 41.

D. Subcalcic clinopyroxenite inclusion in alkaline trachybasalt, 2R MIN-Y, 'Mindora', New South Wales. From J.F.G.Wilkinson, 1973, Contr.Miner. Petrol, 42, Table 6, p 26.

megacrysts have similar Ca-Ts / jadeite ratios to the sub-calcic pyroxenes co-existing with garnet formed in the high temperature (greater than 1300°C) runs described by O'Hara (1969). The fact that these megacrysts are closely associated with pyrope in the tuff suggests that they may have crystallised together within the eclogite facies at high temperatures. In common with the garnets they have significantly higher TiO_2 and lower Cr_2O_3 than similar pyroxenes from eclogites and garnet peridotites (see table 5-1), supporting the theory that they crystallised from an alkaline magma.

The spinel-clinopyroxenites from Duncansby Ness, and the spinel-bearing wehrlite from Fidra both have pyroxenes containing a high proportion of Ca-Ts, suggesting a high temperature origin at elevated pressures. The difference between the Duncansby Ness lherzolites and wehrlites and the lherzolites from other localities is again apparent, the Duncansby Ness specimens plotting with much lower jadeite contents. Bearing in mind the limitations of this type of diagram discussed previously in this chapter it is considered unwise to place too much emphasis on the amount of P-T variance which may appear to exist between any two plotted pyroxenes in quantitative terms. The diagram does, however, serve to indicate the overall high-pressure nature of the pyroxenes discussed, and the high temperature origins of some of them.

CHAPTER SIX

Evidence of mineral parageneses from high-pressure and temperature experiments

In the course of the previous discussions three hypotheses have emerged which can be tested by experimental duplication of possible conditions of mineral origin.

a) The chrome-free spinel in the Duncansby Ness clinopyroxenites may have exsolved from the augite.

b) Large anorthoclase megacrysts, apparently not in reaction with their host-rocks crystallised from the magma at high temperatures and possibly at depth within the crust.

c) The sub-calcic clinopyroxene megacrysts from the Elie Ness tuff co-precipitated with the associated pyrope garnets under conditions of high pressure within the mantle.

In order to test these theories a series of experiments has been performed at elevated pressures and temperatures using solid-media apparatus and internally heated gas-vessels. The techniques of operation are described in Appendix 3. All results, unless otherwise noted, are from dry natural material and are listed in Tables 6-1 to 6-3.

a) Spinel-clinopyroxenite.

The amount of spinel present in the Duncansby Ness clinopyroxenites is difficult to determine due to the large crystal size relative to the size of the nodules. Three methods have been attempted

to gain an estimate of the possible overall proportions. Simple point-counting on ten thin-sections gives the widest scatter of data with 3 to 11% modal spinel depending on the specimen. Simple extract calculations using whole-rock XRF analysis of a nodule and microprobe analyses of the constituent spinel and pyroxene give answers of 5-7% (by weight) spinel. Digestion of the clinopyroxene in hydrofluoric acid leaves the spinel unattacked and two experiments in which the spinel residue is compared with the initial sample weight gave slightly more than 4 wt % spinel. All the methods suffer from sample inhomogeneity, so in the runs it was decided to use four compositions to bracket the estimated values, and to produce a spinel-clinopyroxene phase diagram. The compositions used were: $Sp_{2.5}Px_{97.5}$, $Sp_{6}Px_{94}$, $Sp_{8.2}Px_{91.8}$, $Sp_{11}Px_{89}$ (in weight percent).

The aim of the runs was to determine whether and to what extent spinal could be dissolved in the pyroxene under sub-solidus conditions, and hence show whether it was possible for all the spinel to have exsolved from the pyroxene. All the runs were performed at 18kb, in the region where spinel would be expected to exsolve from a pyroxene rather than garnet. The results are shown in figure 6-1. An XRD peak-height ratio method (Sp-Px) was used to estimate the amount of free spinel remaining in the charge after each run. Concurrent with the solution of spinel in the pyroxene a marked increase was noted in the pyroxene $22\bar{1}$ XRD peak, due to increase in alumina content. Analyses of the starting material and the pyroxenite nodules are presented in Table 6-4.

In Fig 6-1 it can be seen that an estimated 6 out of the 11%

Fig. 6-1

Results of dry 18kb runs on spinel-clinopyroxenite compositions.

cpx...clinopyroxene sp...spinel gl...glass

Numbers adjacent to run points indicate estimated weight percent of spinel remaining in the charge after the run.

X----X is estimated composition of the nodules.

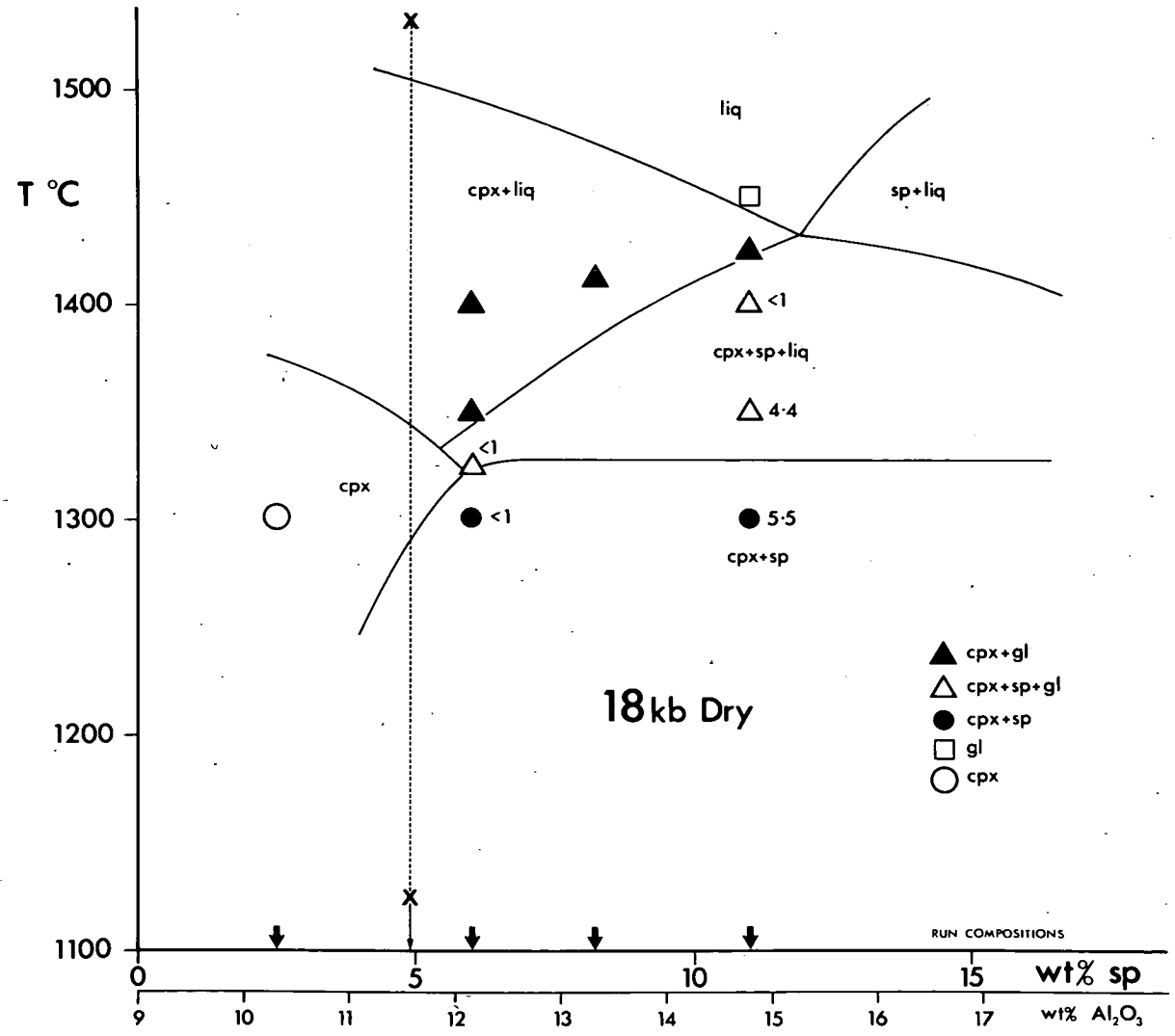
1500
T °C
1400
1300
1200
1100
liq
cpx+liq
sp+liq
<1
cpx+sp+liq
4·4
<1
cpx
<1
5·5
cpx+sp
18kb Dry
cpx+gl
cpx+sp+gl
cpx+sp
gl
cpx
RUN COMPOSITIONS
0
5
10
15
wt% sp
9
10
11
12
13
14
15
16
17
wt% Al_2O_3

spinel in the $Sp_{11}Px_{89}$ composition dissolved in the augite below the solidus. Similarly it is seen that the bulk of the spinel in the Sp_6Px_{94} composition entered the augite structure below the solidus. Within the limits of the data available from the experiments it appears that the maximum amount of spinel able to enter the natural augite before liquid appears, is about 6%. The decrease in the amount of free spinel remaining in the $Sp_{11}Px_{89}$ charges above the solidus may be due solely to spinel entering the liquid phase, and it is thus possible that no more spinel dissolves in the augite above the solidus. If 6% spinel can dissolve in the augite under sub-solidus conditions, it follows that an equivalent amount could exsolve from the spinel-saturated augite (which would contain over 12% Al_2O_3). The best available data shows the actual spinel content of the nodules to be about 5%. It is thus possible for all the spinel in the nodules to have exsolved from the augite. In this case the homogenised augite would have contained over 11.5% Al_2O_3 prior to spinel exsolution, and would be correspondingly depleted in calcium (18.4% CaO). Fig 6-1 shows that isobaric crystallisation of a composition equivalent to that of the bulk-nodule would commence at about 1500°C with clinopyroxene as the liquidus phase. The solidus would be encountered at about 1350°C and at a temperature of about 1300°C the cooling augite would intersect the Sp-Cpx solvus and spinel would be exsolved. Hence at this pressure and under dry conditions, the spinel in the pyroxenite nodules could have been entirely exsolved from the augite provided the original pyroxene crystallized from some magma of its own or other suitable composition at a temperature greater than 1300°C but less than 1350°C. Chemical data (see Chapter 5)

also indicates the augite to have had a high temperature and moderately high pressure origin.

It would appear that the conditions chosen for the runs closely parallel the actual conditions of formation. At higher pressures ($P > 20kb$) garnet may have exsolved instead of spinel. The fact that the apparent saturation limit of 6% spinel is close to the observed natural composition of the nodules is consistent with the proposition that the pressure conditions were close to the natural condition of formation. Similarly, had water activity been significant at the time of formation amphibole would be expected to be present in quantity, and the depression of the solidus and liquidus temperatures would have restricted the extent of the aluminous pyroxene field to less than Sp_5Px_{95}.

A similar black spinel-pyroxenite described by Kutolin and Frolova (1970) from Siberia has a whole-rock alumina content of 16.5% and on Fig 6-1 would fall close to the Sp-Cpx-Liq eutectic at 1430°C, indicating that this nodule may have formed as a spinel-pyroxene co-precipitate.

b) Anorthoclase stability at 5, 10 and 15kb.

The intention of this project was to determine the upper P-T stability limits of anorthoclase megacrysts in their host-rock. For this purpose the Ruddons Point locality was chosen to provide starting material as the host-rock is relatively fresh.

Anorthoclase was cleaned and crushed down to relatively large fragments (up to 140 microns, average of 40 microns) and mixed with

the crushed basalt (RPB) which had a grain size of 5-20 microns, to attain a composition with 10.07% anorthoclase. This allowed for easy optical identification of anorthoclase. XRD identification is complicated by the overlap of anorthoclase $1\bar{3}0$ and plagioclase $1\bar{3}0$ peaks, though the excess peak heights due to addition of 10% anorthoclase allows for determination of the approximate amount present in a run.

Runs were carried out at 5, 10 and 15kb and the results are shown in Fig 6-2. The estimated solidus and liquidus positions for RPB are shown; the liquidus coincides closely with that determined for the tholeiite NM5 by Cohen et al though the solidus is some 40-50° lower. Significant iron-loss to the Pt capsules was noted in the 10 and 15kb runs (solid-media) so only short run-times (15-30 minutes) were used. In the gas-media runs where the run length was ten days welded iron capsules were used to prevent iron-loss, although some gain in iron or reduction of the charge may take place.

Anorthoclase is a near liquidus phase at 5kb. At 10kb it is stable below the solidus, showing no signs of corrosion, but disappears above the solidus. At 15kb the anorthoclase is metastable, showing signs of marginal corrosion in short sub-solidus runs, and if the run time is increased disappears altogether, though in a two hour run the iron-loss is substantial. The loss of magnetite above the solidus may also be caused by severe depletion of iron in the charge.

If anorthoclase crystallised from a melt of similar composition to RPB then the upper pressure limit beyond which it is no longer present in the melting interval is 8-9kb, with an upper temperature

Fig. 6-2

Results of dry runs on 10 % anorthoclase 90 % RPB composition.

Dashed line is estimated stability limit of anorthoclase in the presence of liquid.

cpx...clinopyroxene mag...magnetite gl...glass anr...anorthoclase

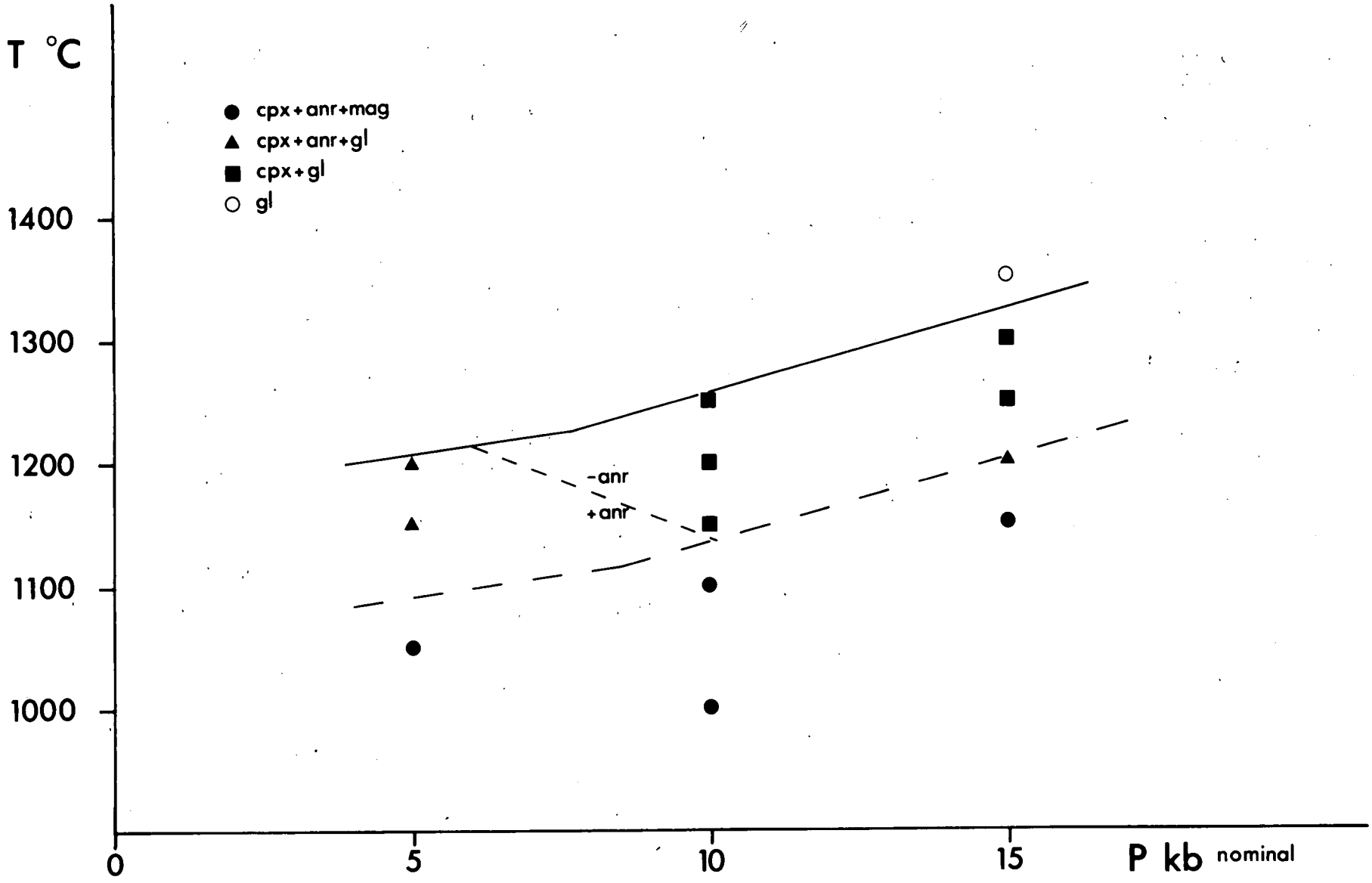
T °C
cpx+anr+mag
cpx+anr+gl
cpx+gl
gl
1400
1300
1200
1100
1000
-anr
+anr
0
5
10
15
P kb nominal

limit of 1150-1200°C, and this limit is tentatively portrayed on Fig 6-2 as a dashed line. It is, however, more probable that the anorthoclase megacrysts crystallised from a highly alkaline body of trapped residual liquid, probably in a wet system which would tend to lower its P-T stability range, possibly to a maximum of 5-6kb. These experiments, however, serve to put a limit on the P-T conditions under which anorthoclase could be expected to crystallise from this basic liquid.

c) Elie Ness garnet-clinopyroxene.

The aim of this series of experiments was to determine the conditions under which the Elie Ness glassy sub-calcic augite megacrysts are just stable with garnet, and to compare the compositions of garnet exsolved from the augite with that of the pyrope megacrysts.

Experiments were carried out on finely crushed powder at pressures from 20 to 30kb, with an average run length of seven hours. Iron-loss was found to be appreciable only at temperatures approaching the pyroxene solidus. Microprobe data suggests iron-loss 250° below the solidus to be minimal. The results of the runs are presented in Fig 6-3. Garnet which exsolved from the augite at 30kb (1250°C) was analysed, the results being compared with the Elie pyrope in Table 6-5. As can be seen the exsolved garnet is richer in grossular than the Elie pyropes though displaying similar chemistry in all other respects. TiO_2 and Cr_2O_3 are comparable with the values from the pyrope which reinforces the supposition that the garnets from Elie may have crystallised from a basaltic melt. Fig 6-4 shows the phase relations determined for the augite on which are superimposed data

Fig. 6-3

Results of dry runs on Elie Ness, glassy, sub-calcic augite.

Upper dashed line represents pyroxene solidus, lower dashed line represents upper limit of garnet exsolution.

cpx...clinopyroxene gt...garnet

A...run from which final charge components were analysed.

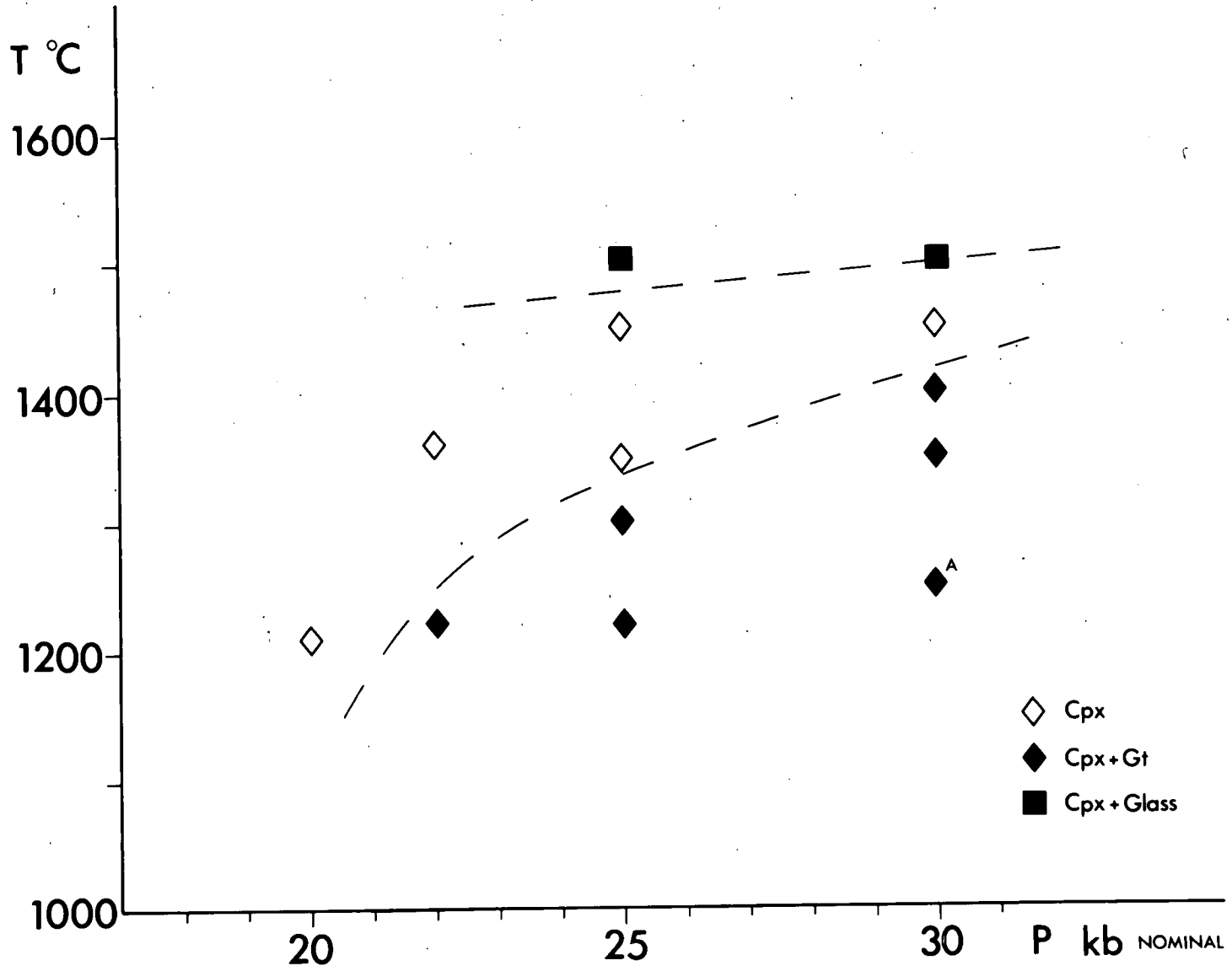
T °C
1600
1400
1200
1000
20
25
30
P kb NOMINAL
A
Cpx
Cpx + Gt
Cpx + Glass

taken from Cohen, Ito and Kennedy (1967), O'Hara et al (1971), and the present work.

Cohen's tholeiitic liquidus coincides with that determined for RPB, and the lower temperature RPB solidus is also shown. The 'garnet-in' of the tholeiitic melting interval is taken from Cohen et al, and the spinel to garnet lherzolite facies boundary from O'Hara et al..

The Elie augite readily exsolves large quantities of garnet at temperatures up to 250°C below the solidus, but at higher temperatures outside the garnet exsolution field shows no signs, either optically or on X-ray trace, of enstatite exsolution. Examination of Fig 6-4 shows a lengthy univariant condition on which this clinopyroxene could co-exist with garnet in a basaltic liquid. It will be noted that this univariant lies below the tholeiite solidus but above the extrapolated RPB solidus, thus allowing an alkali basalt melt to crystallise clinopyroxene and garnet within the garnet-lherzolite facies.

The most probable host-liquid would be a partial melt of garnet-peridotite at pressures not less than 30kb, with crystallisation of garnet and augite taking place possibly down to 25kb and 1350°C. From Fig 6-4 it can be seen that any gradual drop in temperature would cause augite to exsolve garnet whilst still in the basalt liquid field at pressures in excess of 25kb, a feature which is not observed in the Elie augites. Similarly the progressive drop in P experienced by a magma rising along the basalt liquidus would result in garnet becoming unstable at $P < 20$kb and reacting back into the liquid, a

Fig. 6-4

Results from Fig. 6-3 on which are superimposed basalt melting data.

A is tholeiite (NM5) liquidus (Cohen et al. 1967) and also the extrapolated RPB liquidus (this work).
B is the tholeiite solidus (NM5).

RPB is the extrapolated RPB solidus.

Spinel to garnet-lherzolite facies boundary after O'Hara et al. (1971).

'garnet in' line after Cohen et al.

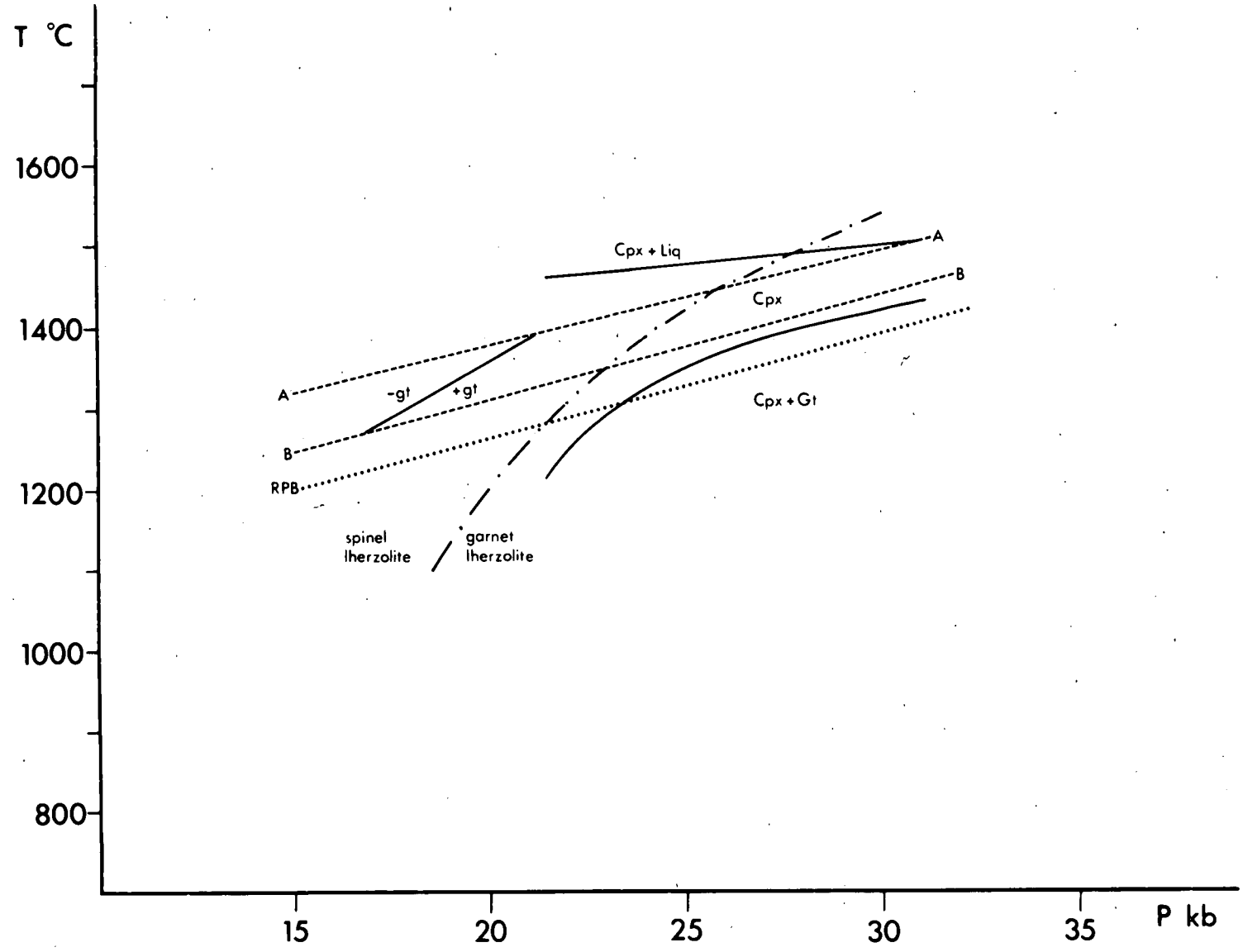
T °C
1600
1400
1200
1000
800
15
20
25
30
35
P kb
Cpx + Liq
A
B
Cpx
A
-gt
+gt
Cpx + Gt
B
RPB
spinel
lherzolite
garnet
lherzolite

feature which is obviously not observed with the Elie pyropes.

Hence any model for the formation of the Elie Ness pyropes and augites must allow for:-

a) An initial partial melt at P in excess of 30kb.

b) Co-precipitation of garnet and augite at 1350-1400°C, 25-30kb.

c) An ensuing rapid rise to the surface from depths in the order of 75-100kms before garnet becomes unstable in the liquid.

All the experiments described in this chapter have been under dry conditions. The presence of water would undoubtedly depress the RPB liquidus a little, and this should be borne in mind when considering the figures discussed above.

Table 6-1

Plotted run results on anorthoclase-RPB samples.

Run No.	P kb	T °C	Time mins.	Cap.	Phases.
An-1	10	1000	360	Pt	Cpx, Anl, Mag
An-3	10	1000	60	Pt	" " "
An-4	10	1100	30	Pt	" " "
An-6	10	1200	30	Pt	Cpx, Gl
An-7	10	1150	30	Pt	Cpx, Gl, ?Anl
An-8	10	1250	20	Pt	Cpx, Gl
An-9	15	1150	40	Pt	Cpx, Anl, Mag
An-10	15	1200	30	Pt	Cpx, Anl, ?Gl
An-11	15	1250	30	Pt	Cpx, Gl
An-12	15	1300	20	Pt	Cpx, Gl
An-13	15	1350	20	Pt	Gl
An-14	15	1200	144	Pt	Cpx, Gl
Gas-1	5	1050	60	Pt	Cpx, Anl, Mag
Gas-2	5	1150	10 days	Fe	Cpx, Anl, Gl
Gas-3	5	1200	12 days	Fe	Cpx, Anl, Gl

Cpx.....Clinopyroxene Anl.....Anorthoclase

Gl.....Glass Mag.....Magnetite

Table 6-2

Plotted run results on spinel-clinopyroxenite nodule.

Run No.	P kb	T °C	Time mins.	Cap.	Phases
11-4	18	1300	360	Pt	Cpx, Sp
11-5	18	1400	360	Pt	Cpx, Sp, Gl
11-X	18	1350	360	Pt	" " "
11-6	18	1450	360	Pt	Gl, QuCpx, Cpx
11-7	18	1425	305	Pt	Cpx, Gl
6-6	18	1300	370	Pt	Cpx, Sp
6-B	18	1325	330	Pt	Cpx, Sp, Gl
6-7	18	1350	360	Pt	Cpx, Gl
6-X	18	1400	360	Pt	" "
2.5-1	18	1300	360	Pt	Cpx
8-1	18	1410	290	Pt	Cpx, Gl

Cpx.....clinopyroxene

Sp.....Spinel

Gl.....Glass

QuCpx.....Quench clinopyroxene

Table 6-3

Plotted run results on Elie sub-calcic augite megacrysts.

Run No.	P kb	T °C	Time mins.	Cap.	Phases
E-1	30	1250	355	Pt	Cpx, Gt
E-2	25	1220	360	Pt	" "
E-3	20	1210	450	Pt	Cpx
E-4	22	1220	450	Pt	Cpx, Gt
E-5	22	1360	450	Pt	Cpx
E-6	25	1350	450	Pt	"
E-7	25	1300	480	Pt	Cpx, Gt
E-8	25	1450	360	Pt	Cpx
E-9	30	1350	390	Pt	Cpx, Gt
E-10	30	1450	405	Pt	Cpx
E-11	25	1500	360	Pt	Gl, QuCpx, Cpx
E-12	30	1400	420	Pt	Cpx, Gt
E-13	30	1500	420	Pt	Gl, QuCpx, Cpx

Cpx.....Clinopyroxene Gt.....Garnet Gl.....Glass

QuCpx.....Quench clinopyroxene

Table 6-4

Composition of Duncansby Ness spinel-pyroxenite phases.

Oxide	Nodule (XR-1)	Augite	Spinel
SiO_2	45.66	49.05	0.12
Al_2O_3	9.53	9.19	61.57
Fe_2O_3	3.08	2.51	NA
FeO	4.14	3.55	17.70
MgO	15.02	14.49	19.76
CaO	17.26	19.16	0.00
Na_2O	1.37	1.24	0.01
K_2O	0.13	0.01	0.00
TiO_2	0.96	1.17	0.48
Cr_2O_3	-	0.01	0.02
MnO	0.06	0.00	-
Total	97.21	100.38	99.65

Trace elements (XR-1)ppm

Ba	T	Ce	T
Zr	T	V	362
Sr	68	La	95
Rb	T		
Ni	266		
Cr	54		

CIPW Norm (XR-1)wt %

Or	0.79	Mag	4.60
Ab	1.53	Il	1.88
An	20.04		
Ne	5.64		
Di	53.52		
Ol	12.01		

T denotes concentrations less than 5ppm.

Table 6-5

Analysis of garnet exsolved from Elie Ness augite at 1250°C, 30kb (point A Fig 6-3) compared with that of an average pyrope megacryst from the same locality.

Oxide	A	Pyrope
SiO_2	41.30	41.60
Al_2O_3	23.20	23.30
FeO	10.20	10.60
MgO	16.00	18.20
CaO	8.30	5.30
TiO_2	0.80	0.40
Cr_2O_3	0.04	0.08
MnO	0.00	0.35
Total	99.84	99.83
Mole % end-members based on CaO, MgO and FeO.		
Pyrope	57.80	66.30
Grossular	21.50	13.70
Almandine	20.70	19.30

CHAPTER SEVEN

Petrogenesis

Spinel-lherzolite inclusions as upper-mantle xenoliths.

There has been much controversy as to whether spinel-lherzolite inclusions in basalt represent primary or depleted mantle materials, or whether they are cognate accumulates from basaltic liquids at depth. The bulk of evidence is interpreted as supporting the former possibilities, and a mantle-fragment origin has been accepted by most authors. O'Hara and Mercy (1963) and O'Hara (1965, 1968) devised a mechanism whereby lherzolite fractionation could account for the production of ne normative liquids from originally hy normative liquids, and he pointed out the rarity of spinel-lherzolites in kimberlites. This absence is explained if they are not normally mantle components. The spinel-lherzolite inclusions in basalt have higher alumina, iron, soda and lime and lower magnesia than garnet-lherzolite nodules in kimberlite. This is the reverse of what would be expected if they were residua of partial melting of garnet-lherzolite. These chemical features will be referred to again later in this discussion. Brothers (1960), in an early paper on lherzolite inclusions from New Zealand, suggested them to be cumulates which developed a fabric within the olivine by convective flow during settling.

Much of the refutation of a cognate origin is based on various isotope data which usually show isotope ratios to differ significantly

between inclusions and their host basalts. Kleeman et al (1969) and Kleeman and Cooper (1970) maintain that U, Th, K and Pb isotopic ratios indicate a primary upper mantle origin for lherzolites from Victoria and show that they are not residua of partial-melting. Leggo and Hutchison (1968) and Laughlin et al (1971) produced similar results from Sr^{87}/Sr^{86} ratios. A theory has often been put forward that spinel-lherzolites cannot be accumulations from their host basalts owing to the high Cr content of the inclusions relative to the basalts. This has been criticised by O'Hara (1967). The main point of O'Hara's argument is that if the lherzolites cannot be chemically related to the basalts, then how can the basalts in turn be derived from the lherzolites. (If one assumes spinel lherzolite to represent primary mantle material).

The argument has been advanced that spinel-lherzolite inclusions are samples of a refractory layer in the mantle from which basaltic liquids have been extracted, which may account for their absence in kimberlite pipes. This theory does not, however, account for the higher Mg, Na, Fe, Al etc. of the basalt lherzolites mentioned earlier in this chapter. Reid and Frey (1971) concluded from rare-earth studies that Hawaiian lherzolites were the barren (Ca, Al, Na, K, Ti poor) residue of partial-melting of a garnet pyroxenite, and thus suggested that spinel lherzolite may only be common in mantle regions where basalt genesis has occurred. Indirectly they also concluded that pyroxenite is a common mantle component. Nishimura (1972) also suggested that U isotope studies indicate lherzolite to be a barren mantle residuum. Work by Gramlich and Naughton (1972)

on He/Ar ratios, also on Hawaiian inclusions, again supported a barren mantle residuum origin. Nagasawa et al. (1969), in an extensive study of REE abundances in nodules and basalts, concluded that nodules were the REE depleted residua of partial-melting which produced REE enriched basaltic liquids.

If this refractory model is correct then it is clear that primary mantle material must be richer in the more fusible elements, particularly Na and K, in order to produce basaltic melts. Griffin and Murthy (1969) proposed the presence of phlogopite, hornblende or plagioclase to account for the estimated mantle concentrations of K, Rb, Sr, and Ba, and many occurrences of hornblende or mica-bearing lherzolites (c.f. Duncansby Ness sample, this work) have been noted (Dawson et al. 1970, Dawson and Smith 1973, Varne 1970).

However, experimental work by Kushiro, Syono and Akimoto (1968) has shown that spinel-lherzolite <u>can</u> be partially melted to produce liquids of olivine-tholeiite composition under dry conditions, which brings the generalised 'residuum' theory into question. The fact that spinel-lherzolite inclusions in basalt have a chemistry contrary to that expected were they residua from garnet-lherzolite, and that they have a much lower pressure of equilibration (< 25kb) than the kimberlite nodules, has been brought out in a new review paper by O' Hara, Saunders and Mercy (in press). In any group of spinel-lherzolite inclusions there is positive correlation between high-alumina pyroxene, high mutual solubility of the pyroxenes, and low Mg/Mg+ Fe ratios in the minerals, a correlation that is linear with decreasing pressure and temperature.

This linear correlation also represents the path taken by a rising basaltic liquid such as those in which the inclusions are transported to the surface, and cannot be explained simply by any other known phenomenon (such as diapiric uprise of peridotite). O'Hara et al. conclude that chemical data are only reasonably complied with if spinel-lherzolites are crystal cumulates formed on pipe-walls. Other theories are inadequate in explaining the chemistry. Frey and Green (1974) proposed an initial residual origin for the Victorian lherzolites followed by chemical modification due to contamination by a later phase of basanite liquid to produce the observed REE distributions. This might also explain the higher soda, alumina, and iron concentrations of spinel-lherzolite inclusions, but as a generalised theory would not allow for the texture of many lherzolites which are highly sheared. Chemical modification of a residual lherzolite would demand substantial recrystallisation and re-equilibration prior to transport to the surface to produce the observed textural and chemical features, and even then would not allow for the sheared inclusions often found. It is not disputed that residual spinel-lherzolite would tend to rise in the mantle due to its loss in density, and hence accumulate at a high level where low-pressure equilibration could take place, and also possible contamination by basaltic liquids. However, the speed of eruption of tuff-pipes precludes the lengths of time required for such contaminative recrystallisation to take place. A more likely theory to account for both the chemistry and texture is that put forward by O'Hara et al. for pipe-wall precipitation. Any accumulation at

depth would be subject to a great deal of plastic deformation, such as that observed, due solely to the stresses applied in a rising magma column.

From the above discussion it seems clear that spinel-lherzolite inclusions are intimately associated with basalt genesis and may only be present in areas of the upper mantle where partial melting has taken place. At the present state of knowledge the mantle residuum theory is the most widely held, though it should be stressed that each occurrence has its own unique features and chemistry and in many discussions of spinel-lherzolite origin the conclusions are often over-generalised. Whilst both sides of the argument have compelling features, no one theory can adequately explain all the data from experimental, geochemical, geophysical and isotope sources. When the crystal cumulate theory of O'Hara and others is applied to the Fife specimens it could explain the observed field data, particularly the absence of spinel-lherzolite nodules in the tuff-pipes. These might be expected to occur in a primitive, rapidly erupted gas and liquid stream, were they residual mantle material. It also accounts for the absence of crustal fragments in the spinel lherzolite-bearing sheets, as any eruption violent enough to bring up mantle fragments would also carry crustal fragments to the surface, as was the case with the tuff-pipes.

Cumulate nodules ?

Nodules mineralogically similar to the Elie-type are of wide-spread occurrence in undersaturated basalts. The best documented

examples are from New South Wales, Japan, New Zealand, Dreiser Weiher, and the southern USA and Mexico. They are often associated with feldspar and pyroxene megacrysts, and have generally been assigned a cumulate origin from alkaline magmas within the lower crust. The New South Wales examples (Binns 1969, Binns, Duggan and Wilkinson 1970, Wilshire and Binns 1961) include amphibole-pyroxenite nodules and megacrysts of sub-calcic augite, pleonaste, kaersutite, anorthoclase and ilmenite. Binns et al. (1970) concluded that substantial fractionation of the megacryst phases would only slightly alter the nature of the host liquid and would be insufficient to act as an important agent in the evolution of widely varying basalt types. Dickey (1968) did, however,use this medium to explain the production of a host melanephelinite from alkali-olivine basalt by fractionation of megacrystal anorthoclase, pyrope and hy normative pyroxene. Binns (1969) proposed that both the NSW nodules and megacrysts were cognate phases crystallised near the crust-mantle interface.

Discussing the kaersutite-bearing nodules from Iki Island (Japan) Aoki (1970a) concluded that they were cognate accumulations from within the stability field of kaersutite, which he placed at a maximum of 13kbs (40kms). In a further paper (1970b) he places the co-precipitation of andesine and aluminous clinopyroxene megacrysts at depths of 30 to 60kms in dry conditions. Le Maitre (1969) concluded that since the breakdown of kaersutite (Tristan da Cunha) took place at pressures less than 1.4kb ($P_{H2O} = P_{Tot}$) then the assemblage kaersutite-clinopyroxene-plagioclase would be stable from 1.4 to 6kb in hydrous basalt melts. Borley et al. (1971) limited the conditions

of formation of kaersutite-pyroxenites from Teneriffe to 9-10kb at 960-1015°C. At T > 1015° kaersutite would disappear and clinopyroxenites would be formed. These data agree with the crust-mantle interface origin conditions proposed by Binns.

The Dreiser Weiher locality has been studied in detail by Frechen (1948, 1963) and Aoki and Kushiro (1968) and is very similar in most respects to the Fife tuff-pipes. Mica- and hornblende-wehrlites are considered by Aoki and Kushiro to be cognate, formed in the lower crust from an alkali magma. A similar conclusion is drawn by Trask (1969) for the black pyroxenite nodules from Nevada. Mason (1968) considered kaersutite megacrysts from San Carlos, Arizona to be fragments of mantle material, whilst Forbes and Starmer (1974) consider kaersutite to be a possible source of alkali-olivine basalts rather than crystallising from them. They consider that since wet crystallisation of tholeiite can produce amphibole with up to 4% TiO_2 then fractionation of this could produce an amphibole-rich cumulate which could later melt to form alkaline liquids. This seems sufficiently unlikely on textural and chemical grounds to be unconnected with the origin of kaersutite-rich pyroxenites and wehrlites. Best (1970) describes amphibole-pyroxenites from the Grand Canyon which show the same chemical features as those studied from previously noted areas, and which display poikilitic amphiboles enclosing olivine and pyroxene euhedra. These are very similar to some Type 1 Elie nodules and Best considers them to be cumulates at pressures of about 10kb.

Thermodynamic calculations carried out by Bacon and Carmichael

(1973) purport to give estimates of P-T conditions of equilibration of lavas, nodules and megacrysts from Baja California, Mexico. The results for spinel-lherzolite-lava equilibration are 1330-1410°C at 27.5 to 31.6kb. Calculation for sub-calcic (17.1% CaO) augite and plagioclase megacrysts are based on the equilibrium buffer reaction

jadeite + quartz = albite

and gives a value of 10.5kb, though this is solely an equilibration pressure and does not represent formation conditions in a liquid which may have been of different composition to that in which the megacrysts were found.

Megacrysts of pyrope garnet and glassy sub-calcic pyroxene of very similar composition to those phases from Elie Ness are found in alkaline rocks from northern Nigeria. Frisch and Wright (1971) tentatively proposed that these phases might have crystallised together at depths exceeding 60kms. They are found associated with titanium-pargasite, plagioclase, ilmenite and spinel megacrysts. Dickey (1968) found pyrope and sub-calcic augites as coarse-grained aggregates in tuff from Kakanui (New Zealand), again associated with anorthoclase and hornblende megacrysts. As noted previously Dickey also considered these phases to be cognate, altering the magma composition as they precipitated.

From the above discussion it is clear that most workers have concluded that kaersutite and mica-bearing wehrlites and pyroxenites are cumulates from alkaline magmas, and there is a general agreement on a crust-mantle boundary region for their place of origin.

In the discussion so far a cognate origin has been assumed for

the Elie-type nodules and megacrysts. On a chemical basis alone this is a logical conclusion for the types 1 and 2 nodules. The mineralogical similarity between the pyroxenes of groups 1 and 2 nodules and the pyroxenes of alkali basalts has been discussed in Chapters 4 and 5, and the relevance of the type 1 and 3 amphibole chemistry to the compositions of the Fife basalts is reiterated below. From these data it seems probable that the types 1 and 2 nodules are cumulates from an alkali melt. In Chapter 4 the linearity of the chemical trend linking the types 1, 2 and 3 pyroxenes was taken to indicate a closely related origin. The type 3 biotite-pyroxenite nodules have compositions which consistently place them at the basic end of the Fife basalt trend on simple Harker diagrams, suggesting that they may represent totally crystallised liquids early on the evolutionary cycle. The pyroxene compositions show them to be the earliest formed of the types 1, 2 and 3 augites, with the highest pressure chemistry. On the basis of Ti-Ts content it was suggested that types 1 and 2 pyroxenes must have formed at pressures less than 10kb. It is suggested that the type 3 pyroxenes formed at pressures slightly greater than 10kb, due to their low Ti-Ts and relatively higher jadeite content.

Nodules of type 4 are unusual in containing green, sodic amphibole. Superficially it seems unlikely that this type of nodule could be cognate from a liquid similar to any of the Fife basalts, but the composition of the mica it contains is very similar to that of the type 3 nodules, assumed to be cognate, and, in common with the other phases crystallised from the magma, the biotite is titaniferous.

It is thought that this type of nodule may be a late stage cumulate of a particularly silica-deficient and alkaline liquid, as is indicated by the sodic nature of the amphibole and the albite and the potassic biotite. A similar origin is proposed for the type 5 mica-albite nodules. The titanium- and iron-rich nature of the biotite in these nodules suggests it to have crystallised from a more evolved liquid than those of types 3 and 4.

Thus it is considered that all the Elie nodule types represented in the Fife rocks are cognate fragments from alkaline liquids.

Turning to the megacryst assemblage present in the Fife rocks, previous discussion in Chapters 5 and 6 has shown that both the garnet and sub-calcic augite megacrysts from Elie Ness could represent high-pressure phenocrystsof an alkaline magma. It has not been possible to show conclusively that the anorthoclase megacrysts are cognate but when one considers the widespread occurrence of this type of megacryst in alkali basalts (Best, Hoffer and Hoffer 1973, Laughlin et al. 1974, Grant et al. 1972, Aoki 1970b etc.) and the fact that it is a stable phase within its host-rock, it seems unlikely that any exotic origin could account for this regularity of occurrence. Experimental work has shown that anorthoclase is a near-liquidus phase in the more basic members of the Fife series at relatively high pressures. The presence of a variety of sodic plagioclases and alkali feldspars as nodule components and megacrysts, considered to be cognate, presupposes a highly alkaline liquid to have been present at depth during the evolution of the Fife basalts.

Such a liquid could be formed by closed-system fractionation of pyroxene from a basic alkaline magma. In Chapter 3 it was seen that the concentrations of alkalis in the Fife basalts could only have been significantly increased by the fractionation of pyroxene. It is now proposed to study this proposition more closely.

Fife series.

It was seen in Chapter three that the Fife basalts form a series of limited chemical variation which is controlled largely by the fractionation of olivine and pyroxene though more significantly by pyroxene. Simple fractionation of the nodule or megacryst phases has no significant control over the path taken by the evolving basalts. The most important points of note regarding these basalts are:-

a) Lherzolite inclusions occur only in the most basic, least evolved members of the series. At Coalyard Hill they occur in a sheet occupying a ring-fracture which is indicative of a late stage of intrusion.

b) Alkali-pyroxenite nodules are not found associated with lherzolite inclusions. The host-rocks to these nodules and the basalts associated with them in tuff-pipes are generally of intermediate composition on the Fife trend.

c) Amphibole compositions from nodules and megacrysts closely mirror those of the basalts of intermediate composition, and it is suggested that these amphibole compositions reflect the chemistry of the magma from which they crystallised.

d) The most undersaturated rocks in the Fife series are not host to any type of inclusion or megacryst. (e.g. Elie Harbour).

Projections within the system C-M-A-S.

Projections within the pseudo-quaternary system C-M-A-S have been found useful as a means of presenting analytical data from basic and ultrabasic rocks (O'Hara, 1968). The method of projection and use has been described by Jamieson (1969). The C-M-A-S system is the natural analogue of the synthetic quaternary system $CaO-MgO-Al_2O_3-SiO_2$.

Fig 7-1 shows the Fife basalts projected onto the plane CS-MS-A from olivine (M_2S). Superimposed on these are the 30kb, 15kb and 1bar invariant points described by O'Hara (1968) as representing the compositions of the initial partial-melt products of an average garnet-peridotite (AVG on Figs 7-1 and 7-2). As can be seen the basalts lie on the undersaturated side of the hypersthene-gabbro divide which links diopside (CMS_2) with the Fo-An piercing-point (M_2S-CAS_2). The elongated trend displayed by the rocks is largely a distortion inherent in this particular projection, but supports the chemical trends discussed earlier in the study, with RPB being the most basic basalt, and the Chapel Ness flow being the most undersaturated. It was also considered earlier that the bulk of these rocks were rapidly chilled, high level differentiates. This supposition is reinforced by an examination of the trend in Fig 7-1 which is seen to lie close to the 1 bar An-Di-Fo cotectic. As these

Fig. 7-1

Fife basalts projected onto the plane CS-MS-A from olivine (M_2S) in the pseudoquaternary system C-M-A-S of O'Hara (1968). Further description in text.

RPN....Ruddons Point lherzolite nodule (E-1).
AVG....Average garnet-lherzolite in kimberlite (O'Hara, 1968).
G....Hypothetical 50-50 garnet-augite mix (Elie Ness).
Fo-An....Forsterite-anorthite piercing point.
■....Ruddons Point basalt (RPB)
▼....Chapel Ness basalt.

Dotted line represents locus of invariant points linking the 25 and 30kb invariants of O'Hara (1968).

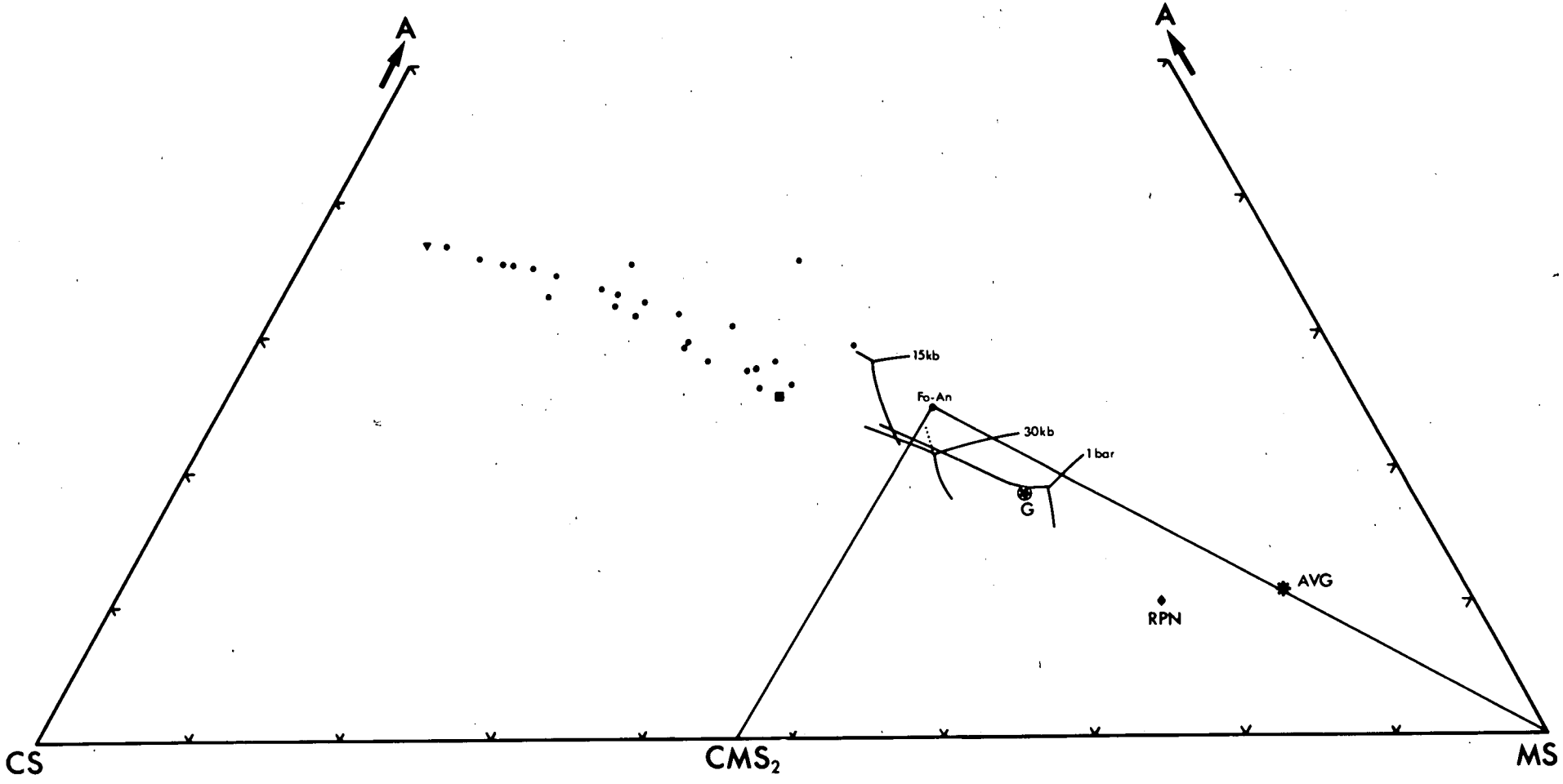
A
A
15kb
Fo-An
30kb
1 bar
G
AVG
RPN
CS
CMS2
MS

three phases are the major phenocryst and microphenocryst constituents of the basalts it seems reasonable to assume that such a low pressure crystallisation trend was followed.

Also shown on this diagram is a hypothetical mixture of 50:50 Elie Ness pyrope and glassy augite megacrysts. In Chapter 6 it was shown that these phases probably crystallised from a primitive magma at pressures of 30-25kb. The locus of invariant points linking the 30kb and 25kb initial partial melts of O'Hara (1968) represents the most MgO and SiO_2 rich liquids from which these would have crystallised. These liquids lie on the silica-saturated side of the Di-Fo/An plane. However, as is discussed later in this Chapter, it is considered that 'vapour-absent' melting of a mica-bearing peridotite would produce liquids which would plot on the under-saturated side of the divide. Fractionation of the garnet-augite mix would produce liquids lying close to the 30kb Gt-Cpx cotectic and close to the basic end of the Fife trend. Fractionation of the 'eclogite' mixture would be unlikely to produce a liquid as undersaturated as RPB, as it would require up to 50% fractionation.

Fig 7-2 shows the same data projected onto the plane C_3A-M-S from diopside (CMS_2). The area occupied by the Fife basalts is shaded and lies below the plane of critical undersaturation in silica. Again it is seen that fractionation of a small amount of the 'eclogite' mix at 30kb from the proposed alkaline, primitive liquid would produce a magma more basic than RPB. The low pressure nature of the more undersaturated members is again emphasised.

Fig. 7-2

Fife basalts projected onto the plane C_3A-M-S from diopside (CMS_2) in the pseudoquaternary system C-M-A-S. (see Fig. 7-1) Further description in text. Symbols are the same as those used in Fig. 7-1.

Di-An....Diopside-anorthite piercing point.

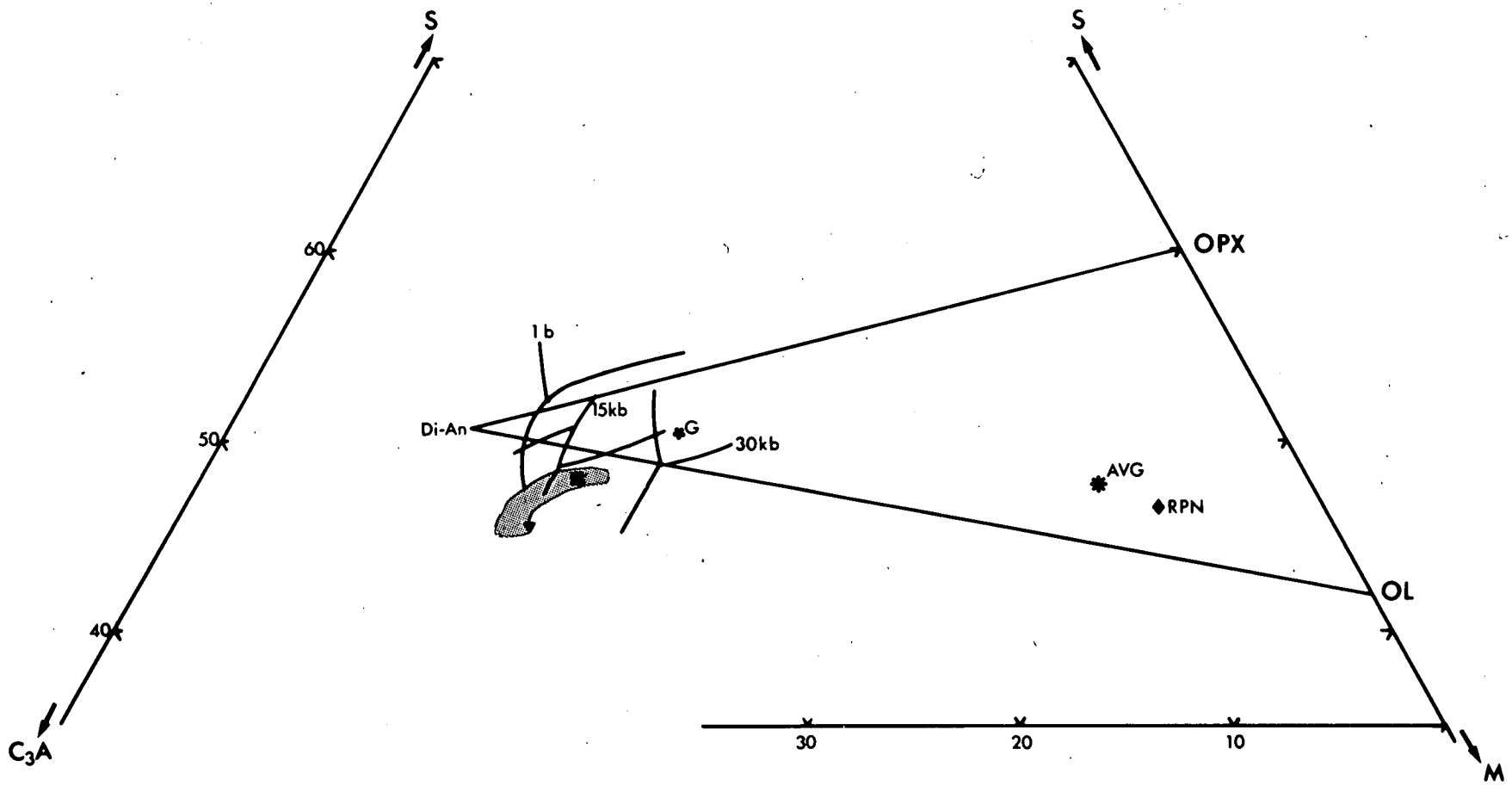
S
60
50
40
C3A
S
OPX
1 b
15kb
Di-An
G
30kb
AVG
RPN
OL
30
20
10
M

Alkali-basalt genesis.

The evolution sequence of the Fife basalts is only represented on the surface by the later differentiates and more basic lavas containing lherzolite inclusions. From chemical data on the garnet and augite megacrysts it is clear that a primitive alkaline liquid existed at depths greater than 80kms and this liquid must have been at least as basic as RPB. This primitive composition may well be represented by the tuff, which is impossible to analyse accurately owing to its content of foreign and cognate material and its carbonated nature. Thus any theory of petrogenesis for the Fife basalts must allow for the liquid already being alkaline at depths greater than 80kms and prior to any known cognate phases crystallising.

It is not within the scope of the present work to provide a full survey of the modern theories of basalt genesis and the following discussion will be restricted to those areas of the controversy which directly affect the deep-seated genesis of alkaline liquids.

In 1965 O'Hara proposed that the various types of lava are not primary magmas but residual magmas after crystal fractionation. The type of magma which finally reaches the surface will be dependant on four main criteria:-

a) The mineralogy of the source rock from which primary liquids are generated by partial melting.

b) The depth at which this takes place, which directly affects

(a).

c) The degree of partial melting which takes place, which will be dependant on the amount of water present in either hydrous phases or as free pore-water, and on the melting interval of (a).

d) The speed at which the liquid ascends and the type of fractional crystallisation it experiences 'en route'.

The controversy surrounding these points has arisen largely through attempts at experimental duplication of the various factors, and the nature of the initial source material. Many disagreements have arisen solely out of the estimates of the validity of varying experimental techniques. A good example of this is the effect on mineralogy of using iron or platinum capsules in high pressure and temperature runs. As noted previously the absorption of Fe by Pt at near solidus temperatures is substantial. Both Green and Ringwood (1967) and Ito and Kennedy (1968) performed similar runs on olivine tholeiite compositions and obtained differing results. Green and Ringwood suggested that the loss of iron was insufficient to modify the phase assemblages or element compositions whereas Ito and Kennedy estimated that iron-loss reduced ol by 25% during the course of most runs, sufficient to radically alter the major liquidus phases at intermediate pressures.

The two most comprehensive theories on basalt genesis which have an experimental basis are those of O'Hara (1968) and Green and Ringwood (1967). They differ considerably in many respects. O'Hara proposes a mantle composition on the kimberlite-nodule basis,

i.e. garnet peridotite, whereas Green and Ringwood propose a 'pyrolite' model, which is a hypothetical mix of peridotite and basalt in the proportions of 3:1. The amount of partial melting required under dry conditions at 30kbs to produce a first liquid, which both agree would be a hy picrite, varies from 10-15% (O'Hara) to 20-40% (Green and Ringwood).

O'Hara explains the origin of undersaturated magmas from this primary hy picrite as being due to fractional crystallisation of eclogite in the high-pressure (25-30kb) regime, or by the fractional crystallisation of four-phase spinel-lherzolite at pressures less than 20kb, which would produce a ne normative residual liquid. In attempting to apply this scheme to the Fife rocks it is seen that whilst aluminous augite and garnet, an eclogitic assemblage, co-precipitated from the liquid, the magma was already alkaline and possible ne normative before this stage (25-30kb). This intimates that partial melting must have taken place at pressures greater than 30kb, i.e. possibly over 100kms down, and that either the primary melt was alkaline rather than a hy picrite, or large scale eclogite fractionation took place prior to the pyrope-augite crystallisation. Since there is no evidence of eclogitic material of non-alkaline affinities in the tuffs, which one would have expected to have been carried to the surface in an eruption which was sufficiently violent to transport garnets from 70kms depth, then it must be assumed that the initial partial melt was probably ne rather than hy.

The schemes discussed so far have considered dry melting only, but as was noted previously most authors agree that a hydrous alkaline phase must be present in the mantle to allow for higher degrees of partial melting and more alkaline initial liquids (K, Na, Ti enriched) (Griffin & Murthy, 1969). Green (1969) suggested that 5-10% wet partial melting would produce an initially ne normative liquid (in the presence of 0.1% H_2O). Increasing partial melting produces more picritic liquids. Green's data however, are not firmly based on experimental evidence, and he shows a very large degree (17-25%) of partial melting at low temperatures below the dry peridotite solidus, in which all garnet and most clinopyroxene dissolves. The scheme has been criticised by Wyllie (1971), and by Kushiro (1969) whose work agrees with that of O'Hara (1965) in that the initial low temperature liquids are silica-saturated and tholeiitic or andesitic in composition. Kushiro's results in the system Fo-Qz-Jd-CaTs (which includes An, En, Ne) help to resolve the argument by allowing for the presence of both free water and a hydrous mineral phase (e.g. amphibole or phlogopite). In a system where no hydrous minerals are stable at the solidus but vapour is present, or where hydrous minerals are present with vapour, then the first liquid produced would be water saturated and andesitic. In a system where a hydrous phase is present but vapour is absent, then the first partial melt will be water under-saturated and nephelinitic. Recent work by Mysen (1973) on the wet-melting of garnet peridotite leads to similar conclusions as those drawn from Kushiro's work. Partial melting of a garnet

peridotite with high water fugacity (mole fraction of H_2O in vapour > 0.6) produces andesitic liquids, while at low water fugacity ($X^{v}_{H2O} \leqslant 0.5$) silica-undersaturated liquids are found. These are strongly alkaline and were likened to melilite nephelinites by Mysen. They are, however, K deficient, though this could be alleviated if phlogopite were present in the peridotite. This compares favourably with the work of Kushiro which indicated partial melting of a dry phlogopite bearing peridotite to produce undersaturated liquids. Melting of such a composition would produce the low water fugacity required by Mysen.

These results are extensions of O'Hara's dry-melting runs on garnet-peridotite into a hydrous environment, and it is thus suggested that the Fife primary liquid was formed by partial melting of a vapour-free garnet-peridotite containing a hydrous mineral, possibly phlogopite, at depths of ca. 100kms. The derivation of subsequently more nephelinitic liquids is due largely to clinopyroxene fractionation.

Petrogenetic model...Fife.

Following the previous discussion on alkali-basalt genesis it has been proposed that the primitive liquid from which the Fife volcanics originated was formed by partial melting of a vapour-free, mica-bearing garnet-peridotite at ca. 100kms depth. The eclogitic assemblage of pyrope-augite crystallised from this liquid as phenocrysts at no less than 70kms. The following petrogenetic model considers a rising body of this alkaline liquid entering, and

becoming trapped in the lower crust, and undergoing fractionation of olivine and pyroxene. Such fractionation would drive the liquid towards more ne normative compositions, and if carried far enough could produce strongly undersaturated magmas such as those from Elie Harbour and Chapel Ness. Such a change in liquid composition would require extensive fractionation of olivine and pyroxene, particularly pyroxene, and would result in a large accumulation of olivine-pyroxenites. This could account for the Types 1 and 2 nodules. The evidence shows that very little fractionation can have taken place at depths over ca. 35kms., the only phases of higher pressure chemistry being the augite and garnet megacrysts from Elie Ness. The cumulate textures of the Types 1 and 2 nodules suggests that any remnant hydrous, interstitial liquid may have crystallised as intercumulate kaersutite, which occurs as a poikilitic phase in many of these types of nodules. This kaersutite is close in composition to the rocks intermediate on the Fife trend. Type 1 nodules presumably accumulated at very shallow levels since the cumulus pyroxenes are nearly identical to the cores of phenocrysts in the associated basanites. Nevertheless, their composition suggests moderately high-pressure growth, probably within the lower crust.

The strongly undersaturated liquid following a) deep-level 'eclogite' fractionation and b) shallower level clinopyroxene-olivine fractionation, probably commenced gas separation and gave rise to violent tuff-pipe eruptions. These first eruptions of strongly undersaturated magmas from above the cumulate layer are

probably represented by the Elie Harbour and Chapel Ness rocks which are free of nodules or megacrysts of ultrabasic material. Thus the initial eruptions may have left a considerable body of 'alkali-pyroxenite' at depth within the crust, possibly preventing further liquids from ascending to the surface.

The origin of the Types 4 and 5 nodules requires crystallisation from a silica-deficient alkaline liquid. This may represent liquid from the first eruptions trapped in the lower crust, or a later surge of liquid trapped below the accumulations of pyroxenite. Experimental data on anorthoclase suggests it to have crystallised at pressures of less than 9kb, and its association with mica indicates formation possibly within the stability field of biotite. It was also seen from the variation diagrams in Chapter 3 that anorthoclase lies at the extremely alkaline end of any projected trend for the Fife basalts and hence might represent a logical final product of crystallisation of a slow-cooling body of trapped alkaline magma.

The composition of the type 3 mica-pyroxenite nodules suggests these may be whole or partial crystallisation products of a magma close to the basic end of the Fife series at pressures greater than 10kb, near to the base of the crust. Any liquid remaining after their formation would be rich in alkalis and volatiles, ideal for the crystallisation of types 4 and 5 nodules and anorthoclase. Similar nodules of biotite-pyroxenite were reported from tuff at Bufumbira, Uganda by Holmes and Harwood (1937). The tendency of these nodules to lie at the more basic end of the magma trend in

variation diagrams was also noted by these authors, who estimated that the biotite-pyroxenite composition might approximate to that of a parental liquid for the local lavas.

With this crystallisation taking place the build up of volatile pressure may have been sufficient to blast through the overlying pyroxenitic body and cause explosive eruptions. If these were sufficiently violent and rapid the ensuing rush of liquid and gas could carry deep-seated garnet and sub-calcic augite megacrysts to the surface before they could be resorbed. If these megacrysts were fractionating at depths in excess of 75kms, as is indicated by the experimental data, then it is tempting to propose that a magma column up to 50kms long existed from this source region to the base of the crust where its upper trapped portion was crystallising alkaline nodules. If this were the case, however, it would be expected to find some evidence of fractionation products from the whole length of the column on the surface, which is not the case, only the high-pressure and low-pressure material being found. This then may indicate that the first alternative mentioned, i.e. that the parental liquid to the highly alkaline phases was a trapped residuum from the initial highly undersaturated eruptions, not a later surge, is sounder. In either case the main eruptive phase would of necessity be rapid and violent, in order to preserve the high-pressure phases intact.

The violent upsurge of liquid and gas would also break up the pyroxenite cumulates and strip them from the pipe-walls higher up, along with fragments of basement rock such as the mica-schist

from Elie Ness, and carry a jumble of fragments and crystals to the surface, sampling all the types and layers of accumulated material on the way.

After this explosive event the more basic magmas could follow through to form flows, sheets and plugs. The late-stage sheet filling the Coalyard Hill ring-fracture is lherzolite-bearing and thus the later erupted liquids may have undergone lherzolite fractionation. The early explosive eruptions could not have precipitated any quantity of this intermediate pressure phase owing to their rapid rise to the surface, hence the absence of lherzolite in the tuff-pipes. That pyroxenitic inclusions are uncommon in these intrusions suggests that most of this material was brought to the surface during the explosive activity. It seems unlikely that the lherzolite inclusions might represent mantle residua associated with the origin of the Fife alkaline magmas, as all the evidence points to initial partial melting at depths approaching 100kms, well outside the stability field of spinel-lherzolite. Also if they were intimately associated with the initial genesis of the liquid then they would be expected to be common occurrences in the Elie Ness tuff.

This model is obviously an oversimplified view of events which may have led to the formation of the Fife tuff-pipes. The wide variety of nodules and inclusions occurring in the various igneous bodies suggests that each individual locality has its own unique origin. The above scheme of petrogenesis does, however, serve to explain the major occurrence of nodules and megacrysts in the Elie Ness vent and their absence in the Elie Harbour vent, and also the main petrological features which all the vents have in

common.

The lherzolite-bearing sheet at Coalyard Hill also contains rare wehrlites and pyroxenite inclusions. The latter show relatively low pressure chemistry which can be equated with the type 2 Elie nodules. This suggests that pyroxenite fractionation may have been a continuous process in the evolution of the Fife rocks. The wehrlites are of deeper origin, possibly being formed well down in the upper mantle. The presence of spinel in the Fidra specimens imposes an upper limit of about 40 to 50 kms depth for this type of inclusion, within the region from which a rising basalt liquid might also be expected to fractionate spinel-lherzolite.

Caithness.

The texture of the spinel-clinopyroxenites does not indicate a cumulate origin but rather suggests slow, progressive crystallisation at temperatures of 1350-1450°C with spinel exsolution taking place on decreasing temperature. The pyroxene shows strong affinities with alkaline magmas in its high TiO_2 and low Cr_2O_3 content and displays a distinctly high pressure and temperature chemistry. It is concluded that these nodules formed at depths close to 50kms and may represent partial crystallisation products of an alkaline magma. Nodules of similar composition containing pleonaste spinel have been reported by Aoki and Kushiro (1968) from Dreiser Weiher, and Kutolin and Frolova (1970) from Minusa (Siberia). The latter are much richer in alumina (16.5%) and may represent co-precipitation of pyroxene and spinel at near eutectic conditions (c.f. Fig 6-1).

Kutolin and Frolova considered them to be cumulates from an alkaline magma.

Whilst the Duncansby Ness vent is similar to the Fife vents it is notable for its lack of amphibole-pyroxenite nodules (Apart from rare green-amphibole aggregates) and also in containing lherzolites and wehrlites in the tuff. Comparison with the petrogenetic model for the Fife vents suggests that pyroxenite fractionation may have been responsible for the undersaturated nature of the basalts, though alkali-pyroxenites have not been carried to the surface. The spinel-clinopyroxenite nodules may thus represent such a fractionated phase.

Other localities.

The Fife localities provide the fullest geochemical data of the areas studied, and as such constitute the only area for which a detailed interpretation can be attempted. In this section it is intended to look at the geochemical data from the nodules and inclusions in other localities and compare them to what is known about similar material from Fife.

The common feature of the East Lothian localities and Calton Hill is the occurrence of spinel-lherzolites in basanites. Apart from the spinel-bearing wehrlite from Fidra there is no evidence of the magmas having gone through a 'pyroxenite' stage in their evolution, yet comparison with the Fife lherzolite localities suggests that such fractionation must have taken place. The East Lothian spinel-lherzolite inclusions are very similar to those from

Fife and Derbyshire, and closely resemble the common occurrences of such inclusions in basalts throughout the world.

The chemistry of the Bute harzburgite inclusions shows an overall more iron-rich nature in the analysed minerals which may indicate a different origin to the lherzolite inclusions of Fife. Lherzolites have not definitely been identified from this locality and it is suggested that many of the Bute inclusions may be cognate accumulates. The host-rock is more basic (MgO = 15%) than its counterparts from Fife and slightly poorer in TiO_2. O'Hara (1968) has suggested that harzburgitic residua may be left after partial melting of peridotites with low CaO / Al_2O_3 ratios, though the iron-rich nature of the Bute samples may exclude such an origin. Conversely fractionation in a deep magma-chamber may produce layered cumulates which could include harzburgites, wehrlites and pyroxenites such as those found in the Bute intrusion.

ACKNOWLEDGEMENTS

During the period of this research I have benefitted not only from the excellent material facilities available at the Grant Institute, but also from much stimulating discussion with many of its members. I am grateful to Professors Sir F.H. Stewart, G.Y. Craig, and M.J. O'Hara for making the facilities available to me.

Professor O'Hara originally suggested this study which was supervised by himself and Dr. B.G.J. Upton. To them I am deeply indebted for continuous guidance and encouragement over the past three years.

I would also wish to express my gratitude to the many other members of the Department for creating a friendly atmosphere, and providing advice and tuition in the many techniques used. Mr. Colin Chaplin and his technical staff provided great assistance in the preparation of materials and running of equipment.

Expert tuition in wet-chemical techniques was given by Mr. Michael Saunders, and Mr. Geoffrey Angell and Dr. Godfrey Fitton offered valuable instruction in the use of X-ray fluorescence equipment.

Mr. Cameron Begg and Dr. Phillip Spencer are gratefully acknowledged for their friendly help and advice in the use of high-pressure equipment.

Miss Kay Stavert and Mr. Ronnie Devine gave great assistance in the preparation of drawings and photographs for the thesis.

For my many hours of trouble-free operation of the microprobe I am indebted to Dr. Peter Hill and Dr. Barry Jefferies. Computer problems were invariably solved by Mr. David Humphries. The author is indebted to Mr. A.K. Ferguson of Melbourne for the use of a computer programme.

To Dr. R.M. Macintyre of the Scottish Reactor Research Centre, East Kilbride, who carried out all the potassium-argon dating of material the author owes a great deal of gratitude. Messrs. R. Elliot and I. Forsyth of the Institute of Geological Sciences, Edinburgh, provided much useful discussion in the fields of petrography and radiometric ages.

The author would also like to thank Dr. William Storey, Dr. Roy Gill, Mr. Claude Herzberg, Dr. Howell Francis (I.G.S., Leeds) and Dr. Aldo Cundari (University of Melbourne) for much useful advice and stimulating discussion. Dr. K. Coe (University of Exeter) kindly provided specimens from Co. Cork.

The research was carried out during the tenure of a Natural Environment Research Council studentship.

I also wish to thank Mrs. E. Courtney for typing this thesis.

APPENDICES

APPENDIX ONE

Whole-rock chemical analyses and electron microprobe analyses of minerals.

List of analysed rock specimens.

XR-1	Spinel-pyroxenite nodule, Duncansby Ness.
XR-2	Basanite block from tuff, Elie Ness.
XR-3	Elie-type 1 nodule, Elie Ness.
XR-4	Basanite block from tuff, Elie Ness. (Q3-1)
XR-5	Analcime basanite, Kidlaw Quarry.
XR-6	Ruddons Point basalt.
XR-7	Gullane sill basalt.
XR-8	Central plug basalt, Kincraig Hill.
XR-9	Basanite block, Elie Harbour. (EHB)
XR-10	Basanite block, Elie Ness. (Q2-32)
XR-11	Elie-type 1 nodule, Elie Ness. (Nod.7)
XR-12	Analcime basanite, Kidlaw Quarry.
XR-16	Basanite block, Kincraig Hill.
XR-17	" " " "
XR-18	" " " "
XR-19	Central plug basalt, Kincraig Hill.
XR-20	Basanite block, Elie Harbour.
XR-21	Chapel Ness basanite.
XR-22	Basanite block, Coalyard Hill.
XR-23	" " " "
XR-24	" " Elie Harbour.
XR-25	" " " "
XR-26	" " " "
XR-27	Analcimic basalt, Calton Hill.
XR-28	Basanite block, Ardross vent.
XR-29	Lherzolite-bearing sheet, Coalyard Hill. (CH-7)
XR-30	Anorthoclase rich sheet, Coalyard Hill. (CHA)
XR-31	Basalt plug, Duncansby Ness.
XR-32	" " " "
XR-33	Monchiquitic dyke near Castletown.
XR-34	Elie Ness dyke.

List of analysed rock specimens (contd).

XR-35	Basanite block, Ardross vent.
XR-36	Lherzolite inclusion, Coalyard Hill. (CH-7)
XR-37	Ardross dyke. (AN-4)
XR-38	Lherzolite inclusion, Ruddons Point. (E-1)
XR-39	Bute host-rock. (B-11)
XR-40	Anorthoclase rich sheet, Coalyard Hill.
XR-41	Monchiquitic block in tuff, Elie Ness. (Q3-20)
XR-43	Kellie Law basalt body (summit).
XR-44	" " " " (roadside).
XR-45	Analcime basanite, Fidra.
XR-46	Elie-type 5 nodule, Elie Ness. (Q2-27)
XR-47	Elie-type 3 nodule, Elie Ness. (Q2-6)
XR-48	Elie-type 4 nodule, Elie Ness. (Q3-6)
XR-49	Lherzolite inclusion, Fidra. (F-1)

List of microprobe specimens.

P-10	Elie-type 1 nodule, Elie Ness. (Q3-2)
P-11	Elie-type 4 nodule, Elie Ness. (Q4-13)
P-12	Elie-type 1 nodule, Kincraig Hill. (H-1)
P-13a	Anorthoclase rich sheet, Coalyard Hill. (CHA2)
P-13b	Pyroxenite (type 1) nodule from same sheet as P-13a. (CHA2)
P-14a	Lherzolite inclusion and host, Coalyard Hill.
P-14b	" " " " "
P-15	Lherzolite nodule (from borehole), Kidlaw. (KI)
P-19a	Lherzolite nodule, Duncansby Ness. (DH-14)
P-19b	" " " "
P-20	Tonalite nodule, Duncansby Ness. (DH-7)
P-21a	Basanite block, Elie Ness. (Q3-28)
P-21b	" " " " (Q2-32)
P-21c	" " " " (Q2-12)
P-22	Vesicular basanite block, Elie Ness. (Q3-11)
P-23	Monchiquite block, Elie Ness. (Q3-20)
P-24a	Lherzolite inclusion, Ruddons Point. (E-1)
P-24b	Ruddons Point basalt (R-2).
P-25	Basanite block, Elie Harbour. (EHB)
P-26	Basanite plug, Duncansby Ness. (DH-21)
P-27a	Harzburgite inclusion, Bute. (B-1)
P-27b	Bute host rock. (B-10)
P-28	Pyroxenite inclusion (borehole), Coalyard Hill.
P-29	Pyroxenite inclusion, Bute. (B-4)
P-30	Elie-type 5 nodule, Elie Ness. (Q2-27)
P-32	Elie-type 2 nodule, Elie Ness. (Q3-15)
P-33	Elie-type 3 nodule, Elie Ness. (Q2-6)
P-34	Elie-type 1 nodule, Elie Ness. (Nod.7)
P-35	Elie-type 2 nodule, Elie Ness. (Q3-16)
P-36	Elie-type 4 nodule, Elie Ness. (Q3-6)
P-37	Lherzolite inclusion, Fidra. (F-1)
P-38	Central plug basalt, Kincraig Hill. (XR-8)
P-39	Wehrlite inclusion, Fidra. (F-5)
P-40	Basanite plug, Duncansby Ness. (DH-24)
P-41	Wehrlite inclusion, Coalyard Hill. (CH-12)

Correlation chart of microprobe and XRF samples.

Locality	Probe No.	XRF No.	Sample
Kidlaw Quarry	P-15	XR-5	K(B)
Ruddons Point	P-24b	XR-6	-
Elie Ness	P-21b	XR-10	Q2-32
Elie Harbour	P-25	XR-9	EHB
Coalyard Hill	P-14a,b	XR-29	CH-7
" "	P-13a,b	XR-30	CHA
Duncansby Ness	P-26	XR-31	DH-24
Ruddons Point	P-24a	XR-38	E-1
Bute	P-27b	XR-39	B-11
Elie Ness	P-23	XR-41	Q3-20
" "	P-30	XR-46	Q2-27
" "	P-33	XR-47	Q2-6
" "	P-36	XR-48	Q3-6
Fidra	P-37	XR-49	F-1
Kincraig Hill	P-38	XR-8	XR-8
Fidra	P-39	-	F-5
Duncansby Ness	P-40	XR-31	DH-24
Coalyard Hill	P-41	-	CH-12
Duncansby Ness	BX	XR-1	DHBX

ABSTRACT OF THESIS

Name of Candidate Neil Anthony CHAPMAN

Address Forkenford Farm, Duddingston Road West, Edinburgh.

Degree Doctor of Philosophy *Date* October, 1974.

Title of Thesis Petrology of Inclusions from Some Late Palaeozoic British Volcanic Rocks.

Ultrabasic inclusions in basanitic rocks are of restricted occurrence in Britain, being found only in rocks of Carboniferous or Permian age. As such they are amongst the oldest known occurrences in the world and yet have never been studied in detail.

The present work has concentrated on a series of late Carboniferous or early Permian tuff-pipes and minor intrusions on the Fife coast near Elie. These contain a wide variety of fragmental materials and megacrysts. Further detailed work was carried out on a vent at Duncansby Ness, Caithness, which is host to spinel-lherzolite, spinel-wehrlite and spinel-pyroxenite nodules. Samples of inclusions were also studied from Fidra, Kidlaw and Weak Law, East Lothian; Hawk's Nib, Bute and Calton Hill, Derbyshire. Geochemical data collected from this material are described, and these, along with results of high-pressure experiments, are used to postulate a petrogenetic model for the Fife volcanics.

Of the six diatremes studied along an 8km stretch of the Fife coast, the Elie Ness vent contains the widest variety of fragments and megacrysts of basic and ultrabasic material. Five types of coarse-grained, alkaline, mafic and ultramafic fragments (Elie-type nodules) were distinguished:-

Type 1. Kaersutite-olivine-pyroxenite.
Type 2. As Type 1 plus oligoclase.
Type 3. Biotite-pyroxenite.
Type 4. Sodic amphibole-biotite-albite.
Type 5. Biotite-albite.

Megacrysts of sodic anorthoclase of high-temperature structure, pyrope, sub-calcic augite and kaersutite are also common in the tuff, and scattered representatives of similar Elie-type nodules and megacrysts occur in other vents. The basaltic rocks associated with this material are alkali-basalts trending via basanites toward monchiquites, with normative nepheline from 1-17%. The most undersaturated rocks, found at Elie Harbour and Chapel Ness, contain no Elie-type nodules or megacrysts. The Ruddons Point basalt (RPB), one of the most basic rocks, contains spinel-lherzolite inclusions, and in common with the other lherzolite-bearing sheet at Coalyard Hill is free of Elie-type nodules.

The composition of the augite and pyrope megacrysts indicates crystallisation from a basic alkaline liquid. Experimental studies show that these phases could have coprecipitated from an alkaline basalt magma at $P > 25kb$, $T = 1300\text{-}1450^{\circ}C$. It is proposed that the primary magma for the Fife volcanics was formed by 10-15% partial melting of a vapour-free, mica-bearing garnet-lherzolite at a depth of ca. 100kms, and that the 'eclogitic' pyrope and augite mixture crystallised from this liquid at depths > 70kms. Geochemical studies of pyroxenes from the Elie-type nodules indicate that they crystallised within the lower crust. It is proposed that the Types 1 and 2 nodules are cumulates from the alkaline/

Use other side if necessary.

alkaline liquid, with intercumulus kaersutite representing the composition of liquids intermediate on the Fife basalt trend. Advanced fractionation of pyroxene could produce the most undersaturated, nodule-free eruptives. The Type 3 nodules may represent basaltic liquids, at the basic end of the Fife trend, crystallised at pressures from 10-15kb. Types 4 and 5 nodules may represent crystallisation products of a trapped body of hydrous liquid, possibly remnant from the formation of Type 3 nodules.

Experimental work on the stability of anorthoclase in RPB shows it to be present in the liquid field at $P < 9$kb (dry), and it is thought that crystallisation of anorthoclase may be the final phase of Types 4 and 5 nodule formation. The build up in volatile pressure led to an eruption so violent as to strip the cumulates from the lower crust, sample fragments of basement rock, and carry unresorbed garnet and augite from depths of over 70kms. This may indicate that a magma column up to 50kms long existed prior to eruption. The spinel-lherzolite inclusions from other localities may represent crystal-cumulates from a late-stage basic liquid, injected into ring-fractures and as sheets within vents.

Experimental studies on black, pleonaste-clinopyroxenites from Duncansby Ness, Caithness, show that up to 5 wt % of the spinel could have been exsolved from the augite at pressures close to 18kb and temperatures of about 1300°C under dry conditions. The large size of these pyroxenites, together with their lack of subsequent low-pressure or hydrous recrystallisation indicates that a deep-seated, violent, eruptive episode similar to that postulated for Elie Ness may have taken place.

Basalts 1

	2	4	5	6	7	8	9	10	12	16	17	18	19	20	21	22	23
SiO_2	45.83	41.66	45.10	44.75	46.13	44.60	45.41	45.36	45.09	45.21	43.76	45.20	44.69	45.82	43.91	39.47	42.53
Al_2O_3	13.94	12.73	14.83	13.69	15.69	14.54	15.19	14.53	14.99	14.78	13.68	15.10	14.40	15.17	14.42	16.39	17.81
Fe_2O_3	7·07	9.79	5.69	3.95	12.77	4.18	5.24	5.84	5.63	5.54	6.43	5.63	4.01	5.87	3.57	7.36	7.34
FeO	4.86	5.41	6.29	8.24	-	7.59	5.06	5.18	6.23	6.01	6.26	5.53	7.42	4.76	7.33	6.37	5.21
MgO	8.03	10.95	8·00	10.09	6.18	9.63	7.00	8.51	8.19	7.76	11.49	8.14	10.14	6.96	9.39	7.51	5.51
CaO	8.65	10.56	8.15	10.38	9.97	10.14	9.33	10.18	8.23	9.76	8.48	8.17	9.89	8.92	9.62	11.58	9.21
Na_2O	3.70	1.79	4.36	2.79	3.51	3.17	5.56	3.74	3.94	2.78	2.31	4.61	3.07	4.64	4.84	1.05	3.50
K_2O	2.00	0.89	1.83	0.67	1.75	0.68	1.38	1.11	2.01	2.10	1.54	1.43	0.45	1.61	1.09	3.66	2.28
P_2O_5	0.18	0.79	0.96	0.16	0.04	0.07	0.44	0.15	0.82	0.87	0.72	1.02	0.92	1.90	1.10	2.09	1.43
MnO	0.97	0.79	0.22	0.20	0.14	0.20	0.97	0.19	0.20	0.68	1.00	1.02	0.20	0.95	0.20	0.06	0.47
TiO_2	2.78	3.12	2.87	2.61	2.45	2.89	2.85	3.15	2.90	2.98	2.79	2.93	2.86	2.86	2.72	3.53	4.09
Total	98.01	98.48	98.30	97.53	98.63	97.69	98.43	97.94	98.23	98.47	98.46	98.78	98.05	99.46	98.19	99.07	99.38
Minor elements ppm (T denotes less than 5ppm)																	
Ba	3960	1980	2083	1054	496	1115	977	1792	1732	3062	710	973	1333	728	849	1054	1494
Zr	278	357	515	311	157	460	393	351	427	384	220	327	412	382	326	318	334
Sr	644	932	1040	1227	382	1514	1031	852	1217	746	497	610	1259	955	858	477	706
Rb	31	15	20	12	58	19	25	20	27	63	28	20	16	37	20	53	37
Ni	317	311	60	239	T	118	117	280	103	166	320	242	191	162	207	240	144
Cr	195	209	125	207	79	214	231	226	102	246	342	288	237	254	227	282	198
Ce	205	357	589	230	128	273	330	338	579	271	81	114	231	296	182	122	108
V	234	229	161	221	249	214	209	207	172	248	230	225	183	200	217	214	278
La	106	129	164	117	78	122	151	122	189	134	66	88	91	105	142	103	90
CIPW norm (with standardised oxidation ratio)																	
Or	12.24	5.45	11.15	4.07	10.64	4.13	8.42	6.74	12.23	12.83	9.43	8.75	2.74	9.87	6.65		13.87
Ab	18·83	11.41	16.73	18.83	12.89	18.80	15.06	17.69	16.02	14.98	16.11	19.35	21.52	16.70	11.19		9.40
An	16.08	24.96	15.97	23.52	22.52	24.06	12.82	20.11	17.80	22.38	23.21	16.86	24.95	16.40	14.86	30.22	26.92
Ne	7.80	2.33	11.55	2.96	9.57	4.73	18.16	8.02	9.93	5.06	2.24	11.40	2.86	11.94	16.83	4.98	11·42
Il	5.47	6.14	5.62	5.10	4.79	5.63	5.59	6.14	5.67	5.85	5.49	5.76	5.60	5.63	5.33	6.94	8.00
Ol	11.85	18.80	12.48	16.05	16.03	14.82	6.97	10.67	13.09	11.10	21.04	12.33	16.19	8.65	12.38	12.10	8.17
Di	22.72	23.52	20.60	23.57	23.56	22.00	27.93	25.27	19.41	22.13	16.23	20.04	20.43	23.59	27.41	20.25	16.14
Woll																	
Mag	5.81	7.38	5.89	5.89		5.83	5.05	5.36	5.83	5.68	6.25	5.50	5.70	5.22	5.34	6.72	6.07
Leuc																17.55	
Ca Ort																1.25	
D·R·	0.59	0.64	0.48	0.32	-	0.36	0.51	0.53	0.48	0.48	0.51	0.51	0.35	0.55	0.33	0.54	0.59

Basalts 2

	24	25	26	27	28	29	30	31	32	33	34	35	37	39	41	43	44	45
SiO_2	46.73	45.30	45.23	44.73	42.56	38.87	41.86	45.87	45.06	40.33	40.28	40.34	43.04	44.18	45.25	41.80	43.58	44.59
Al_2O_3	15.38	15.14	15.18	14.12	13.79	11.58	14.64	10.74	11.04	10.17	12.78	15.29	13.83	12.13	14.73	14.23	15.46	15.61
Fe_2O_3	5.36	6.44	5.31	12.99	6.18	7.59	7.34	5.66	5.57	14.72	8.78	7.90	6.95	4.62	4.72	5.87	5.82	2.66
FeO	5.32	4.25	4.79	-	6.20	6.63	9.00	4.99	4.90	-	6.16	7.10	6.79	7.89	6.18	6.91	6.89	7.89
MgO	7.35	7.07	7.13	11.00	11.25	13.35	7.29	10.80	11.82	14.25	7.35	14.47	13.78	15.00	6.99	10.64	8.70	9.59
CaO	9.09	8.93	9.13	9.15	10.83	13.34	9.46	11.94	10.76	10.09	13.72	4.95	5.86	8.68	10.08	10.41	9.93	9.50
Na_2O	4.53	4.67	5.07	2.52	2.46	1.56	2.31	2.95	3.67	2.48	4.14	1.34	1.76	1.74	4.04	3.21	2.97	4.67
K_2O	1.67	1.67	1.65	1.15	0.74	1.61	2.05	1.53	1.31	1.35	1.22	2.79	2.33	0.97	2.32	1.51	0.63	0.87
P_2O_5	1.92	1.74	1.16	0.69	0.66	0.94	1.32	1.38	1.54	1.53	0.53	0.43	0.94	0.27	0.65	0.37	0.68	0.59
MnO	0.91	0.94	0.86	0.20	0.33	0.16	0.23	0.19	0.19	0.05	0.50	0.33	0.10	0.18	0.17	0.19	0.17	0.15
TiO_2	2.77	2.84	2.85	2.22	3.06	2.77	2.88	2.25	2.29	4.46	2.53	3.35	2.87	2.12	2.95	3.08	3.20	2.72
Total	101.03	98.99	98.86	98.77	98.06	98.40	98.38	98.30	98.15	99.43	97.99	98.29	98.25	97.78	98.08	98.22	98.03	98.84
Minor elements ppm (T denotes less than 5ppm)																		
Ba	940	954	912	438	1581	988	2055	1668	1509	1577	1246	888	1073	455	1313	1428	1369	895
Zr	344	332	354	178	232	244	344	288	278	375	304	267	214	152	330	261	297	264
Sr	1079	944	1131	453	709	701	1137	1107	958	1290	758	471	732	757	938	1067	1138	857
Rb	25	23	25	26	T	39	51	18	20	27	25	36	57	27	59	31	22	18
Ni	216	234	217	311	306	280	122	273	330	404	163	349	175	413	134	174	159	193
Cr	263	269	290	340	310	236	129	394	455	463	194	393	246	461	168	192	152	214
Ce	130	121	132	70	95	104	214	140	165	163	106	112	130	67	144	115	133	100
V	206	189	213	201	217	189	196	166	182	321	226	261	267	264	266	280	281	258
La	87	89	93	44	69	85	179	111	128	117	113	96	91	44	60	55	52	37
CIPW norm (With standardised oxidation ratio)																		
Or	10.07	10.23	10.15	7.01	4.51		12.54	9.37	8.02	0.05		16.95	14.20	5.89	14.11	9.19	3.84	5.24
Ab	18.79	15.44	14.91	18.43	11.38		8.93	9.95	9.82			8.40	15.09	15.14	9.57	3.36	19.23	13.25
An	17.04	14.17	14.36	24.56	25.19	21.91	24.34	11.96	10.13	13.10	13.14	25.24	23.67	23.05	15.65	20.55	27.83	19.43
Ne	11.01	15.69	16.12	1.93	5.47	5.97	6.12	8.62	12.10	11.79	19.65	1.76	0.14		13.87	13.33	3.62	14.64
Il	5.37	5.59	5.64	4.35	6.00	5.44	5.66	4.43	4.50	8.79	4.98	6.54	5.62	4.14	5.77	6.02	6.26	5.27
Ol	9.41	8.26	7.75	19.94	17.28	22.68	14.64	11.15	14.25	28.42	7.29	32.69	29.53	25.48	7.00	15.48	14.62	15.32
Di	23.15	25.39	26.14	17.77	24.08	24.41	19.70	39.30	35.87	31.40	38.92		5.02	16.86	28.65	25.98	18.36	22.92
Mag	5.18	5.22	4.94	6.02	6.08	6.96	8.07	5.23	5.30		7.28	7.33	6.73	6.19	5.37	6.09	6.25	3.93
Leuc						7.71				6.45	5.85							
Ca Ort						4.92					2.89							
Cor												1.10						
Hy														3.25				
O.R.	0.50	0.60	0.53	-	0.50	0.53	0.45	0.53	0.53	-	0.59	0.53	0.51	0.37	0.43	0.46	0.46	0.25

Nodules & Inclusions

	Lherzolites			*Elie Ness nodules*				
	36	38	49	3 A	11 A	47 B	48 C	46 D
SiO_2	48.13	42.76	43.96	42.92	39.75	41.29	38.86	41.58
Al_2O_3	2.25	2.38	2.46	7.32	6.10	8.14	15.49	13.96
Fe_2O_3	5.05	1.78	1.38	4.58	4.50	4.47	5.20	5.68
FeO	6.59	7.00	7.14	7.20	5.16	9.62	8.93	13.72
MgO	26.70	39.45	37.93	16.00	13.19	15.67	8.56	9.76
CaO	9.47	2.60	3.59	13.37	24.45	10.53	11.63	1.57
Na_2O	0.22	0.22	0.57	1.66	1.26	1.17	3.42	2.15
K_2O	0.03	0.01	0.13	2.37	0.36	4.34	2.16	5.90
P_2O_5	0.09	0.62	0.02	0.04	0.06	0.04	0.22	0.01
MnO	0.15	0.06	0.12	0.04	0.16	0.23	0.18	0.22
TiO_2	0.31	0.19	0.20	1.93	2.35	2.52	4.70	4.32
Total	98.99	97.07	97.50	97.43	97.34	98.02	99.35	98.87
Minor elements ppm (T denotes less than 5ppm)								
Ba	67	T	T	406	117	2007	1819	2315
Zr	11	T	7	135	109	119	86	13
Sr	297	T	11	244	306	248	1006	223
Rb	8	10	9	94	T	158	38	220
Ni	1700	2055	1892	264	304	334	83	95
Cr	2608	2782	1995	760	667	473	33	18
Ce	21	29	25	T	T	32	68	21
V	77	61	70	221	272	162	426	302
La	87	23	T	121	67	7	36	6
CIPW norm								
Or	0.18	0.06	0.79					35.34
Ab	1.89	1.76	4.95					2.54
An	5.13	5.78	3.87	5.67	8.87	4.24	20.75	7.90
Ne				7.82	5.16	5.49	15.83	8.61
Il	0.60	0.37	0.39	3.77	3.99	4.90	9.02	8.32
Ol	18.85	66.10	65.82	19.33	45.60	26.67	10.37	27.74
Di	33.42	5.99	11.36	42.70	-2.85	26.62	24.02	
Mag	7.41	2.68	2.05	6.82	5.83	6.63	7.62	8.35
Hy	32.53	17.26	10.76					
Leuc				11.28	1.49	20.57	10.11	
Ca Ort				2.62	31.92	4.89	2.26	
Cor								1.20
O.R.	0.43	0.20	0.16	0.39	0.46	0.32	0.37	0.29

A. Elie-type 1 or 2 nodule B. Elie-type 3 nodule C. Elie-type 4 nodule D. Elie-type 5 nodule

Clinopyroxenes 1

Phenocryst cores

	CHL	CHA			KN									EHB	RPB	BUTE	
	14A-15	13B-2	13B-3	13B-11	21A-1	21A-9	21B-4	21B-5	21C-7	21C-9	22-3	22-5	23-3	25-4	24B-10	27B-1	27B-13
SiO_2	46.41	48.54	47.19	46.60	48.81	48.28	50.10	48.64	47.57	45.75	51.88	50.28	47.67	49.33	49.41	49.69	47.77
TiO_2	2.29	1.89	1.81	1.84	1.78	1.97	1.21	1.35	2.08	3.05	1.33	1.13	1.97	1.40	1.31	1.18	1.80
Al_2O_3	7.90	5.85	7.09	7.22	6.99	5.99	4.45	5.77	7.83	9.68	3.86	4.12	7.05	5.72	6.34	6.50	7.69
Cr_2O_3	-	-	-	-	-	-	-	-	-	-	-	-	-	-	0.10	0.52	-
Fe_2O_3	1.19	2.05	3.03	3.09	3.37	2.36	1.70	3.21	2.90	2.80	0.32	1.84	1.27	1.87	3.28	2.81	2.76
FeO	5.09	4.86	5.08	5.15	4.75	4.82	6.12	4.71	4.77	5.21	6.97	4.63	6.64	3.76	4.18	5.73	6.45
MgO	12.43	12.94	11.98	11.76	13.26	13.49	15.13	14.28	12.82	11.52	13.52	14.28	12.81	14.26	14.56	13.79	12.95
CaO	20.45	21.88	20.76	21.02	19.28	21.38	19.42	20.20	21.14	21.47	22.08	21.72	20.17	21.90	20.67	19.47	19.10
Na_2O	0.88	0.81	1.07	0.91	1.47	0.70	0.64	0.72	0.86	0.90	0.83	0.69	0.74	0.65	0.74	1.06	0.99
K_2O	0.01	0.01	0.02	0.04	0.02	0.00	0.02	0.00	0.02	0.01	0.01	0.01	0.01	0.00	0.03	0.05	0.05
MnO	-	-	-	-	-	-	-	-	-	-	-	-	-	-	0.13	0.16	-
Total	96.67	98.83	98.03	97.63	99.74	98.99	98.79	98.88	99.99	100.39	100.80	98.70	98.33	98.89	100.75	100.96	99.56
Acmite	3.42	5.78	7.95	6.92	9.38	5.07	4.72	5.21	6.27	6.52	0.88	5.04	3.60	4.68	5.39	7.74	7.39
Jadeite	3.14	0.15	0.00	0.00	1.26	0.00	0.00	0.00	0.00	0.00	5.07	0.00	1.85	0.00	0.00	0.02	0.00
Ti-Ts	6.58	5.33	5.16	5.27	4.95	5.54	3.39	3.79	5.79	8.50	3.67	3.17	5.58	3.91	3.60	3.25	5.04
Fe-Ts	0.00	0.00	0.68	1.94	0.00	1.57	0.05	3.81	1.81	1.30	0.00	0.13	0.00	0.55	3.64	0.00	0.35
Ca-Ts	9.63	7.52	10.33	9.97	9.66	6.88	6.36	7.00	10.40	12.01	2.15	5.83	9.15	8.34	8.39	11.53	11.67
FeDi	0.00	0.00	0.00	0.00	0.00	0.00	0.00	0.00	0.00	0.00	0.00	0.00	0.00	0.00	0.00	0.00	0.00
Woll	33.73	37.49	34.03	34.31	30.89	35.83	33.89	33.10	32.95	31.76	40.53	38.88	33.36	37.19	32.69	30.81	29.58
Enst	35.37	36.12	33.80	33.38	36.53	37.58	42.04	39.73	35.39	31.84	36.99	39.73	35.98	39.48	39.69	37.63	35.94
Ferros	8.13	7.61	8.04	8.20	7.34	7.54	9.54	7.35	7.39	8.08	10.70	7.23	10.47	5.84	6.60	9.02	10.04
Al IV	0.228	0.182	0.213	0.225	0.196	0.195	0.132	0.184	0.238	0.303	0.095	0.123	0.203	0.167	0.193	0.180	0.221
Al VI	0.128	0.077	0.103	0.100	0.109	0.069	0.064	0.070	0.104	0.120	0.072	0.058	0.110	0.083	0.081	0.100	0.117

Rims and groundmass

	CHL		KN	CHA				KN								
	14AR-1	14AR-7	38-9	13B-1	13B-4 1	13B-6	13B-14 2	21A-2 3	21B-2	21B-6 4	21B-7	21C-1	21C-5	21C-6	21C-8 5	21C-10 6
SiO_2	46.43	48.95	46.89	46.20	46.43	48.92	46.56	45.10	45.06	48.10	48.79	45.95	50.58	46.58	46.03	48.23
TiO_2	1.96	1.70	0.28	2.90	2.58	1.63	2.34	3.78	3.65	2.75	2.16	2.76	1.58	3.47	3.70	2.33
Al_2O_3	8.12	8.06	7.23	6.71	6.07	3.34	5.74	8.10	7.31	4.72	4.53	8.09	3.55	6.84	6.95	5.14
Cr_2O_3	0.42	1.06	0.08	-	-	-	-	-	-	-	-	-	-	-	-	-
Fe_2O_3	4.39	0.02	6.92	2.83	3.56	3.59	3.97	3.10	2.02	1.86	2.85	6.04	1.66	2.42	2.22	3.66
FeO	2.97	2.75	1.23	5.00	4.19	3.65	3.80	6.07	5.63	6.01	5.27	2.72	4.86	5.82	5.91	4.28
MgO	12.68	15.39	12.92	11.52	12.26	13.66	12.02	11.39	11.59	12.63	13.28	13.03	14.44	11.87	11.65	13.08
CaO	21.80	20.99	21.99	21.97	22.47	22.95	22.73	21.68	22.07	22.37	22.67	22.69	22.89	23.11	22.94	23.33
Na_2O	0.76	0.60	0.74	0.90	0.65	0.54	0.74	0.66	0.56	0.60	0.49	0.52	0.42	0.47	0.49	0.48
K_2O	0.04	0.04	0.01	0.00	0.00	0.02	0.00	0.04	0.00	0.01	0.01	0.00	0.01	0.02	0.01	0.02
MnO	0.14	0.09	0.42	-	-	-	-	-	-	-	-	-	-	-	-	-
Total	99.71	99.65	98.71	98.03	98.21	98.30	97.90	99.92	97.89	99.05	100.05	101.80	99.99	100.60	99.90	100.55
Acmite	5.67	0.06	5.44	6.64	4.79	4.05	5.47	5.00	4.15	4.43	3.59	3.70	3.06	3.49	3.62	3.55
Jadeite	0.00	4.38	0.00	0.00	0.00	0.00	0.00	0.00	0.00	0.00	0.00	0.00	0.00	0.00	0.00	0.00
Ti-Ts	5.49	4.67	0.79	8.30	7.37	4.63	6.71	10.68	10.49	7.80	6.05	7.61	4.40	9.73	10.45	6.50
Fe-Ts	6.62	0.00	14.12	1.47	5.39	6.16	5.92	3.77	1.66	0.84	4.40	12.97	1.56	3.30	2.66	6.67
Ca-Ts	9.63	12.01	8.27	6.02	3.53	0.00	3.23	5.38	5.15	2.27	1.70	3.39	2.56	3.65	3.61	1.40
FeDi	0.00	0.00	0.00	0.00	0.00	0.00	0.00	0.00	0.00	0.00	0.00	0.00	0.00	0.00	0.00	0.00
Woll	32.59	32.70	32.64	36.92	37.58	41.20	38.48	33.74	36.54	39.72	39.18	32.58	41.10	37.80	37.79	39.08
Enst	35.16	41.85	36.15	32.68	34.70	38.46	34.14	31.90	33.01	35.47	36.87	35.59	39.80	32.96	32.60	36.16
Ferros	4.84	4.34	2.60	7.96	6.65	5.77	6.06	9.54	9.00	9.47	8.21	4.17	7.52	9.07	9.28	6.64
Al-4	0.272	0.214	0.240	0.241	0.237	0.152	0.226	0.305	0.278	0.187	0.182	0.316	0.129	0.264	0.272	0.211
Al-6	0.084	0.133	0.080	0.060	0.035	0.000	0.032	0.054	0.052	0.023	0.017	0.034	0.026	0.036	0.036	0.014

1. Rim of 13B-3 2. Rim of 13B-13 3. Rim of 21A-1 4. Rim of 21B-4 and 5 5. Rim of 21C-7 6. Rim of 21C-9

Clinopyroxenes 2

	ES							EHB			DN			RPB			BUTE
	22-4	22-6	22-7	22-10	23-7	23-11	23-12	25-6	25-7	25-9	26-11	26-12	26-15	24B-9	24B-11	24B-12	27B-2
	1	2								3				4	5	6	7
SiO_2	46.78	47.40	50.50	50.05	49.97	44.24	41.98	46.75	45.84	45.16	48.07	43.84	43.81	46.59	46.44	47.59	48.96
TiO_2	2.46	2.41	1.37	1.12	1.62	3.52	4.87	2.83	2.54	4.15	2.34	3.40	2.78	2.46	2.13	2.53	1.92
Al_2O_3	5.74	5.66	3.79	3.65	4.57	8.82	13.03	6.75	7.84	7.75	5.41	8.86	8.32	5.99	7.63	6.02	4.41
Cr_2O_3	-	-	-	-	-	-	-	-	-	-	0.19	-	-	0.00	0.67	0.00	0.08
Fe_2O_3	4.79	3.75	1.32	3.41	2.46	5.56	4.34	2.16	2.42	2.15	1.82	5.95	6.72	3.07	4.26	2.51	2.09
FeO	3.75	4.42	6.33	4.38	4.49	3.27	5.01	3.79	4.31	5.41	4.06	1.97	0.81	5.12	2.78	5.50	5.67
MgO	12.68	12.35	13.63	14.26	14.21	11.39	10.03	12.78	12.46	11.20	13.18	11.49	12.16	12.83	13.13	12.61	13.48
CaO	22.46	22.54	21.44	21.43	22.54	22.93	22.42	22.30	21.48	22.70	23.53	24.03	23.42	20.92	21.79	22.50	22.61
Na_2O	0.64	0.75	0.74	0.77	0.53	0.66	0.62	0.70	0.64	0.70	0.38	0.47	0.51	0.60	0.68	0.47	0.30
K_2O	0.02	0.02	0.03	0.01	0.02	0.02	0.03	0.02	0.03	0.01	0.01	0.02	0.01	0.06	0.01	0.03	0.03
MnO	-	-	-	-	-	-	-	-	-	-	0.09	-	-	0.17	0.16	0.11	0.12
Total	99.32	99.30	99.15	99.08	100.41	100.41	99.33	98.08	97.56	99.23	99.08	100.03	98.54	97.81	99.68	99.87	99.67
Acmite	4.76	5.56	3.71	5.62	3.88	4.88	4.72	5.22	4.86	5.17	2.81	3.51	3.79	4.72	4.95	3.55	2.32
Jadeite	0.00	0.00	1.79	0.00	0.00	0.00	0.00	0.00	0.00	0.00	0.00	0.00	0.00	0.00	0.00	0.00	0.00
Ti-Ts	6.96	6.81	3.85	3.15	4.49	9.89	13.94	8.04	7.26	11.78	6.59	9.58	7.92	7.05	5.96	7.11	5.40
Fe-Ts	8.79	5.05	0.00	3.96	2.94	10.76	7.71	0.92	2.06	0.94	2.32	13.27	15.35	4.08	6.98	3.51	3.56
Ca-Ts	1.37	3.20	3.60	2.91	3.97	4.16	4.71	6.53	9.27	5.00	4.47	3.35	2.98	4.36	8.27	4.40	2.66
FeDi	0.00	0.00	0.00	0.00	0.00	0.00	0.00	0.00	0.00	0.00	0.00	0.00	0.00	0.00	0.00	0.00	0.00
Woll	36.69	37.85	39.20	37.86	38.79	33.50	32.53	37.36	34.63	37.06	40.52	35.13	34.38	34.95	32.84	37.54	39.47
Enst	35.53	34.58	37.95	39.67	39.01	31.71	28.44	35.95	35.28	31.51	36.73	32.08	34.30	36.42	36.41	35.12	37.55
Ferros	5.90	6.95	9.89	6.84	6.92	5.11	7.97	5.98	6.85	8.54	6.50	3.09	1.28	8.43	4.58	8.77	9.05
Al-4	0.241	0.219	0.113	0.132	0.159	0.347	0.403	0.235	0.259	0.295	0.200	0.358	0.342	0.226	0.272	0.221	0.170
Al-6	0.014	0.032	0.054	0.029	0.040	0.042	0.047	0.065	0.093	0.050	0.039	0.034	0.030	0.044	0.063	0.044	0.024

1. Rim of 22-3 2. Rim of 22-5 3. Rim of 25-8 4. Rim of 24B-8 5. Midway out from 24B-10 6. Rim of 24B-10
7. Rim of 27B-1

Elie-type 1 nodules

	BUTE	CHL		KN			EN			KH					
	27B-7	14AB-2	14AE-10	38-1	38-2	38-10	10-5	10-6	10-7	12-1	12-2	12-3	12-5	12-8	12-10	12-12
	1	2				3										
SiO_2	49.51	44.84	48.18	47.26	44.92	46.35	47.92	48.47	48.04	47.29	47.08	46.95	47.92	47.76	46.97	46.66
TiO_2	1.46	3.14	2.76	2.42	3.93	3.55	0.80	0.74	0.78	2.17	2.45	2.47	2.08	2.06	2.26	1.88
Al_2O_3	3.31	8.95	3.88	6.68	8.57	7.40	7.37	7.38	7.20	7.94	7.54	7.78	7.02	6.71	7.53	7.39
Cr_2O_3	-	0.33	0.01	0.55	0.02	0.03	-	-	-	-	-	-	-	-	-	-
Fe_2O_3	3.42	4.25	4.76	2.75	2.92	2.17	3.68	2.32	2.95	3.46	3.32	2.56	2.29	2.58	3.16	2.22
FeO	4.51	2.88	2.92	3.95	5.01	5.36	4.75	6.02	5.36	4.49	4.87	5.42	5.27	5.30	5.14	6.55
MgO	14.71	11.82	12.91	12.98	11.35	11.95	12.88	13.03	12.91	13.15	12.76	12.70	13.46	13.46	12.52	11.20
CaO	21.95	22.27	21.63	22.60	22.65	22.61	19.40	19.35	19.30	20.92	21.29	21.09	21.02	20.59	21.15	20.58
Na_2O	0.32	0.79	1.11	0.54	0.61	0.61	1.17	0.99	1.09	0.80	0.78	0.71	0.63	0.71	0.78	0.94
K_2O	0.06	0.05	0.36	0.01	0.01	0.01	0.01	0.00	0.00	0.02	0.00	0.00	0.02	0.00	0.01	0.08
MnO	-	0.15	0.21	0.11	0.13	0.13	-	-	-	-	-	-	-	-	-	-
Total	99.25	99.47	98.73	99.85	100.12	100.17	97.98	98.30	97.63	100.24	100.09	99.68	99.71	99.17	99.52	97.50
Acmite	2.61	5.97	9.85	3.94	4.48	4.46	8.59	6.55	7.99	5.83	5.62	5.13	4.63	5.14	5.71	6.39
Jadeite	0.00	0.00	0.00	0.00	0.00	0.00	0.00	0.65	0.00	0.00	0.00	0.00	0.00	0.00	0.00	0.97
Ti-Ts	4.11	8.84	7.83	6.77	11.06	9.96	2.27	2.09	2.22	6.03	6.84	6.92	5.81	5.79	6.36	5.41
Fe-Ts	7.02	6.00	3.66	3.76	3.75	1.63	1.84	0.00	0.40	3.80	3.66	2.05	1.77	2.11	3.19	0.00
Ca-Ts	0.00	8.40	0.00	6.81	6.00	5.54	13.18	13.91	13.62	9.37	7.83	9.14	8.67	7.93	8.26	10.77
FeDi	0.00	0.00	0.00	0.00	0.00	0.00	0.00	0.00	0.00	0.00	0.00	0.00	0.00	0.00	0.00	0.00
Woll	38.56	33.05	38.47	36.39	35.01	36.62	30.50	30.91	30.95	31.82	33.19	33.05	33.69	33.29	33.51	34.08
Enst	40.98	32.98	36.28	36.00	31.66	33.22	36.15	36.44	36.35	36.21	35.31	35.26	37.24	37.46	34.92	31.92
Ferros	7.05	4.75	4.94	6.32	8.05	8.57	7.48	9.45	8.47	6.94	7.56	8.45	8.18	8.28	8.05	10.47
Al-4	0.149	0.321	0.183	0.241	0.319	0.271	0.196	0.181	0.185	0.252	0.252	0.251	0.221	0.216	0.242	0.216
Al-6	0.000	0.074	0.000	0.052	0.059	0.055	0.132	0.146	0.136	0.094	0.078	0.091	0.087	0.079	0.083	0.117

1. Rim of xenocrystal orthopyroxene 27B-6 2. Rim of 14AE-1 3. Rim of 38-9

Clinopyroxenes 3

	Elie-type 2 nodules													Type 3
	CHA			EN										
	13B-9	13B-11	13B-13	34-1	34-2	34-3	34-5	35-2	35-3	35-5	35-8	32-2	32-5	32-7	33-1
SiO_2	46.10	46.60	46.61	47.31	48.22	47.46	47.89	49.31	51.52	49.53	49.50	50.54	49.31	51.13	53.09
TiO_2	1.78	1.84	1.91	1.84	1.74	2.03	1.89	1.03	0.93	1.07	1.12	1.07	1.21	0.44	0.18
Al_2O_3	7.50	7.22	7.46	8.49	7.23	8.33	7.46	5.39	4.16	4.91	4.66	4.56	5.55	3.80	1.35
Cr_2O_3	0.07	-	0.02	0.52	0.13	0.15	-	0.07	0.00	-	-	0.33	-	0.00	-
Fe_2O_3	4.52	3.09	2.19	2.96	3.38	3.61	2.90	4.12	1.58	2.85	2.01	1.13	1.56	1.70	2.61
FeO	3.02	5.15	6.00	3.81	4.47	3.44	3.77	4.40	6.51	6.17	6.42	5.98	6.90	7.32	5.63
MgO	12.40	11.76	11.45	12.99	12.79	13.04	13.39	11.60	11.95	11.26	11.54	13.57	12.05	13.02	13.32
CaO	21.11	21.02	20.77	21.52	21.28	21.67	21.80	22.09	22.62	21.02	21.59	20.91	21.10	19.97	21.88
Na_2O	0.92	0.91	0.95	0.76	0.97	0.79	0.72	1.34	1.17	1.50	1.10	0.91	1.00	1.11	1.34
K_2O	0.07	0.04	0.01	0.02	0.02	0.02	0.02	0.03	0.01	0.02	0.02	0.00	0.00	0.01	0.01
MnO	0.08	-	0.00	0.11	0.14	0.40	-	0.21	0.20	-	-	0.22	-	0.24	-
Total	97.57	97.63	97.37	100.33	100.37	100.94	99.94	100.59	100.65	98.33	98.26	99.22	98.68	98.74	99.41
Acmite	7.12	6.92	6.30	5.53	7.04	5.71	5.26	9.74	4.39	8.12	5.73	3.17	4.42	4.81	7.32
Jadeite	0.00	0.00	0.79	0.00	0.00	0.00	0.00	0.00	4.04	2.99	2.45	3.40	2.88	3.33	2.41
Ti-Ts	5.09	5.27	5.49	5.10	4.83	5.60	5.26	2.86	2.58	3.05	3.19	3.00	3.43	1.24	0.50
Fe-Ts	5.81	1.94	0.00	2.69	2.35	4.25	2.81	1.72	0.00	0.00	0.00	0.00	0.00	0.00	0.00
Ca-Ts	8.91	9.97	10.95	12.76	9.92	10.50	9.60	10.30	4.46	6.42	6.00	5.80	7.45	5.51	1.26
FeDi	0.00	0.00	0.00	0.00	0.00	0.00	0.00	0.00	0.00	0.00	0.00	0.00	0.00	0.00	0.00
Wo11	33.06	34.31	34.30	32.22	33.55	32.40	34.35	36.30	41.26	37.90	39.86	37.32	37.13	36.81	42.78
Enst	35.10	33.38	32.60	35.67	35.19	35.64	36.89	31.95	32.90	31.76	32.60	37.66	33.82	36.44	36.97
Ferros	4.93	8.20	9.59	6.04	7.12	5.90	5.83	7.13	10.37	9.77	10.16	9.66	10.87	11.88	8.77
Al-4	0.249	0.225	0.219	0.257	0.220	0.260	0.229	0.178	0.096	0.125	0.124	0.118	0.143	0.080	0.023
Al-6	0.087	0.100	0.117	0.112	0.095	0.101	0.096	0.101	0.085	0.094	0.084	0.082	0.103	0.088	0.037

	Elie 'dark' megacrysts								'glassy' megacrysts				glomeroporphs.		
	EN														
	33-4	33-5	33-6	A-5	A-7	A-9	B-7	B-8	A-1	A-2	A-3	A-10	21B-4	21B-5	23-3
SiO_2	52.52	53.15	53.05	48.53	47.96	48.40	49.37	49.50	49.18	49.80	48.79	51.00	50.10	48.64	47.67
TiO_2	0.20	0.20	0.24	1.32	1.44	1.45	0.92	0.87	0.79	0.78	0.78	0.62	1.21	1.35	1.97
Al_2O_3	2.08	2.21	2.57	8.64	8.76	8.61	8.80	8.82	8.29	8.21	8.32	8.16	4.45	5.77	7.05
Cr_2O_3	0.06	0.07	-	0.00	-	0.00	0.03	-	0.10	0.07	-	0.18	-	-	-
Fe_2O_3	3.03	1.95	1.27	2.75	2.32	3.60	1.82	1.12	2.98	0.90	2.91	0.47	1.70	3.21	1.27
FeO	6.42	7.48	8.40	4.02	4.26	3.66	5.18	5.83	3.88	5.74	3.92	5.84	6.12	4.71	6.64
MgO	13.03	13.15	12.12	13.94	13.66	13.64	14.94	14.79	16.30	15.94	15.89	16.73	15.13	14.28	12.81
CaO	20.75	20.42	20.56	18.65	18.63	19.04	16.73	16.78	15.96	15.88	16.32	15.86	19.42	20.20	20.17
Na_2O	1.36	1.33	1.57	1.37	1.33	1.44	1.39	1.35	1.29	1.21	1.29	1.17	0.64	0.72	0.74
K_2O	0.02	0.04	0.01	0.00	0.00	0.00	0.00	0.01	0.00	0.00	0.01	0.00	0.02	0.00	0.01
MnO	0.38	0.36	-	0.11	-	0.14	0.17	-	0.16	0.14	-	0.14	-	-	-
Total	99.85	100.36	99.79	99.33	98.36	99.98	99.35	99.07	98.93	98.67	98.23	100.17	98.79	98.88	98.33
Acmite	8.49	5.43	3.56	7.62	6.49	9.94	5.02	3.10	8.22	2.49	8.09	1.28	4.72	5.21	3.60
Jadeite	1.42	4.30	7.83	2.16	3.10	0.30	4.86	6.56	0.95	6.13	1.20	6.91	0.00	0.00	1.85
Ti-Ts	0.56	0.56	0.67	3.66	4.03	4.00	2.54	2.40	2.18	2.16	2.17	1.68	3.39	3.79	5.58
Fe-Ts	0.00	0.00	0.00	0.00	0.00	0.00	0.00	0.00	0.00	0.00	0.00	0.00	0.05	3.81	0.00
Ca-Ts	3.38	2.22	1.06	14.02	13.63	14.46	14.08	13.41	15.40	12.67	15.36	12.48	6.36	7.00	9.15
FeDi	0.00	0.00	0.00	0.00	0.00	0.00	0.00	0.00	0.00	0.00	0.00	0.00	0.00	0.00	0.00
Wo11	39.41	39.10	40.16	27.95	28.29	28.18	24.53	25.11	22.55	23.86	23.37	23.60	33.89	33.10	33.36
Enst	36.14	36.26	33.64	38.24	37.85	37.28	40.78	40.47	44.51	43.66	43.76	45.01	42.04	39.73	35.98
Ferros	10.59	12.14	13.08	6.36	6.62	5.83	8.20	8.95	6.19	9.04	6.06	9.03	9.54	7.35	10.47
Al-4	0.045	0.033	0.024	0.213	0.217	0.225	0.192	0.182	0.198	0.170	0.197	0.159	0.132	0.184	0.203
Al-6	0.046	0.063	0.089	0.162	0.167	0.148	0.189	0.200	0.161	0.186	0.166	0.189	0.064	0.070	0.110

Clinopyroxenes 4

Lherzolites

	CHL							DN			KID		RPB				FIDRA
	14A-9	14A-13	14A-14	14A-20	14B-7	14B-10	14B-13	26-5	26-7	26-10	15-1	15-3	24B-3	24B-4	24A-2	24A-4	37-2
			1		2		3			4							
SiO_2	52.06	50.02	43.72	51.34	47.62	52.11	42.07	51.44	51.58	45.74	51.42	51.82	51.77	50.47	52.73	53.05	51.47
TiO_2	0.58	0.49	3.29	0.57	2.73	0.19	4.69	0.35	0.30	2.68	0.80	0.83	0.69	0.70	0.23	0.17	0.62
Al_2O_3	7.49	6.61	8.63	7.14	6.08	5.61	9.85	4.91	5.01	6.99	7.53	7.15	7.41	6.94	5.26	5.31	6.83
Cr_2O_3	-	0.58	0.53	0.72	-	-	-	0.67	-	0.11	0.72	0.73	-	0.79	0.57	-	0.59
Fe_2O_3	0.34	2.28	3.56	1.59	1.29	0.11	2.57	0.64	1.40	4.05	1.76	0.34	0.69	0.65	0.69	1.41	-
FeO	2.77	1.87	4.43	1.52	6.52	3.29	5.86	2.24	1.54	2.69	1.45	2.74	1.58	1.58	1.49	0.94	3.15
MgO	14.42	14.81	11.13	14.50	12.10	14.95	10.33	15.29	15.11	12.48	14.54	14.76	14.53	14.48	15.11	15.53	14.85
CaO	20.38	18.32	22.41	19.93	23.04	19.31	22.02	22.15	22.97	23.75	19.98	19.65	21.05	20.37	21.38	21.41	20.01
Na_2O	1.76	1.83	0.48	1.92	0.38	1.67	0.44	0.82	0.86	0.35	1.95	1.80	1.73	1.59	1.56	1.62	1.43
K_2O	0.01	0.01	0.01	0.01	0.01	0.02	0.00	0.03	0.02	0.03	0.02	0.03	0.02	0.02	0.03	0.01	0.00
MnO	-	0.00	0.00	0.07	-	-	-	0.06	-	0.03	0.14	0.05	-	0.06	0.12	-	0.08
Total	99.81	96.82	98.19	99.31	99.77	97.26	97.83	98.60	98.79	98.90	100.31	99.90	99.47	97.65	99.17	99.45	99.03
Acmite	0.93	6.40	3.60	4.35	2.81	0.31	3.29	1.77	3.87	2.70	4.77	0.93	1.88	1.78	1.89	3.84	-
Jadeite	11.46	6.89	0.00	9.23	0.00	11.79	0.00	4.22	2.35	0.00	8.94	11.83	10.36	9.71	9.26	7.57	-
Ti-Ts	1.58	1.38	9.45	1.56	7.69	0.53	13.58	0.97	0.83	7.59	2.17	2.26	1.88	1.95	0.63	0.46	-
Fe-Ts	0.00	0.00	6.63	0.00	0.83	0.00	4.16	0.00	0.00	8.78	0.00	0.00	0.00	0.00	0.00	0.00	-
Ca-Ts	8.66	10.58	7.47	10.17	5.32	5.83	6.69	8.56	8.85	3.70	10.38	8.11	8.76	9.48	6.85	7.08	-
FeDi	0.00	0.00	0.00	0.00	0.00	0.00	0.00	0.00	0.00	0.00	0.00	0.00	0.00	0.00	0.00	0.00	-
Woll	34.36	30.65	34.09	32.97	39.34	35.16	33.21	38.96	40.37	37.90	32.30	32.88	35.52	34.64	37.95	37.74	-
Enst	38.84	41.19	31.68	39.30	33.79	41.29	29.64	41.98	41.37	35.04	39.04	39.77	39.21	39.90	40.98	41.88	-
Ferros	4.19	2.92	7.08	2.42	10.22	5.10	9.44	3.54	2.37	4.29	2.40	4.22	2.39	2.54	2.45	1.42	-
Al-4	0.118	0.133	0.330	0.133	0.216	0.069	0.380	0.105	0.105	0.277	0.147	0.126	0.125	0.134	0.081	0.080	-
Al-6	0.201	0.158	0.059	0.173	0.053	0.176	0.067	0.108	0.112	0.034	0.173	0.179	0.191	0.169	0.145	0.146	-

1. Rim of 14A-13 2. Rim of 14B-5 (orthopyroxene xenocryst) 3. Rim of 14B-12 4. Titanaugite rim on inclusion

Pyroxenites

	DN					CHL			BUTE				FIDRA	
	19B-2	19B-3	BX-2	BX-3	BX-4	BX-5	28-1	28-2	28-6	29-1	29-2	29-8	29-4	39-1	39-2
SiO_2	52.27	52.37	49.05	48.96	48.63	48.77	48.16	47.92	48.49	48.90	47.78	49.00	48.65	47.99	48.26
TiO_2	0.57	0.57	1.17	1.10	1.09	1.18	1.73	1.54	1.95	1.60	1.83	1.18	1.10	1.61	1.45
Al_2O_3	4.62	4.31	9.19	9.06	8.99	9.15	8.14	8.27	8.00	7.10	7.79	7.44	7.36	8.51	8.09
Cr_2O_3	1.71	-	0.01	-	-	-	-	-	-	-	-	-	-	0.16	-
Fe_2O_3	1.61	2.50	2.51	1.91	1.43	2.10	4.41	4.62	4.98	2.80	2.70	2.53	3.19	0.78	0.45
FeO	1.63	0.79	3.55	4.02	4.45	3.67	3.24	2.63	3.06	4.59	4.73	4.67	4.29	5.54	6.18
MgO	16.42	16.77	14.49	14.17	13.85	14.14	13.90	14.26	14.49	14.08	13.38	14.04	13.91	13.03	13.16
CaO	18.68	19.05	19.16	19.34	19.12	19.35	19.51	19.56	18.86	20.29	20.20	19.81	19.98	20.03	19.20
Na_2O	1.74	1.73	1.24	1.17	1.16	1.22	1.31	1.19	1.43	0.90	0.92	0.97	0.96	0.92	1.03
K_2O	0.00	0.01	0.01	0.02	0.04	0.02	0.02	0.02	0.02	0.02	0.02	0.02	0.01	0.00	0.00
MnO	0.12	-	0.00	-	-	-	-	-	-	-	-	-	-	0.14	-
Total	99.37	98.10	100.38	99.75	98.96	99.60	100.42	100.01	101.3	100.28	99.35	99.66	99.45	98.71	97.82
Acmite	4.41	6.89	6.86	5.26	3.98	5.78	9.39	8.56	10.15	6.50	6.72	7.02	6.93	2.19	1.27
Jadeite	7.86	5.44	1.92	3.13	4.52	2.97	0.00	0.00	0.00	0.00	0.00	0.01	0.00	4.46	6.23
Ti-Ts	1.56	1.57	3.20	3.03	3.03	3.25	4.76	4.25	5.32	4.42	5.11	3.27	3.06	4.51	4.09
Fe-Ts	0.00	0.00	0.00	0.00	0.00	0.00	2.76	4.20	3.44	1.24	0.83	0.00	1.95	0.00	0.00
Ca-Ts	6.87	5.02	15.53	14.94	14.29	15.01	11.42	11.54	10.06	10.33	11.53	12.89	12.01	12.18	10.69
FeDi	0.00	0.00	0.00	0.00	0.00	0.00	0.00	0.00	0.00	0.00	0.00	0.00	0.00	0.00	0.00
Woll	32.17	34.09	27.91	28.90	29.19	28.81	28.79	28.45	27.23	31.93	31.45	31.04	31.08	31.63	31.21
Enst	44.48	45.78	39.20	38.61	38.13	38.56	37.92	38.98	39.16	38.53	37.02	38.58	38.34	36.17	36.81
Ferros	2.66	1.21	5.39	6.15	6.87	5.62	4.96	4.03	4.64	7.05	7.34	7.20	6.64	8.85	9.70
Al-4	0.100	0.082	0.219	0.210	0.204	0.215	0.237	0.242	0.242	0.204	0.226	0.194	0.201	0.212	0.189
Al-6	0.098	0.105	0.174	0.181	0.188	0.180	0.114	0.115	0.101	0.103	0.115	0.129	0.120	0.162	0.169

Wehrlites

Cpx 5

	FIDRA	CHL		
	39-5	41-1	41-2	41-5
SiO_2	49.00	50.39	50.26	50.78
TiO_2	1.36	1.08	0.77	0.97
Al_2O_3	7.87	6.21	6.41	6.18
Cr_2O_3	0.48	0.22	-	0.23
Fe_2O_3	0.14	0.07	1.97	0.21
FeO	6.52	5.71	3.93	5.87
MgO	13.30	14.93	15.23	14.53
CaO	19.30	18.86	19.12	18.56
Na_2O	1.02	1.00	1.12	1.28
K_2O	0.00	0.00	0.01	0.00
MnO	0.13	0.11	-	0.11
Total	99.12	98.58	98.82	98.72
Acmite	0.39	0.20	5.46	0.58
Jadeite	6.95	6.99	2.59	8.59
Ti-Ts	3.79	3.01	2.13	2.70
Fe-Ts	0.00	0.00	0.00	0.00
Ca-Ts	10.65	7.38	10.50	6.81
FeDi	0.00	0.00	0.00	0.00
Woll	31.14	32.22	31.44	32.02
Enst	36.77	41.20	41.83	40.04
Ferros	10.32	9.01	6.06	9.25
Al-4	0.182	0.134	0.148	0.122
Al-6	0.162	0.137	0.131	0.147

Orthopyroxenes

	CHL					DN			KID			BUTE
	14A-2	14A-4	14A-3	14A-5	14B-5	26-2	26-4	26-6	15-2	15-6	15-8	29-3 1
SiO_2	54.15	54.47	54.46	53.72	54.79	55.40	54.23	55.75	55.30	55.24	55.20	52.11
TiO_2	0.10	0.11	0.05	0.15	0.14	0.09	0.12	0.08	0.17	0.19	0.20	0.35
Al_2O_3	4.35	4.37	4.39	4.58	4.46	4.19	4.73	3.56	4.41	4.66	4.74	6.44
Cr_2O_3	-	-	-	-	-	-	0.53	0.29	0.03	-	-	-
FeO	6.48	6.46	6.52	6.07	6.39	7.41	7.25	7.55	6.78	6.63	6.39	10.44
MgO	32.14	32.00	32.39	31.78	32.14	32.35	31.71	32.78	32.51	32.43	32.28	27.18
CaO	0.74	0.76	0.70	2.78	0.76	0.46	0.80	0.34	0.83	0.71	0.83	1.25
Na_2O	0.08	0.06	0.12	0.15	0.13	0.04	0.05	0.05	0.15	0.10	0.16	0.09
K_2O	0.01	0.02	0.02	0.01	0.02	0.03	0.00	0.01	0.02	0.00	0.02	0.00
MnO	-	-	-	-	-	-	0.12	0.18	0.11	-	-	-
Total	98.05	98.24	98.65	99.24	98.83	99.97	99.55	100.60	100.31	99.96	99.80	97.88

	RPB	BUTE			RPB			FIDRA	
	29-7 2	24B-2	24B-6	27A-4	27A-5	27B-6	24A-1	24A-6	24A-11	37-3	37-9
SiO_2	51.92	55.05	55.12	54.49	54.38	52.48	55.23	55.74	55.74	50.47	54.40
TiO_2	0.37	0.13	0.08	0.15	0.11	0.29	0.10	0.05	0.03	0.13	0.14
Al_2O_3	5.56	4.18	3.65	3.81	3.24	3.39	4.30	3.26	3.23	4.84	4.51
Cr_2O_3	-	0.35	-	0.52	-	-	-	0.28	0.25	0.30	-
FeO	11.91	6.44	6.08	8.94	10.61	13.07	6.06	6.07	6.07	6.64	6.63
MgO	27.13	32.86	32.92	31.30	30.06	28.04	32.80	33.55	33.60	31.75	31.67
CaO	2.28	0.44	0.48	1.19	1.07	2.28	0.53	0.45	0.51	0.76	0.79
Na_2O	0.01	0.02	0.08	0.14	0.09	0.14	0.08	0.10	0.09	0.10	0.12
K_2O	0.01	0.13	0.02	0.01	0.01	0.03	0.01	0.01	0.01	0.03	0.00
MnO	-	0.21	-	0.22	-	-	-	0.15	0.16	0.15	-
Total	99.22	99.73	98.44	100.76	99.58	99.72	99.10	99.66	99.69	99.17	98.26

1, 2. Exsolution lamellae in Bute pyroxenite inclusion.

Olivines

	BUTE	RPB		FIDRA		KN					CHL
	27A-2	24A-5	24A-8	37-5	37-7	38-3	38-4	38-5	38-6	38-8	41-4
	A	B	B	B	B	C	C	C	C	C	D
SiO_2	40.64	40.67	40.43	40.86	40.77	39.50	39.40	41.04	39.12	39.55	39.60
TiO_2	0.03	0.00	0.00	0.01	0.02	0.06	0.03	0.03	0.08	0.04	0.04
Al_2O_3	0.07	0.06	0.04	0.07	0.06	0.09	0.10	0.12	0.06	0.07	0.03
Cr_2O_3	-	0.00	-	0.01	-	-	-	0.07	-	-	-
FeO	14.15	9.81	9.53	10.48	10.68	20.16	21.21	13.55	23.15	22.86	17.69
MgO	46.53	49.05	49.15	47.89	47.43	41.48	40.32	46.67	39.07	40.02	42.86
CaO	0.05	0.03	0.06	0.08	0.04	0.22	0.27	0.25	0.37	0.12	0.11
MnO	-	0.14	-	0.12	-	-	-	0.19	-	-	-
NiO	-	-	-	-	-	-	0.15	0.25	-	-	-
Total	101.52	99.78	99.20	99.51	99.00	101.50	101.47	102.16	101.85	102.66	100.33
Mole % Fo	85	90	90	89	89	79	79	86	75	76	81

A. Harzburgite
B. Lherzolite
C. Basalt phenocryst
D. Wehrlite

Feldspars 1

Basalts

	CHL		EN							EHB		RPB		BUTE		CHL	
	14A-11	14B-15	21A-6	21B-1	21B-8	23-10	23-13	23-14	23-15	25-2	25-10	24B-7	24B-15	27B-8 1	27B-9 2	14AE-5	14AE-9
SiO_2	54.47	50.50	53.82	52.54	52.12	58.17	60.76	55.21	57.20	51.37	52.37	52.13	51.55	50.70	55.43	53.28	51.52
Al_2O_3	28.05	30.78	28.79	28.83	29.27	25.93	24.88	25.49	26.81	28.99	29.46	28.70	28.60	29.96	26.43	28.67	30.24
FeO	0.53	0.56	0.49	0.64	0.57	0.28	0.30	0.18	0.39	0.91	0.51	1.12	1.27	0.60	0.79	0.75	0.51
MgO	0.14	0.06	0.07	0.08	0.09	0.07	0.05	0.03	0.04	0.20	0.44	0.42	0.72	0.19	0.75	0.34	0.11
CaO	10.32	13.08	11.04	11.74	11.97	7.52	6.29	9.82	8.60	11.45	11.87	11.82	12.23	13.48	9.56	11.28	13.05
Na_2O	5.22	3.59	4.84	4.68	4.17	6.18	6.98	5.99	6.62	4.54	4.34	4.54	4.10	3.56	5.35	4.66	3.77
K_2O	0.65	0.36	0.46	0.49	0.62	0.90	0.93	1.69	0.66	0.46	0.26	0.45	0.43	0.26	0.58	0.36	0.34
TiO_2	0.19	0.12	0.13	0.18	0.13	0.10	0.03	0.09	0.07	0.19	0.17	0.26	0.19	0.09	0.15	0.22	0.16
Total	99.57	99.05	99.65	99.19	98.94	99.16	100.21	98.69	100.37	98.02	99.40	99.45	99.10	98.74	99.04	99.65	99.69
Or	3.86	2.15	2.73	2.92	3.70	5.26	5.48	10.12	3.88	2.77	1.55	2.67	2.56	1.56	3.46	2.14	2.02
Ab	42.72	30.62	41.10	36.07	34.77	52.74	58.86	40.20	50.80	35.30	36.94	34.70	33.04	30.48	45.71	39.61	32.00
An	51.41	65.51	54.97	56.68	59.95	37.63	31.14	38.15	41.33	57.96	59.23	56.92	58.90	65.55	46.94	56.21	64.78
Ne	0.89	0.03		2.09	0.49			6.04	2.71	2.11		2.13	1.07	0.02			
Il	0.36	0.23	0.25	0.34	0.25	0.19	0.06	0.17	0.13	0.37	0.32	0.50	0.36	0.17	0.29	0.42	0.30
Ol	0.75	0.75	0.52	0.13	0.79				0.13	1.28	0.70	1.36	2.13	0.38		0.98	0.34
Hy			0.17			0.53	0.62				0.81				2.68	0.55	0.44
Cor		0.71	0.26			1.13	0.97			0.21	0.46					0.11	
Qtz						2.42	2.87								0.17		
Rut																	
Di	0.01			1.77	0.06			1.21	1.02			1.72	1.94	1.84	0.85		0.13
Woll								4.11									

1. Core 2. Rim

Zeolites from basalts

	CHL		KM	DM	EN								EHB	CHL
	14AE-11	14AE-12	38-7	20-7	21A-5	21A-8	21B-3	21B-9	21C-2	21C-12	22-1	22-2	22-8	25-1	14AE-3
SiO_2	51.52	51.67	52.97	64.74	55.59	50.46	58.13	56.67	57.82	49.85	66.45	66.46	62.96	60.10	63.15
Al_2O_3	28.93	29.89	28.47	18.71	27.13	26.09	21.56	22.20	22.21	24.69	21.13	18.69	20.60	23.31	21.23
FeO	0.76	0.43	1.28	0.00	0.37	0.10	0.12	0.15	2.58	2.12	0.08	0.11	0.10	0.28	0.49
MgO	0.14	0.14	0.27	0.01	0.03	0.03	0.03	0.05	2.54	0.29	0.00	0.03	0.02	0.03	0.20
CaO	12.02	12.61	11.79	0.03	0.10	0.20	0.12	0.10	0.48	0.29	0.03	0.03	0.00	0.18	2.94
Na_2O	4.46	4.28	3.97	1.78	11.42	12.83	12.01	12.09	9.78	8.09	11.47	7.77	11.72	8.17	4.19
K_2O	0.34	0.57	0.62	11.40	0.70	0.09	0.08	0.08	0.16	0.59	0.05	0.08	0.07	0.28	3.39
TiO_2	0.16	0.13	0.15	0.03	0.02	0.03	0.40	0.24	0.14	0.05	0.02	0.01	0.03	0.14	0.26
Total	98.24	99.72	99.52	96.70	95.35	89.81	92.48	91.58	95.70	85.98	99.21	93.18	94.90	92.50	95.84
Or	2.05	3.38	3.69	69.66	4.34	0.59	0.51	0.52	0.99	4.06	0.30	0.51	0.44	1.79	20.90
Ab	34.80	30.94	33.81	15.58	69.55	60.14	80.86	77.85	78.19	76.66	96.60	70.56	90.42	74.75	36.99
An	58.68	60.83	58.40	0.15	0.52	1.10	0.64	0.54	2.49	1.67	0.15	0.16		0.97	15.22
Ne	1.96	2.91			17.23	32.89	15.74	18.34	4.50	1.61	0.65		7.63		
Il	0.31	0.25			0.04	0.06	0.27	0.35	0.20	0.11	0.04	0.02	0.06	0.29	0.52
Ol	0.46	0.09			0.56	0.17	0.06	0.10	8.33	4.01	0.09		0.15		
Hy			2.84	0.03								0.28		0.39	1.01
Cor				3.50	7.76	5.03	1.62	2.23	5.30	11.88	2.17	2.19	1.31	9.99	5.55
Qtz			0.87	11.04								22.29		11.84	19.82
Rut				0.03			0.29	0.08							
Di	1.74	1.60	0.40												
Woll															

Feldspars 2

	Elie-type 2 nodules					*Type 4*								*Type 5*	
	EN														
	35-4	35-10	32-9	32-10	32-10A	11-8	11-9	11-12	11-15	36-4	36-5	36-8	36-10	30-3	30-4
SiO_2	62.50	62.35	64.12	65.92	66.68	66.67	67.10	70.08	66.53	66.26	70.46	65.61	66.76	68.51	68.88
Al_2O_3	23.36	22.41	21.56	21.24	21.53	20.82	20.72	20.96	20.52	22.73	21.38	22.39	22.61	20.14	20.26
FeO	0.12	0.08	0.10	0.12	0.12	0.20	0.13	0.03	0.03	0.09	0.04	0.09	0.06	0.17	0.16
MgO	0.02	0.02	0.00	0.03	0.03	0.02	0.02	0.01	0.01	0.01	0.01	0.01	0.01	0.02	0.02
CaO	4.70	3.81	2.89	3.01	2.98	1.24	1.21	1.21	1.11	2.69	1.59	2.58	2.82	0.86	0.84
Na_2O	8.29	8.08	6.89	5.25	7.85	10.25	10.47	10.47	10.71	9.71	10.18	10.25	9.73	9.98	10.36
K_2O	0.96	1.85	3.71	6.11	1.27	0.34	0.32	0.32	0.38	0.33	0.40	0.41	0.37	1.04	1.04
TiO_2	0.05	0.10	0.12	0.03	0.03	0.02	0.00	0.02	0.03	0.02	0.02	0.01	0.02	0.01	0.03
Total	99.98	98.70	99.39	101.71	100.50	99.56	99.97	103.10	99.32	101.84	104.07	101.35	102.38	100.74	101.59
Or	5.67	11.08	22.07	35.48	7.49	2.03	1.90	1.97	2.26	1.91	2.25	2.36	2.15	6.10	6.05
Ab	70.15	69.27	58.65	43.69	66.10	87.13	90.89	85.96	91.25	80.64	82.75	83.17	80.42	83.84	86.29
An	23.32	19.15	14.44	14.68	14.71	6.19	6.01	5.81	5.54	13.12	7.57	12.65	13.65	4.24	4.10
Ne												1.29			
Il	0.09	0.17	0.20	0.06	0.06				0.06	0.04	0.03		0.04	0.02	0.06
Ol												0.12			
Hy	0.19	0.05	0.01	0.24	0.24	0.42	0.29	0.08	0.03	0.16	0.05		0.11	0.34	0.29
Cor	0.14	0.19	0.96	0.52	1.82	1.33	0.44	1.13	0.47	1.48	1.27	0.39	1.05	1.03	0.56
Qtz	0.44	0.08	3.66	5.34	9.59	2.90	0.47	5.06	0.39	2.65	6.07		2.57	4.44	2.66
Rut		0.01	0.01												
Di															
Woll															

	CHL	DN												EN	
	28-5 1	20-2	20-3	20-5	20-6	20-8	20-9	26-13	26-14	40-1	40-2	40-3	40-4	40-5	23-1 2
SiO_2	52.96	51.87	55.12	56.98	64.48	56.53	56.46	63.57	61.55	66.51	64.91	62.70	62.58	66.84	62.38
Al_2O_3	28.89	30.85	28.29	26.14	23.21	27.09	27.06	19.07	19.63	21.16	18.43	22.95	23.22	18.49	23.43
FeO	0.70	0.27	0.09	0.37	0.08	0.14	0.13	0.23	0.15	0.10	0.09	0.17	0.10	0.36	0.20
MgO	0.12	0.26	0.00	0.03	0.00	0.05	0.01	0.06	0.00	0.00	0.00	-	-	-	0.04
CaO	12.40	12.44	10.66	8.60	4.62	9.31	9.99	0.19	0.65	2.22	0.08	4.71	4.73	0.11	4.98
Na_2O	4.17	4.21	4.86	6.07	8.43	5.17	5.47	4.95	4.54	10.44	1.57	8.78	8.67	5.85	7.87
K_2O	0.37	0.17	0.07	0.13	0.16	1.22	0.14	8.96	8.33	0.16	14.35	0.19	0.17	8.05	0.74
TiO_2	0.22	0.05	0.05	0.08	0.04	0.09	0.06	0.13	0.50	0.00	-	-	-	-	0.04
Total	99.84	99.32	99.15	98.40	101.04	99.60	99.32	97.15	95.35	100.59	99.44	99.48	99.47	99.71	99.67
Or	2.19	1.01	0.42	0.78	0.94	7.24	0.83	54.49	51.62	0.94	85.28	1.13	1.01	47.71	4.39
Ab	35.35	35.40	41.48	32.20	70.61	43.92	46.60	43.09	40.29	87.82	13.36	74.67	73.75	49.65	66.81
An	59.12	62.14	53.34	43.36	22.69	46.37	49.20	0.97	3.38	10.34	0.40	22.76	23.59	0.42	24.78
Ne		0.25						0.01							
Il	0.42	0.10	0.10	0.15	0.08	0.17	0.11	0.24	0.33						0.08
Ol		0.78						0.27							
Hy	0.12		0.08	0.63	0.08	0.23					0.17		0.18	0.60	0.40
Cor		0.32	0.85	0.38	0.76	0.34		0.91	2.06		0.17				0.63
Qtz	0.66		3.74	2.49	4.85	1.72	2.79		1.96	0.46	0.62	0.83	1.29	1.50	2.91
Rut									0.35						
Di	2.15						0.32			0.34		0.59		0.11	
Woll							0.14			0.09		0.02			

1. From Coalyard Hill pyroxenite inclusion 2. Megacryst in Elie Ness monchiquite

Amphiboles

	EN	CHA	EN							CHL	CHA			EN		KH	
	23-2	13A1	B-1	B-2	B-3	B-4	B-5	B-10	B-11	28-3	13B-5	13B-10	13B-12	10-1	10-4	12-4	12-9
	A	B	B	B	B	B	B	B	B	C	B	C	D	B	D	D	D
SiO_2	38.97	39.86	39.87	40.01	38.98	38.82	39.90	38.59	38.65	40.47	38.87	38.29	38.37	39.10	39.17	39.73	39.53
TiO_2	6.30	4.59	4.34	2.19	5.43	5.46	4.17	5.49	5.36	6.48	4.97	4.29	4.83	4.48	2.97	6.12	6.11
Al_2O_3	13.83	13.45	14.71	14.05	13.61	13.67	14.03	14.51	14.56	12.78	13.27	14.56	13.56	13.88	14.67	13.49	13.59
Cr_2O_3	-	-	0.00	0.00	0.01	-	-	0.01	-	0.11	-	-	0.04	-	-	-	-
FeO	11.56	13.16	8.89	13.14	12.13	11.92	12.06	10.07	9.68	6.19	12.85	11.77	12.80	11.02	10.69	10.60	10.40
MgO	11.12	10.86	13.25	10.48	11.23	11.33	11.72	12.03	12.16	17.03	11.18	11.42	10.79	12.24	13.12	12.44	12.58
CaO	11.37	10.64	10.75	11.04	11.48	11.48	10.83	11.60	11.92	10.97	10.21	11.42	11.28	10.47	10.02	11.45	11.65
Na_2O	2.70	2.55	2.31	3.36	2.33	2.31	2.50	2.38	2.46	2.33	2.46	2.71	2.38	2.44	2.82	2.25	2.11
K_2O	1.50	2.06	2.39	1.50	1.79	1.80	2.18	1.94	1.99	1.70	1.99	1.19	1.56	2.23	1.01	1.69	1.81
MnO	-	-	0.12	0.14	0.09	-	-	0.06	-	0.02	-	-	0.13	-	-	-	-
Total	97.34	97.17	96.63	95.91	97.06	96.79	97.38	96.68	96.79	98.09	95.90	95.65	95.73	95.86	94.47	97.77	97.78
Formula based on 23 oxygens.																	
Si	5.825	6.001	5.926	6.102	5.869	5.852	5.965	5.785	5.782	5.856	5.933	5.822	5.915	5.919	5.952	5.878	5.850
Al	2.437	2.386	2.577	2.526	2.415	2.429	2.472	2.564	2.567	2.180	2.387	2.609	2.432	2.476	2.627	2.353	2.371
Fe	1.445	1.657	1.105	1.676	1.527	1.503	1.508	1.263	1.211	0.749	1.640	1.497	1.629	1.395	1.359	1.312	1.287
Mg	2.478	2.437	2.936	2.382	2.520	2.546	2.612	2.688	2.711	3.673	2.543	2.588	2.447	2.762	2.972	2.744	2.775
Ca	1.821	1.716	1.712	1.804	1.852	1.854	1.735	1.863	1.911	1.701	1.671	1.860	1.839	1.698	1.631	1.815	1.847
Na	0.783	0.744	0.666	0.994	0.680	0.675	0.725	0.692	0.714	0.654	0.728	0.799	0.702	0.716	0.831	0.645	0.605
K	0.286	0.396	0.453	0.292	0.344	0.346	0.416	0.371	0.380	0.314	0.387	0.231	0.303	0.431	0.196	0.319	0.342
Ti	0.708	0.520	0.485	0.251	0.615	0.619	0.469	0.619	0.603	0.705	0.570	0.491	0.553	0.510	0.339	0.681	0.680
mg	0.632	0.595	0.726	0.587	0.623	0.629	0.634	0.680	0.691	0.831	0.608	0.634	0.600	0.664	0.686	0.677	0.683

	EN															
	34-7	34-8	34-11	34-12	35-1	35-7	35-11	32-1	32-3	32-4	11-4	11-5	11-6	36-3	36-7	36-9
	D	D	D	D	E	E	E	E	E	E	F	F	F	F	F	F
SiO_2	39.18	39.06	39.03	40.39	40.87	39.51	39.43	40.70	40.06	39.98	44.87	44.37	43.63	40.16	40.98	39.68
TiO_2	5.68	5.63	6.02	4.23	4.42	5.67	5.66	4.35	4.32	4.70	2.39	2.44	2.51	2.78	2.89	2.89
Al_2O_3	14.17	14.21	14.48	13.97	12.83	13.52	13.32	12.87	13.66	13.35	10.68	10.40	11.30	14.47	13.48	15.37
Cr_2O_3	0.06	0.03	-	-	0.10	0.04	-	0.06	0.06	-	-	0.20	-	0.00	0.02	-
FeO	10.43	10.46	10.31	10.38	12.87	11.93	12.01	12.06	11.15	11.50	13.18	12.94	13.43	15.50	15.65	14.93
MgO	12.60	12.68	12.42	13.11	10.74	10.76	10.75	11.68	11.92	11.41	12.52	12.38	11.71	9.42	9.85	9.59
CaO	11.34	11.33	11.44	11.42	11.16	11.22	11.00	10.98	11.32	11.27	9.63	9.92	9.55	9.59	9.18	9.89
Na_2O	2.63	2.52	2.50	2.82	2.93	2.74	2.64	2.75	2.54	2.73	4.90	4.63	4.51	4.70	5.09	4.48
K_2O	1.56	1.57	1.65	1.54	1.47	1.65	1.56	1.54	1.60	1.60	0.69	0.63	0.75	0.72	0.73	0.81
MnO	0.12	0.09	-	-	0.19	0.14	-	0.14	0.13	-	-	-	-	0.21	0.19	-
Total	97.76	97.58	97.84	97.85	97.56	97.08	96.36	97.12	96.76	96.54	98.76	97.91	97.39	97.56	98.05	97.65
Formula based on 23 oxygens.																
Si	5.803	5.798	5.770	5.954	6.121	5.935	5.954	6.094	6.004	6.010	6.560	6.559	6.483	6.062	6.155	5.960
Al	2.476	2.486	2.523	2.427	2.265	2.394	2.370	2.271	2.413	2.365	1.840	1.812	1.979	2.574	2.386	2.721
Fe	1.293	1.299	1.275	1.280	1.612	1.486	1.517	1.510	1.397	1.446	1.612	1.600	1.669	1.957	1.966	1.876
Mg	2.784	2.806	2.737	2.881	2.397	2.409	2.419	2.607	2.663	2.557	2.728	2.728	2.594	2.119	2.205	2.147
Ca	1.801	1.802	1.812	1.804	1.791	1.806	1.780	1.762	1.818	1.815	1.509	1.571	1.520	1.551	1.477	1.592
Na	0.756	0.725	0.717	0.806	0.851	0.798	0.773	0.798	0.738	0.796	1.361	1.327	1.299	1.375	1.482	1.305
K	0.295	0.297	0.311	0.290	0.281	0.316	0.300	0.294	0.306	0.307	0.129	0.119	0.142	0.139	0.140	0.155
Ti	0.633	0.628	0.669	0.469	0.498	0.641	0.643	0.490	0.487	0.531	0.263	0.271	0.280	0.316	0.326	0.326
mg	0.683	0.684	0.682	0.692	0.598	0.618	0.615	0.633	0.656	0.639	0.629	0.630	0.608	0.520	0.529	0.534

A. Phenocryst in monchiquite B. Megacryst in tuff or basalt C. Alteration of clinopyroxene D. Elie-type 1 nodule
E. Elie-type 2 nodule F. Elie-type 4 nodule

Opaques etc

Titanomagnetites & sulphides

	CHA	BUTE	EN							BUTE	EN				
	13B-15	27B-12	A-14	A-15	21C-3	22-9°	23-4°	23-5	23-6	27A-3	34-9°	35-6°	32-8°	32-11	32-12
								1	2		A	B	B	B	B
SiO_2	0.35	0.60	0.00	0.00	0.75	0.36	0.19	0.12	1.51	8.65	0.06	0.50	2.08	0.11	0.04
Al_2O_3	7.19	2.38	0.02	11.69	2.55	0.10	0.08	2.43	2.09	0.04	0.07	0.17	0.04	6.71	0.27
FeO	64.79	63.72	58.81	26.63	57.52	61.70	64.28	60.41	73.64	73.04	59.16	60.21	60.45	73.90	42.88
MgO	2.74	1.28	2.35	14.59	0.04	0.15	0.06	0.03	0.10	4.02	0.04	0.09	0.06	1.74	4.56
CaO	0.01	0.01	0.00	0.00	0.13	0.12	0.19	0.00	0.38	0.01	0.29	0.26	0.02	0.10	0.12
TiO_2	15.27	24.50	0.06	0.17	26.65	0.15	0.13	24.77	8.00	0.00	0.02	0.03	0.02	10.07	49.46
Cr_2O_3	-	0.03	0.00	0.00	-	-	-	-	-	-	0.00	0.01	0.02	0.24	0.04
MnO	-	0.95	0.00	0.14	-	-	-	-	-	-	0.05	0.01	0.02	0.46	0.59
Total	90.35	93.48	61.23	53.22	86.51	62.58	64.93	87.76	85.72	85.76	59.69	61.28	60.71	93.31	97.96

1. Core zone 2. Rim of 23-5 * denotes pyrite (FeS_2)

Chrome-spinels

	EN				CHL				DN	KID		RPB			CHL
	36-1	13-8°	11-7°	11-11°	14A-1	14A-2	14A-17	14A-1A	26-1	15-5	15-7	24B-5	24A-3	24A-10	14AE-4
	C	A	A	A											3
SiO_2	0.02	1.03	0.03	0.16	0.05	0.16	0.03	0.05	0.07	0.04	0.12	0.08	0.05	0.02	0.19
Al_2O_3	0.05	0.57	0.00	0.02	58.14	59.41	52.11	58.16	53.57	57.91	57.81	59.14	55.45	58.12	54.11
FeO	44.17	60.07	60.17	57.66	10.91	10.39	13.95	10.91	15.25	12.00	11.81	9.54	9.54	9.53	12.41
MgO	1.92	0.00	0.07	0.38	21.12	21.24	19.00	21.13	18.39	21.22	20.30	20.62	20.75	20.97	19.89
CaO	0.04	0.03	0.01	0.71	0.03	0.26	0.03	0.03	0.00	0.00	0.00	0.02	0.02	0.00	0.12
TiO_2	51.76	0.00	0.01	0.08	0.04	0.13	0.13	0.04	0.08	0.28	0.22	0.07	0.02	0.07	0.48
Cr_2O_3	0.00	-	-	-	9.59	7.36	9.75	9.87	11.93	8.36	8.17	8.30	11.96	9.69	12.78
MnO	1.40	-	-	-	0.00	0.08	0.07	0.07	0.19	0.10	0.08	0.09	0.14	0.15	0.16
Total	99.35	61.70	60.29	59.01	99.88	99.03	95.07	100.26	99.49	99.91	98.51	97.85	97.92	98.53	100.14

A. Type 1 Elie nodules B. Type 2 Elie nodules C. Type 4 Elie nodules

Pleonastes

	CHL	FIDRA					DN			
	14AE-8	37-1	37-6	39-3	39-4	37-8	BX-1	BX-8	BX-9	
	4									
SiO_2	0.25	0.05	0.07	-	-	0.08	0.12	0.08	0.09	
Al_2O_3	53.85	59.01	58.97	56.37	53.37	58.53	61.57	61.10	61.50	
FeO	13.12	10.60	9.90	22.25	24.00	10.33	17.70	17.66	17.33	
MgO	18.64	20.61	20.91	16.59	15.28	20.68	19.76	19.57	19.48	
CaO	0.12	0.00	0.01	-	-	0.00	0.00	0.01	0.00	
TiO_2	0.77	0.13	0.24	0.56	0.86	0.10	0.48	0.44	0.51	
Cr_2O_3	11.52	8.32	8.35	3.18	5.14	8.98	0.02	-	-	
MnO	0.15	0.14	0.15	0.20	0.12	0.13	-	-	-	
Total	98.42	98.85	98.59	99.03	98.97	98.82	99.65	98.86	98.91	

3 and 4. Spinels from quench vein in lherzolite inclusion.

Garnets (Elie)

	C- - - - R			C- - - - R			
SiO_2	41.79	41.69	41.69	41.61	41.52	41.64	41.40
Al_2O_3	23.44	23.43	23.34	23.39	23.26	23.41	23.22
FeO	9.96	9.83	10.69	10.66	10.90	10.66	9.84
MgO	18.64	18.50	18.43	18.07	18.10	18.30	18.94
CaO	5.33	5.26	5.27	5.33	5.25	5.33	5.45
TiO_2	0.36	0.36	0.40	0.42	0.40	0.42	0.38
Cr_2O_3	0.08	0.08	0.01	0.07	0.07	0.06	0.19
MnO	0.35	0.32	0.33	0.33	0.33	0.38	0.34
Total	99.99	99.50	100.20	99.86	99.82	100.20	99.76

C- -R denotes core and rim analyses.

Anorthoclase

	CHA	RPB	AN	CHA		END			KL		ENT
SiO_2	68.39	67.79	67.73	67.82	67.45	69.19	71.02	71.35	66.73	66.78	69.62
Al_2O_3	19.25	19.36	19.55	19.49	19.59	18.76	19.28	19.38	18.88	19.25	19.49
FeO	0.17	0.17	0.14	0.14	0.13	0.16	0.14	0.19	0.15	0.14	0.16
MgO	0.00	0.02	0.00	0.03	0.03	0.04	0.01	0.04	0.02	0.04	0.03
CaO	0.47	0.43	0.37	0.45	0.51	0.21	0.29	0.28	0.33	0.45	0.45
Na_2O	8.93	8.84	8.88	8.33	8.61	9.51	9.38	9.31	5.78	5.92	8.58
K_2O	2.69	3.36	3.03	2.89	2.92	3.03	2.32	2.29	7.96	7.94	3.09
TiO_2	0.02	0.02	0.00	0.05	0.00	0.03	0.02	0.01	0.07	0.04	0.05
Total	99.92	99.99	99.70	99.20	99.24	100.92	102.46	102.85	99.90	100.55	101.50
Or	15.91	19.86	17.96	17.22	17.39	17.75	13.38	13.16	47.11	46.68	18.00
Ab	75.62	74.81	75.37	71.05	73.41	78.92	77.48	76.60	48.98	49.83	71.55
An	2.33	2.13	1.84	2.25	2.55		1.40	1.35	1.64	2.22	2.18
Ne											
Il	0.04	0.04		0.10							0.09
Ol											
Hy	0.28	0.33	0.26	0.25	0.32		0.28	0.44	0.33	0.35	0.28
Cor	0.79	0.40	0.99	1.85	1.35		0.79	1.05	0.16	0.10	1.20
Qtz	5.02	2.43	3.58	7.28	4.99	2.32	6.67	7.40	1.79	0.81	6.70
Rut											
Di						0.76					
Woll						0.06					

LOCALITIES

CHA. Coalyard Hill sheet

RPB. Ruddons Point sheet

AN. Ardross Neck dyke

END. Elie Ness dyke

KL. Kellie Law

ENT. Elie Ness tuff

Biotites

	EN									DN			
	33-2 A	33-3 A	33-7 A	11-2 B	11-3 B	11-14 B	36-2 B	36-6 B	30-1 C	30-2 C	20-1 D	20-10 D	19B-1 E
SiO_2	37.18	37.10	37.54	37.70	37.99	37.16	35.53	35.18	35.72	35.93	36.20	35.98	37.94
TiO_2	3.57	3.63	3.23	3.05	2.98	2.76	3.73	3.81	5.23	5.23	2.18	1.91	3.77
Al_2O_3	14.47	14.53	14.34	14.27	14.41	13.73	15.79	15.53	13.40	13.26	16.26	15.15	15.76
Cr_2O_3	0.06	-	-	0.04	-	-	0.00	-	0.00	0.00	-	-	1.90
FeO	14.95	15.03	15.16	14.11	14.11	13.69	17.23	17.02	23.48	23.15	19.72	21.56	3.70
MgO	14.71	14.78	15.33	15.80	15.98	16.43	13.74	13.69	9.14	9.00	10.85	10.73	21.35
CaO	0.00	0.06	0.05	0.01	0.00	0.01	0.00	0.00	0.00	0.01	0.00	0.04	0.07
Na_2O	0.91	0.88	0.83	1.08	0.95	1.09	0.98	1.12	0.75	0.87	0.37	0.28	0.96
K_2O	8.93	8.48	8.62	8.23	8.23	8.17	8.50	8.28	8.59	8.48	9.13	8.81	9.04
MnO	0.13	-	-	-	-	-	0.21	-	0.32	0.30	-	-	0.03
Total	94.91	94.48	95.10	94.29	94.65	93.04	95.70	94.62	96.63	96.22	94.71	94.45	94.51
MgO /FeO	0.98	0.98	1.12	1.12	1.13	1.20	0.80	0.80	0.39	0.39	0.55	0.50	5.77

A. Elie-type 3 nodules B. Elie-type 4 nodules C. Elie-type 5 nodules D. Tonalite inclusion E. Lherzolite inclusion

APPENDIX TWO

Geochemical techniques

Sample preparation

Rock-samples intended for bulk-analysis were initially selected for minimum weathering and alteration. Weathered surfaces were removed from the samples by means of a Cutrock hydraulic splitter, leaving an average sample of 50-500gms. Crushing down to chips of less than 5mm size was carried out using a Sturtevant jaw-crusher. The chips and powder so obtained were homogenised by 'coning and quartering' and approximately 50gms of the sample was crushed down to a grain size in the order of 100 mesh (BS) in a tungsten carbide barrel Tema. A portion of this powder was retained for wet-chemical analysis. A final sample of 20-30gms of homogenised powder was then ground under acetone for about 20 minutes in an agate Micronizer to reduce the grain size to less than 20 microns. For XRF analysis 5-6gms of the fine powder was dried overnight at 110°C and pressed into discs on a boric acid backing at 15 tons pressure. Material intended for use as standards was prepared similarly.

Mineral separation

The spinel and augite samples used as starting material in the spinel-pyroxenite experimental runs were separated by a dense liquid technique. Clerici solution used with a centrifuge separator was found to give excellent results on 100 mesh powder from the pyroxenite

nodules. The resulting separates were 'micronised', a technique used on all the materials selected for experimental work.

X-ray fluorescence.

All analyses for major and trace elements were performed on whole-rock powder discs using a Phillips automatic PW1212 X-ray fluorescence spectrometer. The use of whole-rock discs for major-element analysis was found preferable to the use of fusion discs as samples are more easily prepared and one set of discs can be used for both major and trace-element analysis. The length of count-time required by individual samples is also reduced. Machine conditions for major-element analysis are outlined in Table A2-1. A monitor disc of USGS standard W-1 was used in each batch of four samples and counts were automatically corrected back to a standard monitor count to compensate for machine instability. A group of 15-20 NBS, USGS and departmental standards was used and the weight percent values were calculated using an iterative programme correcting for mass-absorption. The analytical technique and computer programme were developed by Brown, Hughes and Esson (1973). The reliability of this method was checked by comparison with wet-chemical Na_2O analyses. Na_2O is not normally determined by XRF, in common with other elements of low atomic number. However, the finely crushed nature of the samples used in the above method is found to give reliable values. The table below presents six widely spread Na_2O values determined by XRF and wet-chemically, the latter method being generally accepted as being the more accurate.

Table A2-1

XRF machine conditions for major-element analysis.
(As preset on automatic pegboard.)

Channel	Counts	kV	mA	Coll.	Crystal	Time on W-1. (secs)
Si	10^5	40	24	C	2-1	17.8
Al	3×10^4	40	24	C	2-1	14.2
Fe	10^5	40	24	F	3-1	14.3
Mg	10^4	40	32	C	1-1	17.9
MgBg	Timed	40	32	C	1-1	17.9
Ca	10^5	40	8	F	2-1	15.5
Na	3×10^3	40	32	C	1-1	24.5
NaBg	Timed	40	32	C	1-1	24.5
K	10^5	40	24	C	2-1	32.5
Ti	3×10^4	40	24	F	3-1	16.7
P	10^3	60	24	F	2-1	26.0
PBg	Timed	60	24	F	2-1	26.0

Coll...collimator (fine or coarse).
Timed...background count set to count-time of peak.
Time on W-1...approximate time to attain preset counts on USGS standard W-1 under good operating conditions.

Sample	16	16(dup)	21	25	29	38
XRF wt %	2.78	2.78	4.84	5.06	1.26	0.20
Wet-chem. wt %	2.67	2.70	4.31	4.69	1.56	0.22

As an estimate of precision of the above method several samples were analysed using the standard fusion technique (Rose et al. 1963) and Table A2-2 presents a comparison of analyses of sample XR-26. This sample was also subjected to five repeated runs both in the same batch and at a later period in another batch, using the whole-rock disc method. The precision of the results is also presented in Table A2-2.

Electron-microprobe analysis.

All the microprobe analyses presented were performed on a Cambridge Instruments Microscan 5 machine in Edinburgh. The standards used were all polished minerals or Specpure metals and are listed below:-

SiO_2	Wollastonite
Al_2O_3	Corundum
TiO_2	'Specpure' metal
CaO	Wollastonite
FeO	'Specpure' metal
MgO	Periclase
Na_2O	Jadeite
K_2O	Orthoclase
MnO	'Specpure' metal
Cr_2O_3	'Specpure' metal

Each analysed point was subjected to 4 ten second counts for each element and 2 ten second background counts on either side of

Table A2-2

Precision of XRF major-element procedure.

All analyses for sample XR-26.

Oxide	Mean	σ	C %
SiO_2	45.29	0.073	0.16
Al_2O_3	14.89	0.274	1.84
TiO_2	2.94	0.075	2.55
MgO	7.27	0.103	1.42
Fe_2O_3Tot	10.55	0.078	0.74
CaO	9.28	0.089	0.96
Na_2O	4.93	0.112	2.27
K_2O	1.67	0.013	0.78
P_2O_5	1.19	0.008	0.67

Comparison with fusion technique.

Oxide	Powder method (mean)	Fusion method
SiO_2	45.29	45.53
Al_2O_3	14.89	14.35
TiO_2	2.94	2.79
MgO	7.27	6.71
CaO	10.55	10.57
Fe_2O_3Tot	9.28	9.18
K_2O	1.67	1.65
P_2O_5	1.19	1.19

σ ...standard deviation.

C % ...relative deviation (100σ/mean)

the main peak. An average count was then obtained. This, along with dead-time correction and apparent concentration was calculated manually using a programmed Compucorp calculating machine. The apparent concentrations were fed into a computer programme and corrected for atomic number, characteristic fluorescence and mass-absorption, and converted into oxide weight percent. The methods of analysis and correction are similar to those of Sweatman and Long (1969).

Modal analyses.

Modal data were obtained by point-counting using a Swift mechanical microscope stage and counter. Between 500 and 800 points were used for each analysis.

Wet-chemical techniques.

a) Ferrous iron

FeO was determined using the method of Wilson (1955) involving solution of rock-powder in cold hydrofluoric acid in the presence of excess ammonium vanadate in PTFE crucibles. This process takes from 3 to 7 days. The vanadate is titrated against ferrous ammonium sulphate in the presence of sulphuric and boric acids. A sodium diphenylamine sulphonate indicator is used. The samples were treated in two batches, XR-9 being analysed in each batch. The results obtained were 5.06% FeO and 4.95% FeO, an estimated precision of $\pm$3%.

b) Na_2O

Soda was determined by flame-photometer after solution in cold HF and dilution in distilled water and sulphuric acid. The results of the six analyses are presented earlier in this Appendix. XR-16 was subjected to duplicate analysis, the values obtained being 2.67 and 2.70% Na_2O.

APPENDIX THREE

High-pressure experimental procedure

All the experiments described in Chapter 6 were performed on dry, micronised, natural materials. Preparation of crushed powders is described in Appendix 2. Runs above 5kb were carried out on single-stage, piston-cylinder, solid-media apparatus, similar to that described by Boyd and England (1960, 1963). Pressure is applied by means of a hydraulically operated, half-inch diameter, tungsten carbide piston.

About 15 to 20mgs of homogenised sample powder were loaded into platinum capsules which had been annealed overnight at 1200 to 1300°C. The crimped capsule was then dried for one hour at 800°C in a nitrogen atmosphere and welded-up, using a DC carbon-arc microwelder, immediately on removal from the furnace. Furnace assemblies were made up several days in advance and stored in a dessicator until use. After 'forming' the capsule was inserted into the furnace cell and loaded into the press. Temperature control was maintained by use of a $Pt/Pt_{87}Rh_{13}$ thermocouple in contact with the capsule and connected to an automatic Eurotherm temperature controller.

After compressing the assembly under 170tons pressure the operating piston was driven into the cylinder to apply the required pressure. All the runs were carried out using the 'piston-out' technique described by Richardson et al (1968) in which the effect

of friction on the measured 'nominal pressure' is taken to result in $P_{actual} > P_{nominal}$. An overshoot of about 5kb was used in all cases. The apparatus and methods of calibration used in Edinburgh are described by O'Hara et al (1971). After bringing the furnace to temperature the pressure was bled back to the required pressure, and over the initial period of any run continual adjustment was required to compensate for the thermal expansion of the apparatus.

Samples were quenched by cutting off power to the furnace. Charges were accepted in which the thermocouple joint was found to be welded to the top of the platinum capsule. The precision of the temperature measurements is high, generally being less than $\pm 1^{\circ}C$ during the course of a run. Bravo (1973) estimated the error in temperature measurement to be in the order of $\pm 10^{\circ}C$. Estimates of pressure accuracy are confused. Unpublished data of Herzberg suggests that at low temperatures the error may be minimal, possibly less than ± 0.5kb, but as temperature increases the error rises and at temperatures greater than $1400^{\circ}C$ it may be as much as ± 2kb.

All the 5kb runs were performed in internally-heated gas-vessels, as described by Ford (1972). Sample preparation was the same as that for the higher pressure work, except where iron capsules were used. In those cases welding was performed with an oxy-acetylene torch. A thin film of carbon deposited on the outside of the capsules after welding indicated that no oxidation had taken place. Several capsules can be inserted into the furnace at one time. Argon, passed through an intensifier pump, acted as the

pressure medium and $Pt/Pt_{87}Rh_{13}$ thermocouples were used as temperature sensors. Pressure was measured by a manganin coil connected through a Wheatstone Bridge circuit. Temperature was controlled by a West Viscount controller. The errors in these procedures are discussed by Ford (1972). It is thought that the error and precision in temperature are similar to those experienced with the solid-media apparatus. The error in measured pressure is thought to be in the order of 10bars per kilobar, which would be an error of $\pm$50 bars in the 5kb runs.

Identification of phases.

After extraction of the charges from the capsules the material was coarsely ground under acetone and a portion was mounted for examination under a Zeiss Ultraphot microscope. The remainder of the sample was retained for X-ray diffraction analysis. It was generally found that all phases could be identified optically. Small amounts of some phases were observed microscopically whilst not being present in the large enough quantities to show on an XRD trace.

APPENDIX FOUR

Computer methods.

Programmes for the reduction of XRF and microprobe data have been outlined above. Further programmes in general use in the Department estimate norms, projections in the C-M-A-S system, extract calculations, mineral formulae and various ratios and subprojections from the above data.

Two programmes used a great deal in the preparation of this work are those for handling clinopyroxene data. FE3CALC3 is a slightly modified version of a charge-balancing method for the estimation of ferric iron in clinopyroxenes devised by A. K. Ferguson (University of Melbourne). This programme assumes perfect stoichiometry in the pyroxene structure and estimates ferric iron by charge-balancing and cation site occupancy. A full cation site value of 4 is assumed and any deficiency is made up for by ferric iron. This method has obvious drawbacks and does not provide an accurate ferric analysis. Its main advantage is in giving an estimation of the approximate ferric-ferrous proportions, and to this extent works best on the more iron-rich pyroxenes. Table A4-1 lists seven clinopyroxene analyses taken from Deer, Howie and Zussman (vol. 2) which were recalculated using FE3CALC3. As noted the higher iron values produce a more accurate answer though the lower values also produce an acceptable result.

The clinopyroxene end-members were calculated according to the

Table A4-1

Accuracy of ferrous-ferric recalculation by FE3CALC3

	D.H.Z.		FE3CALC3	
Clinopyroxene	FeO	Fe_2O_3	FeO	Fe_2O_3
Ferrohedenbergite 7-4	29.10	1.66	28.67	2.13
Ferrosalite 5-31	17.33	0.70	17.95	0.01
Chromian-augite 17-1	3.53	2.66	4.53	1.55
Augite 17-6	7.71	0.72	7.21	1.38
Aegirine 12-1	0.14	32.98	3.27	29.50
Augite 17-18	14.25	0.59	14.08	0.78
Augite 17-12	5.03	7.83	4.19	8.76

(Numbers after titles refer to table and analysis number in volume 2 of Deer, Howie and Zussman--Chain Silicates--1963)

Table A4-2

Error effects on results of PXENDCR

Oxide	A	B	C	D	P15-3
SiO_2	52.86	50.78	52.86	50.78	51.82
Al_2O_3	7.29	7.01	7.29	7.01	7.15
Fe_2O_3	0.34	0.34	0.34	0.34	0.34
FeO	2.74	2.74	2.74	2.74	2.74
MgO	15.06	14.46	14.46	15.06	14.76
CaO	20.04	19.26	19.26	20.04	19.65
Na_2O	1.80	1.80	1.80	1.80	1.80
K_2O	0.03	0.03	0.03	0.03	0.03
Cr_2O_3	0.73	0.73	0.73	0.73	0.73
TiO_2	0.83	0.83	0.83	0.83	0.83
Acmite	0.13	1.44	-6.08	7.70	0.79
Soda-Cr.	2.05	2.13	2.08	2.09	2.09
Jadeite	10.35	9.44	16.72	3.01	9.89

Iron values recalculated from above data and substituted into PXENDCR to obtain the above end-member values.

Fe_2O_3	0.05	0.52	-2.24	2.82	0.34
FeO	3.00	2.58	5.07	0.51	2.74

A....Si, Al, Mg, Ca all raised by 2 %
B....Si, Al, Mg, Ca all decreased by 2 %
C....Si, Al raised; Mg, Ca decreased by 2 %
D....Si, Al decreased; Mg, Ca raised by 2 %

method of Kushiro (1962) using another programme, PXENDS. This was developed by R. G. Cawthorne and amended by the author. As discussed in Chapter 5 two versions of the programme were used, the latter (PXENDCR) calculating a 'soda-chrome' molecule in addition to the other nine end-members. The values fed into these programmes were the ferric-corrected versions from FE3CALC3, hence allowing for calculation of acmite etc.

In order to test the precision of the programmes when allowing for experimental error in analysis several values of P15-3, a chrome-diopside, were run through PXENDCR. It was assumed that changes in the values of SiO_2, MgO, Al_2O_3 and CaO are most likely to affect the sensitivity of the programme, since these oxides represent over 90% of the total analysis. Four sets of values were used assuming a maximum of 2% individual oxide error from the microprobe analyses. The results are listed in Table A4-2. A 2% increase or decrease in all four oxides induces an error of $\pm$4.5% in the jadeite value, and $\pm$2.1% in the Ca-Ts value, two of the most significant end-members. The end-member values calculated from such analysis manipulations are unlikely enough to suggest that an overall error of the magnitude tested is unlikely to occur without being noticed. Similarly, the values obtained from simultaneous increase and decrease of two oxide-pairs produce highly improbable end-member values for a chrome-diopside. It is thus assumed that the overall analytical error is small, though the error in individual oxides might approach 2% or more. Such small errors would induce small variations in the calculated end-members, probably of less than 2% of any individual molecule.

BIBLIOGRAPHY

AOKI, K. 1968. Petrogenesis of ultrabasic and basic inclusions in alkali-basalts, Iki Island, Japan. Am.Mineral. 53, 241-256.

AOKI, K. 1970a. Petrology of kaersutite-bearing ultramafic and mafic inclusions in Iki Island, Japan. Contr. Miner. Petrol. 25, 270-283.

AOKI, K. 1970b. Andesine megacrysts in alkali-basalts from Japan. Contr. Miner. Petrol. 25, 284-288.

AOKI, K. & KUSHIRO, I. 1968. Some clinopyroxenes from ultramafic inclusions in Dreiser Weiher, Eifel. Contr. Miner. Petrol. 18, 326-337.

BACON, C.R. & CARMICHAEL, I.S.E. 1973. Stages in the P-T path of ascending basalt magma; an example from San Quintin, Baja California. Contr. Miner. Petrol. 41, 1-22.

BENNET, J.A.E. 1939. The analcite and leucite-basanites of East Lothian. Unpublished Ph.D. Thesis, Univ. of Edinburgh.

BEST, M.G. 1970. Kaersutite-peridotite inclusions and kindred megacrysts in basanitic lavas, Grand Canyon, Arizone. Contr. Miner. Petrol. 27, 25-44.

BINNS, R.A. 1969. High-pressure megacrysts in basanitic lavas near Armidale, New South Wales. Am.J.Sci. 267-A (Schairer volume) 33-49.

BINNS, R.A., DUGGAN, M.B., WILKINSON, J.F.G. 1970. High-pressure megacrysts in alkaline lavas from north-east New South Wales. Am.J.Sci. 269, 132-168.

BORLEY, G.D., SUDDABY, P. & SCOTT, P. 1971. Some xenoliths from the alkalic rocks of Teneriffe, Canary Islands. Contr. Miner. Petrol. 31, 102-114.

BOYD, F.R. & ENGLAND, J.L. 1960. Apparatus for phase-equilibrium measurements at pressures up to 50 kilobars and temperatures up to 1750°C. J.Geophys. Res. 65, 741-748.

BOYD, F.R. & ENGLAND, J.L. 1963. Effect of pressure on the melting of diopside, $CaMgSi_2O_6$ and albite, $NaAlSi_3O_8$ in the range up to 50kb. J.Geophys.Res. 68, 311-323.

BRAVO, M.S. 1973. Melting of synthetic phlogopite-bearing spinel- and garnet-lherzolites at high pressures. Unpubl. Ph.D. Thesis. Univ. of Edinburgh.

BROTHERS, R.N. 1960. Olivine nodules from New Zealand. Report 21st Int.Geol.Cong. Copenhagen. Part 13, 68-81.

BROWN, G.C., HUGHES, D.J. & ESSON, J. 1973. New XRF data retreival techniques and their applicability to USGS standard rocks. Chem.Geol. 11, 223-229.

CHAPMAN, N.A. in press. Ultrabasic inclusions from Coalyard Hill, Fife. Scott.J.Geol.

CLOUGH, C.T. 1910. In "The Geology of East Lothian". Mem.Geol. Surv.Scot. No.33.

COHEN, L.H., ITO, K. & KENNEDY, G.C. 1967. Melting and phase relations in an anhydrous basalt to 40 kilobars. Am.J.Sci. 265, 475-518.

COLVINE, R.J.L. 1968. Pyrope from Elie, Fife. Scott.J.Geol. 4, 283-286.

COOMBS, D.S. 1963. Trends and affinities of basaltic magmas and pyroxenes as illustrated on the diopside-olivine-silica diagram. Min.Soc.Am.Spec.Paper 1, 227-250.

COOMBS, D.S., & WILKINSON, J.F.G. 1969. Lineages and fractionation trends in undersaturated volcanic rocks from the East Otago province (New Zealand) and related rocks. J.Petrol. 10, 440-501.

DAWSON, J.B., POWELL, D.G., & REID, A.M. 1970. Ultrabasic xenoliths from the Lashaine volcano, Northern Tanzania. J.Petrol. 11, 519-548.

DAWSON, J.B. & SMITH, J.V. 1973. Alkalic pyroxenite xenoliths from the Lashaine volcano, Northern Tanzania. J.Petrol. 14, 113-131.

DEER, W.A., HOWIE, R.A. & ZUSSMAN, J. 1963. Rock-forming minerals. 2. Chain silicates. Publ. Longmans, London.

DEER, W.A., HOWIE, R.A. & ZUSSMAN, J. 1966. An Introduction to the Rock Forming Minerals. Publ. Longmans, London.

DEWEY, J.F. 1969. Evolution of the Appalachian/Caledonian Orogen. Nature, Lond. 222, 124-129.

DICKEY, J.S. 1968. Eclogitic and other inclusions in the Mineral Breccia Member of the Deborah Volcanic Formation at Kakanui, New Zealand. Am.Mineral. 53, 1304-1319.

DUNCAN, A.M. 1972. The occurrence of an ultramafic xenolith in the vent at Weak Law Rocks, East Lothian. J.Arthur Holmes. Soc. (Durham), 5-1, 31-36.

FITCH, F.J., MILLER, J.A. & WILLIAMS, S.C. 1970. Isotopic ages of British Carboniferous rocks. C.R. 6th Int.Congr.Carb.Strat.Geol. Sheffield, 2, 771-789.

FITTON, J.G. & HUGHES, D.J. 1970. Volcanism and plate tectonics in the British Ordovician. Earth Planet.Sci.Lett. 8, 223-228.

FLETT, J.S. 1914. In 'The Geology of Caithness'. Mem.Geol.Surv.Scot.

FORBES, R.B. & KUNO, H. 1965. The regional petrology of peridotite inclusions and basaltic host rocks. Upper Mantle Symposium, New Delhi, 161-179, 1964.

FORBES, R.B. & KUNO, H. 1967. Peridotite inclusions and basaltic host rocks. In 'Ultramafic and related rocks' ed. P.J. Wyllie. Publ. J. Wiley.

FORBES, W.C. & STARMER, R.J. 1974. Kaersutite is a possible source of alkali-olivine basalts. Nature, Lond. 250, 209-10.

FORD, C.E. 1972. Furnace design, temperature distribution, calibration and seal design in internally heated pressure vessels. Prog.in Exptl. Petrol. 2, 89-96. N.E.R.C., London.

FRANCIS, E.H. 1960. Intrusive tuffs related to the Firth of Forth volcanoes. Trans. Edinb. Geol. Soc. 18, 32-50.

FRANCIS, E.H. 1969. In 'Field excursion guide to the Carboniferous volcanic rocks of the Midland Valley of Scotland. ed. B.G.J. Upton. Scot.Acad.Press. Edinburgh, 23-30.

FRANCIS, E.H. 1970. Bedding in Scottish (Fifeshire) tuff-pipes and its relevance to maars and calderas. Bull.Volcanol. 34, 697-712.

FRANCIS, E.H. & HOPGOOD, A.M. 1970. Volcanism and the Ardross Fault, Fife. Scott.J.Geol. 6, 162-185.

FRECHEN, J. 1948. Die genese der Olivinausscheidungen vom Dreiser Weiher (Eifel) und Finkenberg (Siebengebirge). Neues Jb. Miner. Geol. Palaeont. 79A, 317-406.

FRECHEN, J. 1963. Kristallisation, Mineralbestand, Mineralchemismus und Förderfolge der Mafitite vom Dreiser Weiher in der Eifel. Neues Jb. Miner. Monatshefte. 205-225.

FREY, F.A. & GREEN, D.H. 1974. The mineralogy, geochemistry and origin of lherzolite inclusions in Victorian basanites. Geochim. cosmochim. Acta. 38, 1023-1059.

FRISCH, T. & WRIGHT, J.B. 1971. Chemical composition of high-pressure megacrysts from Nigerian Cenozoic lavas. Neues Jb. Miner. Monatshefte. 289-304.

GAST, P.W. 1968. Trace element fractionation and the origin of tholeiitic and alkaline magma types. Geochim. cosmochim. Acta, 42, 1057-1068.

GEIKIE, A. 1902. The Geology of Eastern Fife. Mem.Geol.Surv. Scotland.

GRANT, N.K., FREETH, S.J., & REX, D.C. 1972. Potassium-argon data and the origin of feldspar megacrysts in basalt. Nature Physical Sci. 238, 42-43.

GRAMLICH, J.W. & NAUGHTON, J.J. 1972. Nature of source material for ultramafic minerals from Salt Lake Crater, Hawaii, from measurement of Helium and Argon Diffusion. J.Geophys.Res. 77, 3032-3042.

GREEN, D.H. 1969. The origin of basaltic and nephelinitic magmas in the earth's mantle. Tectonophysics, 7, 409-422.

GREEN, D.H. & RINGWOOD, A.E. 1967. The genesis of basaltic magmas. Contr.Miner.Petrol. 15, 103-190.

HAMAD, S.El D. 1963. The chemistry and mineralogy of olivine nodules from Calton Hill, Derbyshire. Miner.Mag. 33, 483-497.

HARRIS, P.G., HUTCHISON, R. & PAUL, D.K. 1972. Plutonic xenoliths and their relation to the upper mantle. Phil.Trans.Roy.Soc. Lond. A 271, 313-323.

HAYS, J.F. 1967. Lime-alumina-silica. Carnegie Inst. Wash. Yrbk. 65, 234-239.

HEDDLE, M.F. 1878. Chapters on the mineralogy of Scotland. Chapter 4th - augite, hornblende and serpentinous change. Trans. Roy. Soc. Ed. 27, 453-555.

HEDDLE, M.F. 1901. Mineralogy of Scotland. Publ. Douglas, Edinburgh.

HERZBERG, C.T. 1974. Phase assemblages of the system $CaO-Na_2O-MgO-Al_2O_3-SiO_2$ in the plagioclase and spinel-lherzolite mineral facies. Unpubl. Ph.D. Thesis. Univ. of Edinburgh.

HOFFER, J.M. & HOFFER, R.L. 1973. Composition and structural state of feldspar inclusions from alkali-olivine basalt, Portrillo Basalt, southern New Mexico. Bull.geol.Soc.Am. 84, 2139-2142.

HOLMES, A. & HARWOOD, H.F. 1937. The Volcanic area of Bufumbira. Geol.Surv. Uganda Mem. 3, part 2.

HUCKENHOLZ, H.G. 1973. The origin of fassaitic augite in the Alkali-basalt Suite of the Hocheifel area, W. Germany. Contr.Miner.Petrol. 40, 315-326.

ITO, K. & KENNEDY, G.C. 1968. Melting and phase relations in the plane tholeiite-lherzolite-nepheline basanite to 40 kilobars with geological implications. Contr.Miner.Petrol. 19, 177-211.

JACKSON, E.D. 1969. Discussion on the paper 'The origin of ultramafic and ultrabasic rocks' by P.J.Wyllie. Tectonophysics, 7, 517-518.

JAMIESON, B.G. 1969. Natural Rock Projections into a Pseudo-Quaternary system. Prog.in Expt.Petrol. No. 1, 152-155. N.E.R.C. London.

KLEEMAN, J.D., GREEN, D.H. & LOVERING, J.F. 1969. Uranium distribution in ultramafic inclusions from Victorian basalts. Earth Planet. Sci.Letts. 5, 449-458.

KLEEMAN, J.D. & COOPER, J.A. 1970. Geochemical evidence for the origin of some ultramafic nodules from Victorian basanites. Phys.Earth Planet.Interiors. 3, 302-308.

KNOPF, A. 1936. Igneous geology of the Spanish Peaks region, Colorado. Bull.geol.Soc.Amer. 47, 1727-1784.

KUNO, H. & AOKI, K. 1970. Chemistry of ultramafic nodules and their bearing on the origin of basaltic magmas. Phys.Earth Planet.Interiors. 3, 273-301.

KUSHIRO, I. 1962. Clinopyroxene solid-solutions. Part 1: The $CaAl_2SiO_6$ component. Jap.Jour.geol.Geog. 33, 213-220.

KUSHIRO, I. 1969. Discussion of the paper "The origin of basaltic and nephelinitic magmas in the earth's mantle" by D.H. Green. Tectonophysics, 7, 427-436.

KUSHIRO, I., SYONO, Y. & AKIMOTO, S. 1968. Melting of a peridotite nodule at high-pressures and high water pressures. J. Geophys. Res. 73, 6023-6029.

KUTOLIN, V.A. & FROLOVA, V.M. 1970. Petrology of ultrabasic inclusions from basalts of Minusa and Transbaikalian regions (Siberia, USSR). Contr.Miner.Petrol. 29, 163-179.

LAUGHLIN, A.L., BROOKINS, D.G., KUDO, A.M. & CAUSEY, J.D. 1971. Chemical and strontium isotopic investigations of ultramafic inclusions and basalt, Bandera Crater, New Mexico. Geochim. cosmochim. Acta. 35, 107-113.

LAUGHLIN, A.W., MANZER, G.K. & CARDEN, J.R. 1974. Feldspar megacrysts in alkali basalts. Bull. geol. Soc. Am. 85, 413-416.

LEAKE, B. 1968. A catalog of analysed calciferous and sub-calciferous amphiboles together with their nomenclature and associated minerals. Geol.Soc.Am.Spec.Paper 98.

LEGGO, P.J. & HUTCHISON, R. 1968. A Rb-Sr isotope study of ultrabasic xenoliths and their basaltic host rocks from the Massif Central, France. Earth Planet. Sci. Letts. 5, 71-75.

LE MAITRE, R.W. 1968. Chemical variations within and between volcanic rock series - a statistical approach. J.Petrol. 9, 220-52.

LE MAITRE, R.W. 1969. Kaersutite-bearing plutonic xenoliths from Tristan da Cunha, S. Atlantic. Miner.Mag. 37, 185-197.

MACDONALD, G.A. & KATSURA, T. 1964. Chemical composition of Hawaiian lavas. J.Petrol. 5, 82-133.

MASON, B. 1968. Kaersutite from San Carlos, Arizona, with comments on the paragenesis of this mineral. Miner. Mag. 36, 997-1002.

MÉTAIS, D. & CHAYES, F. 1963. Varieties of lamprophyre. Carnegie Inst. Wash. Yrbk. 62, 156-157.

MYKURA, W. 1967. The upper Carboniferous rocks of south-west Ayrshire. Bull.Geol.Surv.Gt.Br. 26, 23-98.

MYSEN, B. 1973. Melting in a hydrous mantle; phase relations of mantle peridotite with controlled water and oxygen fugacities. Carnegie Inst. Wash. YrBk. 72, 467-478.

NAGASAWA, H., WAKITA, H., HIGUCHI, H. & ONUMA, N. 1969. Rare earths in peridotite nodules: An explanation of the genetic relationship between basalts and peridotite nodules. Earth Planet.Sci.Letts. 5, 377-381.

NISHIMURA, S. 1972. Partition of Uranium between peridotite nodules and host basalt. Chem.Geol. 10, 211-221.

NOCKOLDS, S.R. 1941. The Garabal Hill-Glen Fyne igneous complex. Ql. J.geol.Soc.Lond. 96, 451-511.

NOCKOLDS, S.R. 1947. The relation between chemical composition and paragenesis in the biotite micas of igneous rocks. Am.J.Sci. 245, 401-420.

O'HARA, M.J. 1965. Primary magmas and the origin of basalts. See 3H Ref. Notes. Scott.J.Geol. 1, 19-40.

O'HARA, M.J. 1967. Crystal-liquid equilibria and the origins of ultramafic nodules in basic igneous rocks. in 'Ultramafic and related rocks' ed. P.J. Wyllie.

O'HARA, M.J. 1968. The bearing of phase equilibria studies in synthetic and natural systems on the origin and evolution of basic and ultrabasic rocks. Earth Sci.Rev. 4, 69-133.

O'HARA, M.J. 1969. The origin of eclogite and ariégite nodules in basalts. Geol.Mag. 106, 322-330.

O'HARA, M.J. & MERCY, E.L.P. 1963. Petrology and petrogenesis of some garnetiferous peridotites. Trans.Roy.Soc.Edinb. 65, 251-314.

O'HARA, M.J., RICHARDSON, S.W. & WILSON, G. 1971. Garnet peridotite stability and occurrence in crust and mantle. Contr.Miner.Petrol. 32, 48-68.

O'HARA, M.J., SAUNDERS, M.J. & MERCY, E.L.P. in press. Garnet peridotite, primary ultrabasic magma and eclogite; interpretation of upper-mantle processes in kimberlite. in 'Physics and Chemistry of the Earth', Pergamon press (publ.)

PEARCE, T.H. 1968. A contribution to the theory of variation diagrams. Contr.Miner.Petrol. 19, 142-157.

REID, J.B. & FREY, F.A. 1971. Rare-earth distributions in lherzolite and garnet-peridotite xenoliths and the constitution of the upper mantle. J. Geophys. Res. 76, 1184-1196.

RICHARDSON, S.W., BELL, P.M. & GILBERT, M.C. 1968. Kyanite-sillimanite equilibrium between 700° and 1500°C. Am.J.Sci. 266, 513-541.

RINGWOOD, A.E. 1966. The chemical composition and origin of the earth. Advances in Earth Sciences. M.I.T. Press, Cambridge, Mass.

ROSE, H.J., ALDER, I. & FLANAGAN, R.J. 1963. X-ray fluorescence analysis of the light elements in rocks and minerals. Appl.Spectrosc. 17, 81-85.

ROSS, C.S., FOSTER, M.D., & MYERS, A.T. 1954. Origin of dunites and olivine-rich inclusions in basaltic rocks. Am.Mineral. 39, 693-737.

SIMPSON, J.B. 1932. Geology of the Kidlaw district, East Lothian. Trans.Edinb.Geol.Soc. 12, 111-113.

SMELLIE, W.R. 1915. The Igneous rocks of Bute. Trans.Geol. Soc.Glasg. 15, 334-373.

SWEATMAN, T.R. & LONG, J.V.P. 1969. Quantitative electron-probe microanalysis of rock-forming minerals. J.Petrol. 10, 332-379.

THOMPSON, J.B. 1947. Role of Al in rock-forming silicates. B.G.S.A. 58, 1232.

TRASK, N.J. 1969. Ultramafic xenoliths in basalt, Nye County, Nevada. U.S.G.S. Professional Paper 650-D 43-48.

TURNER, F.J. 1968. Metamorphic petrology. McGraw Hill Co.

UPTON, B.G.J. & MACDONALD, R. in press. In "Edinburgh Geology; an excursion guide" 2nd edition. Ed. Craig, G.Y & Duff, P.McL.D. Publ. Scot.Acad.Press.

VARNE, R. 1970. Hornblende-lherzolite and the upper mantle. Contr.Miner.Petrol. 27, 45-51.

VINCENT, E.A., WRIGHT, A.B., CHEVALLIER, R. & MATHIEU, S. 1957. Heating experiments on some natural titaniferous magnetites. Miner.Mag. 31, 624-655.

WALKER, G.P.L. & ROSS, J.V. 1954. A xenolithic monchiquitic dyke near Glenfinnan, Inverness-shire. Geol.Mag. 91, 463-472.

WHITE, A.J.R. 1964. Clinopyroxenes from eclogites and basic granulites. Am.Mineral. 49, 883-888.

WILKINSON, J.F.G. 1962. Mineralogical, geochemical, and petrogenetic aspects of an analcite-basalt from the New England district of New South Wales. J.Petrol. 3, 192-214.

WILSHIRE, H.G. & BINNS, R.A. 1961. Basic and ultrabasic xenoliths from volcanic rocks of New South Wales. J.Petrol. 2, 185-208.

WILSHIRE, H.G., SCHWARZMAN, E., & TRASK, N.J. undated. Distribution of ultramafic xenoliths at twelve North American sites. U.S.G.S./ N.A.S.A. Interagency report, Astrogeology, 42. (Preliminary report only).

WILSON, A.D. 1955. A new method for the determination of ferrous iron in rocks and minerals. Bull.Geol. Surv. Gt.Brit. 9, 56-58.

WRIGHT, T.L. 1968. X-ray and optical study of alkali feldspars, Part II; X-ray method for determining the composition and structural state from measurements of 2θ values for three reflections. Am.Mineral. 53, 88-104.

WYLLIE, P.J. 1967. Ultramafic and related rocks. Publ. J. Wiley & Sons.

WYLLIE, P.J. 1971. The Dynamic Earth. John Wiley & Sons.

YAGI, K. & ONUMA, K. 1967. The join $CaMgSi_2O_6$-$CaTiAl_2O_6$ and its bearing on the titanaugites. J.Fac.Sci.Hokkaido Univ. 13, 463-483.

YAMAGUCHI, M. 1964. Petrologic significance of ultrabasic inclusions in basaltic rocks from south-west Japan. Mem.Fac.Sci.Kyushu Univ. Series D, 15, 163-219.

YODER, H.S. 1969. Calc-alkaline andesites: experimental data bearing on the origin of their assumed characteristics. Proc.Andesite Conference, 77-89.

YODER, H.S. & TILLEY, C.E. 1962. Origin of basalt magmas. J.Petrol. 3, 342-532.

ADDENDUM TO BIBLIOGRAPHY

BAILEY, E.B. 1910 — The geology of East Lothian. Mem.Geol.Surv. Scotland.

BALSILLIE, D. 1927 — Contemporaneous volcanic activity in East Fife. Geol.Mag. 64, 481-494

COE, K. 1966 — Intrusive tuffs of west Cork, Ireland. Ql.J.geol.Soc. Lond. 122, 1-28

MACGREGOR, A.G. 1949 — Geology of central Ayrshire. Mem.Geol.Surv. Scotland.

SIMPSON, J.B. and RICHEY, J.E. 1936 — The geology of the Sanquhar coalfield and the adjacent basin of Thornhill. Mem.Geol.Surv. Scotland.

TYRELL, G.W. 1918 — Igneous geology of the Ayrshire coast from Downfoot to the Heads of Ayr. Trans. geol. Soc. Glasg. 16, 339-348

WHYTE, F. 1963 — The Heads of Ayr vent. Trans. geol. Soc. Glasg. 25, 72-97

Ultrabasic inclusions from the Coalyard Hill Vent, Fife

N. A. CHAPMAN
Grant Institute of Geology, Edinburgh

SYNOPSIS

The petrography and field relations of a hitherto undescribed occurrence of lherzolitic and amphibole-biotite pyroxenite inclusions in basanite and monchiquite sheets associated with one of the Fife tuff-pipes are briefly discussed.

INTRODUCTION

Two small basanitic and monchiquitic sheets associated with the Coalyard Hill volcanic vent contain an assemblage of megacrysts which may be fragments of inclusions or representative of a relatively high-pressure phenocryst assemblage, and ultrabasic inclusions.

Although these occurrences have been known for many years, no description of the inclusions has hitherto been published. The purpose of this note is to provide a preliminary account of the sheets which are of interest in that whereas both are likely to represent intrusive events very close in time, they contain contrasting lherzolitic and amphibole-biotite pyroxenitic suites of inclusions.

The Coalyard Hill diatreme is one of a number of Upper Carboniferous volcanic necks aligned along a 4 km stretch of coast (where the Ardross fault is a dominant structural feature), between Elie and St. Monance in Fife. The diatremes were first described by Geikie (1902) and subsequently by Cumming (1928, 1936), Francis (1960, 1969, 1970) and Francis and Hopgood (1970).

The lherzolite locality (Fig. 1) lies on the margin of the diatreme, about 200 m ENE. of Ardross Farm and a little below High-Water Mark [NO511008]. The inclusions occur in a steeply inclined basanite sheet approximately 1·5 m thick, exposed over a distance of a few metres around the margin of the vent, flanked by tuff to the east and highly disturbed sediments to the west.

The host rock is a fine-grained, slightly porphyritic basanite, with a groundmass of labradorite (An_{55}), titanaugite, magnetite, nepheline and analcime. It contains xenocrysts of olivine, clinopyroxene, orthopyroxene and spinel, believed to be derived from the inclusions. The spinels are commonly marginally altered to magnetite. Most of the olivine is serpentinized and the host rock is highly carbonated and cut by many fine fractures radiating from the inclusions.

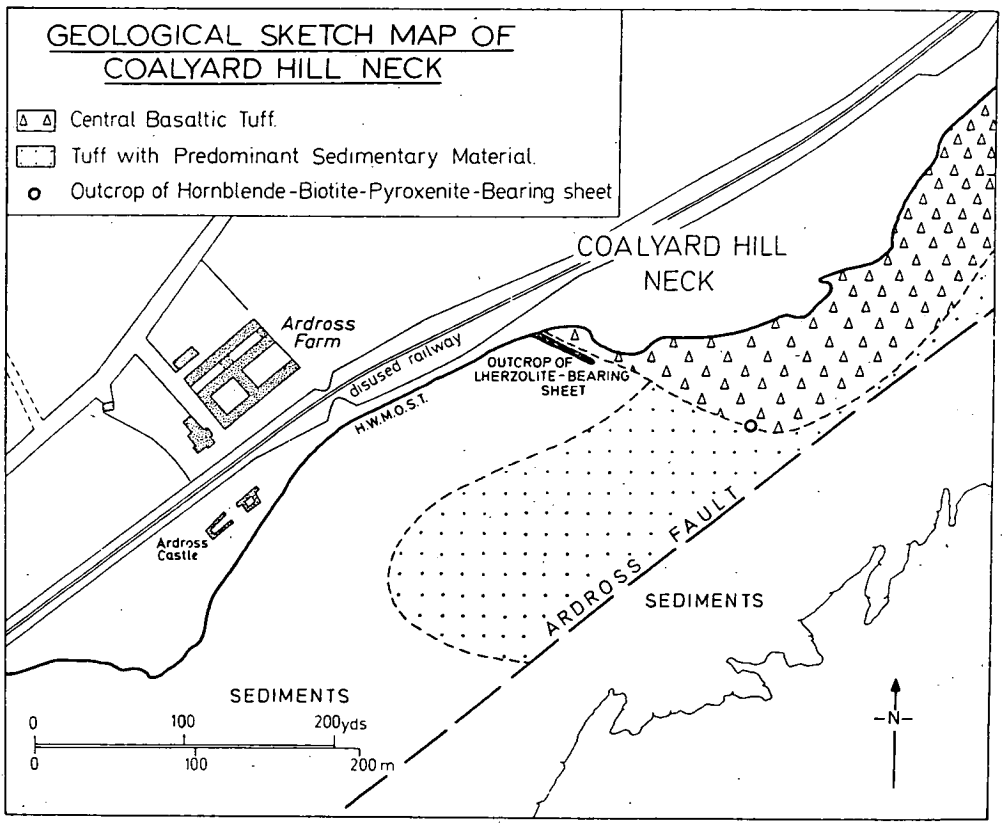

FIG. 1.

THE INCLUSIONS

The inclusions are concentrated at the base of the sheet where they comprise at least 70 per cent of the rock volume. They vary in size from 300 mm across down to a few millimetres, and are generally sub-rounded in outline. Many are in extreme stages of alteration and the whole outcrop is riddled with thin calcite veins. In thin section the edges of the inclusions are seen to be ragged, and fragmentation is indicated by the xenocrysts and small ultrabasic crystal aggregates in the basanite host.

The inclusions are spinel-bearing lherzolites with rare wehrlites and clinopyroxenites. The majority of the lherzolites are highly serpentinized and carbonated so that in most samples only a little fresh olivine can be seen, and in general, a colourless mosaic of alteration products is all that remains. These contain scattered blebs of sulphide and some ilmenite lamellae. Texturally there is little variation in this suite of inclusions, and all can be described as granoblastic, having undergone enough recrystallization to obliterate any primary igneous textures. One specimen consists of a single large clinopyroxene crystal twisted along its length, and surrounded by a mosaic of small

altered olivine crystals, probably representing cataclasis and recrystallization of the olivine matrix (*cf.* Spry 1968).

The spinel is a uniform pale greenish-brown in all specimens, and is often rimmed by magnetite. Some very fine exsolution lamellae are visible in some of the orthopyroxenes, and rarely small lamellae of exsolved spinel are present in the diopside. Where diopside occurs at inclusion margins it is often rimmed with overgrowths of titanaugite, as are many of the diopside and enstatite xenocrysts in the host. Fractures in some of the ultrabasic blocks have been invaded by the host basanite. Thin veinlets of the latter show quench crystals of titanaugite and plagioclase with some glass. Rutile was found in one such vein, and biotite was also noted.

A second, monchiquitic, sheet was also examined, showing a much greater degree of alteration than the basanite. This sheet is nearly horizontal and about 2 m thick, outcropping some 50 m to the south-east of the last locality between high and low water marks, also near the vent margin. It consists of a fine-grained matrix of clinopyroxene, analcime, carbonate and chlorite with small phenocrysts of olivine, augite and apatite. It also contains abundant amphibole and feldspar megacrysts as well as some xenoliths of sandstone. Only one ultrabasic inclusion was found, consisting of

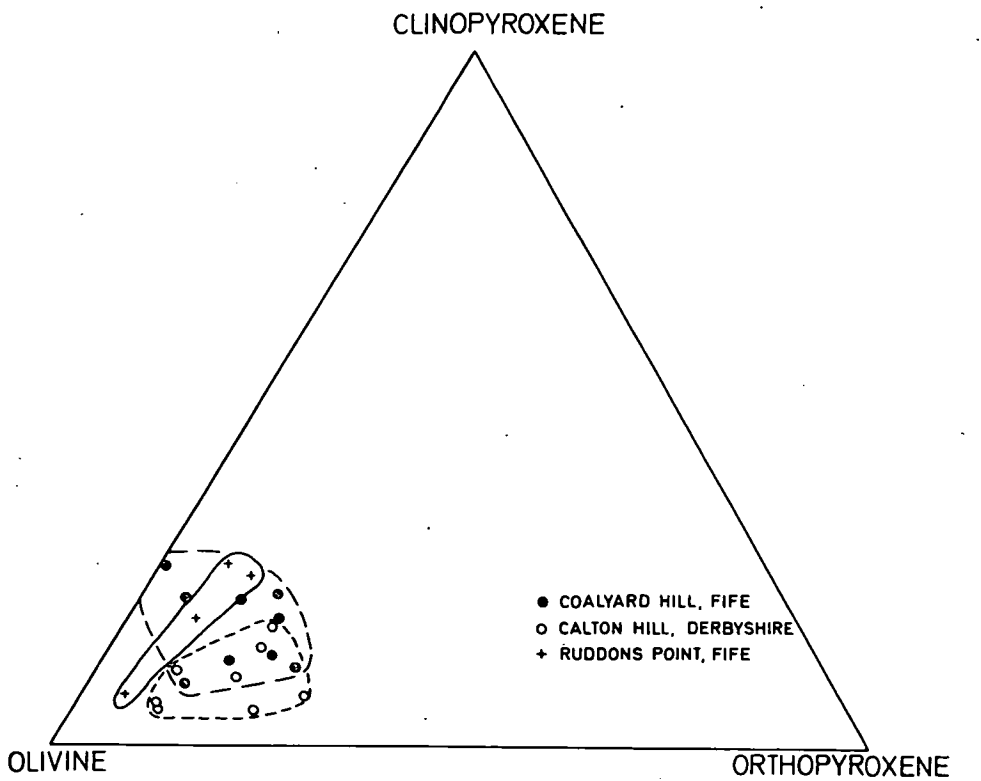

FIG. 2. Modal analyses of spinel-lherzolites from British Carboniferous localities. (Some Calton Hill analyses after Hamad, 1963)

titanaugite, olivine and minor opaque phases. Kaersutite and biotite occur interstitially. The host rock contains abundant rounded megacrysts of amphibole similar to that seen in the inclusions, up to 10 mm across and rimmed by magnetite. The feldspar megacrysts consist of anorthoclase (sometimes with associated biotite), of composition $Or_{17}Ab_{81}An_2$. One perfect euhedral twinned anorthoclase was found, about 80 mm long, although the majority of the big feldspar crystals are well rounded and anhedral. Scarce clinopyroxene megacrysts were also noted.

Discussion

The occurrence of ultrabasic inclusions is well known in the minor intrusions and vents of Fife. Thus spinel lherzolites occur in basaltic blocks from the Ardross Neck tuff, and also in basanite at Ruddon's Point. Inclusions of amphibole-biotite pyroxenite, consisting of clinopyroxene, kaersutite, biotite, olivine and plagioclase, in widely varying proportions, are found in tuff at Elie Ness and Kincraig Hill, and in dykes cutting the Elie Ness and Ardross Necks. Anorthoclase megacrysts from the basanite at Ruddon's Point, and from a dyke cutting the Ardross Neck have been analysed, and have compositions respectively of $Or_{21}Ab_{77}An_2$ and $Or_{19}Ab_{79}An_2$, very similar to those from Coalyard Hill. Megacrysts of amphibole and pyroxene are common to the tuffs and minor intrusions of nearly all localities where pyroxenitic inclusions are found, and pyrope is well known from the Elie Ness tuff.

The importance of the Coalyard Hill locality lies in the close association of the lherzolitic and pyroxenitic inclusion suites, and in the occurrence of anorthoclase megacrysts in the monchiquite. These latter most probably represent high-pressure phenocrysts, as any xenocrystal origin seems unlikely. Dickey (1968) noted similar anorthoclase megacrysts ($Or_{12}Ab_{84}An_4$) in melanephelinites from New Zealand, and suggested that their co-precipitation with augite and pyrope from an alkali-basaltic magma could change the composition of the liquid to that of the host melanephelinite. It is intended to carry out further analytical work and high-temperature controlled pressure simulations to ascertain the effects of megacryst extraction on the Coalyard Hill host rock.

The evidence from this locality shows no genetic affinities between the two groups of inclusions, which would appear to represent two quite different modes of origin. Comparison of the lherzolite suite of inclusions with those of other localities (*cf.* Harris *et al.* 1972) would indicate a mantle origin, while data so far available on the mineralogy of the pyroxenitic inclusions suggests a higher level cognate origin for this suite.

Acknowledgements

The author wishes to express his thanks to Dr. B. G. J. Upton for drawing his attention to the locality, and to Dr. E. H. Francis for discussion on the structure of the area.

References

CUMMING, G. A. 1928. The lower limestones and associated volcanic rocks of a section of the Fife coast. *Trans. Edinb. geol. Soc.* **12**, 124–140.

—— 1936. The structure and volcanic geology of the Elie-St. Monance district. *Trans. Edinb. geol. Soc.* **13**, 340–365.

DICKEY, J. S. 1968. Eclogitic and other inclusions in the mineral breccia member of the Deborah Volcanic Formation at Kakanui, New Zealand. *Am. Miner.* **53**, 1304–1319.

FRANCIS, E. H. 1960. Intrusive tuffs related to the Firth of Forth volcanoes. *Trans. Edinb. geol. Soc.* **18**, 32–50.

—— 1969. *In* Upton, B. (ed.), *Field excursion guide to the Carboniferous volcanic rocks of the Midland Valley of Scotland*, 23–30. Edinburgh.

—— 1970. Bedding in Scottish (Fifeshire) tuff-pipes and its relevance to maars and calderas. *Bull. volcan.* **14**, 697–712.

—— and HOPGOOD, A. M. 1970. Volcanism and the Ardross Fault. *Scott. J. Geol.* **6**, 162–185.

GEIKIE, A. 1902. The geology of Eastern Fife. *Mem. geol. Surv. Gt Br.*

HAMAD, S. EL D. 1963. The chemistry and mineralogy of the olivine nodules of Calton Hill, Derbyshire. *Mineralog. Mag.* **33**, 483–497.

HARRIS, P. G., HUTCHISON, R. and PAUL, D. K. 1972. Plutonic xenoliths and their relation to the upper mantle. *Phil. Trans. R. Soc.* **271A**, 313–323.

SPRY, A. H. 1969. The interpretation of the textures of peridotites, eclogites and granulites. *Spec. Publs. geol. Soc. Australia* **2**, 307–321.

MS received 11th January 1973
Revised MS received 15th June 1973